N° d'ordre : 2283

THESE

présentée

pour obtenir

LE TITRE DE DOCTEUR DE L'INSTITUT NATIONAL POLYTECHNIQUE DE TOULOUSE
&
THE TITLE OF DOCTOR OF PHILOSOPHY OF THE INSTITUTE OF CHEMICAL TECHNOLOGY, PRAGUE

École doctorale : Energétique et Dynamique des Fluides

Spécialité : Energétique et transferts – Systèmes et Procédés

Par M. Jaroslav BLAŽEK

Titre de la thèse :

- français **ETUDE DES SCHEMAS REACTIONNELS DE DEGRADATION THERMIQUE DES POLYMERES**
- anglais **STUDY OF THE REACTION KINETICS OF THE THERMAL DEGRADATION OF POLYMER**
- tchèque **TERMICKÁ DEGRADACE ORGANICKÝCH MATERIÁLŮ**

Soutenue le 11 Novembre 2005 devant le jury composé de :

M.	Bohumil KOUTSKÝ	Président
MM.	Didier LECOMTE, Petr BURYAN	Directeurs de thèse
	André FONTANA, Pavel STRAKA, Ivan VÍDEN	Rapporteurs
	František HRDLIČKA	Membre
	Yannick SOUDAIS	Membre
	Florent LEMORT	Membre
	Josef VEJVODA	Membre

Contents

Appendices

List of figures

Appendix C

Appendix D

Appendix F

Appendix G

List of tables

Appendix B

Appendix E

Appendix G

Acknowledgements

Firstly I must express my appreciation to my Czech thesis director Prof. Ing. Petr Buryan, DrSc. and Ing. Viktor Tekáč who fostered me throughout the whole thesis, as well as all other members of the Department of Gas, Coke and Air Protection of the Institute of Chemical Technology in Prague.

Prof. Didier Lecomte, my French thesis director, has always been ready to lend me a helping hand. Prof. Didier Grouset has given me some good tips to make my thesis more sound and complete. And every credit for the organizational success of the thesis goes to Dr. Yannick Soudais, who was at the same time the initiating factor of the thesis. Expert laboratory assistant Ludivine Moga has often spontaneously come with new ideas how to enhance quality of data treatment by modifying the output of machines. My thanks are to the entire team of the Centre énergetique-environnnement of the Ecole des Mines d'Albi-Carmaux, for their encouragement and suggestions.

Next are my thanks aimed unto Miguel Sanchez Amoros (Universidad Politécnica de Cartagena) and Daniel Barrabes Pradal (Escola Tècnica Superior d'Enginyers Industrials de Barcelona) for their assistance in FTIR analyses; and Shan Jiang (Ecole des Mines d'Albi-Carmaux) for his calculations in Sidolo.

Special acknowledgements are expressed to the French Embassy in Prague, which has offered the possibility to launch this joint thesis project and provided the consecutive support in the practical implementation of the thesis by enabling to benefit from the grant by the French government, in the programme BGF (bourse du gouvernement français).

A part of the study was cofinanced by CEA (*Commissariat à l'Energie Atomique*, i.e. the French Atomic Energy Commission), SCDV (Service de Conditionnement des Déchets et Vitrification). Appreciation of this fact is expressed as well.

Shrnutí

Disertační práce se zabývá pyrolýzou polymerů za atmosférického tlaku, v oblasti teplot 20-1000°C.

Teoretická část práce uvádí historické mezníky ve vývoji termické degradace polymerů a přehledně shrnuje současný stav problematiky. Nadto obsahuje základní poznatky týkající se metod výroby polymerů a v několika tabulkách seznamuje s průmyslovou produkcí těchto materiálů v Evropě.

Cílem experimentální práce bylo ověřit možnost aplikace specifické metody k výpočtu kinetických parametrů pyrolýzy (aktivační energie a frekvenčního faktoru) a jejich porovnání s údaji uváděnými v literatuře.

Experimenty byly prováděny v laboratorním měřítku. Byl použit termogravimetr sériově napojený na spektrometr FTIR. Výstupními údaji byl úbytek hmotnosti v korelaci s narůstající teplotou. Množina spekter odpovídajících různým stádiím pyrolýzních experimentů podpořila předpokládané mechanizmy rozkladu.

K výpočtu kinetických parametrů pyrolýzy polymerů byla použita integrální metoda Ozawa-Flynn-Wall a metoda využívající speciálního programu vytvořeného za tímto účelem v programu MatLab. Potřebné kinetické parametry byly získány pomocí „solverů" (rutin) využívajících soustavy diferenciálních rovnic. Výsledky obou metod byly porovnány.

Sledovanými polymery byly dva „přírodní polymery" – lignin a celulóza, a průmyslově připravené polymery: EVA, PS a PVC. Ve většině případů byla konstatována velmi dobrá shoda s kinetickými parametry nalezenými v dostupné literatuře.

Vypočtené hodnoty aktivační energie jsou v rozsahu od 118 $kJ.mol^{-1}$, std. odch. 2,73 $kJ.mol^{-1}$, (první fáze degradace PVC) do 454 $kJ.mol^{-1}$, std. odch. 78,1 $kJ.mol^{-1}$ (pyrolýza ligninu). Hodnoty frekvenčního faktoru se nacházejí v rozmezí od $7{,}66.10^{9}$ s^{-1}, std. odch. $1{,}58.10^{9}$ s^{-1} (Difuzní model 3), a to pro 1. stupeň degradace PVC, do $1{,}84.10^{45}$ s^{-1} pro Model F1 (řád reakce = 1), std. odch. $5{,}5.10^{45}$ s^{-1} pro pyrolýzu ligninu. Vypočtené hodnoty pyrolýzy ligninu vykazovaly jisté zvláštnosti. Další hodnotou frekvenčního faktoru je $1{,}77.10^{22}$ s^{-1}, std. odch. $8{,}22.10^{21}$ s^{-1} pro druhé stádium degradace „EVA 25" (řád reakce = 1).

Detailní studium pyrolýzy binárních sloučenin EVA/PVC, EVA/PS a EVA/celulóza, doprovázena analýzou uvolněných plynných termodegradentů pomocí spektrometrie FTIR přispěla lepšímu pochopení pyrolýzních jevů a byla uplatněno i k řešení problémů v průmyslovém měřítku.

Předkládaná disertační práce je součástí spolupráce Vysoké školy chemicko-technologické v Praze a Institut National Polytechnique de Toulouse, v rámci programu Doctorat en cotutelle (společně řízená doktorská práce), financovaného z prostředků francouzské vlády. Experimentální práce byly uskutečněny převážně na Ecole Nationale Supérieure des Techniques Industrielles et des Mines d'Albi-Carmaux.

1. Introduction

Accumulation of various plastic wastes begins to pose a serious problem. By creating waste sites, valuable chemical raw materials are lost. Moreover, in many countries, laws and regulations are fighting disposal of used plastic materials. Therefore, other solutions such as thermal treatment have to be taken into account.

Destruction of wastes by means of thermal treatment (combustion, pyrolysis) very often leads to pollution of the atmosphere by toxic pollutants as e.g. HCl, HCN, NO_X, SO_2, fly ash, compounds of the type of PCDD and PCDF. However, the pyrolysis process allows recovery of chemical products and energy from wastes.

The actual level of knowledge or state of arts, as well as the sustainability approach, do not allow us to adopt any new technology without considering its influence on our environment. It is therefore necessary to eliminate the production of toxic compounds. For this to be done effectively, understanding of the reaction pathways of polymer pyrolysis is vital. Thus, the best concepts and methods of the elimination of pollutants can be found and chemical resources as well as energy can be obtained. Using this information, processes may be designed for better control of flue gases and chemical compounds as well as energy consumption or recovery.

2. Theoretical backgrounds

2.1 Pyrolysis

Pyrolysis and thermolysis, commonly referred to as *destructive distillation*, are defined as an irreversible chemical change brought about by the action of heat in an oxygen-deficient (less than 2 %), inert-gas environment. The pyrolysis process requires temperatures ranging from 400 °C to 900 °C. Pyrolysis systems use a source of heat to drive the endothermic pyrolysis reactions in the complete absence of oxygen. The only difference between pyrolysis and thermolysis is that the former employs a direct heat source within the reactor (retort), while the latter employs an indirect external source of heat to the reactor (retort). Depending on particular reaction conditions (temperature, partial pressure of oxygen, total pressure), the organic fraction decomposes into gas, oil, and solid carbonaceous residues. Mild temperatures favour production of oils against gases. These products are recuperated at the end of the process, with the intention of being valorised.

Low oxygen content can be obtained under partial vacuum, by reinjecting one part of produced gases in the reactor or by injecting gaseous nitrogen into input riddle. The thermolysis technologies differ from each other by the reactor type, methods of reactor heating and conversion operating conditions.

Pyrolysis leads to decomposition of matter into various by-products (gas, oil, char, etc.). Yields of particular products are very variable, according to pyrolysis technology used. Some processes lead only to gases, others will produce a great quantity of oil. Pyrolysis products are gas, liquid, and char, the relative proportion of which depend very much on the pyrolysis method and process. Pyrolysis products are synthetic gas, oil, and carbonaceous residue. Synthetic gas produced in pyrolysis consists generally of a mixture of volatile organic compounds, some more heavy than others, methane, hydrogen, carbon dioxide and monoxide, and water coming largely from a humid fraction of the waste. After its treatment, gas can contain yet more volatile organic compounds (oil or tar). Most often, it is valorised in a boiler or directly in a thermolysis reactor, producing energy necessary for the thermal dissociation.

Oil is produced by condensation of a fraction of synthetic gas. Liquid thus obtained is refined by extraction and catalysis and then energetically valorised. Oil is an interesting product because it enables storage of energy that can be consequently used in a combustion turbine or a diesel engine.

Carbonaceous residue is a material relatively akin to lean coal, containing between 10 and 40 % of carbon. It can be valorized in situ in a classical boiler to give heat. The final residue is thus composed of fly ash from coal combustion. Some systems use a gasification stage to convert coal into synthetic gas. Carbonaceous residue can also be forwarded to a thermal power station or a cement factory and valorized ex situ.

Plastic materials cover a considerable spectrum of applications in our daily life. In France, in connection with evolution of legal regulations concerning waste sites, there cannot be used dumping for wastes, beginning the 1st of January 2002. They must be treated otherwise, e.g. by pyrolysis.

Pyrolysis is an alternative process of reuse of plastic materials to incineration and recycling. Recycling is being encouraged – it is compulsory for the EU members to recycle a minimum of 25 % and a maximum of 45 % of the total waste. By chemical recycling, plastic wastes can be converted to chemical feedstock, which can be used to produce new valuable products. Nevertheless, chemical recycling has the drawback of high-energy demand, and furthermore non-catalytic thermal degradation of polyolefin results in a wide range of products. Thus, pyrolysis seems to be an environmentally friendly process; yet, there are some disadvantages associated with it. The energy consumption is high and the molecular weight distribution of the products obtained tends to be quite broad, depending on the conditions used. The products can be used mostly as a low quality combustible. Elevated operating costs and the costs involved in the separation of the complex mixture lower the economical attractiveness of the process.

Pyrolysis (thermal cracking) of plastic waste allows recovering monomers and other petrochemical products. It is possible to obtain a mixture of hydrocarbons working at atmospheric pressure and moderate temperatures (500-850°C). During this process, quite a small gas volume can be obtained compared to incineration [Escola 1998]. Moreover, metallic toxic products are concentrated in the ashes, thus preventing undesirable emissions.

Howbeit, in the last few years the catalysed pyrolysis of plastics is being considered as a chance to avoid the problems mentioned above. However, this is not feasible without a perfect mastering of the kinetics of degradation for each and every polymer and all their possible mixtures, i.e. understanding their kinetic schemes and in parallel evaluating their thermodynamic parameters as well. It is imperative to know energy balances, released gases, products, by-products, … In this perspective, development of pyrolysis should be favoured.

Therefore, it has become interesting to know pyrolysis behaviour of certain number of polymers. And finally, in the domain of medical wastes, or even nuclear wastes, pyrolysis has to be preferred.

The study of kinetics and the knowledge of the main evolved gases are the main objectives of the present thesis.

2.1.1 Various possible methods of use of plastic polymers

According to the obligation in matter of wastes with the 2002 deadline, plastics cannot be from now on put on dumping sites. First of all, they must be treated by some method. However, the method of recycling depends on their nature and source.

Fig. 1: Plastic materials susceptible to recycling.

There are 4 main techniques of recycling and valorisation of wastes:

Thermal recycling by combustion (incineration) methods. This one is applied on mixed and unsorted wastes. The generated energy is thus in the form of calorific energy. In fact, combustion of polymers, particularly plastic materials (in which 60 % constitute carbon and hydrogene) produces a lot of heat. For example, plastic materials, representing approx. 10 % of domestic waste, deliver 50 % of heat of incineration.

Physical recycling by collection of pure thermoplastic wastes. They are reprocessed and enter again into the process of transformation of plastic materials. Certain mixtures of plastic wastes are combined with other materials to give composite materials as e.g. those which serve to be formed into public benches.

Chemical recycling consists in chemical treatment of wastes with aim of obtaining basic molecules of chemical industry. This method, analogously to pyrolysis, grows up to be developed more and more in future. It could even become an unfailing and regular supply of raw materials.

Pyrolysis (breaking of certain bonds under the effect of heat) is heating of a material in an inert atmosphere. In comparison with combustion (thermal degradation in the presence of air), lower temperatures (from 400 to 700°C) is generally used.

Generated products are: oily residue that is composed of organic products (it is also called synthetic oil); tar; combustible gases with enhanced calorific properties.

In the case of polymers, these products can be valorised in the form of reusable energy, but also in the form of recyclable products.

The figure on the next page (Fig. 2) presents the P.I.T. Pyroflam pyrolysis process unit by Serpac Environnement. It is a gasification process aimed at the valorisation and conversion to energy of various solid wastes, including municipal solid wastes, industrial wastes, sludges, animal and meat wastes. The reactor comprises two chambers that rotate around a common horizontal axis on a slight incline. The waste pyrolysis chamber is cylindrical and the char gasification reactor is in the form of a truncated cone.

Fig. 2: Industrial pyrolysing unit P.I.T. – PYROFLAM® with energy valorization.

2.2 Thermal analysis

A typical method of investigating degradation kinetics of a pyrolysed substance is to measure its mass evolution in time, and commensurate with temperature.

In the present work, the problem of the influence of heat on polymers will be treated.

The word analysis comes from the greek $\eta\ \alpha\nu\alpha\lambda\upsilon\sigma\iota\varsigma$, solution of a problem. The word thermal comes from the greek $\tau o\ \theta\varepsilon\rho\mu o\nu$, heat. Hence, the expression "thermal analysis" (TA) means literally the resolution of the heat problem.

The first documented thermogravimetric (TG) experiments were carried out in 1887 by Le Chatelier [Ozawa 2000]. The next pioneering work was done by Nernst & Riesenfeld [1903], who used a Nernst quartz torsion microbalance, equipped with an electric furnace, to study the mass-loss on heating of Iceland spar, opal, zirconia, and other minerals. The method of differential thermal analysis (DTA) was invented in 1899. The so-called "French school of thermogravimetry" began with Urbain [1912], when he modified a two-pan analytical balance into a crude thermobalance. In 1915, Japanese physicist Honda invented another thermogravimetric technique. Back then, the TA was used for materials such as minerals, metals, ceramics, inorganic compounds and refractory materials. Generally, two persons had to tend the machine and register data.

A fully automated TA apparatus was commercially available at the end of the years 50 of the previous century. The "First International Conference on Thermal Analysis" was held in 1965 in Aberdeen, Scotland.

The currently accepted definition of thermal analysis, as given by Mackenzie [1979] and the International Confederation for Thermal Analysis and Calorimetry (ICTAC) is: "A group of techniques in which a physical property of a substance and/or its reaction products is measured as a function of temperature whilst the substance is subjected to a controlled temperature program."

As the definition implies, there are three criteria to be satisfied in order that a thermal technique be regarded as thermoanalytical:

1. A physical property has to be measured;

2. This measurement has to be expressed as a function of temperature;

3. And it has to be done under a controlled temperature program.

The measured physical property and the corresponding thermal analysis technique are cited in Table 1. Note that the technique called "Emanation thermal analysis" (ETA) and "Thermoparticulate analysis" could well be inserted into the category of techniques used to measure mass. As can be seen in the table, other properties that can be determined by means of thermal analysis, in addition to direct thermal properties, are e.g.: mechanical properties (thermal expansion, softening, …), catalysis, corrosion, phase transformations and equilibriums.

As Wendlandt [1980], Liptay [1982] or Dunn [1980] observe in their surveys of the types of thermal analysis techniques used and their applications in numerous areas of research, the most widely used techniques are TG and DTA, followed by DSC and TMA. Materials that are the most frequently studied are inorganic ones, high polymers, metals and metallic alloys, and organic substances. Thermal analysis is used for supportive research relating to quality control, troubleshooting and for innovative research into processes, base materials, materials and products. According to Lombardi [1980], there were some 10,000 thermoanalytical instruments used throughout the world at the outset of 1990s.

Thermal analysis has become the most frequently used polymer characterization method.

Prior to 1969-1970, thermal analysis papers were published in a large number of international scientific journals, making a literature search very time-consuming, as notes Wendlandt [1986]. In 1969, the Journal of Thermal Analysis was founded by Buzagh and Simon in Hungary. In 1970, the Thermochimica Acta journal was founded (by Wendlandt). As an illustration of the growth of publications on the subject matter of thermal analysis, it can be mentioned that the Thermochimica Acta has increased its volume from about 400 pages in 1970 to over 3600 pages in 1983. Two useful abstracting journals are available: Thermal Analysis Abstracts (Heyden & Sons, London), and Chemical Abstracts CA Selects: Thermal Analysis (Chemical Abstracts Service, Columbus, Ohio, USA).

In the present outline, the state of the arts of thermal analysis will be briefly discussed with a focus on recent literature. For a more detailed description of the historical developments and reflections about possible future trends, the article of Mathot [2000] is recommended.

Tab. 1: Principal thermoanalytical methods (after Turi [1981], Brown [1988], Mathot [2000]).

Measured property	Name of the technique	Abbreviation
Mass	Thermogravimetry	TG
	Derivative thermogravimetry	DTG
	Evolved gas detection	EGD
	Evolved gas analysis	EGA
	Thermoparticulate analysis	
Temperature	Differential thermal analysis	DTA
	Heating-curve determination	
Enthalpy	Differential scanning calorimetry	DSC
Dimensions	Thermodilatometry	
Mechanical properties	Thermomechanical analysis	TMA
	Dynamic mechanical analysis	DMA
Optical properties	Thermoptometry	
Magnetic properties	Thermomagnetometry	TM
Electrical properties	Thermoelectrometry	
Acoustic properties	Thermosonimetry	TS
	Thermoacoustimetry	
Evolution of radioactive gas	Emanation thermal analysis	ETA
Evolution of particles	Thermoparticulate analysis	TPA

2.2.1 Thermogravimetric analysis (TGA)

The change in sample mass in the TG is determined as a function of temperature and/or time. Three modes of thermogravimetry are found to be used in literature: (a) isothermal thermogravimetry, in which the sample mass is recorded as a function of time at constant temperature, (b) quasi-isothermal thermogravimetry, in which the sample is heated to some constant temperature, (c) dynamic thermogravimetry, in which the sample is exposed to the effect of some temperature programme, usually a linear rate.

The mass-change versus temperature curve that results from such experiments has various synonyms, e.g.: thermolysis curve, pyrolysis curve, thermogram, thermogravimetric curve, thermogravigram, thermogravimetric analysis curve, and so on. It gives us information concerning the characteristic of the sample in question, as are the thermal stability and composition of the initial sample or any intermediate compounds that can be formed, and the composition of the possible residue as well.

The characteristic magnitudes of any single-stage nonisothermal reaction are two temperatures: the *initial temperature* T_i (sometimes called also the *procedural decomposition temperature*, *pdt*), defined as the temperature at which the cumulative change of mass reaches a value that the thermobalance can detect; and the *final*

temperature, T_f, which is the temperature at which the cumulative change of mass first reaches its maximum value, corresponding to complete reaction. At a linear heating rate, T_f is necessarily greater than T_i; the difference $T_f - T_i$, is called the *reaction interval*. For an endothermic decomposition reaction, T_i and T_f both increase with increasing heating rate, the effect being greater for T_f rather than for T_i.

Some factors affecting thermogravimetric experiments

There is a large number of factors, which affect the nature, precision, and accuracy of the experimental results in TG. Basically, the factors fall into the following two categories: 1. Instrumental (thermobalance) factors, 2. Sample characteristics.

Of course, many of these factors are fixed with a given thermobalance. And also because of the diversity in sample materials, it is difficult to reproduce such variable factors as the sample-particle size, the sample packing, furnace convection currents, and electrostatic effects, to mention the most significant. Unfortunately, some type of standard sample is not available to compare one given experimental apparatus with another.

Now some instrumental factors will be glanced upon. To begin with, the effect of the *rate of heating* will be considered. For a single-stage endothermic reaction, Simons and Newkirk [1964] have pointed out the following changes for T_i and T_f, as a function of fast (F), and slow (S) heating rates. For the initial procedural decomposition temperature, $(T_i)_F > (T_i)_S$. For the final procedural temperature, $(T_f)_F > (T_f)_S$, while the reaction interval is characterized by the following term: $(T_f - T_i)_F > (T_f - T_i)_S$.

For any given temperature interval, the decomposition is greater at a low rate of heating than for a similar sample heated at a faster rate [Wendlandt 1986]. If the reaction involved is exothermic, the sample temperature will rise above that of the furnace, and Coats & Redfern [1963] have shown that the difference between the furnace temperature and the sample temperature is greatest for the faster rate of heating when a reaction is occurring.

When successive reactions are involved, the rate of heating may well determine whether or not these reactions will be separated on the TG curve. The appearance of

a point of inflection at a faster heating rate may resolve itself into a horizontal plateau at a slow heating rate.

If a small sample is used, very fast heating rates may be employed and one will still be able to detect the presence of intermediate compounds formed during the decomposition reaction.

Now, the term "very fast heating rate" may correspond to various absolute values of heating rate, depending on the sample material used and other experimental conditions. However, one experiment that was taken as an instance justifying the conclusion remembered in the previous paragraph can be mentioned. In Perkin-Elmer Thermobalance brochure, a fast heating rate of 160° $C.min^{-1}$ was used for the experiment with $CuSO_4 \times 5H_2O$ (2.37 mg, in a N_2 atmosphere).

Nevertheless, as Popescu [2003] confirms, the higher the heating rate, the more the heat transmission effect through the walls of the crucible plays a role; one looses the reaction information due to this. In particular, for pyrolysis experiments of the type used in our study, he recommends, as a general rule, heating rates inferior to 20 $K.min^{-1}$. He advises to combine heating rates from 20 K.min-1 with sample weights of less than 10 mg.

Results of DeClerq & Duval [1951] indicate that when samples containing a large amount of water are studied, a slow heating rate should be employed. Otherwise, inflection points can be made undistinguishable, as mentioned earlier. However, as Lukaszewski & Redfern [1961] have observed, a sudden inflection in the mass-loss curve may be caused by a sudden variation in the rate of heating and thus be false. To detect this phenomenon, furnace temperature as a function of time should always be recorded.

As far as the effect of *furnace atmosphere* is concerned, it depends on the type of reaction, the nature of the decomposition products and the type of atmosphere employed. Different types of reactions can be met with, taking into account both the condition of original substances and products and the reversibility or irreversibility of reactions. In the field of thermogravimetric analysis, a dynamic (flowing) gas atmosphere is recommended, as the static (fixed) atmosphere implies changes of the gas concentration around sample that are virtually unquantifiable, thus making any attempts to attain reproducible results fruitless.

Moreover, the inert and oxidative types of atmosphere are being distinguished. Oxidation reactions can have effect on the mass-loss curve in both senses.

The rate of reaction is also dependent on how quickly heat is supplied to the system. Figure 3 below shows the thermal conductivity of He, N_2, and Ar as a function of temperature (according to Caldwell et al. [1977]).

Apparent mass gains are occasionally observed in the thermal decomposition of a sample under high vacuum conditions, if the sample layer is of a critical thickness and if a certain type of sample holder is employed.

Brown et al. [1971] report opposite effects to those encountered in low-pressure atmosphere when high-pressure is used.

Numerous other studies on the effect of furnace atmosphere are available by Newkirk [1960], Paulik and Paulik [1972], etc.

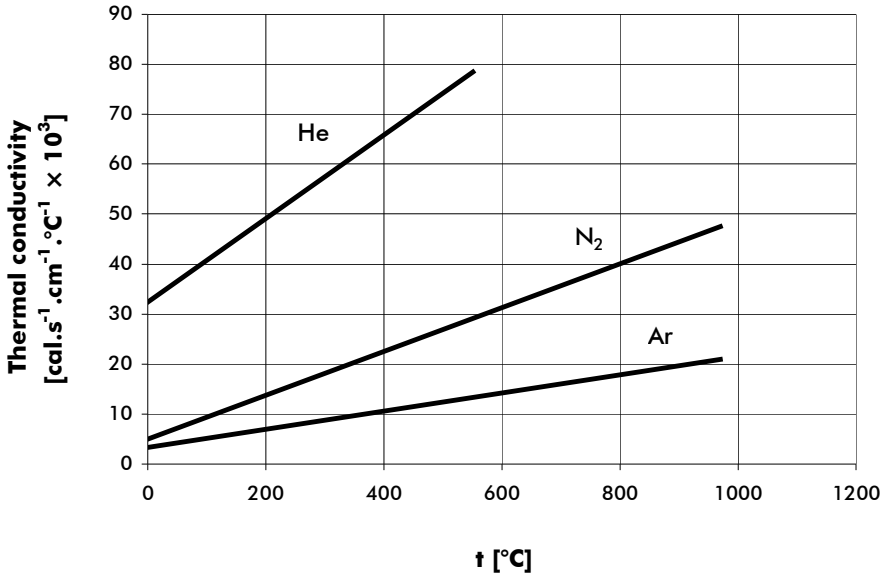

Fig. 3: Thermal conductivity of furnace atmosphere gases.

Sample holders range from flat plates to (deep) crucibles of various capacities. Materials used in their construction vary from glass, alumina, and ceramic compositions to various metals and metallic alloys. Newkirk & Aliferis [1958] have shown that sodium carbonate

can react with porcelain or alumina crucibles at high-temperatures, thus producing a mass loss. The catalytic properties of platinum were reported by Ramakrishna et al. [1970] to affect TG curves of certain metal sulfides.

Regarding the sample characteristics, the most important property is the amount of sample.

The *sample masses* can affect thermogravimetric experiments mainly in three ways, as Coats and Redfern [1963] report it:

a) the *endothermicity* or *exothermicity of reactions* will cause the sample temperature to deviate from the temperature programme of TGA apparatus; this effect aggravates with increasing sample masses;

b) the *diffusion conditions* of the product gas around the solid sample particles; a convenient gas flow, rather than static conditions, does not allow the atmosphere immediately surrounding the reacting particles to be governed by the bulk of the sample;

c) the *thermal gradients* in the sample, increasing with its low thermal conductivity.

Another aspect that could be taken into consideration is the *size of sample particles*. Generally, a decrease in particle size of the sample lowers the temperature at which thermal decomposition begins, and also the one at which it is completed. A sample consisting of large crystals or particles will often decompose more slowly than a sample of equal mass but consisting of very small particles; undoubtedly, the ratio of surface areas/mass is playing its role in this phenomenon.

Other properties are the nature of sample, heat of reaction, thermal conductivity, solubility of evolved gases in sample, etc.

Discussion on the above mentioned factors would not be more expanded. In the next chapter, the main subject matter will be presented.

2.3 Kinetics

The term kinetics derives from the ancient greek ($\eta\ \kappa\iota\nu\eta\sigma\iota\varsigma$, action of moving or moving oneself, movement, change). Used in the modern chemistry language, it designates the study of the reaction rate of chemical or enzymatic reactions.

Chemistry and kinetics of the thermal degradation of hydrocarbons is important in several different domains of process and environmental engineering. These are e.g. geochemistry, conversion of petroleum, coal, and biomass to liquid fuels, cracking processes, and recycling of polymers.

The kinetics of polymer decomposition can be studied in order to determine the appropriate conditions for hindering or limiting the evolution of toxic compounds and recuperation of raw materials from the thermal treatment of plastic wastes.

The principal objectives common to the majority of kinetic studies are the determination of the rate equation, i.e. the description of the extent of conversion of reactant(s) or formation of product(s) with time, and the assessment of the influence of temperature on the rate of reaction.

The rate of conversion, $d\alpha/d\tau$, is usually assumed to be a linear function of a single temperature-dependent rate constant, k, and a temperature-independent function of the conversion, α, i.e., $d\alpha/d\tau = k.f(\alpha)$.

The quantitative representation of the rate-temperature dependence of k has been almost universally expressed by the Arrhenius equation, $k = A.\exp(-E_a/RT)$, where A is the "frequency factor" (usually assumed to be independent of temperature), E_a is the activation energy, and R is the ideal gas constant.

Values of the Arrhenius equation, or else the Arrhenius parameters E_a, the activation energy, and A (called also the "pre-exponential factor") describe quantitatively the energy barrier to reaction and the frequency of occurrence of the situation that may lead to product formation, respectively. As such, these parameters facilitate the concise reporting of kinetic data, and the comparison of different systems from the point of view of their chemical reactivities. Moreover, they can be used to forecast behaviour at temperatures outside the intervals of different conditions of the experimental measurements.

The use of Arrhenius equation which has been applied to the study of the kinetics of homogenous reactions for some hundred years, was also extended to the thermal analysis of polymers.

The reactions that take place during the thermal decomposition of polymers are classified as heterogeneous. The question arises whether or not the validity of the Arrhenius equation may cope with such an extension, as the kinetics of homogenous and heterogeneous reactions are fundamentally different. In homogenous reactions, the reaction takes place at a uniform rate in every space unit of the single phase, while in heterogeneous reactions, the reactions takes place only on the phase boundaries of the contacting phases and at a rate permitted by the predominant mass and heat transport processes. The elementary chemical reaction taking place on the surface of the phase boundary is generally faster than the other elementary processes, and the course of transformations is usually defined by slow heat- and gas-transport processes, which are greatly influenced by experimental conditions.

Arnold et al. [1981] noticed that the course of conventional thermoanalytical curves is more characteristic of the experimental conditions (the above-mentioned transport processes) than of the reaction itself. They conclude that the correctness of reaction kinetic calculations on the basis of curves obtained by dynamic thermoanalytical methods is rather questionable. However, if the experimental conditions are taken into account in appropriate way as to their further exploitation in kinetic analysis, this limitation can be overcome.

As Arnold et al. [1981] noticed, the estimated parameter values are dependent on the mathematical methods used rather than on the thermoanalytical curve itself. But their affirmation that "It is shown experimentally that dynamic thermoanalytical curves provide insufficient information for the purpose of reaction kinetic calculations" seems to be rather exaggerative, as they estimate parameter triplets (A, E, n) from a ***single*** measured curve. No doubt that such calculations can lead to many deviating results while using different kinetic calculation methods. The standard practice that will be applied in this thesis is that the kinetic parameters estimation must be backed up not only by different kinetic calculation methods that complement themselves, but also by a set of curves measured in different experimental conditions, i.e. in the case of non-isothermal techniques, at various heating rates.

The methods of kinetic analysis of thermogravimetric data are divided into five categories (Flynn and Wall [1966]): 1) "Integral" methods utilizing weight loss versus temperature data directly, 2) "Differential" methods utilizing the rate of weight loss, 3) "Difference-differential" methods involving differences in rate, 4) methods specially applicable to initial rates, and 5) nonlinear or cyclic heating rate methods.

In the next few paragraphs, the advantages and disadvantages of the first three methods will be briefly mentioned, as these groups are used most. A detailed description of the integral method applied in the thesis will be presented in the experimental protocol section dealing with the TGA data treatment methods.

In integral methods, results are less affected by experimental errors, as these methods evaluate the whole experimental data set and are based on the primary experimentally acquired data, α and t.

Differential methods based on rate of mass loss versus temperature data are much simpler in application and some of them are able to circumvent difficulties of many integral methods. However, they have a strong weakness: experimental noise is magnified, which renders the whole task of evaluating kinetic parameters very difficult, sometimes even impossible.

The difference-differential method of Freeman and Carrol and its modifications are the most widely used methods for the kinetic analysis of thermogravimetric data. It was used for the investigation of both inorganic materials and polymers. In general, one may obtain the initial parameters only if high accuracy data can be obtained at low conversions. The experimental noise, being magnified by interpreting the difference of a derivative, will not – in many cases – allow the determination of order at low conversion. As Flynn and Wall [1966] have noted, these methods seem to be of limited applicability to polymeric systems with complex kinetics.

On the top of that, Ozawa [1975] have found that the Freemann and Carroll, Coats and Redfern, and Sharp and Wentworth methods cannot be applied to a second-order reaction, random scission in main chains of polymers, and a system of two parallel competitive first-order reactions. As he pointed out: "… when one does apply them [i.e. the methods mentioned above] to these cases [the above-mentioned reactions], nearly straight relations are observed and false unreal kinetic parameters are obtained". In other words, the methods yield data that fit the thermogravimetric experimental data, but

their kinetic parameters are false. Ozawa's method, however, gives correct kinetic parameters. As Wendlandt [1986] notes, one of the methods of avoiding false parameters is to observe a process at different heating rates. If the kinetic parameters estimated by analyzing the curves at different heating rates coincide with each other, the kinetic parameters are not false. He recommends also application of two or more methods to corroborate the resulting kinetic parameters. And as a most desirable way, he considers the use of a method based on a more fundamental kinetic equation, such as that of Ozawa [1965].

Before entering the chapter on the subject matter of the theoretical study of individual polymers, the procedure employed in the experimental study will be presented. It consisted of:

1) choosing the conditions of pyrolysis convenient to a particular polymer,

2) conducting a set of experiments at chosen heating rates, usually repeating the same experiment three times,

3) simultaneously registering FTIR data during the whole experiment, with one scan about each 30 seconds,

4) evaluating infra-red spectra, correlating them with the assumed reaction history,

5) eventually carrying out the FTIR analysis of residues (systematically done only in the case of lignin, as there were no reference data found on other polymers or the specific study was not considered as a contribution from the point of view of theoretical and/or practical meaning),

6) calculating of kinetic parameters, according to the integral method presented in the sub-chapter entitled TGA data treatment (p. 62),

7) eventually evaluating of kinetic parameters by means of a MatLab program, making use of the differential method presented in the chapter mentioned above (point 6).

Below see a special chapter giving more details on issues concerning especially the so-called isothermal and non-isothermal kinetics. For a more exhaustive review of the problem, we invite the reader to kindly refer to the special section with selected references dealing with kinetics (section 6).

2.3.1 Isothermal vs. non-isothermal kinetics and other issues

As Vyazovkin [2000] explains, for both isothermal and nonisothermal kinetics, the currently dominating approach appears to be force-fitting of experimental data to different reaction models. Following these indiscriminate model fitting methods, Arrhenius parameters are determined by the form of f(α) chosen. Such methods tend to fail to meet even the justifiable expectations. The application of these methods to isothermal data gives rise to believable values of Arrhenius parameters that, however, are likely to conceal the kinetic complexity. In a nonisothermal experiment both T and α vary simultaneously. The application of the model-fitting approach to single heating-rate data generally fails to achieve a clean separation between the temperature dependence, k(T), and the reaction model, f(α). As a result, almost any f(α) can satisfactorily fit the data at the cost of drastic variations in the Arrhenius parameters, which compensate for the difference between the assumed form of f(α) and the true but unknown reaction model. For this reason, the application of the model-fitting methods to single heating-rate data produces Arrhenius parameters that are highly uncertain and, therefore, cannot be meaningfully compared with the isothermal values. Unfortunately, for years, the model-fitting analysis of single heating rate data has been the most prevalent computational technique in nonisothermal kinetics. That is why the failures of this technique have been mistaken for the failures of nonisothermal kinetics as a whole. Vyazovkin [2000] points out that an alternative approach to kinetic analysis is to use model-free methods that allow for evaluating Arrhenius parameters without choosing the reaction model. The best known representatives of the model-free approach are the isoconversional methods. These methods yield the effective activation energy as a function of the extent of conversion. Knowledge of the dependence E_a on α assists in both detecting multi-step processes and drawing certain mechanistic conclusions. Secondly, it is sufficient to predict the reaction kinetics over a wide temperature region. Thirdly, the isoconversional methods yield similar (but not identical!) dependences of the activation energy on the extent of conversion for isothermal and nonisothermal experiments.

He stipulates that fitting data to reaction models cannot be used as the sole means of identifying the reaction mechanisms. Note that this is equally true in the case when

statistical analysis allows one to unequivocally choose a single reaction model – statistical analysis evaluates the reaction models by the goodness of fit of the data, but not by the physical sense of applying these models to the experimental data. Even if a reaction model does not have any physical meaning at all, it may well be the best fit to the experimental data.

According to Vyazovkin, the most important feature of a reliable method of kinetic analysis is its ability to handle multi-step processes that are rather typical for reactions of solids. He founds the model-free and model-fitting methods that use sets of isothermal or/and nonisothermal data obtained at different temperatures or/and at different heating rates to be very effective in detecting this feature in the data provided. The model-free methods reveal the kinetic complexity in the form of a dependence of the activation energy on the extent of conversion (isoconversional methods) or in the form of a temperature dependence (the NPK method) – the 'non-parametric kinetics' method of Nomen and Sempere [Serra, 1998]. While too young to reveal all the ups and downs, the NPK method makes a promising debut. It is easy to appreciate the value of the isoconversional method, which is a seasoned veteran of kinetic battles. As seen from the results of the project, various isoconversional methods applied by different workers to the same set of nonisothermal data have produced consistent dependences of the activation energy on the extent of conversion. This fact bears a great meaning for nonisothermal kinetics that for years has been a subject of acidulous criticisms and humiliating mockery for its alleged inability to produce sensible kinetic data. The isoconversional methods may also be helpful in providing some mechanistic clues. … the mechanistic clues are not yet the reaction mechanism, but rather a path to it that can further be followed only by using species-specific experimental techniques.

According to Vyazovkin [2000], the isoconversional method of Friedman presents the most straightforward way to evaluate the effective activation energy, E_a, as a function of the extent of reaction. This is a differential method, which can be applied to integral data (e.g. TG data) only after their numerical differentiation. As we have indicated before (in the paragraph about differential methods), because this procedure may lead to erroneous estimates of the activation energy, the use of the integral isoconversional methods appears to be a safer alternative.

The consistency of the kinetic parameters derived from isothermal and nonisothermal data should not be used, as it follows from Vyazovkin's analysis, as a decisive criterion to determine if the values are trustworthy. It is not a sufficient condition. He exemplifies this on the fact that although fitting isothermal and nonisothermal data to single-step models resulted in incorrect values of the kinetic triplets, the latter are also in perfect agreement.

Vyazovkin [2000] further shows that there are some rather insignificant differences between the E_a-dependences obtained by using integral and differential methods. These differences arise partially from the fact that the equations of the integral methods are usually derived under the assumption of the constancy of the activation energy. On the other hand, the differential methods may suffer from imprecise numerical differentiation, even in the case of artificial data that are free of 'experimental noise'.

In conclusion, he declares that model-free techniques have been very successful in detecting multi-step kinetics in the data provided. Fitting data to multi-step kinetic models has allowed the 'true mechanism' to be guessed for the simulated data. For the real data, the mechanistic guesses happened to be uncertain. The fact that the obtained E_a-dependences allow one to unmistakably recognize a multi-step process taken alone is, according to him, already a very important piece of mechanistic information.

Brown et al. [2000] say that use of small samples has decreased the problems of heat transfer at the expense of a possible decrease in the homogeneity of the sample.

On the assumption that the data obtained are reliable and that random noise in the data is negligible, one can proceed in the search for a mathematical description of the data.

A mathematical description of the data is usually sought in terms of a 'kinetic triplet' (i.e. Arrhenius parameters A and E_a, and the reaction model, f(α), also called the conversion function).

Attempts have to be made to relate the computational results to the actual sequence of physico-chemical processes occurring, i.e. the reaction mechanism. Formulation of such a relationship is generally only possible with the aid of complementary information from microscopic, spectroscopic and structural studies.

The ability to handle multi-step reaction mechanisms is a desirable feature of a computational method. Multi-heating rate and isoconversional methods have proven to be particularly effective and most of the recent interest in the field of kinetic computations has been concerned with these methods.

The goodness of fit is only the necessary, but not the sufficient condition for the identified reaction model to be physically sound.

Maciejewski [2000] demonstrates by experimental data that the kinetic description of the process depends strongly on the experimental conditions. The very limited applicability of the kinetic methods that use single-heating rate data is emphasized.

Direct comparison of the kinetic parameters obtained by different computational methods is very problematic because it is unclear whether the observed differences in the values originate from differences in the experimental conditions of from the differences in the computational methods.

(Project provides a unique opportunity to compare computational methods, because different methods are applied to the same sets of experimental and simulated data.)

The kinetic description of the solid state reactions is influenced not only by the complicated nature of the process but also by the method of calculation.

Besides, we cannot choose 'the best' method, because we do not know the correct mechanism and kinetic parameters. This is possible only for simulated data for which the kinetics triplets are known exactly.

Only computational methods, which use multi-heating rate data, can produce a reliable mathematical description of the reaction kinetics. The methods that use single heating rate data should simply be avoided in serious kinetic analyses.

He further notes that the dependence of E_a on α is observed when a process involves several steps that have different activation energies. There is, however, a danger of missing the multi-step character of a process in the case when different steps have practically equal activation energies, but have different pre-exponential factors and/or obey different kinetic models.

In real experiments, there are two reasons that can prevent consistent kinetic triplets from isothermal and non-isothermal data being obtained: (i) the temperature ranges of isothermal and non-isothermal experiments are not the same; (ii) truly isothermal

conditions cannot be accomplished for the very low and very high ranges of the reaction extent α.

Isothermal experiments cannot be carried out at temperatures when the reaction rate is too fast and significant decomposition may occur during settling of the experimental temperature at the beginning of the experiment. This undefined period depends upon the experimental conditions (applied temperature ramp, sample mass, the kind of carrier gas) and reactant properties (c_p, thermal conductivity, the mechanism of the decomposition) and makes it experimentally impossible to achieve strictly isothermal conditions over the full range of conversion. For many kinetic models the maximum rate of decomposition, under isothermal conditions occurs at the beginning of the reaction.

As far as non-isothermal experiments, he noticed difficulties of the determination of the α-T dependence at the beginning of the decomposition. Due to the specific shape of this dependence for some functions, especially for the contracting geometry and diffusion models, the change of the reaction progress from 0.001 to 0.02 required, at a heating rate of 5 $K.min^{-1}$, the temperature change of 63 K (R2) or 109 K (D3), respectively. Due to buoyancy effects, the determination of such small mass changes over a relatively long period of time is uncertain.

Another important factor that affects the reliability of kinetic data obtained for very low and very high a values is self-heating/cooling. The distortion of the preset temperature program is especially high at the beginning of isothermal and at the end of non-isothermal experiments due to the occurrence of the greatest thermal effects at these stages of the process. The effect of self-heating/cooling increases with increasing sample mass. The deviation of the actual T from the preset temperature may invalidate any evaluation of the kinetics triplets.

Comparison of the kinetic parameters obtained under isothermal and non-isothermal conditions is aggravated by unavoidable experimental phenomena that affect the kinetic data. In the case of a relatively simple process, whose kinetics can be described by a single kinetic triplet, the difference is primarily determined by these experimental phenomena, but not by computational methods (provided they are valid).

In the narrower ranges used under iso-thermal conditions, the difference between different models are much less visible.

The solution for avoiding these problems would seem to be the opposite procedure: determination of kinetic parameters should be done from non-isothermal experiments carried out over a wide temperature range.

The results of experiments carried out indicate that the same process cannot be characterized by the same kinetic triplet under different experimental conditions.

As a first test for reaction complexity, one should use isoconversional methods. The complexity is easily detectable as a variation of the activation energy with α.

In a real system, the influence of the experimental conditions disturbs, in a different way, the course of the isothermal and non-isothermal dependencies, …, making the comparison of isothermal and non-isothermal kinetic parameters more difficult. Due to the fact that non-isothermal parameters are calculated from the data obtained in a much wider temperature range, it is logical to use them for the prediction of isothermal runs. The opposite procedure, i.e. the prediction of non-isothermal relationships based on the isothermal parameters may be erroneous.

He thinks it proven that the original isoconversional methods (Ozawa, Friedmann) are very sensitive to experimental noise which leads, despite their mathematical simplicity, to a great scatter of the results, etc.

In Burnham's [2000] opinion, isoconversional methods give kinetic parameters that agree qualitatively with those from subsequent nonlinear regression to appropriate models. Single-heating-rate methods work poorly and should not be used or published. He summarizes his contribution to the ICTAC kinetics projects in these words: the isoconversional analyses of various workers tend to agree fairly well and give qualitatively good predictions of the activation energies ultimately obtained from non-linear regression to appropriate models.

He found that the isoconversional methods give a narrower set of results and uniformly agree that the activation energy decreases during conversion.

According to him, the isoconversional analyses of various workers tend to agree fairly well and give qualitatively good predictions of the activation energies ultimately obtained from non-linear regression to appropriate models.

As is also recommended in a recent material by the ICTAC [Roduit 2000], the computations should be carried out with experimental data obtained from at least two or three different heating rates (non-isothermal) or temperatures (isothermal). Moreover, the data should be collected under similar experimental conditions because the kinetic parameters of solid-state reactions are not intrinsic properties of an investigated compound, but can change depending on the experimental conditions applied. This is known as PSTA-principle or parametric sensitivity of thermal analysis [Roduit et al. 1996].

Isoconversional methods are known to allow the calculation of model-independent estimates of the activation energy, E(α), related to different extents of conversion, α [Roduit 2000].

In 2000, a series of 5 papers was published containing the results of an ICTAC kinetics project. Besides the model-fitting analysis, most of the participants have tried to recover the hidden activation energies by applying isoconversional methods (Friedman, Ozawa-Flynn-Wall). The kinetics results computed for a hypothetical simulated process and experimental data for the thermal decompositions of calcium carbonate and ammonium perchlorate were presented. The comparison of the kinetic parameters obtained from isothermal and non-isothermal (a.k.a. „dynamic“) experiments was presented and discussed. Experiments were carried under vacuum and nitrogen. In Part E, dealing with numerical techniques and kinetics of solid state processes, Roduit [2000] commented that measurements of experimental data carried out under isothermal conditions are usually investigated in a narrow temperature range due to technical problems. Therefore, they may not contain the information necessary for determining the complexity of a process. He stated also that the use of heating rates which are higher than 2-3 $K.min^{-1}$ helps to discern between the different reactions involved in the kinetic scheme. In his experiments, he found that if heating rates are too similar, they narrow the temperature region of non-isothermal experiments, and model-fitting analysis becomes comparable to that using single heating-rate methods and may fail to determine the best kinetic models, just as for isothermal experiments carried over a narrow range of temperatures. He argued that consideration of the wide range of temperatures achieved with non-isothermal experiments provides very important insights in interpreting and

quantifying the experimental results and non-isothermal experiments appear to be more advantageous than isothermal conditions.

Bockhorn et al. [1996] worked on the decomposition kinetics of PVC. It is assumed that the dehydrochlorination mechanism at moderate temperature can be distinguished in an endothermal and exothermal part. The benzene formation is identified as a second order reaction. A great advantage of the isothermal method is, that changes in the mechanisms are detectable, i.e. changes in the apparent order of the reaction and the apparent activation energy. From that, new mechanistic aspects of the decomposition kinetics of polyethylene were obtained.

A disadvantage of isothermal measurements is that various measurements at different temperatures are necessary entailing a higher amount of sample and, therefore, perhaps varying sample properties. Another problem is the period of time in which the sample is instationarily heated up to the isothermal temperature. To overcome this drawback the reactor design has to be optimized for this purpose. However, isothermal measurements also have numerous advantages. The main advantage is that changes in the mechanism are detectable because decomposition rates are obtained for single temperatures. Thereby, for instance changing orders of reaction can be determined. In contrast to dynamic measurements the rate equation can be solved analytically enabling easy parameter evaluation. Another great advantage is the homogeneous sample temperature after attaining the isothermal reaction temperature, whereas in dynamic measurements a temperature gradient in the sample occurs due to the non stationary heat conduction.

It is possible to compensate this effect by low heating rates and, if necessary, by isothermal measurements. Additionally, the sample temperature is dependent on the occurring chemical reactions and its reaction enthalpies as well as the changing heat capacities.

The method of deriving kinetic data in the work is based on the assumption that the sample temperature is very close to the measurable temperature of the surrounding gasphase. In practice, the heat capacity of the sample and the reaction enthalpy cause a difference between the sample and the surrounding temperature. Furthermore, due to non stationary heat conduction a temperature gradient may occur in the sample. This temperature gradient depends on the Biot number, which is a measure of the ratio of the

resistance of heat conduction (X/λ) in the sample and the resistance of outer heat transfer ($1/\alpha_o$), $Bi = \alpha_o X/\lambda_{,,}$ with X being a characteristic length, for example half the thickness of a layer.

For the used thermobalance, the main contribution to heat transfer is from heat radiation.

2.4 Polymers

The word polymer has its origins in the ancient Greek. The first of its two components, *πολυ*, means *a lot of*, *many*, the second, *η μερη*, means *a part*. The meaning of the word is that the polymer is composed of a lot of units with the same nature.

History of polymers begins around 1830. In 1833, vinyl chloride (CAS No. 75-01-4) was synthesized by Binn [Salamone & Westlake 1998]. In 1839, Goodyear discovered the process of vulcanization. In 1860, Greville Williams obtained a liquid with the formula C_5H_8 by distilling rubber; he called it "isoprene". Synthetic rubber technology started in 1879, when Gustave Bouchardat found that heating isoprene with hydrochloric acid produced a rubberlike polymer (however, Bouchardat had obtained isoprene from natural rubber; the first truly synthetic rubber was made by William Tilden three years later, by cracking turpentine) [ACS]. Other polymers followed gradually. In 1880, methylmethacrylate was prepared. The treatment of cellulose by means of acetic anhydride (1865) allowed Chardonnet to spin the first artificial silk. During World War II, the economical and political situation foster the development of classical plastic materials: PVC, PS, vinyl polyacetate, PMME, and of important synthetic elastomers – Buna in Germany, BRS in the United States – that use butadiene, styrene, and acrylonitril. Polychloroprene was invented in the same period, as well as polyamides 6 and 66, and polytetrafluorethylene (Teflon®). The direct synthesis of silicium chloride opens the door to industrial silicones. Since the beginning of the war, low-density polyethylene (high-pressure ICI process) plays a determining role in the manufacturing of radars. In the 50s, the petrochemical industry and the industry of classical plastics (PVC, LDPE, HDPE, PP, PET, PBT, ABS, PA, PC, PPO, etc.) were widely developed. In the 60s, the period of the race to the space, high-performance polymers were developed. These are, e.g.: polysulfones, polyetherketones, liquid crystal polymers (both thermotropic and lyotropic; Kevlar®), and a huge number of polymers at the boundary of thermoplastics and thermosets, as e.g. polyimides (Kapton®). The oil crisis in 1973 awoke the idea of economy of oil derivatives, of re-utilization of plastics[1] and search of natural raw materials that would be easy to recycle. Thus, the automobile industry

[1] The word "plastic(s)" comes from the Greek word *πλαστικος* (adj.), which designates the ability to be molded.

organizes itself to recycle its own parts. Some inventions in the domain of catalysis allow the diversification of molecular structures, particularly of polyethylenes. The consequences of this are the possibility of fine adjustment of products regarding end-use, price reductions, and recycling ability. The 90s' globalization brings a high concentration of production and an increased standardization of qualities. The hasty evolution of the polymer industry raises a question: is it still possible to make new discoveries in this field, to develop new types of polymers with new properties? In short, have polymers still a future? Human biology polymers are just on their beginning. Electronics and optoelectronics are also sectors that demand new materials. New markets are developed. Even though the tonnage of such polymers is not so important and classical models of industrial companies is less and less implicated in new developments, the level of scientific research remains virtually the same.

Classification

Polymers can be classified according to their configuration, thermophysical properties, and polymerization reactions.

Polymer Configurations

A polymer can have any of three basic molecular shapes. The shape is determined by the functionality of the monomers, which make up the polymer. The three configurations are (see Fig. 4):

linear – long, linear polymer chains;

branched – long chains with arms coming from branch points;

network – long chains linked together by crosslinking arms; a crosslinked network of chains.

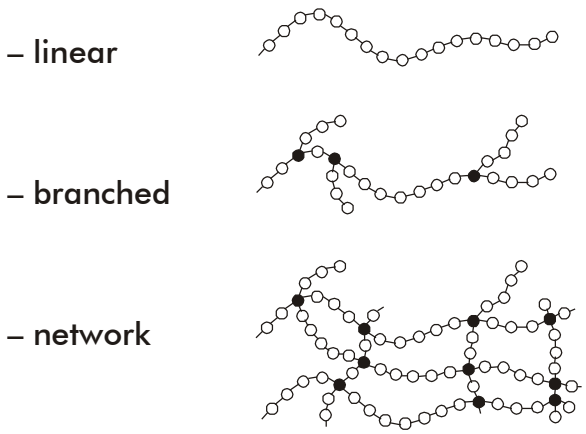

Fig. 4: Linear, branched, and network polymer configurations.

Linear polymers

Some polymer molecules are linear, similar to a normal alkane such as *n*-decane. An example is high-density polyethylene (HDPE), which can contain more than 1,000 CH_2 groups (HDPE has a high density because the linear molecules can pack closely).

Nonlinear (branched) polymers

Some polymers, such as low-density polyethylene (LDPE), have branches of different sizes irregularly spaced along the main chain. Such polymers are said to be nonlinear. However, polymers with pendant groups[2], such as the methyl group in polypropylene, are considered to be linear.

The branches prevent the nonlinear molecules from packing as closely as the linear, reducing their density.

Network polymers

Some polymers have cross-links between polymer chains creating three-dimensional networks. A high density of cross-linking restricts the motion of the chains and leads to a rigid material.

[2] A group attached to the polymer backbone and present in the repeating unit is called a pendant group.

Classification based on Thermophysical Properties

According to their behaviour, polymers that soften and flow upon heating are termed thermoplastic; those, which do not, are called thermoset polymers.

Molecules in *a thermoplastic* are held together by relatively weak intermolecular forces so that the material softens when exposed to heat and then returns to its original condition when cooled [PR.COM]. Thermoplastic polymers can be repeatedly softened by heating and then solidified by cooling, which is a process similar to the repeated melting and cooling of metals. Most linear and slightly branched polymers are thermoplastic. All the major thermoplastics are produced by chain polymerization [Seymour 1988].

Thermoplastics have a wide range of applications because they can be formed and reformed in so many shapes. Some examples are food packaging, insulation, automobile bumpers, and credit cards.

A *thermosetting plastic*, or thermoset, solidifies or "sets" irreversibly when heated. Thermosets cannot be reshaped by heating. Thermosets usually are three-dimensional networked polymers in which there is a high degree of cross-linking between polymer chains. The cross-linking restricts the motion of the chains and leads to a rigid material. Thermosets are strong and durable. They are primarily used in automobiles and construction. They also are used to make toys, varnishes, boat hulls, and glues [PR.COM].

<u>Characteristics of thermoplastic polymers</u>

- Linear or branched structure
- Polymer melts and flows upon heating
- Easy to process with application of heat
- Heat sensitive properties
- Individual polymer molecules are held together by weak secondary forces:

  * Dispersion forces (these are due to instantaneous dipoles that form as the charge clouds in the molecules fluctuate),

* Hydrogen bonds (hydrogen bonding can take place when the polymer molecule contains -OH or -NH groups),

* Dipole-dipole interactions (resulting from the attraction between polar groups, such as those in polyesters and vinyl polymers with chlorine pendant groups).

– Examples: polyethylene, polypropylene, nylon, polymethyl methacrylate, polystyrene.

Notes on intermolecular forces

1. Dispersion forces, the weakest of the intermolecular forces, are present in all polymers; they are the only forces possible for nonpolar polymers such as polyethylene. Dispersion forces depend on the polarizability of a molecule. Larger molecules generally are more polarizable, so large polymers with high molecular weights can have significant dispersion forces. Ultra high molecular weight polyethylene (UHMWPE), which has a molecular weight in excess of 3,000,000 $g.mol^{-1}$, is used to make bulletproof vests [PCOL].

2. Hydrogen bonding is the strongest of the intermolecular forces; polymers such as poly(vinyl alcohol) and polyamides are hydrogen bonded.

3. Examples of pendant groups are the methyl group in polypropylene and the benzene ring in polystyrene. The presence of pendant groups modifies the properties of a polymer.

4. All intermolecular attractions are known collectively as van der Waals forces. The various different types were first explained by different people at different times. Dispersion forces, for example, were described by London in 1930; dipole-dipole interactions by Keesom in 1912 [Clark].

Advantages and disadvantages of thermoplastics

Advantages of thermoplastics

• Unlimited shelf life – won't undergo polymerization during storage or in processing unit

• Easy to handle (no tackiness)

• Recyclable – they undergo melt and solidify cycles
• Easy to repair by welding, solvent bonding, etc.
• Postformable

Disadvantages of thermoplastics

• Thermoplastics are prone to creep
• They have poor melt flow characteristics

Characteristics of thermoset polymers

• Upon application of heat, liquid resin becomes rigid via vitrification process
• End polymer is less temperature sensitive than thermoplastics
• Crosslinked network structure (formed from chemical bonds) exists throughout part
• Crosslinking provides thermal stability such that polymer will not melt or flow upon heating

– Examples: epoxy, unsaturated polyesters, vinyl esters, phenol formaldehyde, bismaleimide, urethane.

Advantages and disadvantages of thermosets

Advantages of thermosets
• Low resin viscosity
• Good fiber wet-out
• Excellent thermal stability once polymerized
• Chemically resistant
• Creep resistant

Disadvantages of thermosets
• Brittle

• Non-recyclable via standard techniques
• Must mold polymer in shape of final part – not postformable

Classification Based on Polymerization Reactions

There are two fundamental polymerization reactions: chain polymerization and step polymerization (Fig. 5). This classification is of particular importance to thermosetting systems that polymerize in situ when used in processes.

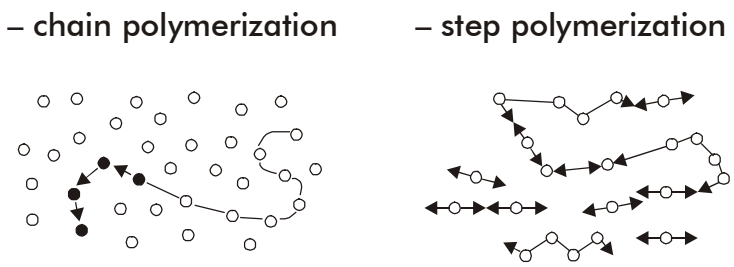

Fig. 5: Chain polymerization and step polymerization.

Chain (or Addition) Polymerization

Chain polymerization is characterized by the presence of a few active sites, which react and propagate through a sea of monomers. Sometimes called also chain-reaction polymerization, it requires an initiator to start the growth of the reaction. The largest family of polymers [PSRC], vinyl polymers, are produced by chain polymerization reactions from vinyl monomers. A good example is the free-radical polymerization of styrene, which is initiated by a free radical (R) that reacts with styrene. The compound that is formed still is a free radical, which can react again (see Fig. 6).

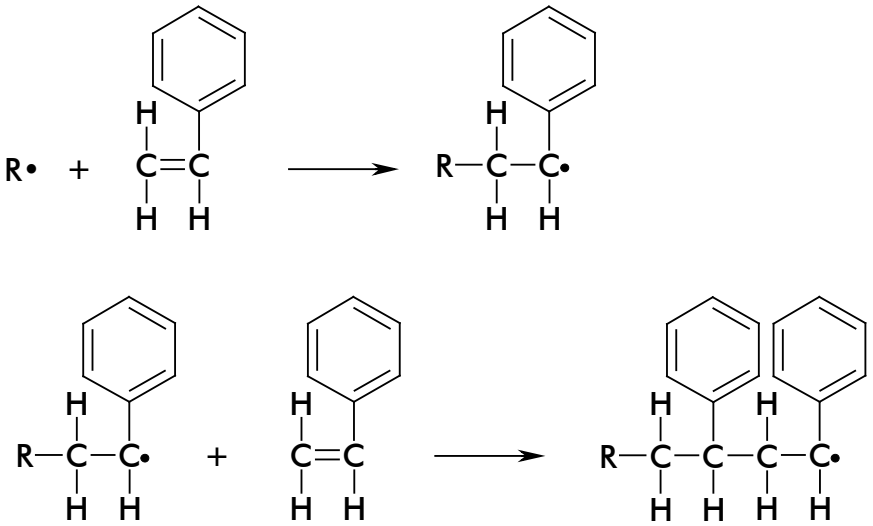

Fig. 6: Free-radical polymerization: example of styrene.

This reaction eventually leads to the formation of polystyrene, a portion of which is shown below. Polystyrene prepared by free-radical polymerization is shown on Fig. 7 (see below).

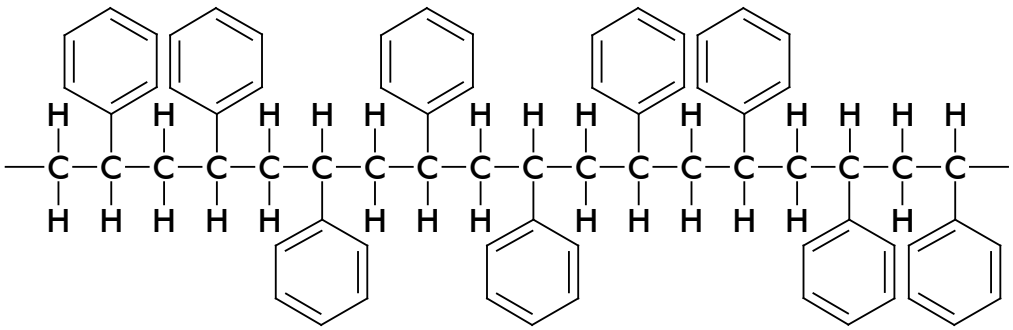

Fig. 7: Polystyrene prepared by free-radical polymerization.

Polymerization may occur by any of three mechanisms:

free radical,

cationic,

anionic.

Polymers formed via this process include: polyethylene, polystyrene, polypropylene, polyvinyl chloride, polyvinylidene chloride, polymethylmethacrylate.

Step Polymerization

In a step reaction mechanism, sometimes called condensation polymerization (because water is often liberated when the polymer bonds form), monomers react with any nearby monomer. In contrast to chain polymerization, no special activation is needed to allow a monomer to react. Frequently, these reactions are copolymerizations, where two types of monomer are present and each reacts only with the other (and not with monomers like itself).

Example reactions include:

polyester formation, where the monomers are diols and diacids; the acid groups react with the alcohol groups to form ester linkages,

polyamide formation; amine groups react with carboxylic acids.

The sample reactions shown both yield linear polymers.

An example of polyester formation is the polymerization reaction involving terephthalic acid and ethylene glycol, both of which are bifunctional (Fig. 8):

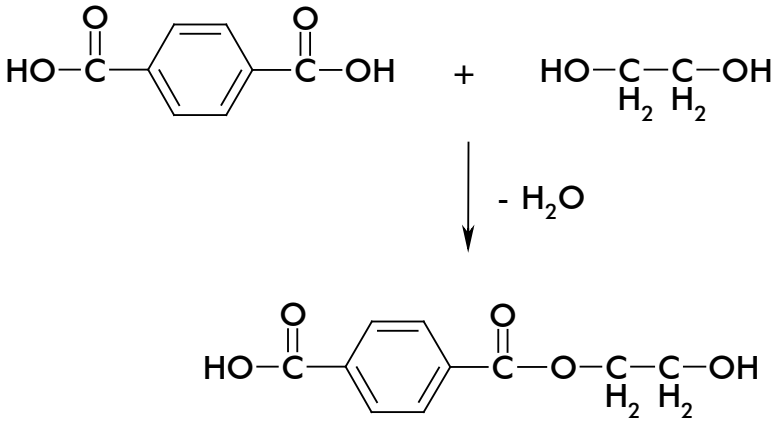

Fig. 8: Polymerization of terephthalic acid and ethylene glycol.

Polymer formation begins with one diacid molecule reacting with one dialcohol molecule to eliminate a water molecule and form an ester. The ester unit has an alcohol on one end and acid on the other, which are available for further reactions.

The eventual result is a polyester called polyethylene terephthalate or more commonly, PET (Fig. 9).

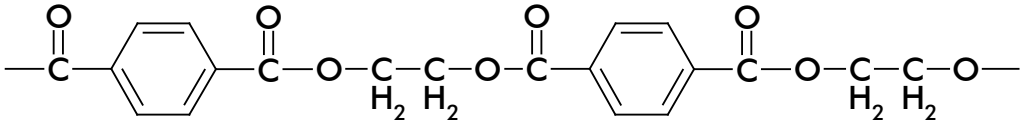

Fig. 9: Polyethylene Terephthalate.

Thus, polyesters and polyamides are condensation polymers, which contain fewer atoms within the polymer repeat unit than the reactants because of the formation of by-products, such as H_2O or NH_3, during the polymerization reaction. Most synthetic fibres are condensation polymers.

Typically, polyester, polyamide, polyurethane, and polycarbonate polymers are made by step polymerization.

The table below compares the two types of polymerization reactions and summarizes their characteristics:

Tab. 2: Types of polymerization reactions [TRP Project].

Step Polymerization	**Chain Polymerization**
Any two molecular species present can react.	Reaction occurs only at active centres by adding repeating units one at a time to the chain.
Monomer disappears early in the reaction.	Monomer concentration decreases steadily throughout the reaction.
Polymer molecular weight rises steadily throughout the reaction.	High polymer is formed at once, polymer molecular weight changes little throughout the reaction.
Long reaction times are essential to obtain high molecular weights.	Long reaction times give high yields but have little effect on molecular weight.
At any stage all molecular species are present in a calculable distribution.	Reaction mixture contains only monomer, high polymer, and a minuscule number of growing chains.

There is yet another classification of polymers that should not be overlooked: natural polymers vs. artificial polymers. Natural polymers are categorized in three major groups

[Mathias]: proteins, polypeptides, and polysaccharides (e.g. cellulose, RNA, and DNA). Artificial polymers have their roots in the coal industry developed in the 19th century by Germany and Britain. It produced acetylene, methanol, and phenol, which serve as a main source of an array of polymers, by decomposing coal at high temperatures (cracking). Today, the leading chemical industry called the petroleum industry (started in United States in 1920 and in Europe in 1950) produces most monomers and polymers within the petrochemical industry, and ventures within crude-oil distillation products.

Applications

The highest demand of plastics is traditionally raised in the sector of packaging, accounting for about 40 wt. % of plastics consumed. Follow the building and construction sector with some 20 wt. %, household and domestic applications with around 18 wt. %, automobile industry with 7 wt. % and the electric devices and electronics industry with 8 wt. %; the rest share basic industry and the agricultural sector [APME 1999].

There are six main plastic materials that occur in European municipal solid waste: high density polyethylene (HDPE), low density polyethylene (LDPE), polypropylene (PP), polyvinyl chloride (PVC), polystyrene (PS) and polyethylene terephthalate (PET) [APME 1996].

For bonus information on generalities concerning polymers, please refer to Appendix G.

2.4.0 Studied polymers

The studied polymers in this thesis are: lignin, cellulose, EVA, PS, and PVC.

2.4.1 Lignin

Lignin is a macromolecular substance formed in the cellular membranes of vegetal cells that changes them into wood. The term itself comes from the latin word *lignum* that means "wood", the fact reminding of which is probably as superfluous as to "bring wood in the forest" (*in silvam ligna ferre* [Horatius]). The precise structure of this substance has not yet been completely determined. Thus the term "lignin" has to be understood to designate a complex of aromatic rings with methoxyl groups. It's an amorph substance that, once liberated from its linkage with cellulose in the cellular membrane, has brown or black-brown colour. This is why wood becomes brown when its cellulose is disturbed and lignin liberated.

Lignin is the second most wide-spread organic compound of the biosphere. This abundant natural resource is present in all plants, particularly in trees. In wood, it comes second after cellulose, representing between 15 and 30 % of its weight. Lignin is an indispensable substance in vegetal kingdom.

Lignin is embedded in between polysaccharidic constituents of cell walls; its function is the support and conduction. First, it is deposited in the vicinity of intercellular space, and then, on the level of primary and secondary plant diaphragms. Thus, lignin is in a state of quasi-total gel, it is situated in the walls in form of cords.

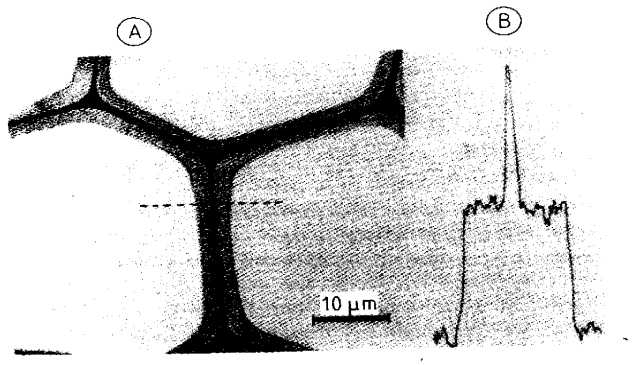

Fig. 10: Cut through a young black conifer [Lin et al.]. (A) Transversal cut of a bark of a young black conifer; an ultra-violet (λ = 240 nm) photograph; (B) Densimetric curve of the mentioned cut, demonstrating variation of concentration of lignin along the dashed line (see (A)).

Lignin supports the vertical posture of vegetals, resisting the force of gravitation and wind. It contributes to water and mineral salts alimentation of various plant organs.

As it is little sensible to biologic degradation, it creates a morphologic barrier to the penetration and progression of pathogenic agents that protects the plant in a natural fashion against various parasitic attacks.

Structure and composition

Even though it is the second most important constituent of wood, lignin has not yet been scientifically defined with respect to its structure. The term lignin is used to refer to the whole set of organic components of cell wall that are not formed from polysaccharides and that partake in consistency and rigidity of the wall. In other words, the term lignin is a generic name for a group of polyphenolic polymers with high molecular masses, containing a considerable proportion of aromatic nuclei.

Thus, we can speak of lignins in plural, because this proportion in coniferous and leafy woods will be different. In the first case, the basic structure stems from coniferine, in the second case, it stems from syringine. These are organic substances contained in coniferous woods and leafy woods, respectively.

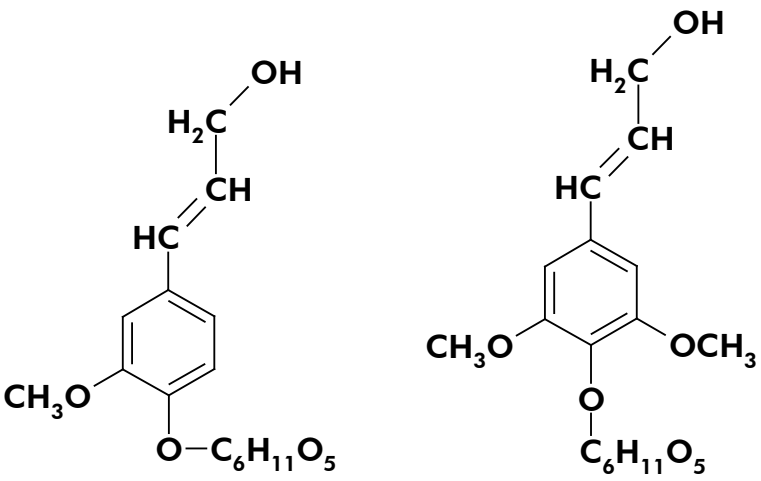

Fig. 11: Lignin monomer; coniferine (left) and syringine (right).

Lignins result from the oxidative polymerization of three phenolic alcohols.

Biosynthesis of these alcohols is carried out in one sequence of enzyme-induced stages. From aromatic aminoacid (phenylalanine, PhAla) comes the double bond CH=CH and then, hydroxyl groups -OH are introduced into the aromatic nucleus. Lastly, transformation of these groups in methoxylic substituents supervenes.

In the course of this process, three principal acids are formed, esterified, and reduced to phenolic aldehydes or alcohols.

The formulae of these alcohols follow [Lin et al.]:

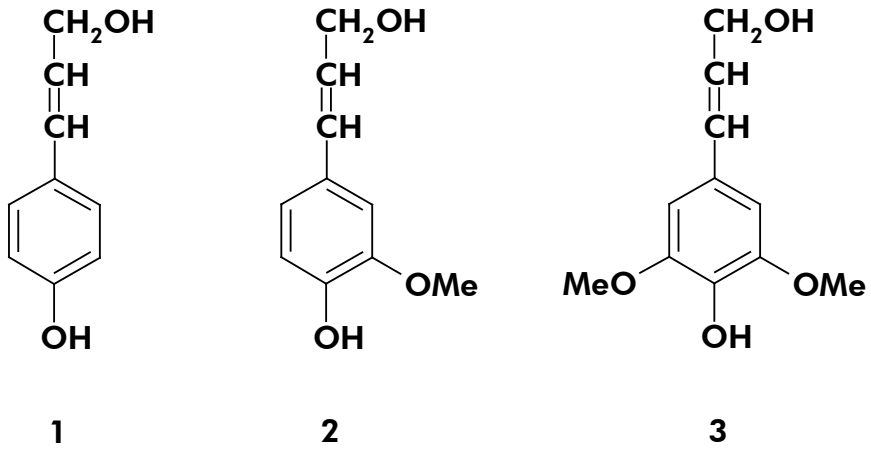

Fig. 12: Formulae of three principal lignin alcohols. 1: 3-(4-Hydroxyphenyl)-2-propen-1-ol (alcohol coumaryle), 2: 3-(3-methoxy-4-hydroxyphenyl)-2-propen-1-ol (alcohol coniferyle), 3: 3-(3,5-dimethoxy-4-hydroxyphenyl)-2-propen-1-ol (alcohol sinapyle).

The first stage of lignin polymerisation consists in enzymatic dehydrogenation of these alcohols that gives phenoxy radicals characterised by four isometric forms. This degradation of alcohols takes place in the presence of peroxydase enzymes.

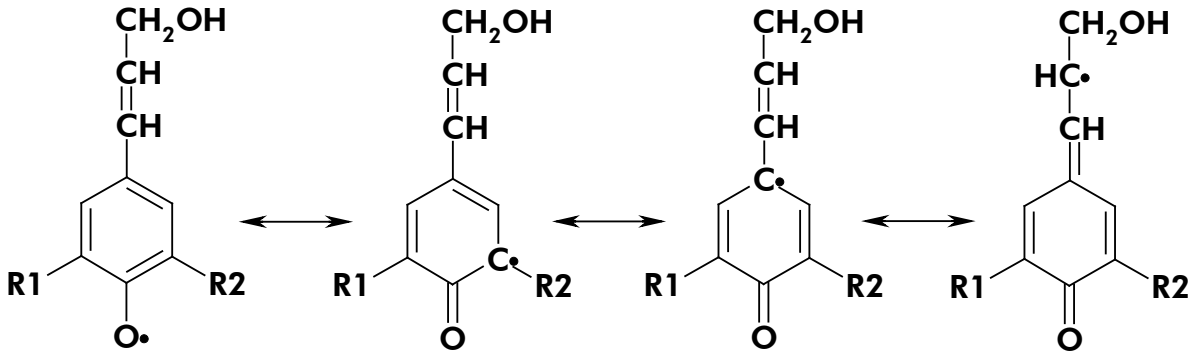

Fig. 13: Lignin polymerisation. R_1, R_2 = H or OCH_3.

The second stage of polymerisation consists in formation of random bonds between these radicals that give rise to the three-dimensional molecule of lignin.

The nature of bonds originated in this procedure is varied, as is shown in Fig. 14 below:

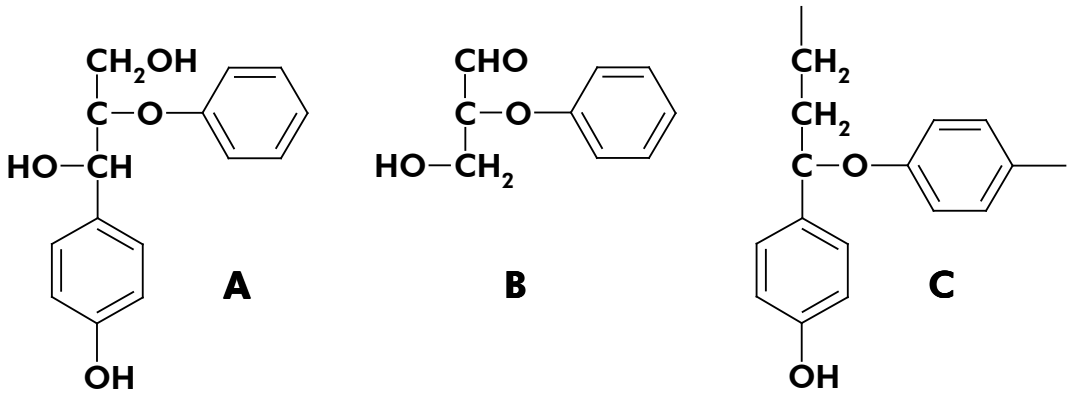

Fig. 14: Types of bonds that occur in lignine [Lin et al.] (See continuation on p. 52). A) Arylglycerol β-aryl ether, B) Glyceraldehyde 2-aryl ether, C) Noncyclic benzyl aryl ether.

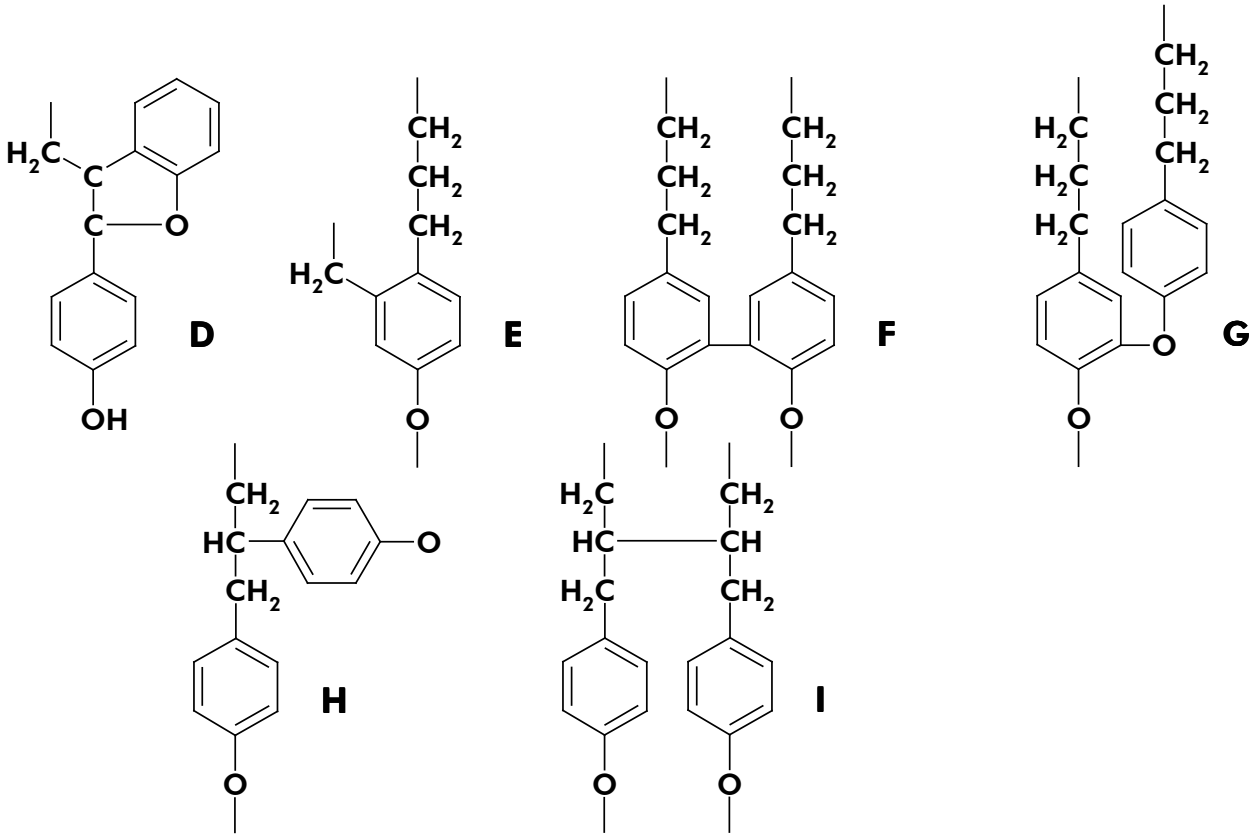

Fig. 14 (contd. from p. 51): Types of bonds that occur in lignine [Lin et al.]. D) Phenylcoumaran, E) Condensated structure on 2nd or 6th positions, F) Biphenyl, G) Diarylether, H) 1,2 Diarylpropane, I) joined β, β-structures.

From this, the multiplicity of basic units, types of bonds and their combination determine a great number of lignin structure that are known very poorly.

Depending on whether the basic radicals contain the group R_1 = H and R_2 = OCH_3 (radical called guaiacyle derived from the degradation of alcohol coniferyle) or R_1 = R_2 = H (radical called syringyle that comes from the degradation of alcohol sinapyle), lignin is considered to stem from coniferyne or syringine, respectively.

Trees containing lignin based on coniferine are gymnosperms (conifers like pine-tree, yew, etc.), the ones containing lignin based on syringine are angiosperms (leafy trees like birch, beech, etc.).

On the ground of a considerable amount of lignins present in nature and a difficult extraction of wood (cf. below), only two models were broadly discussed in literature in a precise manner: the one stems out from coniferine, the other from syringine.

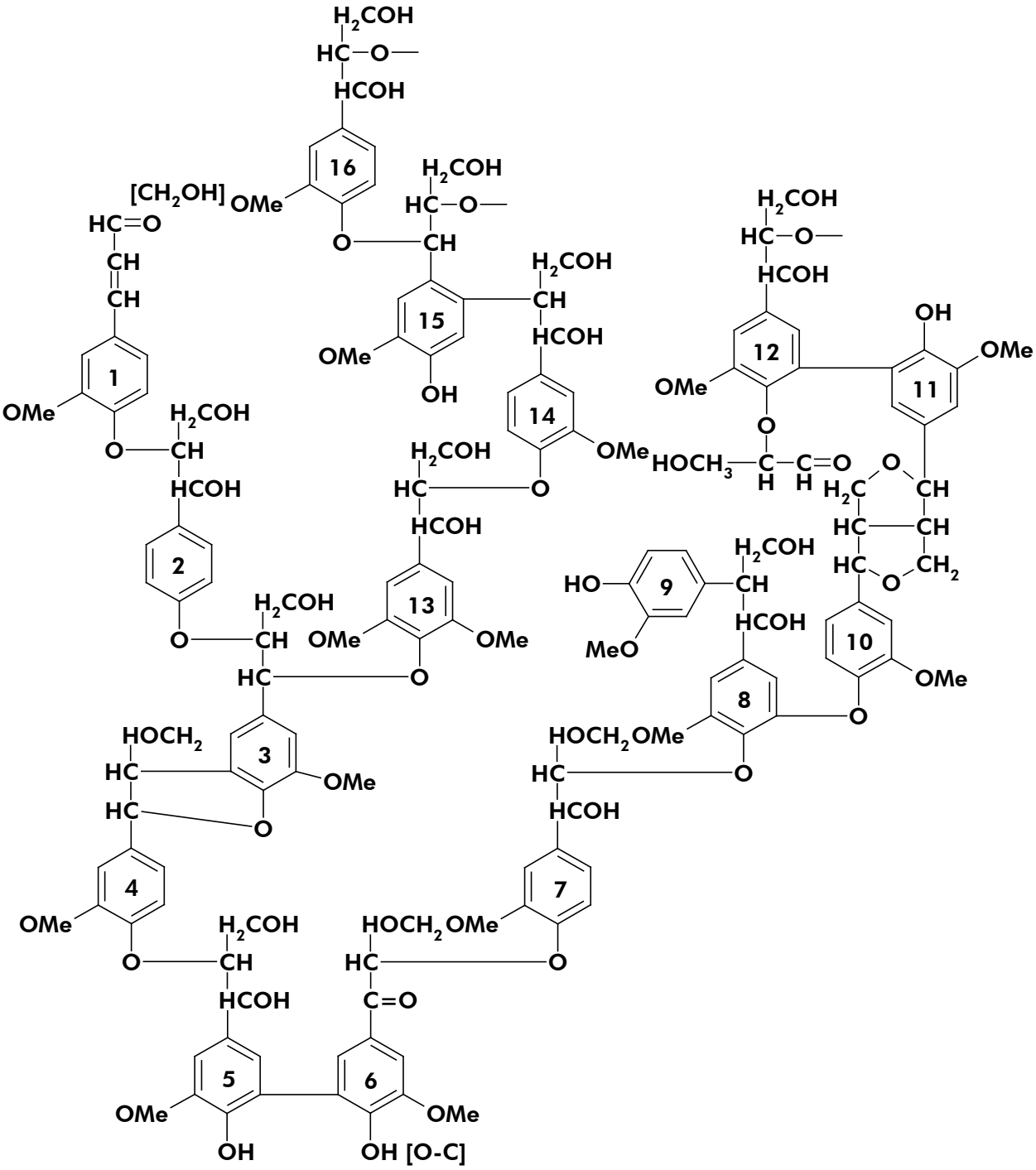

Fig. 15: Model of lignin based on coniferyne [Lin et al.].

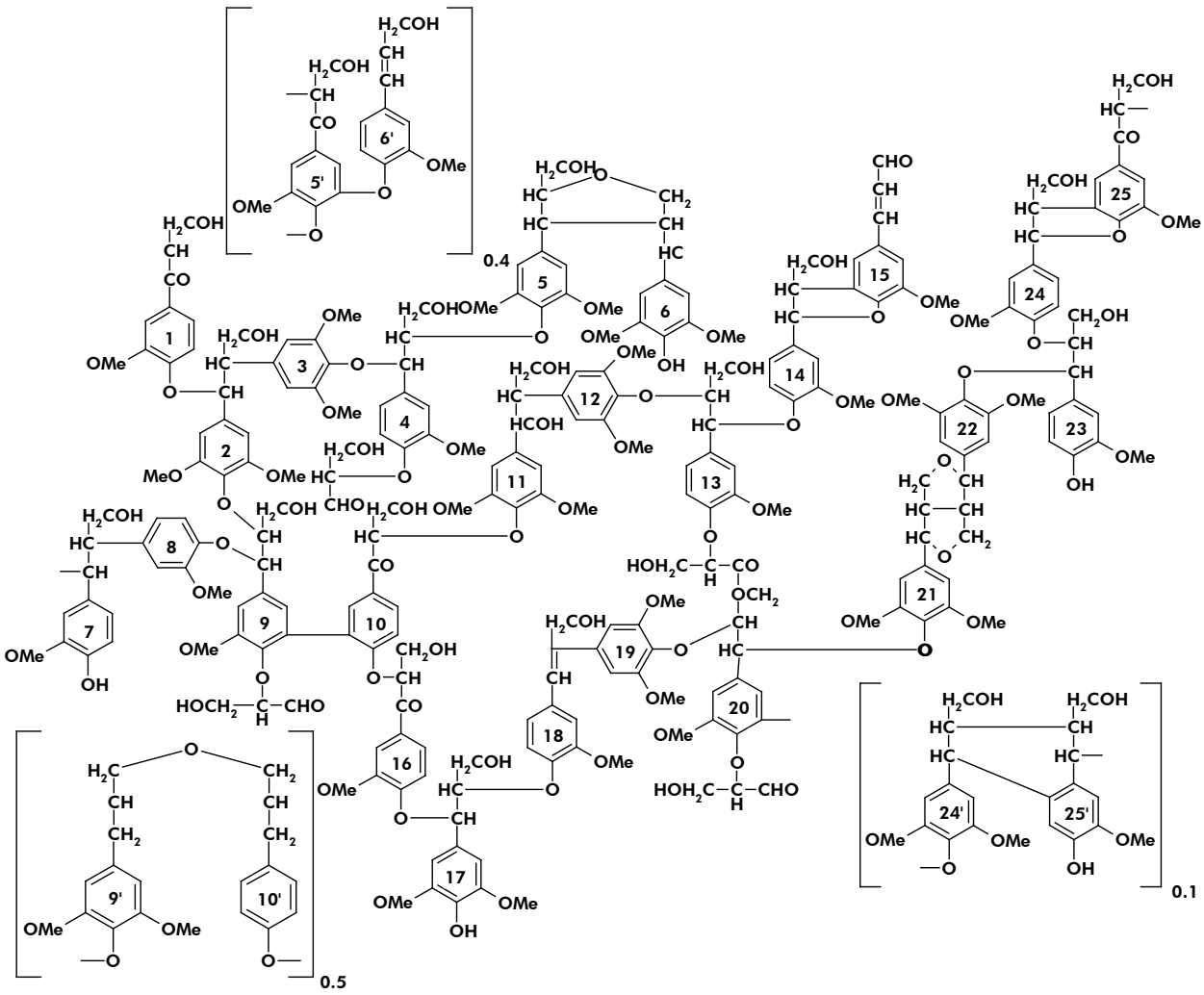

Fig. 16: Model of lignin based on syringine [Lin et al.].

Industrial use of lignin

The study of lignin structure is difficult by the reason of impossibility of its isolation from vegetals without degrading it. Therefore, the true molecular mass of lignin in wood is unknown.

Various measuring methods enable to evaluate the molecular mass of lignin in leafy woods (around 20,000 units). On the other hand, for coniferous woods, lower values were found.

Notwithstanding, lignins can be made use of in a multitude of industrial applications.

They contribute e.g. to wood quality in furniture. At present, several processes are operating to combat with their biodegradation.

On the other hand, lignins constitute a handicap in agro-alimentary or industrial exploitation of some trees. As they are not very digestible, some types of much lignified vegetation are not suitable for fodder purposes.

The presence of lignins also conduces to a number of inconveniences in pulp industry of which they are principle by-products.

All the same, industrial or residual lignin materials represent an important portion of polyphenols. Once an efficient procedure of degradation of polymer chains or another method of transformation is set in motion, it can turn into an interesting source of raw material.

Methods of lignin extraction

There are several methods of lignin extraction. These reactions can be divided in two large groups:

– basic extraction (caustic soda, kraft and anthraquinone),

– sulfite extraction.

As for the basic extractions, a simple treatment of wood chips by means of soda provokes degradation of lignin and polysaccharides. To improve this process, sulfites as e.g. Na_2SO_3 and anthraquinone (AQ) are used in small quantities that accelerate lignin depolymerization and limit losses of polysaccharides caused by hydrolysis.

Kraft extraction (soda – sulfite)

In this extraction method, lignin goes essentially through nucleophilic reactions that provoke rupture of arylglycerol β-aryl bonds of the phenolic group.

The products of these reactions are lignin monomers (little modified) and methylmercaptane (CH_3SH), responsible for the smell of Kraft packing-paper. [Lin et al.]

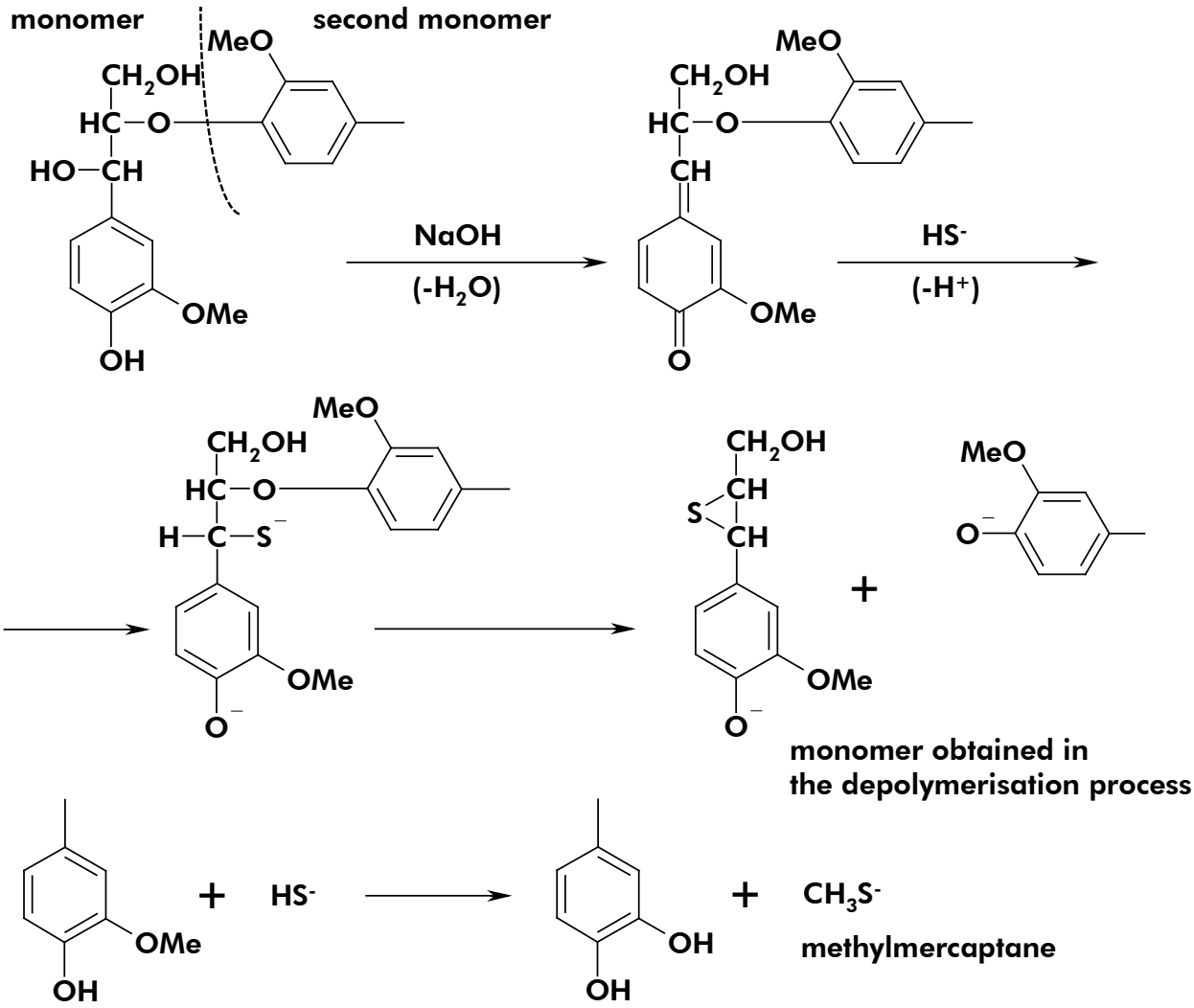

Fig. 17: Kraft extraction process.

Sulfite extraction

In this extraction, lignin is sulfonated and becomes water-soluble. The principal reaction of sulfonation is the following [Lin et al.]:

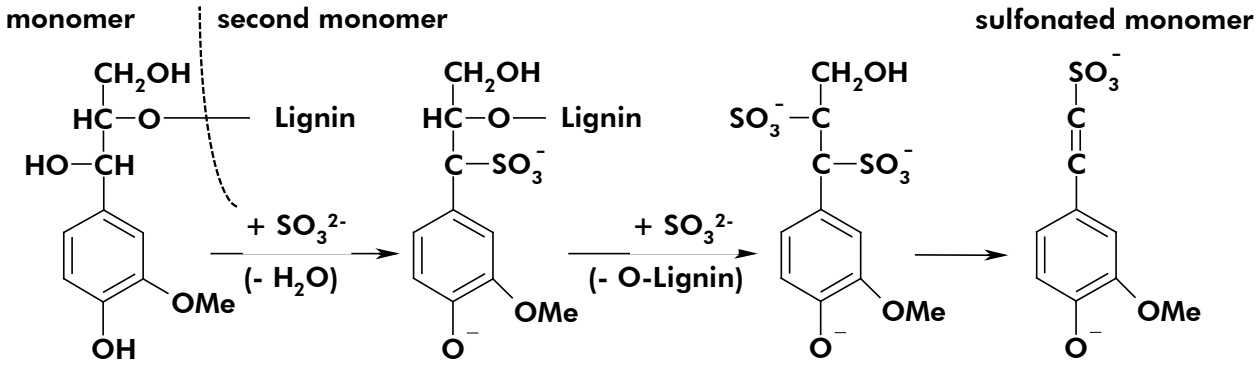

Fig. 18: Sulfite extraction.

Lignins on market

For industrial utilization, only two types of lignin were commercialised: lignosulfates, and Kraft lignins.

Other types of molecules are used rather in research.

World annual production of lignins is estimated at $1.4.10^9$ tons (see the table below):

Tab. 3: World annual production of different types of lignin.

Producer	**Country**	**Annual capacity [10^6 kg]**
Daishowa Chemicals	United States, Canada	220
Georgia Pacific	United States	190
Holmes	Sweden	180
ITT Rayonier	United States	160
Borregaard Industries	Norway	120
G. A. Serlachius	Finland	90
Chemische Werke Zell	Federal Republic of Germany	60
Societe i Avebene	France	60
Dresser Industries	United States	45
Westvaco*	United States	45
Others		215
Total		1385

Legend: * The only producer of Kraft lignin.

Lignosulphates (or lignin sulfonates and lignin sulphites)

From the point of view of their mass distribution and structure, they are heterogenous. Lignosulfates come from sulfite extraction.

They are soluble in solutions of all possible pH values. Nevertheless, in ethanol, acetone, and other similar organic solvents, they are insoluble.

Lignosulfate polymers have a small tendency to reduce surface tensions between liquids, but they don't allow any micelles to be formed.

"Basic" lignosulfates, obtained in sulfite extraction, can undergo a number of other chemical reactions (oxidation, introduction of amin chains, …) in which they obtain more specific properties according to the intended usage.

Kraft lignins (or sulphate lignins)

These are obtained from the Kraft liqueur pulp (Kraft extraction) by means of precipitation in the presence of sulphuric acid, hydrochloric acid and carbon dioxide.

Principal commercialised Kraft lignins are sulfonated (aside from a negligible part). The conditions employed are different for different types of processes:

- with sodium sulfite – at temperatures between 150 and 200 °C,
- with sulfite and formaldehyde – at temperatures around 100 °C,
- with oxygen and sulfite in oxidative sulfonation.

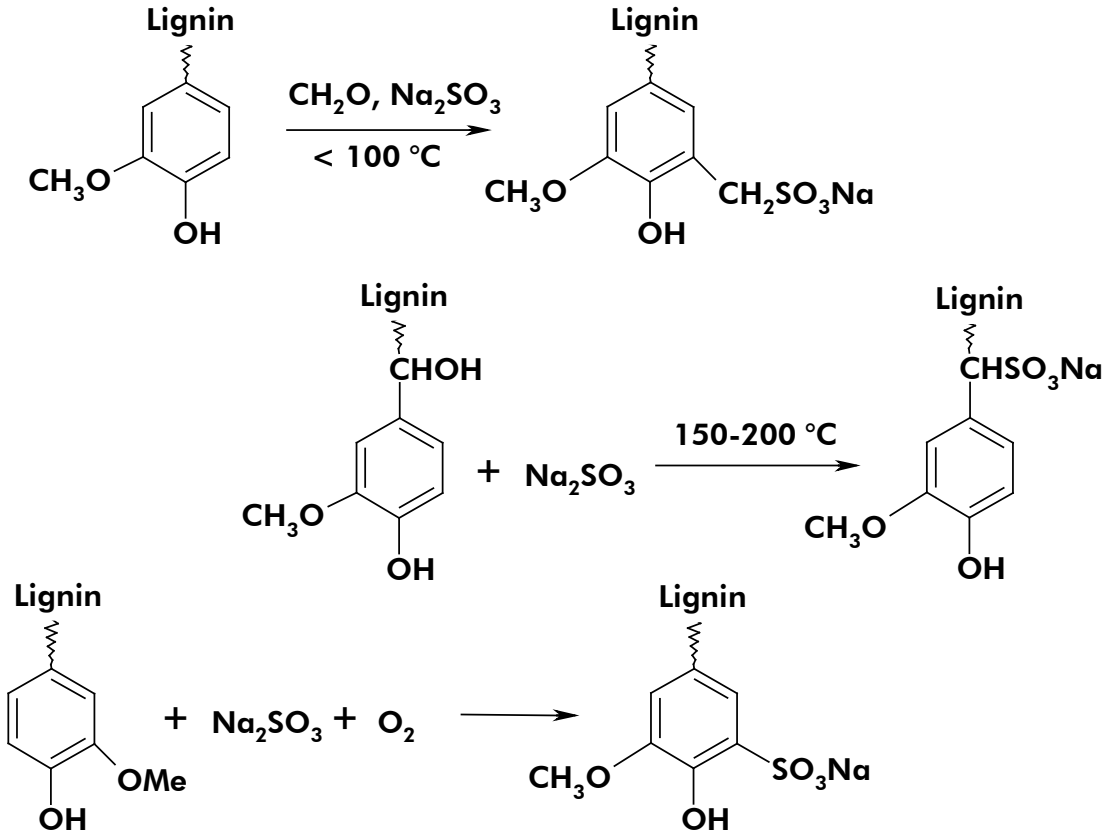

Fig. 19: Sulfonation of Kraft lignins.

A lot of other reactions are applied on Kraft lignins with a view to obtain specific properties.

Kraft lignins have a more homogenous mass distribution than lignosulfates. They are soluble in basic solutions (pH > 10.5), in acetone and in dimethyl formamide.

Some properties of lignosulfates and kraft lignins: [Lin et al.]

Tab. 4: Properties of lignosulfates and kraft lignins.

Property	**Lignosulfates**	**Kraft lignins**
Molecular mass	20,000-50,000	2,000-3,000
Polydispersity (M_w/M_n)	6-8	2-3
Sulfonate groups, meq/g	1.25-2.5	0
Organic sulfur, %	4-8	1-1.5
Solubility	Soluble in water at all pH's; insoluble in organic solvents	Insoluble in water; soluble in alkaline water (pH > 10.5), acetone, dimethyl formamide, methyl cellosolve, etc.
Color	Light brown	Dark brown
Functional groups	Smaller quantities of phenolic hydroxyl, carboxyl, and catechol groups; little side-chain unsaturation.	Larger quantities of phenolic, hydroxyl, carboxyl, and catechol groups; some side-chain unsaturation.

2.4.2 Cellulose

Cellulose, the most important constituent of cellular walls of plants, is the most wide-spread polymer in nature. Its structure determines to a great extent properties of pulp, paper, and of a great number of other materials based on wood. It's a chiral molecule and thus, it can endow products made of it with unexpected properties.

The cellulose molecule is a monotonous polymer composed uniquely of cellobiose monomer (2 glucose molecules linked by β-1-4 bond).

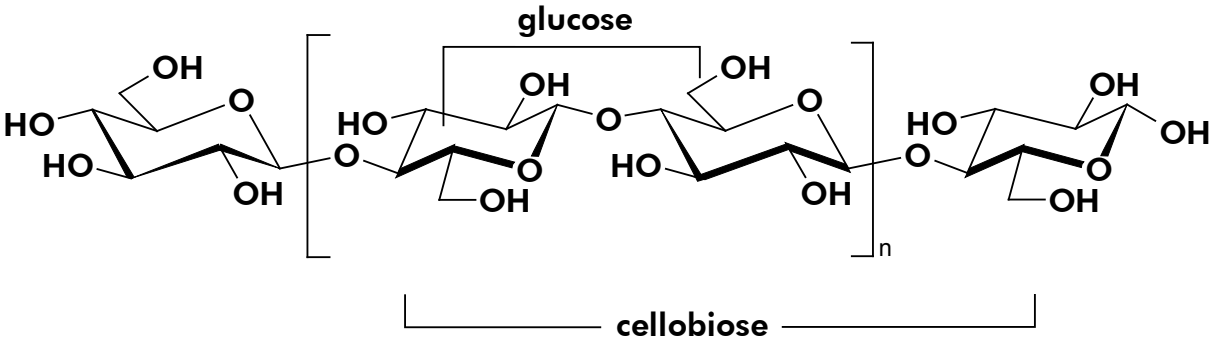

Fig. 20: Chemical formula of cellulose.

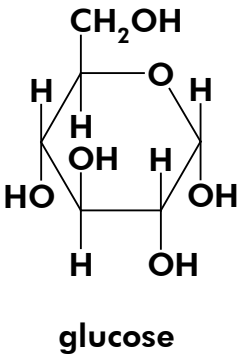

Fig. 21: Principal cellulose monomer.

By reason of β-1-4 bond, homologous monomer groups are situated alternatively above and below the plane. The molecule is linear. Its flexibility bears on degrees of freedom at each and every bond's level.

Cellulose is a component part ensuring protection and posture in vegetal organisms. It is situated in cytoplasmic membrane of cells and it is the most wide-spread organic substance in nature. It is estimated that a tree produces approx. 10 g of cellulose in one day. Thus, on a world-wide scale, the production of this compound amounts to $1.3.10^{10}$ tons per year.

Cellulose is also present in the composition of natural fibres, as well as lignin and hemicellulose. Unlike other constituents of fibres that are characteristic by amorphous structure, the structure of cellulose is to a great extent crystalline.

Crystalline cellulose is one of the world's most elastic polymers. Its elasticity coefficient is 136 GPa (for comparison, the value of this coefficient for glass fibre is 75 GPa).

2.4.3 EVA

Ethylene vinyl acetate is prepared from ethylene by oxyacetylation, using the acid group of ethanoic acid and air oxygen.

See below the chemical formula of EVA.

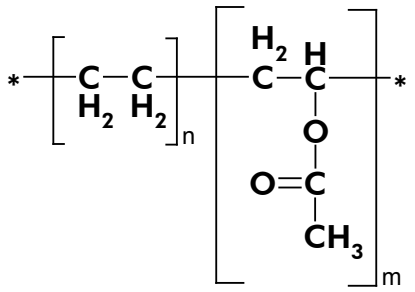

Fig. 22: Chemical formula of EVA.

Its monomer is composed of two parts: vinyl acetate or VA – $C_4H_6O_2$, i.e. $CH_3COOCH{=}CH_2$ – and ethylene. These two constituents can be co-polymerized in all proportions. With increase of VA contents, the material becomes more soft and transparent. Its properties acquire values over the range from semi-crystalline thermoplastic to an amorphous one. EVA is the first commercialised thermoplastic elastomer (it is easy to process it, and its properties resemble those of vulcanised caoutchouc).

EVA copolymers are very wide-spread thermoplastic copolymers.

They are known for good physico-chemical properties, good mechanical endurance, great easiness of treatment, and, finally, low cost. When the ration of vinyl acetate is equal to or greater than 28 %, it is possible to class the corresponding plastic material into elastomers. Still, it will lose its mechanical properties totally at temperatures above 100 °C. High percentage of vinyl acetate is the reason why it can be used in the production of thermo-fusible glues and adhesives, for manufacturing of cables, and for modifications of properties of bitumen materials.

EVA is used in numerous domains; three processes can shape it:

1) Extrusion of films:

food packaging, sheathing material (shopping bags, films bulking of packs, …) and industrial packaging (plastic foils for packing of palettes, industrial bags, ...);

agricultural films (ensilaging, straw treatment, greenhouses);

industrial films (lamination films, surface-protecting films...).

2) Injection:

sports material (shoe soles and webs, ...);

plastic plugs;

medical accessories.

3) Compoundage for producing of cables.

Properties of EVA

The properties of EVA depend on percentage of vinyl acetate (VA). Usually, concentrations between 5 and 40 % are used; they also relate to a particular moulding process. Inherent to the moulding procedure and the composition are various notable properties:

- good inertia;
- vigorous resistance to low temperatures;
- excellent transparency.

2.4.4 Polystyrene

Polystyrene is a hard, cheap thermoplastic. Probably only polyethylene and PVC are used more extensively than polystyrene in everyday life. Polystyrene molecule was found in 1839. Its synthesis in the industrial scale has started some hundred years after. There are three main types of polystyrene: crystalline polystyrene (GPPS), polystyrene resistant to impact (HIPS), and expanded polystyrene (PSE).

Polystyrene (PS) is a versatile thermoplastic resin available in a wide range of formulations from general purpose crystal and impact grades to highly specialized grades for applications where engineering resins were once the only choice.

Grades of GPPS and HIPS are available to meet the needs of various fabrication processes such as extrusion, injection, thermoforming, blow moulding, foam sheet extrusion, and biaxially oriented sheet.

The wide range in physical properties and relative ease of processing make polystyrene an extremely attractive material, capable of competing quite favourably with more expensive resins in a number of demanding applications.

GPPS or Crystal polystyrene

GPPS is a clear, amorphous polymer which exhibits high stiffness, good dimensional stability and electrical insulation properties. The commercial grades of crystal PS offer a wide range in melt flow index with high-heat, high-molecular-weight grades around 2 g.10 min^{-1} (ASTM D 1238; 2000 C.5 kg^{-1}) and other grades as high as 30+g.10 min^{-1} for easy flow. Changes in molecular weight distribution, as well as specialised additives, account for the variety available in general-purpose PS.

The versatility and sparkling clarity of GPPS make it an ideal selection for an extensive range of applications including food packaging, food service items, medical care products, and packaging for audio cassettes, compact discs, and other consumer electronic media.

HIPS or Impact polystyrene

Commercial impact polystyrene make use of polybutadiene elastomers for impact modification. A number of impact grades are available and these are generally classified as being either medium impact PS (notched Izod values between 4 and 8 kg cm.cm^{-1}), high impact (8 to 16), or extra high impact (greater than 16).

The mechanical properties of impact PD vary significantly depending on the level of rubber modification. Impact PS ranges from translucent to opaque in its natural colour.

HIPS are widely used in toys, furniture, housewares, food packaging, food service, medical care products, appliances, building materials, consumer electronics, and packaging for electronic media.

EPS or Expanded polystyrene

Expanded polystyrene (EPS) is used for the production of a number of applications. However its major application is as a protective packaging for consumer electronic products and white goods. Its excellent thermal insulation and mechanical protection properties make it ideal to package fish and other foodstuffs. EPS also has applications in horticulture as seed trays.

The outstanding shock absorbency of expanded polystyrene packaging ensures the protection of a broad range of products. Moreover, its compression resistance means that EPS is ideal for stackable packaging goods. When safety is paramount, EPS comes into its own. It is used in the manufacture of children's car seats and cycling helmets, where its protective qualities, strength and shock-absorbency are vital.

Speciality polystyrene

The properties of polystyrene can be further enhanced by incorporation of a variety of additives to tailor its performance for specific applications. These performance features can include extra-high impact strength, enhanced heat resistance, antistatic features and various combinations of these characteristics.

Speciality polystyrenes have replaced engineering resins in many applications and are gaining wide industrial acceptance due to ease of processing, secondary finishing characteristics, and cost effectiveness.

Compounded polystyrene

Is polystrene resin (GPPS / HIPS) modified with additives to impact special properties to improve performance. Typically compounding imparts any of following characteristics to polystrene resin:

- flame retardancy,
- light stability,
- colour,
- alter electrical properties like resistivity, dielectric strength, arc resistance etc.,
- higher strength and modulus,
- better toughness,
- better heat resistance,
- modified surface properties like COF, scratch resistance and glass.

These modifications can also be combined together. For example, it is possible to increase strength, modulus and toughness of polystyrene resin along with importing better heat resistance and flame retardancy together with specific colour. Thus modified polystyrene resin can be put into new applications or replace expensive resins.

Chemical formula of polystyrene is the following:

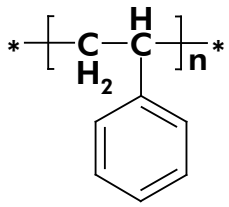

Fig. 23: Elementary motive of polystyrene molecule – styrene.

Around 120 °C, polystyrene becomes doughy, and above 150 °C, he reaches its melting point. Its pyrolysis begins at 350 °C; a rapid temperature slope allows attaining its flash-point (at 490 °C), before any form of thermal degradation.

Tab. 5: Identity card for styrene.

Usages	Thermoplastics
Monomer	Styrene
Polymerisation	Radical chain (atactic), Ziegler-Natta (syndiotactic)
Morphology	Very amorphous (atactic), very crystalline (syndiotactic)
Melting point	270 °C (syndiotactic)
Glass transition	100 °C

Transparent plastic bottles are made of polystyrene, as well as a great portion of stampings in the interior or cars. Polystyrene is also used in toy industry and in fabrication of casings of objects like personal computers, hair driers, and other household products.

Styrene (or vinylbenzene, C_6H_5-CH=CH_2) polymerisation in the Ziegler-Natta process (or radical polymerisation) produces transparent plastic material. Polystyrene is therefore a vinyl polymer (that consist in vinyl monomers, i.e. small molecules containing double bonds carbon-carbon; this is the largest group of polymers). From the structural point of view, it is a long chain of hydrocarbons, with phenyl groups attached to specific carbon atoms. Polystyrene can be fabricated by radical polymerisation from styrene monomer:

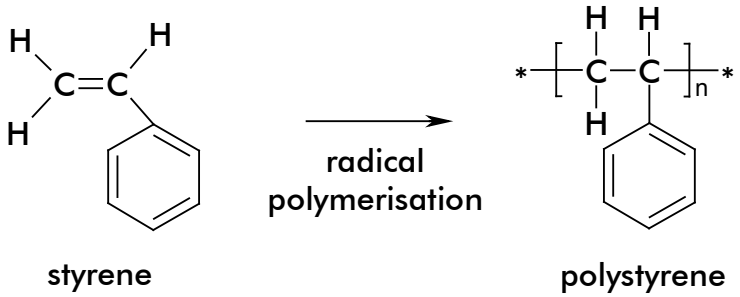

Fig. 24: Radical polymerisation of styrene into PS.

2.4.5 PVC

PVC is the second most utilised plastic in the world, after polyethylene. Besides, its structure is very comparable to that of polyethylene, the PVC monomer differs from that of polyethylene just by a chlorine atom replacing a hydrogen atom.

PVC is a member of a family of thermoplastic polymers (polymers that are easy to mould and form when they are heated). This type of polymers is constituted by linear macromolecules that can slide over one another under influence of heat or strong stress.

PVC can be either flexible or rigid, depending on different additives.

PVC is produced by radical polymerisation of vinyl chloride, which is made by chloration of acetylene.

Polyvinyl chloride (PVC), also known as "vinyl," is produced in several steps. In the first step, ethylene dichloride (EDC) is produced by the chlorination of ethylene through either direct chlorination or oxychlorination. Direct chlorination reacts ethylene with chlorine. Oxychlorination is done by reacting ethylene with dry hydrogen chloride (HCl) and oxygen at temperatures generally less than 325°C. The resulting EDC is then subjected to pressures between 20-30 atmospheres and temperatures between 550-650°C. This process is known as pyrolysis, or thermal cracking. Equal parts of vinyl chloride monomer (VC) and hydrogen chloride (HCl) are created during this stage. The VC is then isolated. And finally, PVC is made by the polymerization of the VC. Polymerization is a chemical reaction linking the molecules of a simple substance (monomer) together to form large molecules whose molecular weight is a multiple of that of the monomer. There are two general types of polymerization reactions, addition polymerization, and condensation polymerization. PVC is made by addition polymerization, which occurs when VCM reactive monomers unite without forming any other products. Its resulting molecular structure is similar to that of polyethylene.

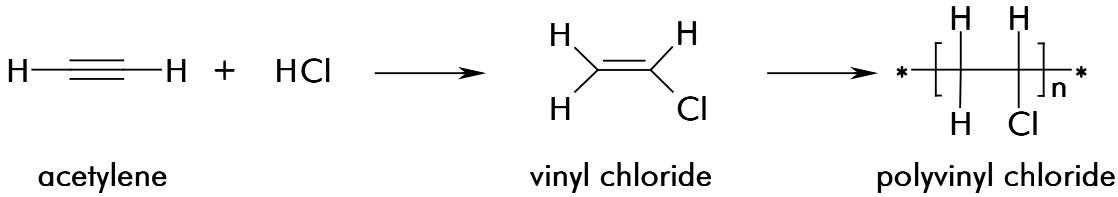

Fig. 25: Reaction of synthesis of polyvinyl chloride.

PVC is being transformed in the following processes:

- **extrusion;**
- **injection;**
- **rolling;**
- **rotation moulding.**

It is present in the following products: bottles, domestic items, sheets, cables, badges, pipes, thin films, bags, gloves, toys, gutters, shutters, …

PVC, e.g., dominates the market of packing plain and fizzy drinks, as is illustrated by the following chart:

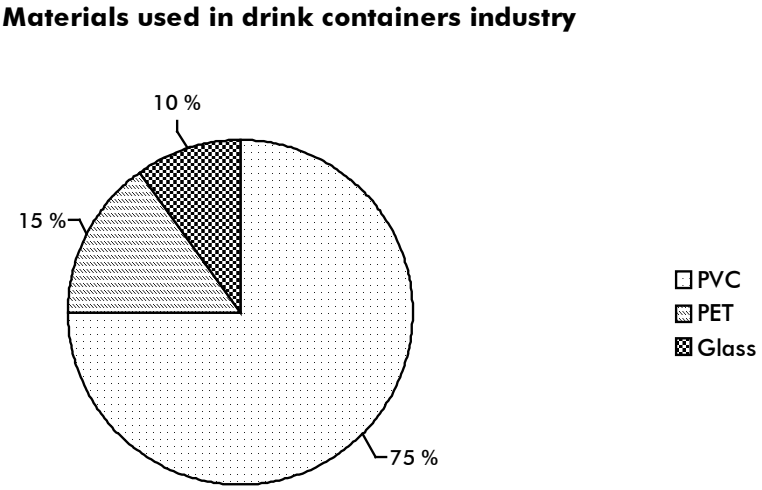

Fig. 26: Distribution of various materials used in conditioning of drinking waters, either plain or fizzy drinks [Syndicat des Producteurs de Matieres Plastiques].

As a matter of fact, PVC is more and more replaced in consequence of environmental problems caused by this polymer. It is being systematically replaced by PET, at least in production of beverage bottles. For example, *Société des eaux d'Evian*, a well-known producer of packed waters Evian, has begun with this exchange in 1998.

Most appreciated properties of PVC are:

- **transparency;**
- **inertia;**
- **good elasticity;**
- **excellent memory;**
- **stress resistance.**

PVC is water resistant (and consequently used for fabrication of cloaks or drapes in shower bath; naturally also for water pipelines). It is also resistant to fire to some degree, due to the presence of chlorine atoms. These are released when one tries to burn PVC inhibiting thus combustion.

Tab. 6: Identity card for vinyl chloride.

Usages	Thermoplastics
Monomer	Vinyl chloride
Polymerisation	Radical chain
Morphology	Very amorphous, crystallinity ~ 11 %
Glass transition	~ 84 °C

3. Experimental part
– Study of the kinetics of the thermal degradation of polymers –

The kinetic study of the thermal degradation of above-presented polymers was realised using two ways that are traditionally found in literature. These are:

- **Isoconversional methods (in the present study, we use that of Ozawa-Flynn-Wall), that comes under so-called model-free methods,**
- **Numerical resolution of kinetic equations obtained from pseudo-schemes of reactions, that belongs to model-fitting methods.**

3.1 Materials and experimental apparatuses

All samples used are products of the Aldrich Chemical Company (now Sigma-Aldrich), if not mentioned otherwise. Their properties are stated in the table below. No other properties were measured:

Tab. 7: Used sample materials.

Material	Nomenclature	Ref. No.	Molecular structure	Other characteristics
PVC	Polyvinyl Chloride, secondary standard	18,026-1	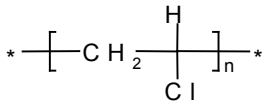	MW = 83,500 MN = 37,400 white powder
Lignin	Lignin, alkali, Kraft	37,095-9	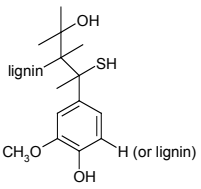	*Merck Index* 11,5363 dark brown powder
Cellulose	Cellulose	31,069-7	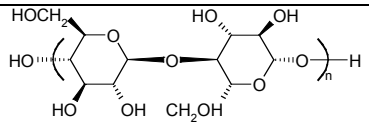	*Merck Index* 11,1961; white powder (particles of c. 20 μm)
EVA	Ethylene Vinyl Acetate	43,724-7	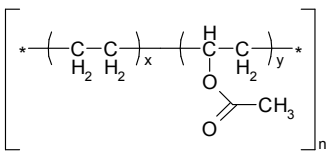	m. p. 95 ° d 0.933; melt index 8; 12, 25, 40 wt. % vinyl acetate 200-900 ppm BHT
PS	Polystyrene	18,242-7	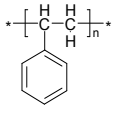	average MW ca. 280,000 (GPC)

In all experiments, samples of EVA with 12, 25 and 40 % content of VA were used. In the case of studied mixture we have chosen the following ratios: 25/75 ; 50/50 ; 75/25. The sample weight was between 20 and 40 mg. The heating rates used were in the range 10-30 °C.min^{-1} and the pyrolysis was carried out in a N_2 atmosphere (99.995 %), with the gas flow maintained at 27 cm^3.min^{-1}. The thermobalance is a Setaram model TGA 92-16. Its connection with the FTIR spectrophotometer (Perkin-Elmer, model System 2000) by means of a heated line has made it possible to make continuous recordings of the IR-spectra corresponding to evolved gases. The analysis of the spectra was performed with KnowItAll Analytical System.

In the experimental work, focus was primarily on these objectives:

(i) Analysis of TGA curves,

(ii) Assessing of a chosen kinetic model by means of the alluded MatLab programme or by other convenient method,

(iii) Correlation of a presumed degradation mechanism with the resulting FTIR spectra.

On the next page, the items on which modes of action appropriate for each of the elements designated (i), (ii), and (iii) (vide ante) will be applied are delineated.

Below see the scheme of experimental configuration (Fig. 27).

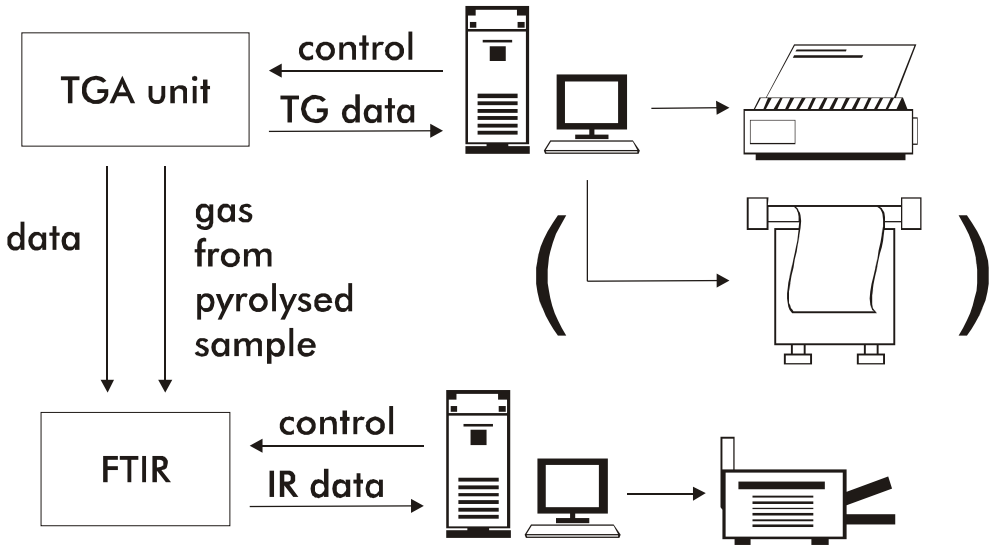

Fig. 27: Experimental apparatuses.

As for the location of the temperature sensor in the termobalance, see the figure below:

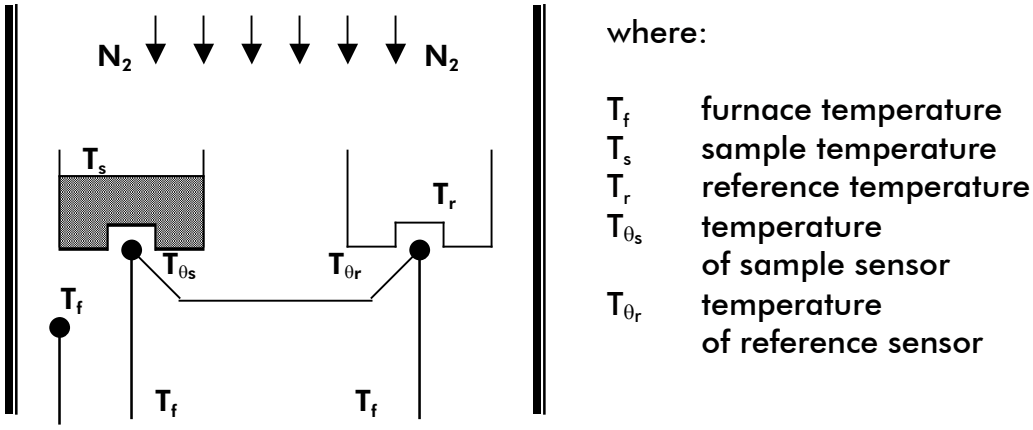

Fig. 28: Temperature sensor location [Lecomte et al.].

It can be seen that the temperature sensor touched the bottom of crucibles. Measurements studied in the work by Lecomte and Bodoira [2002], on the same equipment as that used in the thesis, show that there is really a delay between the sample temperature and the temperature of sensor. As is documented by Lecomte and Bodoira, the difference amounts to several degrees centigrade, for the samples studied in their work. A similar difference is surely to be expected in the case of our study. For our purposes, this influence was not considered in the numerical evaluation of experimental data. A deeper study into relevant phenomena would certainly prove fruitful.

As far as the heating rates used, slow-pyrolysis conditions were employed, as required by our experimental configuration. Conventionally, fast pyrolysis conditions are considered to amount to the rise of temperature of several hundreds of degrees centigrade in time periods of order of seconds or less (e.g. 500 ms). In the case of the scale of our heating rates, one could also consider that the heating rate of 30°C.min^{-1} is to be designated as a fast pyrolysis and the one of 1°C.min^{-1} as a slow pyrolysis. However, taking the conventional approach, we have selected the slow heating rates between 1 and 30 °Cmin^{-1}.

Also, it is important to note that for the purposes of the thesis, heat transfer phenomena were neglected. Otherwise, it is accepted that the heat transfer to the particles and within the material itself could be the slow determining step. Though, samples were prepared with regard to the diminution of the above-mentioned problem.

3.2 Part A
Kinetic study of the thermal degradation of polymers – isoconversional method (model-free method)

3.2.1 TGA data treatment

In evaluating of our experimental data, two methods were adopted. Firstly, the integral method described in the following section was used.

The second approach, serving as a confrontation of both methods, was to assume a kinetic model appropriate for each polymer and to employ the procedure of fitting developed for these experimental data, by means of a specific software application conceived in MatLab for this purpose.

The second method described more in detail would be presented in this way: a set of kinetic parameters found in literature (e. g. those in Tab. 11, p. 93, for PS activation energy) was put into a MatLab differential equations solver functions (e. g. "ode45"). The other parameters (i. e. the frequency factor) were adjusted – by computation – to fit experimental curves. The converse was also executed, that is starting with frequency factor values. Correlations of thus computed curves were evaluated and parameters corresponding to the most fitting one were considered to be the result of the process. The advantage of this method is relative rapidity of obtaining results (once the program is written or adjusted for pyrolysis conditions of the polymer in question).

Description of the Popescu's variant on the Ozawa-Flynn-Wall method

This method is based on the use of the degree of conversion for a particular reaction measured for the same temperature values on curves recorded at various heating rates. The main advantage of this method is that it does not stem from any assumption concerning the temperature integral, thus giving a higher degree of precision to the calculated results.

It is assumed that the reaction rate for the heterogeneous process under non-isothermal conditions depends only on the degree of conversion α and temperature T, and that these two variables are independent,

$$\frac{d\alpha}{d\tau} = f(\alpha)k(T)\,, \tag{1}$$

where τ is time; α is defined as: $\alpha = (m_0\text{-}m_\tau)/(m_0\text{-}m_f)$, where m_0 stands for the initial sample mass, m_τ for the sample mass in a given time τ, and finally m_f for the final one). By introducing the heating rate, β, where $\beta = dT/d\tau$, Eq. (2) is obtained:

$$\frac{d\alpha}{dT} = \frac{1}{\beta} f(\alpha)k(T)\,. \tag{2}$$

The integral form of Eq. (2) is, then

$$\int_{\alpha_m}^{\alpha_n} \frac{d\alpha}{f(\alpha)} = \frac{1}{\beta}\int_{T_m}^{T_n} k(T)dT\,, \tag{3}$$

where α_m, α_n are two different degrees of conversion and T_m, T_n are their corresponding temperatures. By using the notations

$$F(\alpha)_{mn} = \int_{\alpha_m}^{\alpha_n} \frac{d\alpha}{f(\alpha)}\,, \tag{4}$$

and

$$I(T)_{mn} = \int_{T_m}^{T_n} k(T)dT\,, \tag{5}$$

for the integral of conversion and temperature, respectively, Eq. (3) can be written in a short form as

$$F_{mn} = \frac{1}{\beta} I_{mn}\,. \tag{6}$$

Now, several experiments using various heating rates will be considered. Two straight lines $T = T_m$ and $T = T_n$, drawn on the TG plot just described, will determine, on each curve corresponding to a distinct heating rate, a pair of values of α, i.e. (α_{m1}, α_{n1}), …, (α_{mi}, α_{ni}). With the help of these pairs and using various conversion functions, such as those given in Table 8 (at the end of this section), the values of F_{mn1}, …, F_{mni} can be computed according to Eq. (4). As the temperatures T_m and T_n are the same for all the experiments, according to Eq. (5) it follows that I_{mn} is constant (because $k(T) = A \exp(-E/RT)$), and, from Eq. (6), a plot of the values of F_{mn} versus $1/\beta$ has to lead to a straight line with an intercept of zero if the analytical form of $f(\alpha)$ is properly chosen. This procedure may be repeated for other pairs of temperatures. Finally, a family of straight lines will indicate the best kinetic model, out of those that were considered, of course, for the acquired experimental data. To choose the proper kinetic function, the best correlation coefficient can be used.

In order to calculate the values of the activation energy E and the frequency factor A, it is assumed that $k(T)$ obeys the Arrhenius-type relationship

$$k(T) = A \exp(-E/RT) \tag{7}$$

The frequency factor A is considered independent of temperature. By merging Eq. (7) into Eq. (3), Eq. (8) emerges:

$$\int_{\alpha_m}^{\alpha_n} \frac{d\alpha}{f(\alpha)} = \frac{A}{\beta} \int_{T_m}^{T_n} \exp(-\frac{E}{RT}) dT \,. \tag{8}$$

By introducing the notation

$$H_{mn} = \int_{T_m}^{T_n} \exp(-\frac{E}{RT}) dT \,, \tag{9}$$

and in a parallel way to Eq. (4), it may be written that

$$F_{mn} = A/\beta \, H_{mn}. \tag{10}$$

To evaluate the integral H_{mn}, the simplest approach is to use the first mean value theorem for definite integrals and thus write

$$H_{mn} = (T_n - T_m)\exp(-E/RT_\zeta), \tag{11}$$

where T_ζ belongs to the range T_m, T_n. Eq. (10) then becomes

$$F_{mn} = A/\beta(T_n - T_m)\exp(-E/RT_\zeta) \quad , \tag{12}$$

or, when using logarithms,

$$\ln\frac{\beta}{T_n - T_m} = \ln\frac{A}{F_{mn}} - \frac{E}{RT_\zeta}. \tag{13}$$

Now, the plot of $\ln[\beta/(T_n - T_m)]$ versus $1/T$ leads to a straight line whose slope, equal to $-E/R$, allows us to calculate the value of the activation energy E. As the form of the conversion function is already known, the value of F_{mn} may easily be substituted, and, from the value of the intercept of the above mentioned plot, $\ln(A/F_{mn})$, the frequency factor A can also be calculated.

Why a variant on the Ozawa-Flynn-Wall method?

The method proposed by Popescu [1996] is a variant on the Ozawa [1965] method, elaborated on by Flynn & Wall [1966]. The major difference between them lies in the fact that the Popescu's method uses definite integrals, i.e. conversion degree and temperature intervals with both limits defined. The Ozawa-Flynn-Wall method takes into consideration intervals whose first limit is assumed to be zero. This assumption made, one can use the Doyle's approximation [Doyle 1962] for computing the temperature integral. As Popescu [1996] has outlined it, this assumption requires two conditions to be fulfilled:

1) The value of the temperature integral from zero to the onset temperature T_0 (the highest temperature for which the conversion degree is still zero), may be neglected.

Otherwise, its value would have to be considered and, consequently, the Doyle approximation does not apply. This condition is mathematically written as follows:

$$\int_0^{T_0} \exp\left(-\frac{E}{RT}\right) dT = 0. \tag{14}$$

In reality though, the value of the integral is never zero. One can just assume that up to a certain temperature the value of the integral is small enough to be neglected.

2) For all experiments with the same reaction carried out at various heating rates, the value of the onset temperature is the same. If this condition is satisfied, the onset temperature could be used to characterize the chemical reaction in a better way than the kinetic parameters do. And this condition is even more dubious than the first one. Consider a reaction, for which the onset temperature changes when the heating rate is changed. Thus, T_1 for β_1 and T_2 for β_2, and $T_2 > T_1$ are obtained. According to the first condition, the value of the temperature integral may be neglected for temperatures up to T_1. It follows that the integral from T_1 to T_2 cannot be neglected. Thereby, the Doyle's approximation is invalid. However, this is closer to reality than the second condition, which has to be met in order to apply Doyle's approximation.

The Popescu's method avoids the necessity of these two conditions by taking into consideration definite limits of the integrals and performing calculations accordingly.

It can be noted that the second condition is not required when the integral method is used to analyse the experimental data obtained from only one heating rate.

Tab. 8: Analytical forms of various conversion functions.

Symbol	$f(\alpha)$	$g(\alpha)$	**Current denomination**	**Mechanism**
F1	$(1-\alpha)$	$-\ln(1-\alpha)$	1st order, random nucleation	random nucleation uni-molecular decay law; 1st order
F2	$(1-\alpha)^2$	$(1-\alpha)^{-1}$	2nd order	second order
F3	$(1/2)(1-\alpha)^3$	$(1-\alpha)^{-2}$	3rd order	third order
R1	1	α	(1st order)	1st-order reaction
R2	$(1-\alpha)^{1/2}$	$2[1-(1-\alpha)^{1/2}]$	contracting cylinder	2-Dimensional phase-boundary-controlled reaction
R3	$(1-\alpha)^{2/3}$	$3[1-(1-\alpha)^{1/3}]$	contracting sphere	3-Dimensional phase-boundary-controlled reaction
A2	$2[-\ln(1-\alpha)]^{1/2}(1-\alpha)$	$[-\ln(1-\alpha)]^{1/2}$	Avrami-Erofeev equation	2-Dimensional growth of nuclei
A3	$3[-\ln(1-\alpha)]^{2/3}(1-\alpha)$	$[-\ln(1-\alpha)]^{1/3}$	Avrami-Erofeev equation	3-Dimensional growth of nuclei
A4	$4[-\ln(1-\alpha)]^{3/4}(1-\alpha)$	$[-\ln(1-\alpha)]^{1/4}$	Avrami-Erofeev equation	
D1	$\alpha/2$	α^2		one-dimensional diffusion law
D2	$-1 / \ln(1-\alpha)$	$(1-\alpha)\ln(1-\alpha) + \alpha$		two-dimensional diffusion law
D3	$3(1-\alpha)^{2/3} / 2[1-(1-\alpha)^{-1/3}]$	$[1-(1-\alpha)^{1/3}]^2$	Jander equation	three-dimensional diffusion law
D4	$3 / 2[(1-\alpha)^{-1/3}-1]$	$(1-2\alpha/3)-(1-\alpha)^{2/3}$	Ginstling-Brounstein equation	three-dimensional diffusion law
B1	$\alpha(1-\alpha)$	$\ln[\alpha/(1-\alpha)]$	Prout Tompkins	
P1	$n\alpha^{1-1/n}$	$\alpha^{1/n}$	Mampel power law	
E1	α	$\ln \alpha$	Exponential law	

3.2.2 Kinetic model in literature

3.2.2.1 Lignin

Three principal constitutive units of lignin are *p*-hydroxyphenyl, guaiacyl, and syringyl. Billa et al. [1998] noticed that there are significant variations in the yields of aromatic aldehydes (*p*-hydroxybenzaldehyde, vaniline, syringaldehyde), as well as their corresponding acids – hydroxycinnamic, *p*-coumaric and ferullic – depending on the temperature and time of the degradation of samples of straw and foliage. The yields of monomeric lignin units of the guaiacyl and syringil have also changed significantly. The decrease of the yields of vanilline and syringaldehyde, above 170°C, can be explained [Adachi 1992] by the thermal instability of benzaldehydes.

The major stage of the degradation of ground lignin obtained from real samples of wood and plants [Jakab 1997] is between 200 and 700°C.

The principal products of lignin pyrolysis are phenyls, alkenes, alkanes, and aldehydes. According to Britt et al. [1995], the dominant reaction pathway is the free radical mechanism.

In the pyrolysis of organic materials, two types of processes can be distinguished:

(a) primary reactions, forming products directly from the biomass, and

(b) secondary reactions, i.e. reactions of the volatiles formed by primary reactions.

The first stage of the degradation of lignin consists in the fragmentation to lignin units. The ether α-O-4 bond is found to be the weakest.

The pyrolysis products can be classified into: gaseous hydrocarbons (CH_4, C_2H_4, …), CO, CO_2, H_2, liquid volatiles (water, methanol, acetone, acetaldehyde), mono phenols (phenol, guayacol or *o*-methoxyphenol, catechol or *o*-dihydroxybenzene, and other polysubstituted phenolic compounds. Many hydrocarbonous and complex phenol compounds with high boiling point are formed. The quantity of carbon produced depends strongly on the temperature of pyrolysis. With higher temperatures, the carbon yield and the time of pyrolysis are reduced, and more liquid products are obtained.

The basic constituents of tar, guaiacyl and syringyl (aromatic compounds), are usually stable up to about 500°C. During the treatment at temperatures above 500°C, the secondary decomposition occurs, resulting e. g. in the conversion of guaiacols into

catechols, and in the formation of tars. Thereafter, the decomposition of catechols into phenols can occur. Phenol and its derivatives are the only stable products of pyrolysis [Dorrestijn 2000].

In the products formed during the thermal treatment of our sample, one should find also some sulphuric compounds. These are usually present in Kraft lignins in amounts of c. 1.5 % (w/w). The reaction path of our sample could therefore be represented by the following scheme:

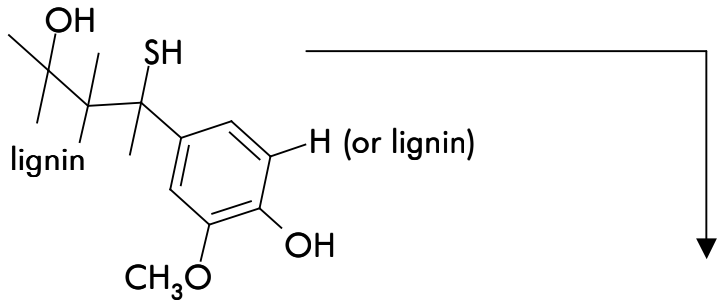

$CO_2 + CH_4 + H_2 + CO + C_2H_n + C_2$ + tar + sulphuric compounds

In the sulphuric compounds of the pyrolysis of the Kraft lignin, one could expect H_2S, CS_2 (in the experiments at high temperature), CH_2CSH, Ph-CH-SH, and other compounds.

In the table below (Tab. 9), kinetic parameters found by different researchers are cited.

Tab. 9: Kinetic parameters of lignin pyrolysis.

Reference	***k* [min^{-1}]**	***E* [kJ.mol^{-1}]**
Stamm [1956]	1.4×10^{10}	96.1
Nunn et al. [1985]	3.39×10^{5}	81.9
Cordero et al. [1990]	0.655	36.7
Suuberg et al. [1978]	10^{9}-10^{22}	125-292
Tang [1967]	0.93	37.6
Wenzl [1970]	—	97.8
Domburgs & Sergeeva [1971]	—	71-158
Avni & Coughlin [1985]	1.59×10^{10}	$58+250X$, if $X < 0.4$[a] 171, if $X > 0.4$[a]
Caballero et al. [1996]	$\ln(k_0) = 18.8 + 0.0208\ T^{*}$[d]	$52.64 + 0.172\ T^{*}$[d]

[a] X … degree of conversion; [b] using data from Nunn et al. [1985]; [c] using data from Avni and Coughlin [1985]; [d] $T^{*} = (T_R\text{-}273.15)$.

3.2.2.2 Cellulose

From the point of view of history, the most popular mechanism of the degradation of cellulose has been the mechanism of Shafizadeh (also called the Broido-Shafizadeh mechanism). This mechanism consists of three first-order reactions. The initial reaction (transformation of cellulose into active cellulose) is followed by a couple of competitive reactions accompanied by a weight loss. The first reaction is the depolymerization of cellulose in levoglucosan and other products that come up from its breaking, the second one generates carbon and gases as CO_2 and water vapour.

However, this mechanism is based on weight loss data. It has been discovered, from gaseous products analysis, that the major product of the cellulose pyrolysis is hydroxyacetaldehyde or glycol aldehyde. On that account, a modification of the mechanism appeared to be necessary.

Banyasz et al. [2001], on the basis of their evaluations of complex kinetic analyses (with the help of FTIR) of gases released in the course of rapid pyrolysis (upto from 400 to 800°C), have recently proposed the mechanism represented by this diagram:

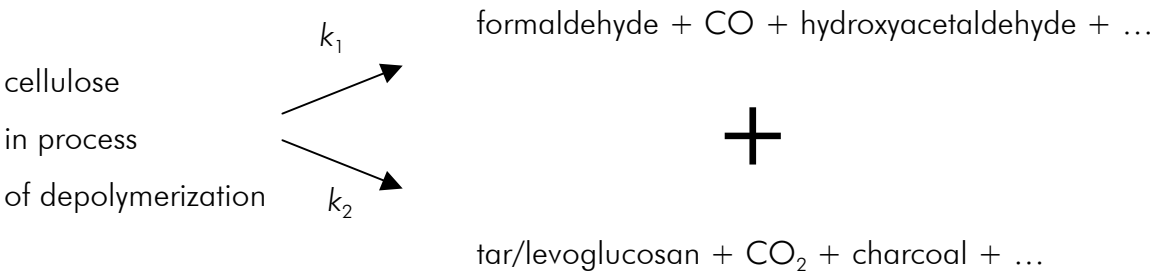

Fig. 29: Cellulose depolymerisation scheme.

Formaldehyde and CO are formed very rapidly prior to hydroxyacetaldehyde. The characteristic temperature of cellulose degradation is 350°C (623.15 K).

Using the coupling of DSC (differential scanning calorimetry) and TGA (thermogravimetric analysis), the influence of modifications of experimental conditions on the thermodynamic aspect of the decomposition process was studied [Milosavljevic et

al. 1996], under these conditions: purging inert gas (nitrogen or helium), with the heating rate of 0.1 to 60 $K.min^{-1}$, sample mass of 0.5 to 15 mg (in the form of powder).

The effect of the heating rate on the kinetics of the weight loss during the pyrolysis was important. On the basis of experimental results, heating rates can be classified into two groups: the high heating rate and the low heating rate, where the separating line is at 10 $K.min^{-1}$. The lower the heating rate, the higher the production of charcoal.

The main products of the pyrolysis were (w/w): tar (83 %), CO_2 (1.5 %), water (6.5 %), and charcoal (approx. 6 %). Some trace substances (e.g.: CO, methanol, acetaldehyde) were neglected and the missing weight was attributed to tar. Charcoal is considered here to be pure carbon.

The formation of charcoal is an exothermal process; the production of volatiles is endothermic. It is convenient to note that there is no value of the enthalpy of formation of cellulose that would be accepted by all research workers, as it depends on a particular type of cellulose, or, more precisely, on its properties as e.g. crystallinity.

For Broido-Shafizadeh mechanism, Di Blasi [1998] presents the following kinetic parameters:

$A_1 = 1.10^{18}\ s^{-1}$, $E_1 = 238\ kJ.mol^{-1}$,

$A_2 = 1.10^{9.4} s^{-1}$, $E_2 = 147\ kJ.mol^{-1}$, with the following experimental conditions:

T up to 703 K, heating rate 40 $K.min^{-1}$, 0.5-3 mg of cellulose, TGA;

and

$A_1 = 4.10^{17}\ s^{-1}$, $E_1 = 217.5\ kJ.mol^{-1}$,

$A_2 = 1.6.10^{14} s^{-1}$, $E_2 = 179\ kJ.mol^{-1}$, with the following experimental conditions:

$523\ K < T < 633\ K$, 90 mg of 0.076 thick cellulose disks; isothermal fluid bed.

In the same paper, along the above-mentioned Broido-Shafizadeh (sometimes also referred to as Modified Broido-Shafizadeh mechanism) other pyrolysis mechanisms are presented: Broido mechanism and Shafizadeh mechanism (semi-global pyrolysis mechanisms used for cellulose degradation); Koufopanos et al. mechanism, and Three-step mechanism (semi-global pyrolysis mechanisms usually used for wood and biomass degradation).

3.2.2.3 Ethylene vinyl acetate

At present, EVA (ethylene vinyl acetate) copolymers with different percentages of vinyl acetate (VA) are employed very broadly, particularly in the cable industry. Other uses can be cited: striped films, pipes, coatings, and adhesives [Gilby 1982]. EVA copolymers represent the most important part of the copolymer market. Their properties depend chiefly on the VA percentage. Usually, polymers containing from 2 to 40 % w/w VA can be found [Odian 1991].

The thermal degradation of EVA occurs in two stages. The first stage comes between 300 and 400°C (according to Mothé and Tavares [1997] around 340°C) and consists of the elimination of a molecule of acetic acid (desacetylation), whose consequence is the creation of an ethylene structure on the rest of the carbon chain, where the carbonyl function group was situated previously. Mechanisms proposed for this reaction are the radical one and that of the ionic β-elimination (McNeill [1989], Camino [1974]). According to Oliveira et al. [1999], the acetic acid formation is initiated by thermal scission of the C-O bond of the PVA (poly[vinyl-acetate]) chain. This break of the C-O bond is accompanied by the release of hydrogen atom of the adjacent carbon atom. A double bond is thus formed in the chain (i.e. the ethylene structure is formed) and the just adjoining C-O bond (on that account weaker than the others) is breaked in the sequence that marks the origin of the propagation stage of the chain reaction.

Munteanu and Turcu [1977] maintain that the decomposition of acetoxy groups is favoured by the aptitude to form (through the hydrogen bonds with the active methylene group) an intermediate cyclic structure state that promotes the transfer mechanism. This activated complex decomposes thereafter while eliminating acetic acid. Moskala and Lee [1989] have remarked that the acetic acid thereby produced can react with other polymer chains and so accelerate the overall weight loss. According to McGrattan [1993], the first stage of the degradation, characterised by the pyrolysis of acetate and the formation of polyunsaturated hydrocarbon chain, takes place around 370°C. A competitive reaction generating carbon monoxide, carbon dioxide and methane can occur also, but the acetate pyrolysis is always favoured over the others. In EVA (with 17.6 % of VA) pyrolysis products, Munteanu and Turcu [1977] have also found an indispensable quantity of acetone that can result from the acetic acid decomposition.

The elimination of acetic acid is the critical stage by reason of its relatively high volatility (its b. p. corresponds to 118.2°C at 1 atm). The reaction of elimination of the lateral group, in the course of which acetic acid is formed, occurs at temperatures lower than that which is indispensable for the PEA degradation (poly[ethylene-co-(acetylene)]). Acetic acid is completely eliminated before any explicit degradation of the resting chain of PEA begins [Oliveira 1999].

After the formation and removal of acetic acid, PEA begins to decompose in smaller chains through the random scission mechanism. The second stage of the EVA decomposition occurs around 425°C [Dutta 1995]; or at 470°C [Moskala 1989]. It is characterised by the stage of formation of "transvinyls", accompanied by the scission of the principal chain. The "trans" configuration of vinyl double bonds favours an intermolecular transversal concatenation (cross-linking) of molecules thus obtained [Munteanu and Turcu 1981].

McGrattan [1993] have observed that the saturated radical fragment formed by the scission of the chain on the bond neighbouring the double bond can either capture one hydrogen and produce a terminal methyl group, or loose one hydrogen and produce a vinyl group. From these two paths, he considers the first one to be more significant. Regarding the unsaturated fragment, it adds one hydrogen to produce a vinyl group. By the recurrence of this mechanism at the other end of the fragment, during the consecutive decomposition, alkane, alkene or 1,*n*-diene are finally generated.

The same authors have observed that after the treatment of EVA sample at the temperature of 530°C, there was no residue left.

Figures 30 and 31 on the next page represent the first and the second stage of the EVA decomposition, respectively.

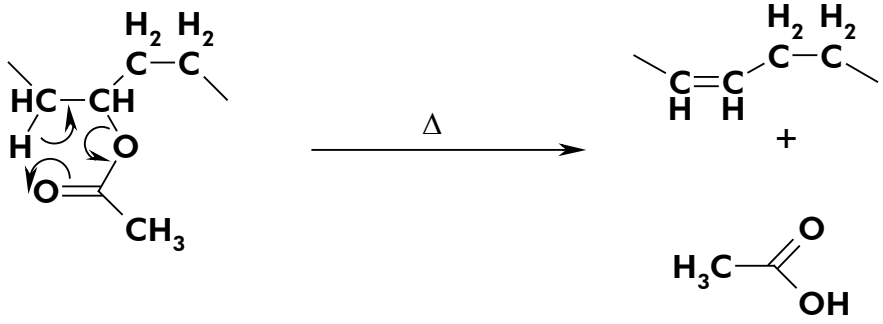

Fig. 30: Scheme of the first stage of the EVA decomposition.

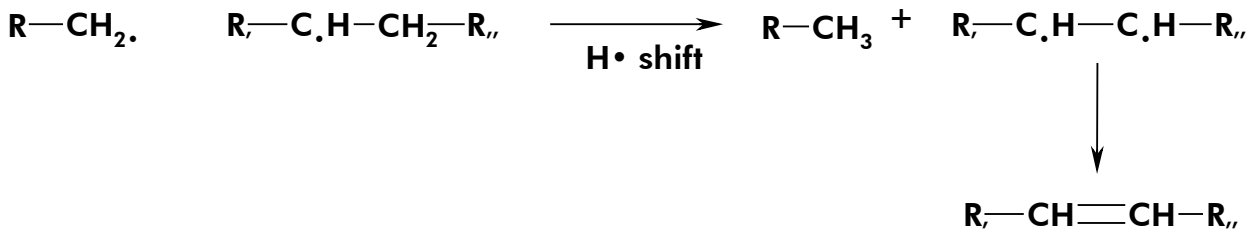

Fig. 31: Scheme of the reactions of the second stage of the EVA decomposition – formation of transvinyls and disproportionation of free radicals.

According to Dutta et al. [1995], the kinetic parameters of the thermal decomposition for both stages are the following:

- **activation energy of the $1^{st}/2^{nd}$ stage [$kJ.mol^{-1}$]:** 171.5 / 175.7,
- **frequency factor of the $1^{st}/2^{nd}$ stage [min^{-1}]:** $2.1.10^{14}$ / $3.9.10^{12}$,
- **reaction order for both stages:** 1.0.

Dutta et al. [1995] have done one FTIR analysis of pyrolysis products as well. Their results can thus be compared with those presented in this thesis. The spectrophotometric analysis carried out in framework of this work should also answer the question of whether the above-mentioned products are the only ones from the EVA pyrolysis. It seems that the formation of lactone or ketones described below (Fig. 32) could intervene in the stage of formation of acetic acid.

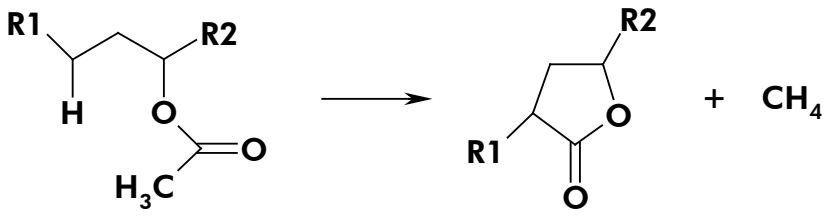

(*a*)

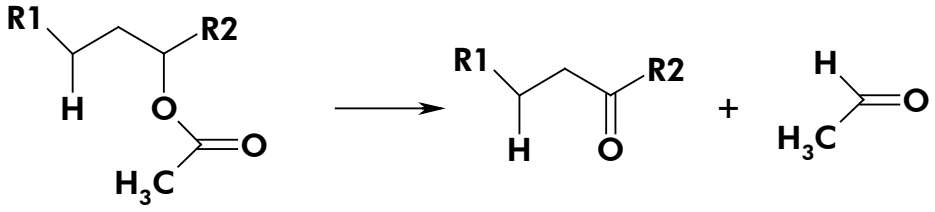

(*b*)

Fig. 32: Formation of lacton (*a*), formation of ketones and acetaldehyde (*b*).

Still for this first stage, Oliveira et al. propose more complex mechanisms. According to them, the formation of acetic acid is initiated by a thermal scission of C-O bond in the VA chain. This breaking of C-O bond is accompanied by elimination of hydrogen atom of the neighbouring carbon atom. Thus, double bond is produced in the chain.

3.2.2.4 Polystyrene

The PS degradation occurs mainly via photooxidation or thermal degradation. The thermal degradation consists of a single stage characterized by the rapid initial diminution of its molecular weight. The major volatile product of the pyrolysis of PS is monomeric styrene.

The primary products of the polystyrene pyrolysis are styrene and its oligomers. In the case that these are not immediately withdrawn from the reactor, the secondary products such as benzene, toluene, ethyl benzene and naphthalene begin to form by interactions of the primary products. From all the products of the polystyrene pyrolysis, the one that is the most in demand is styrene. It is one of the most important monomers worldwide and its polymers and copolymers are used in an increasingly wider range of applications, such as plastics, latex dyes and enamels, synthetic elastic materials, polyesters and styrene-alcyde coatings (Collins [1992], Miller [1994]).

In the process of polystyrene pyrolysis, styrene is produced as the liquid fraction. Thus, the industrial interest is to find conditions favourable to the formation of a higher amount of this fraction. In his experiments at vacuum, Karaduman and al. [2001] observed that the liquid fraction does not change its quantity significantly in the course of the increase of temperature. However, the quantity of the solid fraction is by this effect reduced and the gaseous fraction (that consists of CH_4 and some hydrocarbons of the series C_2, C_3, and C_4), as well as the total yield, puts on.

The graph on the next page (Fig. 33) represents the distribution of fractions in the course of the temperature variation.

From the point of view of the reaction mechanism, different speculations can be found in literature. Majority of them suppose the radical mechanism to be responsible for the thermal degradation of PS (e.g. Ebert [1982]). The initial elevated rate of the molecular weight diminution was elucidated by Jellinek [1948] and Grassie & Kerr [1959]. According to their interpretation, it is just the intervention of the scission of the weak bonds formed by the incorporation of oxygene in the form of peroxide groups into the chain during the polymerization. The depolymerization appears only after it. For Grassie and Kerr [1962], it is the presence of unsaturated structures of the polymer chain that is at the origin of the depolymerization. Others (Mardosky [1962], Wall [1966]) claim that

weak bonds do not play any important role in the degradation of polystyrene and that there is no essential difference in the mechanism regardless of the degradation stage. They affirm that molecular weight changes are firstly caused by transfer reactions of the intermolecular chain that succeed to the initiation stage. The reaction at the end of the chains generates primary radicals. Richards and Salter [1967] suggest that both processes, scission of weak bonds and intermolecular transfer, are similarly important.

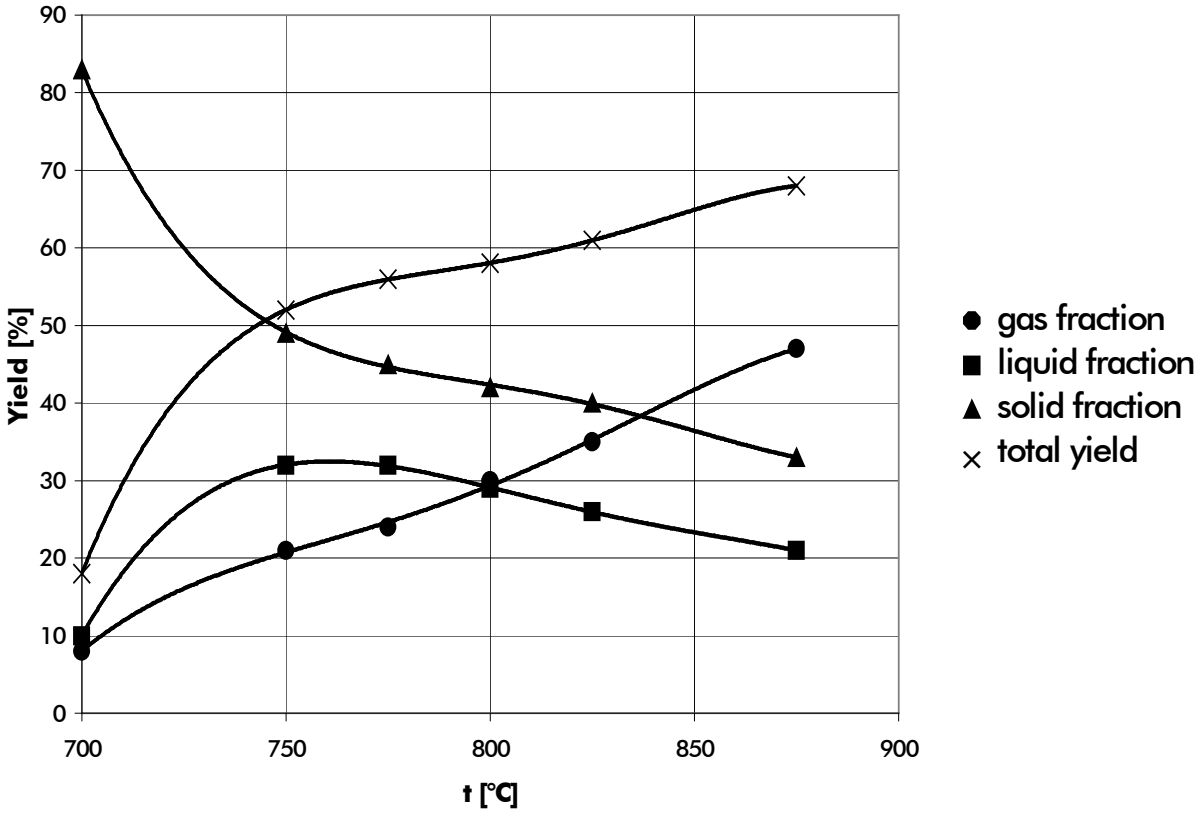

Fig. 33: Influence of temperature on PS degradation products; (experimental dots are inlaid with the curves of polynomials of the fourth order). N.B.: The correlation of experimental points with the polynomial curve ot the 4th order (added by the author of the present thesis) is motivated purely by an effort for graphical lucidity, as its appearance corresponds well with the experimental points and should answer the need for an interpolation.

Marcilla and Beltrán [1995b] have studied the PS kinetics and thermal degradation postulating two models. The first model, which is used most often, supposes that the polymer decomposition takes place in one and only stage. The second model assumes the formation of an intermediate state of PS. The decomposition of this one leads to the

formation of gases that add to those released during the first stage of their model of the PS degradation.

Follows a table (Tab. 10) with the corresponding kinetic parameters:

Tab. 10: Kinetic parameters of the PS decomposition [Marcilla and Beltrán 1995b].

Parameters / Model	Reaction order n [–]	Frequency factor k [min^{-1}]	Activation energy E_a [$kJ.mol^{-1}$]	Variation coefficient [%]
First model	0.07 / 1.0	$6.29.10^{14}$ / $1.27.10^{16}$	203.3 / 217.9	0.119 / 0.218
Second model	n_1: 0.51 / 1.0 n_2: 1.02 / 1.0 n_3: 0.80 / 1.0	k_1: $4.11.10^{16}$ / $2.01.10^{14}$ k_2: $3.67.10^{19}$ / 0 k_3: $8.58.10^{13}$ / $2.60.10^{16}$	E_1: 220.3 / 189.8 E_2: 276.6 / 2085.4 E_3: 186.9 / 216.5	0.054 / 0.064

3.2.2.5 Polyvinyl chloride

PVC or polyvinyl chloride is a thermoplastic material (atactic, and amorph). It is made by the process of radical polymerisation. The glass transition temperature is 80°C. Its most significant properties are hardness and rigidity. It is used in form of sheets, tubes, pipes, and as an insulator. Its chemical formula is $[CH_2CHCl]_n$.

From the point of view of pyrolysis, PVC is the most problematic among the polymers studied in the present thesis, due to release of HCl. It was also shown that the thermal decomposition of PVC can lead to the production of chlorinated hydrocarbons like e.g. chlorobenzene [Ida 1974].

PVC incineration can eventuate in the production of precursors of extremely toxic emissions, such as polychlorinated dibenzodioxins (PCDD), dibenzofurans (PCDF), and biphenyls (PCB) [Christmann 1989]. Corrosive effects of HCl were also, among other things, the reason for closing one pilot plant for pyrolysis of plastic wastes in Ebenhausen in Germany (1990) [Hinz 1994]. A detailed study of the PVC pyrolysis, particularly with a focus on the conditions of the HCl formation thus seems to be an important area of research with respect to recycling and environmental emissions.

Numerous studies have revealed two stages of the thermal decomposition of PVC. The first stage is found in the region of 200-360°C, the second one in the region from 360 to 500°C. The first stage consists in dehydrochlorination that is followed by the formation of conjugated double bonds accompanied by the formation of low quantities of hydrocarbons, essentially aromatic ones, as benzene, toluene, naphtalene, indene, anthracene, o-xylene, etc. In the course of the second stage, the polyene sequences formed in the first stage give place to scission.

Series model

The SIC (single ion current) analysis [Ballistreri 1980a, 1980b] has lead Marcilla & Beltrán [1995a] to propose a series model comprising three reactions to describe two stages of weight loss of PVC. The analysis has indicated that the formation of aromatic compounds takes place immediately on the apparition of polyene sequences in the chain. This means that a small proportion of unsubstituted aromatic compounds (benzene,

naphtalene and anthracene) is formed simultaneously with HCl, in the first stage of pyrolysis. Marcilla and Beltrán [1995a] have proposed the following reaction scheme:

$$\text{PVC} \xrightarrow{k_1} \text{a HCl} + \text{b I},$$

$$\text{b I} \xrightarrow{k_2} \text{c } V_1 + \text{e } R_1,$$

$$\text{e } R_1 \xrightarrow{k_1} \text{f } V_2 + \text{g } R_2,$$

where I designates the intermediate PVC, V_1 and V_2 volatile fractions produced in the second and the third reactions, respectively, R_1 solid residue generated during the second reaction and R_2 that produced in the third reaction.

The first reaction corresponds to the formation of HCl and of the intermediate product (I). The second reaction consists of the formation of some volatile substances (benzene, naphtalene, and anthracene), still a little of HCl that remained from the first process (V_1), and the formation of polyene chains (R_1). The third reaction represents the final stage of the PVC decomposition; it is made up of the formation of toluene and other aromatics (V_2), as well as the final residue R_2.

The first two reactions form the first stage of the degradation, the third reaction corresponds to the second stage of degradation, as is indicated in the table below.

The differential equations based on the above-mentioned kinetic model, together with corresponding kinetic parameters are cited below (Tab. 11). These equations are usually expressed in moles.

$$\frac{dR_2}{d\tau} = gk_3 \exp(-E_3 / RT){R_2}^{n_3} . \qquad (15)$$

Tab. 11: Kinetic parameters of PVC pyrolysis [Marcilla & Beltrán 1995a].

	Reaction order, n [–]	Frequency factor, k [min^{-1}]	Activation energy, E_a [kJ.mol^{-1}]	Yield coefficient	Variation coefficient [%]
1st stage	$n_1 = 0.46$	$k_1 = 1.65.10^{12}$	$E_1 = 136.8$	b = 0.889	0.031
	$n_2 = 1.54$	$k_2 = 3.95.10^{12}$	$E_2 = 146.5$	e = 0.380	
2nd stage	$n_3 = 1.62$	$k_3 = 4.70.10^{16}$	$E_3 = 239.1$	g = 0.123	

Parallel model

Miranda et al. [1999] have observed three stages of PVC decomposition, of which first two have a common domain. Their corresponding temperature regions (for the heating rate of 10°C.min^{-1}) are: 200-330°C (weight loss of 46 %), 220-375°C (weight loss of 18 %) and 375-512°C (weight loss of 30 %). The mass of solid residue was approx. 6 %. The cited values hold for experiments under vacuum; in experiments under nitrogen and atmospheric pressure, the quantity of the solid residue was nearly twice as high. Other parameters do not exhibit any important variation. The use of light-weight samples and small heating rates have apparently contributed to an easy discernment of the two first stages.

This model takes into account two structural varieties of PVC, the "head-to-head" (PVC_1) and the "head-to-tail" (PVC_2) structure. The first mentioned type presents the threshold value of thermal degradation that is inferior to one of the other type. The reason of this behaviour is an increased fragility of the bonds between atoms of chlorine in the "head-to-head" type of PVC.

$$PVC_1 \xrightarrow{k_1} \alpha_1 HCl + \gamma_1 Rs_1,$$
$$PVC_2 \xrightarrow{k_2} \alpha_2 (HCl + V_1) + \gamma_2 Rs_2,$$
$$\alpha_3 Rs \xrightarrow{k_3} \alpha_4 V_2 + \gamma_3 Rs_3;$$

where $Rs = Rs_1 + Rs_2$, and $\alpha_i \neq \gamma_i$.

The first equation represents the formation of HCl from the first type of PVC (PVC_1). Once the intermediate polyene (Rs_1) sequences develop in the chain, the third reaction begins. The second reaction shows that the second type of PVC (PVC_2) produces HCl. The formation of aromatics also takes place (V_1; principally benzene from the already formed polyene). The third reaction describes the evolution of substituted aromatics (toluene, naphtalene-methyl) from both the Rs_1 polyene that did not produce aromatics in the second reaction and the Rs_2 polyene formed from PVC_2.

On the contrary, Sakata et al. [1996] have observed just two regions of the weight loss, even if they have, likewise, chosen a low heating rate (4°C.min^{-1}). The sample weight (around 20 g) had apparently played an important role in this case, and did not allow

them to find the third stage that was mentioned just above. Other results (of Sakata et al. [1996]) are in a good agreement on these two regions: from 200 to 340°C and from 400 to 500°C. Howbeit, the attribution of decomposition products to different stages of the weight loss seems to be very problematic and unsound.

Some authors propose that the thermal decomposition of PVC takes place in two stages under atmospheric pressure and three stages under vacuum (Miranda et al. [1999], Chang [1974], Guyot [1973]).

Below, differential equations based on the before-mentioned model by Miranda et al. are presented.

For the purpose of calculation of kinetic parameters, the overall rate of PVC thermal decomposition can be considered as a summation of the rates of each individual reaction. Kinetic equations corresponding to the apparent reactions are described by the following equations:

$$1 = \sum_{i=1}^{3} \alpha_i , \tag{16}$$

$$\frac{dX}{d\tau} = \sum_{i=1}^{N} \alpha_i \frac{dX_i}{d\tau} , \tag{17}$$

where X_i is the conversion degree, the ratio between the weight loss at time "τ" of the reaction and the weight loss at the end of each stage; thus:

$$\frac{d[PVC]}{d\tau} = \alpha_1 \frac{d[PVC_1]}{d\tau} + \alpha_2 \frac{d[PVC_2]}{d\tau} + \alpha_3 \frac{d[(R)]}{d\tau} , \tag{18}$$

$$\frac{d[PVC]}{d\tau} = \alpha_1 (-A_1 e^{\frac{-E_{a1}}{RT}} [PVC_1]^{n_1}) + \alpha_2 (-A_2 e^{\frac{-E_{a2}}{RT}} [PVC_2]^{n_2}) + \alpha_3 (-A_3 e^{\frac{-E_{a4}}{RT}} [R]^{n_3}) . \tag{19}$$

In Table 12, the kinetic parameters obtained by Miranda et al. [1999] are presented, based on calculations using both the series model discussed in the previous section and the parallel one.

Tab. 12: Kinetic parameters of PVC pyrolysis [Miranda et al. 1999].

Heating rate [°C.min^{-1}]	**Stage**	**E_a [kJ.mol^{-1}]**	**n**	**A [min^{-1}]**	**Yield coefficient**
Series model	1	198	1.04	$3.57.10^{18}$	$b = 0.52$
(under vacuum)	2	143	1.15	$9.95.10^{10}$	$e = 0.36$
1, 5, 10, 20	3	243	1.58	$5.77.10^{16}$	$g = 0.06$
Series model	1	200	0.98	$2.18.10^{18}$	$b = 0.53$
(in N_2 atmosphere)	2	153	1.10	$1.26.10^{11}$	$e = 0.35$
1, 5, 10, 20	3	243	1.55	$6.47.10^{16}$	$g = 0.11$
Parallel model	1	182	0.98	$1.31.10^{15}$	$\alpha_1 = 0.47$
(under vacuum)	2	138	1.01	$1.12.10^{11}$	$\alpha_2 = 0.17$
1	3	243	1.55	$3.47.10^{17}$	$\alpha_3 = 0.35$
5	1	189	0.98	$1.82.10^{14}$	$\alpha_1 = 0.45$
	2	145	1.00	$4.86.10^{11}$	$\alpha_2 = 0.19$
	3	245	1.54	$3.26.10^{17}$	$\alpha_3 = 0.35$
10	1	189	0.98	$1.58.10^{14}$	$\alpha_1 = 0.46$
	2	143	1.03	$1.13.10^{11}$	$\alpha_2 = 0.18$
	3	245	1.50	$3.56.10^{17}$	$\alpha_3 = 0.36$
20	1	193	0.98	$3.40.10^{14}$	$\alpha_1 = 0.46$
	2	140	1.00	$1.36.10^{11}$	$\alpha_2 = 0.18$
	3	246	1.52	$3.56.10^{17}$	$\alpha_3 = 0.36$

In their study on municipal waste pyrolysis, Fontana et al. [2000] note that numerous investigations have been performed on the thermal degradation of PVC [Starnes et al., Knümman et al., Hsiung et al., Bockhorn et al., Murty et al., Patel et al.].

3.2.3 Analysis of experimental results

3.2.3.1 Lignin

Analysis of solid residue

In the case of lignin, the analysis of solid residue was carried out, on the ground of the availability of corresponding data for comparison in literature and for purposes of verification of the resolution of the FTIR apparatus. In the cases of other polymers, relevant reference data were not found and the analyses were also omitted because of time considerations.

Lignin samples underwent thermal treatment at 226, 300, 336, and 435°C; the untreated sample material FTIR spectra were compared with them. Spectra characteristic for lignin (see Tab. 13 on the next page) that make it possible to determine its presence in unknown samples are to be found in the following regions: 1510 cm^{-1}, 1600 cm^{-1} (aromatic ring vibration), and between 1470 and 1460 cm^{-1} (C-H deformations and aromatic ring vibration). These are bands of an aromatic skeleton.

The infrared spectra of our solid residues show a considerable decrease of the intensity of the band at 1510 cm^{-1}, beginning from the temperature of 300°C. The 1460 cm^{-1} band decreases from 226°C and almost disappears above 300°C.

The same holds for the bands at 1600 cm^{-1} and 1270 cm^{-1}. The carbonyl band that is situated generally between 1660 and 1770 cm^{-1} (in our case around 1730 cm^{-1}) is not observed at room temperature; however, beginning from 226°C, its intensity remains almost the same for all other temperatures. This could indicate that the C=O groups are not conjugated with the aromatic ring.

In conclusion, it can be said that the experimental data obtained with the help of FTIR spectrometry of solid residues allow affirming that between 226°C and 300°C, substantial modifications of the bands of certain functional groups take place. Between 330°C and 435°C, there is no distinguishable change of spectra, indicating that the structure is stable.

Tab. 13: Lignin IR absorption bands (according to Hergert [1971]).

Position [cm^{-1}]	Band origin
3450-3400	OH stretching
2940-2820	OH stretching in methyl and methylene groups
1715-1710	C=O stretching nonconjugated to the aromatic ring
1675-1660	C=O stretching conjugated to the aromatic ring
1605-1600	Aromatic ring vibrations
1515-1505	Aromatic ring vibrations
1470-1460	C-H deformations (asymmetric)
1430-1425	Aromatic ring vibrations
1370-1365	C-H deformations (symmetric)
1330-1325	Syringyl ring breaking
1270-1275	Guaiacyl ring breaking
1085-1030	C-H C-O deformations

The evolution of lignin structure deduced from the FTIR analysis of solid residue, described in the antecedent text, was compared with results found in literature. Principally, it corresponds with the found data. Still, there are slight deviations that can be ascribed to the lignin used (its different molecule structure) and different experimental conditions as well.

Concerning the thermal degradation of lignin, Fig. F-1[3] presents the TGA curve of the set of experiments with the heating rates of 10, 20, and 30 $K.min^{-1}$.

Next, the relation of α, the conversion degree, and t, the pyrolysis temperature, is shown in Fig. F-2. The curves are very clearly distinguishable from one another and their forms are regular. However, they display some irregularities in the induction region and also at the end of pyrolysis experiments. A more detailed study of the products evolved during the pyrolysis was not effectuated.

The next graphical output (Fig. F-3) shows the temperature history of pyrolysis experiments and any deviations from the linear programme of the TG furnace thereof. As can readily be seen, even from this not much detailed print, there is no significant temperature drift.

Clearly, the scatter of calculated activation energy values is more than significant. The reason for this can be understood from Fig. F-4, the derivative of the mass loss curve. Although it is not so manifest from the thermogram, there are more than one stage of the

[3] The letter F refers to the respective Appendix. Please see the Appendix F, beginning on p. 200.

degradation. Thus, the evaluation of kinetics based on just one degradation step cannot produce good results. Technical reasons obstructed a more detailed study.

Table E-1 presents frequency factors for two models estimated as the most convenient. The scatter seems to be quite important. The next table (E-2) presents activation energies.

3.2.3.2 Cellulose

The thermal degradation of cellulose is shown in Figure F-5, which presents the TGA curve of the experiments with the heating rates from 10 to 30 $K.min^{-1}$.

Next, the relation of α, the conversion degree, and t, the pyrolysis temperature, is shown in Fig. F-6. As you can see, the curves corresponding to the heating rate of 10 $K.min^{-1}$ are almost indistinguishable from one another. Thus, reliability of the runs can be ascertained.

The next graphical output (Fig. F-7) shows the temperature history of pyrolysis experiments and any deviations from the linear programme of the TG furnace thereof. As can readily be seen, even from this not very detailed print, there is no significant temperature drift. Only at about 150°C, for the runs at 20 and 30 $K.min^{-1}$, there is a slight deviation, caused probably by heat transfer.

Figure F-8 depicts energy of activation together with standard deviation values. The figure is presented herein as a matter of example; in the case of lignin and other polymers, the trends were analogous.

Frequency factor for Diffusion model 3 is $2.76.10^{13}$ s^{-1}. For F1 Model, calculation results in $4.61.10^{14}$ s^{-1}. The activation energy values for the whole set of three experiments, and for two separately chosen runs, are, respectively, 154.838, 178.115, and 164.404 $kJ.mol^{-1}$.

Unfortunately, no parallel experimental results were found in the available literature, i.e. no comparison can be made.

Tables E-3 and E-4 present the frequency factors for two models estimated as the most probable and the calculated activation energy values of cellulose pyrolysis, respectively.

3.2.3.3 Ethylene vinyl acetate

The pyrolysis behaviour of EVA will be discussed in this section. As was indicated in the theoretical section, there are different "types" of EVA polymer. They differ by their respective (weight) percentage of VA. Thus, experiments were performed with EVA with 12, 25, and 40 % of VA. Results for the first two types will be presented. The experiments of that with 40 % of VA were not evaluated completely, also because of the fact that this document is not meant to constitute a database of numbers.

The whole collection of figures are disposed as follows: the first set concerns EVA with 12 % of VA – TGA curve in Fig. F-9, $\alpha = f(t)$ in Fig. F-10, $t = f(\tau)$ in Fig. F-11. Fig. F-12 presents the relation between α and temperature, for the temperature values chosen in calculation of the best fitting kinetic model. Figures F-13 to F-19 present values of kinetic models functions corresponding to all heating rates, at different temperature ranges. From these graphs, the need was derived to separate the calculations of the best kinetic model into groups of the following heating rates: 1 and 2 $K.min^{-1}$; 5, 7, and 10 $K.min^{-1}$; and finally 15, 20, and 30 $K.min^{-1}$. The reason is obvious: the points corresponding to one specific particular kinetic model cannot be connected to form one straight line. This holds, to varying degrees, for all temperature ranges explored.

The ensemble of results presented in graphical form for EVA with 25 % of VA follows the same pattern. Their numbering begins at F-20 and ends at F-30.

At the end, the Fig. F-31 compares two curves coming from pyrolysis of "EVA 12" with two others coming from experiments with "EVA 25", at the same two heating rates. In this figure, the first step of degradation of "EVA 12" can be compared with that of "EVA 25". For the last mentioned type of EVA, there is a more significant loss of weight, which corresponds to the escape of VA representing a greater proportion of EVA composition.

The calculated values are higher in comparison with reference data (see p. 87). The number of experiments done in the framework of the present study and the mutual proximity of resulting parameters entitle to claim that the calculated values are reliable.

Tables E-5 and E-6 present frequency factors for two models estimated as the most probable, for the 1^{st} and 2^{nd} degradation step of EVA "12", respectively.

Tables E-7 and E-8 present frequency factors for two models estimated as the most probable, for the 1st and 2nd degradation step of EVA "25", respectively.

The calculated activation energies of the pyrolyses of EVA 12 and EVA 25 are tabulated in Fig. E-9 and E-10.

3.2.3.4 Polystyrene

The pyrolysis behaviour of PS is characterized by one and only degradation step, as is evident from Fig. F-32. It presents the TGA curves of the set of experiments with the heating rates from 1 to 20 $K.min^{-1}$.

The next figure (Fig. F-33) exemplifies a well-known phenomenon of thermogravimetry: the higher the heating rate, the more "to the right" the corresponding TG curves are situated. This is clearly visible even when the initial masses differ.

Next, the relation of α, the conversion degree, and t, the pyrolysis temperature, is shown in a graphical way (Fig. F-34). The curves are very clearly distinguishable and their form is quite regular. However, the curve corresponding to the heating rate of 10 $K.min^{-1}$ displays some odd behaviour. From the preceding charts, this could not be stated with positive certainty, as the corresponding sample mass was smaller and the singularity was not easily explicitly discernible from absolute magnitudes.

We have used the experimental values of the 10 $K.min^{-1}$ run, together with other six runs. Our results are very good even when this anomalous curve is included. No explanation for the behaviour was found nor any substitute data were available.

The next graphical output (Fig. F-35) shows the temperature history of pyrolysis experiments and any deviations from the linear programme of the TG furnace thereof. As can readily be seen there is no significant temperature drift, just occasional slight oscillations not exceeding several units of degrees centigrade.

Now, let us discuss the results concerning the frequency factor parameter, A. Table E-11 demonstrates temperatures at various degree-of-conversion values.

The next table, E-12, presents frequency factors for two models estimated as the most probable. The scatter seems to be quite important.

In Tab. E-13, the calculated activation energies are tabulated.

We could suggest that the value of activation energy for the set containing the heating rate of 10 $K.min^{-1}$ should not be considered a very reliable one. Instead, let us consider recalculating it by using just the heating rates of 5 and 7 $K.min^{-1}$. In Tab. E-14, you can find values for the three heating rates presented once again side by side with more reliable values, corresponding to just the first two of the heating rates.

Tabs. E-15 and E-16 provide a further correction on induction and associated phenomena. In Tab. E-17, summary calculated results for both the "0.1-α" and "0.2- α" values are presented.

To conclude, the final value of the E_a is presented once again: 189.513 $\pm$ 9.752 kJ.mol^{-1}.

3.2.3.5 Polyvinyl chloride

The pyrolysis behaviour of PVC is represented in Fig. F-36 by the TGA curves of the experiments with the heating rates 1, 2, 5, 10, 15, 20, and 30 $K.min^{-1}$.

The relation of α, the conversion degree, and t, the pyrolysis temperature, is shown in a graphical way in Fig. F-37. It can be noticed that the curves are very clearly distinguishable from one another and their forms are quite regular. However, the curve corresponding to the heating rate of 2 $K.min^{-1}$ displays some odd behaviour in the first degradation step. Also the curve corresponding to the heating rate of 20 $K.min^{-1}$ diverges somewhat from what one could expect. This latter fact is clearer from the Fig. F-37; from the Fig. F-36 it would rather appear that it is the curve corresponding to the heating rate of 30 $K.min^{-1}$ that deviates from the linear course to a certain degree. Whatever the case may be, the magnitude of the heating rate employed could readily explain it. Also, the mass of sample employed could play an important role. For the strange behaviour of the curve mentioned before, no explanation has been found.

The next graphical output (Fig. F-38) shows the temperature history of pyrolysis experiments and any deviations from the linear programme of the TG furnace thereof. As can readily be seen, even from this not very detailed print, there is no significant temperature drift.

Tables E-18 to E-20 present frequency factors for two models estimated as the most fitting, for the three degradation steps.

In the two following paragraphs, the mode of presentation of calculated values common to all examined materials will be briefly delineated.

Two columns under the names of models contain values from one set of calculations; thus, the second column does not mention any new value – the majority of them are reiterated and some values from the first one are just "excluded" – to lessen the deviation caused by the induction period, at around $\alpha = 0.1$, and similarly to compensate the behaviour around $\alpha = 0.9$.

In the section below, mean value, standard deviation, maximum value, minimum value, and the difference between two lastly mentioned, are calculated separately for each column, as to make the influence of the induction period and similar phenomena patent.

In Table E-21, calculated activation energies are indicated.

Thus, summary results with corrections are:

1st degradation step:

$A = 7.66.10^{9}$ s^{-1}, std. dev. $1.58.10^{9}$ s^{-1} (D3 model),

$A = 8.70.10^{10}$ s^{-1}, std. dev. $4.33.10^{10}$ s^{-1} (F1 model),

$E_a = 117.586$ kJ.mol^{-1}, std. dev. 2.734 kJ.mol^{-1};

2nd degradation step:

$A = 8.89.10^{15}$ s^{-1}, std. dev. $5.60.10^{15}$ s^{-1} (D3 model),

$A = 8.61.10^{16}$ s^{-1}, std. dev. $4.10.10^{16}$ s^{-1} (F1 model),

$E_a = 197.495$ kJ.mol^{-1}, std. dev. 3.212 kJ.mol^{-1};

3rd degradation step:

$A = 1.22.10^{17}$ s^{-1}, std. dev. $1.67.10^{17}$ s^{-1} (D3 model),

$A = 1.81.10^{18}$ s^{-1}, std. dev. $2.85.10^{18}$ s^{-1} (F1 model),

$E_a = 255.402$ kJ.mol^{-1}, std. dev. 8.778 kJ.mol^{-1}.

The calculated results seem to be very reliable, standard deviation of 3.4 % maximum from the mean value is very low.

Comparing the results with those cited for the series model of Marcilla & Beltrán [1995a], frequency factors values are very dissimilar. Values of the activation energy are closer, but don't match either: 136.8 kJ.mol^{-1}, 146.5 kJ.mol^{-1}, 239.1 kJ.mol^{-1}, for the first, second, and the third degradation reaction, respectively (see Tab. E-21). Frequency factors cited by Miranda et al. for their parallel model (pyrolysis under vacuum), can be seen, together with more closely matching E_as (for the 3rd degradation; the values for the first and second step show opposite tendency to the one observed in our experiments), in Tab. 12 (p. 96); they are (e.g. for the heating rate of 5°C.min^{-1}, parallel model): $1.82.10^{14}$, $4.86.10^{11}$, $3.26.10^{17}$ min^{-1}, and 189, 145, 245 kJ.mol^{-1} — for the frequency factors and activation energies of the first, second, and the third degradation reaction, respectively.

It can be concluded that there is an overall agreement of the calculated activation energy with the values found in literature for all three stages of pyrolysis. The calculated results match with the references especially well in the case of the third stage of the thermal degradation.

3.2.4 Discussion and conclusions

In this first part (Part A) of the presented thesis, evaluation of kinetic parameters of pyrolysis from thermogravimetric data based primarily on the Ozawa-Flynn-Wall method (Popescu's modification) was realized.

Polymers studied include: lignin, cellulose, ethylene vinyle acetate copolymer, polystyrene, polyvinyl chloride.

In the case of *lignin*, it was found that the evaluated values were very scattered. The need of examining the degradation behaviour from the point of view of mass loss derivative came from it; this study, however, could not be completed due to time considerations. The analysis of solid residue of lignin, by the means of FTIR spectrometry, was also briefly discussed.

In section 3.2.3, a more detailed study of pyrolysis can be found, including the analysis of solid residues by the FTIR spectroscopy.

The mean values of the frequency factors were $2.25.10^{44}$ s^{-1} for the Diffusion model 3 and $1.84.10^{45}$ s^{-1} for the F1 Model (Reaction order = 1). The mean value of the activation energy was 454 $kJ.mol^{-1}$. As one can see, two methods of evaluating kinetic parameters did not produce comparable results (see Appendix G and p. 80). The activation energy values found in literature (p. 47) are much lower, their maximum lies around 300 $kJ.mol^{-1}$. However, the analysis of FTIR spectra of pyrolysis gas (not presented due to space considerations) and solid residues gave a valuable insight into and corroborated the reaction mechanism presented in the theoretical section.

In inert atmosphere, *cellulose* is relatively stable. The adsorbed water on cellulose is probably the first compound eliminated when cellulose is heated. This process is not taken for pyrolysis. Between 200°C and 220°C cellulose loses some more water. A more significant weight loss starts only around 300°C. As concluded from FTIR analysis, the main initial pyrolysis steps probably are side group elimination of water (taking place around 350°C) and chain scission reactions (predominant at higher temperatures). The reaction of levoglucosan formation is one of the main paths in pyrolytic decomposition of cellulose above 400°C.

The frequency factor for Diffusion model 3 is $2.76.10^{13}$ s^{-1}. For F1 Model, calculation results in $4.61.10^{14}$ s^{-1}. The activation energy values for the whole set of three experiments, and for two separately chosen runs, are, respectively, 155, 178, and 164 $kJ.mol^{-1}$.

EVA co-polymer was treated in a little bit more detailed manner, especially its kinetic model aspect. Two "types" of EVA were presented, one with 12 % of VA, the other with 25 % of VA. Higher values than those found in literature were calculated for both the activation energy and the frequency factor values.

FTIR analysis of pyrolysis gases confirmed the descriptions of the process found in literature (see the example in Appendix F). The pyrolysis of EVA occurs in two stages. The first stage of the degradation of EVA, characterised by the pyrolysis of acetate and the formation of polyunsaturated hydrocarbon chain, takes place around 370°C. The competitive reactions generating carbon monoxide, carbon dioxide and methane can eventuate also, but the acetate pyrolysis is always favoured over the others. The second stage begins between 420°C and 450°C. It is characterised by the stage of formation of "transvinyls", accompanied by the scission of the principal chain.

The calculated frequency factors for "EVA 12" are: $6.39.10^{15}$ s^{-1}, $2.41.10^{16}$ s^{-1}, for the first stage of degradation and R3 (Contracting volume 3) model and F1 (Reaction order = 1) model, respectively; $2.07.10^{18}$ s^{-1}, $7.75.10^{18}$ s^{-1}, analogously for the second stage of degradation. The values of the activation energy are: 200 $kJ.mol^{-1}$ for the first stage, 271 $kJ.mol^{-1}$ for the second stage of pyrolysis.

The frequency factors calculated for "EVA 25" are: $2.84.10^{15}$ s^{-1}, $1.08.10^{16}$ s^{-1}, for the first stage of degradation and R3 (Contracting volume 3) model and F1 (Reaction order = 1) model, respectively; $4.85.10^{21}$ s^{-1}, $1.77.10^{22}$ s^{-1}, analogously for the second stage of degradation. The values of the activation energy are: 194 $kJ.mol^{-1}$ for the first stage, 317 $kJ.mol^{-1}$ for the second stage of pyrolysis.

The practical importance of the study of *PS* pyrolysis can be inferred from the fact that styrene is one of the most important monomers worldwide and its polymers and copolymers are used in an increasingly wider range of applications.

The thermal degradation consists of a single stage characterized by the rapid initial diminution of the molecular weight. Primary products of the polystyrene pyrolysis are styrene and its oligomers. In the case that these are not immediately withdrawn from the reactor, secondary products such as benzene, toluene, ethyl benzene and naphthalene begin to form by interactions of the primary products. From the perspective of pyrolysis mechanism, PS undergoes some depolymerisation and some side group scission.

Little lower values were calculated than those announced by other authors (see p. 93). The frequency factor values are $3.38.10^{14}$ s^{-1} for the AE2 (Avrami-Erofeev 2) Model and $4.14.10^{14}$ s^{-1} for the F1 Model, the final value of the activation energy was evaluated as 190 $kJ.mol^{-1}$. The corresponding value presented by Marcilla and Beltrán [1995b] is 203 or 218 $kJ.mol^{-1}$.

The determined mean values of kinetic parameters for the three degradation steps of the pyrolysis of *polyvinyl chloride* were correlated with results found in literature; experimental conditions and the way of evaluation were slightly different. However, a good accord was found.

PVC began to volatilize between approx. 230°C and 260°C, depending on heating rate. This first stage of thermal decomposition, ending around 360°C, consisted mainly in dehydrochlorination and the formation of conjugated double bonds accompanied by the formation of low quantities of hydrocarbons, essentially aromatics. The polyene sequences were thereafter subject to scission, from around 370°C up to the end of the weight loss, around 530°C.

From the point of view of pyrolysis mechanism, PVC is characterized by the side group scission (a.k.a. side group elimination or chain-stripping). Theoretically, it is confirmed by the fact that the C-Cl bond has lower energy of 330 $kJ.mol^{-1}$ compared to the energy of the C-C bond of at least 350 $kJ.mol^{-1}$. The groups attached to the side of the backbone are cleaved and the resulting backbone becomes polyene (polyunsaturated). From the conjugated double bond backbone, the formation of aromatic compounds is relatively straightforward. The conjugated chain will readily break randomly at a C-C bond, yielding to aromatic compounds such as benzene, toluene, ethylbenzene, styrene and napththalene. Some authors say that the degradation of PVC starts at about 250°C

and HCl commonly represents more than 95 % of the volatiles produced [Drysdale, 1985; Madorsky, 1984]. This corresponds with our results.

The calculated kinetic parameters were:

1st degradation step:

$A = 7.66.10^{9}$ s^{-1}, std. dev. $1.58.10^{9}$ s^{-1} (D3 model),

$A = 8.70.10^{10}$ s^{-1}, std. dev. $4.33.10^{10}$ s^{-1} (F1 model),

$E_a = 118$ kJ.mol^{-1}, std. dev. 3 kJ.mol^{-1};

2nd degradation step:

$A = 8.89.10^{15}$ s^{-1}, std. dev. $5.60.10^{15}$ s^{-1} (D3 model),

$A = 8.61.10^{16}$ s^{-1}, std. dev. $4.10.10^{16}$ s^{-1} (F1 model),

$E_a = 197$ kJ.mol^{-1}, std. dev. 3 kJ.mol^{-1};

3rd degradation step:

$A = 1.22.10^{17}$ s^{-1}, std. dev. 1.67×10^{17} s^{-1} (D3 model),

$A = 1.81.10^{18}$ s^{-1}, std. dev. 2.85×10^{18} s^{-1} (F1 model),

$E_a = 255$ kJ.mol^{-1}, std. dev. 9 kJ.mol^{-1},

with the maximum standard deviation of 3.4 % from the mean value.

Possible prospects for the present study would be particularly to evaluate kinetic parameters with yet another method, e.g. the method of Friedmann, which is of a different type (differential one). Also, a deeper study of measuring techniques and factors linked to them would surely prove fruitful.

3.3 Part B

Kinetic study of thermal degradation of polymers – numerical resolution of kinetic equations obtained from reaction pseudo-schemes (model-fitting method)

3.3.1 Lignin

Kinetic model used was that developed by Pascali and Herrera [1997]. In pyrolytic experiments, Kraft lignin obtained from Aldrich Chemical Company was used, data relative to its mass loss were collected by a thermogravimetric analysis apparatus. As the calculations relative to the chosen model were programmed in the MatLab software, comparison of experimental data with theoretical ones was possible.

Analysis of these results allows claiming that the choice of the above-mentioned model is pertinent as the theoretical curves correspond well with experimental data. On top of that, reaction order seems to be constant and independent of temperature.

Among studied articles from literature sources in relation to the thermal degradation of lignin and at the same time presenting a mathematical model linked to a kinetic scheme, the work by Pascali and Herrera [1997] came in focus, as it was by far best documented. In fact, the paper expounded in detail operation conditions, contained a table with results and graphical description of experiments in form of thermogravimetric curves.

However, it was found that the mathematical equation representing the model contained a mistake. Data in table did not tally with the equation. Instead of $[-\ln(1-x)^{1/n}] = k.T$, as is found in the paper, $[-\ln(1-x)]^{1/n} = k.T$ is the correct reading.

Expected results

First, it must be noted that the apparatuses used for the present study are not the same as Pasquali and Herrera [1997] used. Also, the type of lignin molecule differs from the one mentioned in the referenced paper.

Results relative to kinetic parameters of the paper are following: activation energy, E_a, rests constant, at 27,500 J.mol^{-1}, whatever the isothermal temperature plateau may be.

Tab. 14: Results obtained by Pascali and Herrera [1997].

Temperature, t [°C]	Reaction order, n [—]	Frequency factor, A [s^{-1}]
226	0.52	63.43
242	0.52	79.02
279	0.48	68.87
315	0.45	50.91
341	0.46	53.07
410	0.43	47.03
435	0.42	52.07

It is supposed that a constant reaction order and activation energy around 0.5 and 28,000 J.mol^{-1} respectively, could be obtained, for all isothermal temperature program plateaus. The frequency factor value oscillates between 50 and 80 s^{-1}.

Numerical resolution of the model, as calculated from kinetic experiments

The values chosen on the basis of the data from the paper by Pascali and Herrera [1997] were used for initialisation of numerical treatment: n = 0.5; A = 59.2 s^{-1}; E_a = 27,440 J.mol^{-1}.

Tab. 15: TGA kinetic analaysis values by Pascali and Herrera [1997].

Temperature, t [°C]	Reaction order, n [—]	Frequency factor, A [s^{-1}]	Activation energy, E_a [J.mol^{-1}]
226	1.01	0.707	27,499
242	1.60	1.88	27,499
279	0.69	0.37	27,498
300	1.57	0.94	27,499
315	0.63	0.31	27,500
336	4.56	0.57	27,499
410	0.42	0.65	27,503
435	0.37	1.27	27,499

After analysing of the above-mentioned results, the following conclusions can be drawn: mean reaction order n = 0.68; mean activation energy E_a = 27,512 J.mol^{-1}; the mean value of A cannot be evaluated on the ground of too significant variations.

Operating methods

The type of lignin studied in the paper is Quebracho Colorado and is coming from one type of so-called hard wood. From the point of view of granulometry, it can be characterized by the range of values 40-60 μm. Lignin used in our experiments is coming from a sample of Aldrich company (see references in Tab. 7). The cost of the sample is 222 F for 100 g. It is distributed as a fine brown powder.

A set of thermogravimetric analyses at different isotherms was carried out. Studied temperatures were: 226°C, 242°C, 279°C, 315°C, 341°C, 410°C, 435°C, the same as were used in the paper. Moreover, experiments with isotherms at 300°C and 336°C were effectuated, because lately, an analysis of solid residue by the means of Fourier transformation infra-red spectrometry (FTIR) was done (see afterwards).

Referenced paper mentioned samples of 2.5 mg, samples used in the thesis were between 40 and 90 mg.

The atmosphere employed was N_2 for both the paper and experiments. In the paper, its flow was 50 $cm^3.min^{-1}$. During experiments, gas flow was not mastered perfectly; it alternated in the range between 33 and 38 $cm^3.min^{-1}$.

In the paper, pyrolysis time was fixed at 1 hour and 30 minutes, while the experiments done took 130 minutes, with the exception of the experiment at 226°C that filled up just 1 hour.

Temperature programme

Temperature programmes consist first of a slope of heating rate theoretically amounting to 50°C.min^{-1}, followed by a phase of adjusting to a milder gradient. As a matter of fact, it can be seen that at the end of the sequence with the high gradient of growth of temperature, the mandatory temperature is not attained. Only during the next sequence with much lower gradient, this mandatory value is arrived at. And this sequence takes the same time as the first one, which doubles the time needed to attain the mandatory temperature value. Consequently, mass loss appearing in the stage of growth of temperature is not insignificant.

Test of determination of the plateau of the temperature in focus

In order to verify that the pyrolysis of a sample of lignin runs well at the temperature plateau used in the paper, a thermogravimetric analysis with the slope from room temperature to 850 °C was carried out.

The mass loss curve contains 3 inflection points:

• the first one corresponds to release of water, is situated at 100 °C, and it is indeed an endothermic process;

• the second one is situated at 320°C and corresponds to the reaction which is running between 130 and 750 °C;

• the third one is situated at 775 °C and corresponds to the reaction between delimited by 750 °C and 800 °C; this one is on a very mild bracket and seems to agree with what is described in literature as a secondary pyrolysis of lignin (secondary pyrolysis is not, however, subject matter of our study); this reaction is endothermic.

The temperature range studied in the article, i.e. 226-435°C, is well included in the reaction zone of our lignin, i.e. 130-750°C.

Results

Obtained curves allow to monitor, in function of time:

- mass loss in percentage of the mass on input;
- derivation of the mass loss (DTG) in percentage by time.

Temperature programme

Tab. 16 gives a comparison of mass loss data obtained in experiments with those from the paper by Pascali and Herrera [1997], together with the time needed to attain the mandatory temperature.

Tab. 16: Comparison of literature and experimental results.

Temperature [°C]	Mass loss – experimental –	Mass loss – referenced –	Time to mandatory temperature
226	8 %	16 %	22min 10s
242	11.5 %	36 %	18min 22s
279	17.4 %	44 %	18min 54s
315	34.7 %	46 %	16min 21s
341	32 %	52 %	13min 30s
410	45.2 %	64 %	10min 00s
435	44.25 %	72 %	16min 27s

It is observed that the loss mass is increasing with rising temperature from 226 to 410°C. Above 410 °C, mass loss seems to lose connection with temperature development.

The observed differences between experimental mass loss and the ones from referenced paper can be chiefly explained by diverse natures of the two lignin types.

Numerical model

The kinetic equation of the lignin pyrolysis is represented by the following mathematical expression:

$$[-\ln(1-x)]^{1/n} = k.t, \qquad (20)$$

where: $x = (m_i-m_t)/(m_i-m_f)$,

and: m_i is the initial mass of lignin sample,

m_t is the instantaneous mass of lignin in the course of pyrolysis,

m_f is the final sample mass;

next: n is the reaction ordee,

and: k is a parameter depending on pyrolysis temperature, as e.g.:

$$k = A.\exp[-E_a/(RT)], \qquad (21)$$

where: A is frequency factor [s^{-1}],

E_a is activation energy [$J.mol^{-1}$],

R is ideal gas constant (R= 8.314 $J.mol^{-1}.K^{-1}$),

T is pyrolysis temperature [°K].

This model is used with constant temperature (a possible slope is neglected), which makes it more easily applicable. For this reason, it was chosen and preferred against other models proposed in the available literature.

Using this model allows us to determine lignin mass within time:

$$m = m_i - (m_i - m_f).(1-\exp(-(k.t)^n)), \text{ where } k = A.\exp[-E_a/(RT)]. \quad (22)$$

Model constraints

Strictly speaking, lignin pyrolysis does not run at constant temperature, because the experimental configuration at our disposal is binding us to submit sample to the temperature slope of the furnace in question. This constitutes an important source of error in exploitation of results.

Another source of error is represented by the necessity of a "blank", carried out in order that the variation of sample mass be determined. In fact, questions regarding reproducibility conditions in relation of a blank to an experiment with sample can gain on importance.

On the ground of these sources of incertitude, it was agreed that as constant temperature conditions, a variation of 1°C would be acceptable.

Numerical resolution of the system

The purpose of the numerical programme developed in MatLab is the determination of kinetic parameters – n, Ea, and A – by methods of parametric identification. In other words, an effort is being made to adjust the parameters of the mathematical model from a series of experimental results by minimisation of objective function (MatLab function "lsqcurvefit").

The developped programme is consists of four main parts:

1) Initialisation of parameters;

2) Loading of experimental data;

3) Minimisation of objective function;

4) Graphical exploitation of results.

Ad 1) Initialisation of parameters: In this stage, constants of the mathematical model are retrieved.

Ad 2) Loading of experimental data: Just some of experimental data was preserved – those where temperature is constant and equals the studied isotherm with tolerance of 1°C.

Ad 3) Minimisation of objective function: The used method is the "least squares method". In MatLab, there are several functions at one's disposal, more or less efficient, as per the problem of parametric identification solved. For the present thesis, function "lsqcurvefit" was chosen.

Ad 4) Graphical exploitation of results: By this expression, a trace of experimental and theoretical masses in function of time is meant. A good degree of superposition of both curves allows validation of mathematical model at experimental temperatures.

Tab. 17: Results of the simulation.

Temperature zone [°C]		N [—]	A [min^{-1}]	Ea [$J.mol^{-1}$]	Residue []
229 ± 1	228 – 230.25	1.012	0.698	27,444	7
286 ± 1	285 – 286.67	0.698	0.366	27,466	27
323 ± 1	322 – 323.32	0.633	0.309	27,459	57
418 ± 1	417 – 418.78	0.421	0.645	27,445	42

Residue is calculated using the following expression:

$$R = \frac{\sum \left(m_{theo} - m_{\exp} \right)^2}{1 + \exp\left(\frac{T_0 - T}{T_0} \right)}, \tag{23}$$

where m_{theo} **is the theoretical sample mass,**

$m_{\exp}$ **is the experimental sample mass,**

T **is the instantaneous temperature,**

and T_0 **is the desired isothermal plateau temperature.**

The term in the denominator is a factor of weight. With its growth, the "credibility" of the calculated point is being diminished. In other words, the more T departs from T_0, the less this term is taken into account in identification of parameters.

Analysis of results

Analysis of results is done in two stages:

-I- by an analysis of theoretical and experimental mass loss evolution of lignin sample in time for each and every isothermal temperature plateau,

-II- by a global analysis of kinetic parameters determined experimentally, and by comparing it with results furnished by Pascali and Herrera [1997].

Ad -I- Analysis of theoretical and experimental mass loss evolution of lignin sample

For each and every isothermal temperature plateau, the numerical programme developed enables to accede to the reaction order, activation energy, frequency factor. Consequently, from these values, the programme calculates the theoretical mass loss of lignin sample in time.

Values of calculated kinetic parameters are considered correct if curves "experimental mass loss of lignin sample in time" and "theoretical mass loss of lignin sample in time" embody a good degree of superposition.

The graphics below exemplifies one of temperature plateaus:

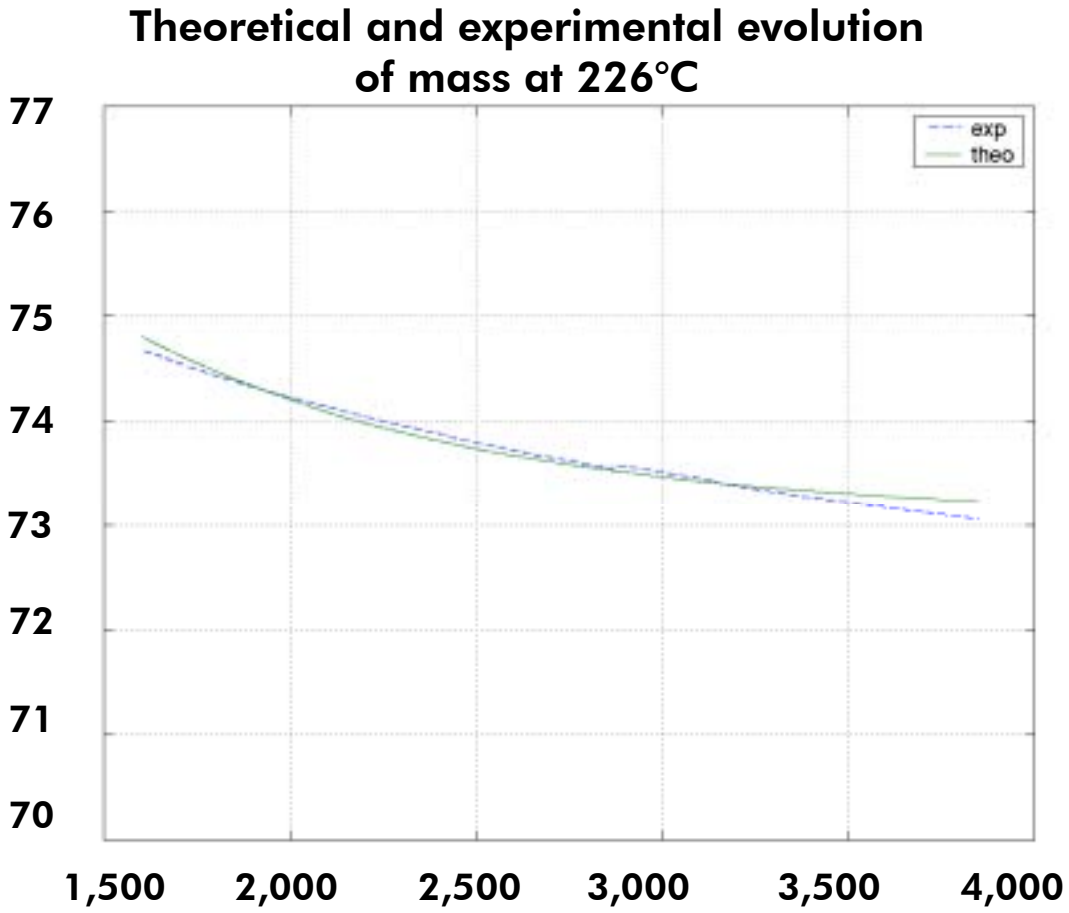

Fig. 34: Mass loss theoretical and experimental values at 226 °C isothermal plateau. X: time in seconds, from 1,500 to 4,000, Y: relative mass, from 70 to 77 %.

Taken as a whole, the superposition of experimental and theoretical curves is good, which gives a good ground for claiming that the chosen kinetic model is appropriate. Likewise, it can be supposed that the kinetic parameters calculated via this model are correct.

Ad -II- Global analysis of kinetic parameters

The following table (Tab. 18) shows the whole set of kinetic parameters calculated for all isothermal temperature plateaus examined.

Tab. 18: Kinetic parameters for isothermal experiments with lignin.

Temperature, t [°C]	Reaction order, n [—]	Frequency factor, A [s^{-1}]	Activation energy, E_a [$J.mol^{-1}$]
226	1.01	0.707	27,499
242	1.6	1.88	27,499
242 (rptd)	0.54	0.71	27,488
279	0.69	0.37	27,498
279 (rptd)	0.66	0.4	27,500
279 (mean value)	0.67	0.38	27,499
300	1.57	0.94	27,499
315	0.63	0.31	27,500
336	4.56	0.57	27,499
336	0.61	0.28	27,521
410	0.42	0.65	27,503
435	0.37	1.27	27,499
435 (rptd)	1.01	0.31	27,607
435 (mean value)	0.68	0.8	27,528

N.B.: Only results in shaded cells were used for analysis. These results seemed to be the most probable with respect to the expected ones. Some of these results were also mean values obtained from duplicating of experiments. Exploitation of these results is interesting only by comparing them with results of Pascali and Herrera [1997].

Comparison of reaction orders

First of all, it is evident that the value of reaction order for the experiment at 300°C (1.57) stands considerably out against the others. Therefore, it could be regarded as an experimental error or a modification of reaction mechanism. Consequently, it was deemed legitimate to eliminate this point in the frame of the used model. Thus, the following chart is obtained:

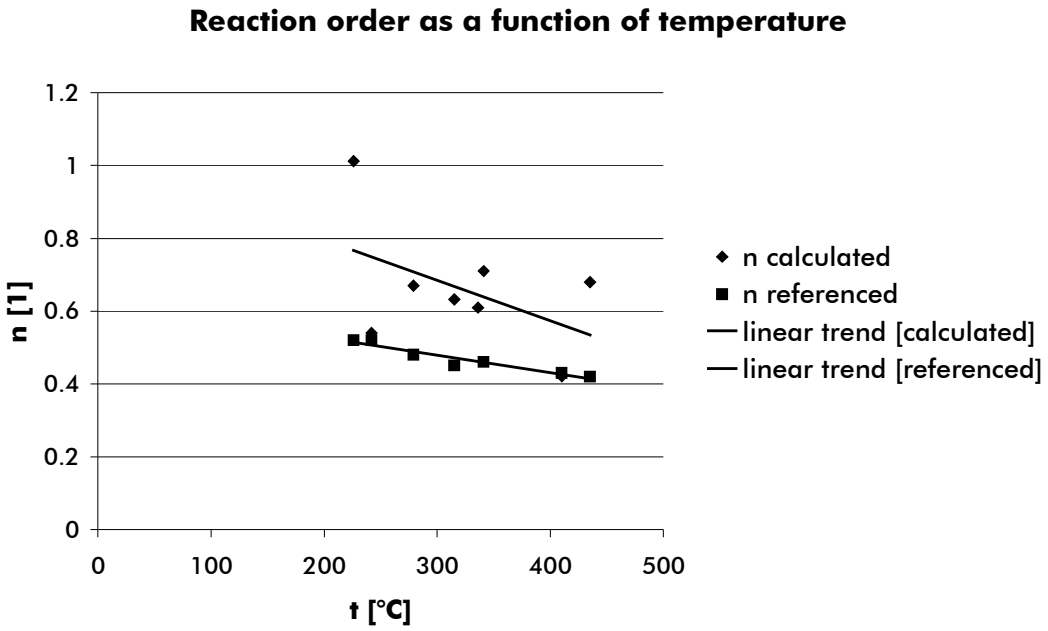

Fig. 35: Reaction order as a function of temperature. For calculated data y = -0.0011.x + 1.0192, R^2 = 0.2372; for referenced data, y = -0.0005.x + 0.623, R^2 = 0.9165.

To conclude, the chosen kinetic model could lead one to suppose a constant reaction order equal to approx. 0.65, in the range of temperatures from 200 to 450°C.

Comparison of frequency factors:

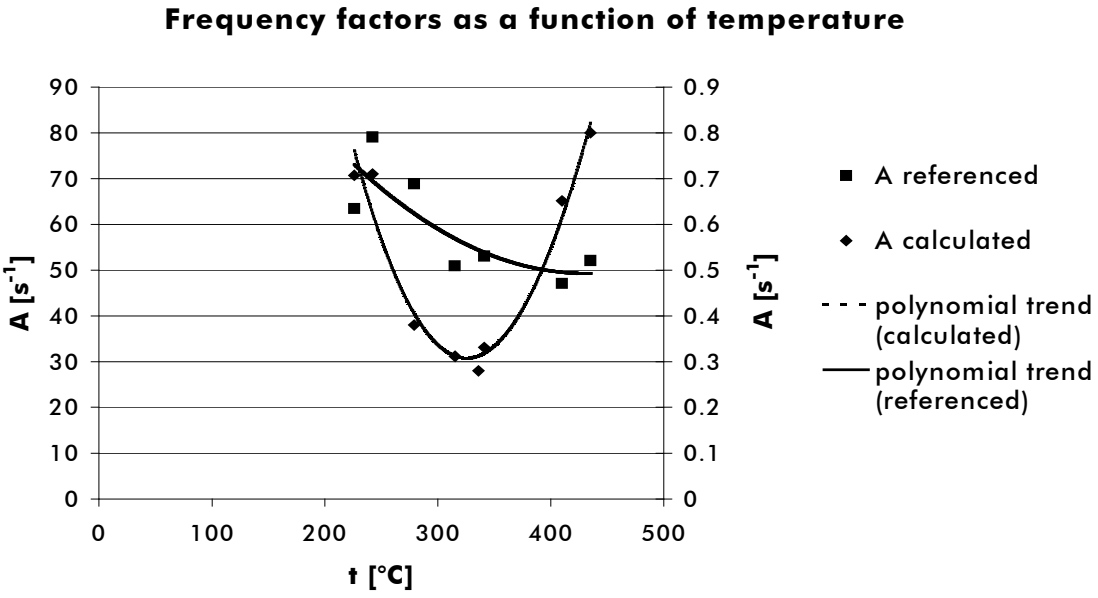

Fig. 36: Frequency factor as a function of temperature.

Results relative to frequency factor are much more ambiguous for analysis.

Very globally speaking, the same variation of frequency factor is found comparing our numerical results with data in the paper in question (minimum for experimental results is found at 315°C, whereas minimum from the data in the paper is at 400°C).

Notwithstanding, the calculated values oscillate between 0.3 and 1 s^{-1}, while the data from the paper oscillate between 45 and 80 s^{-1}. Calculated values are thus 80 to 150 times smaller than what could be expected. Hence, it is difficult, indeed even impossible, to pronounce a conclusion in matter of frequency factor.

Comparison of activation energy values:

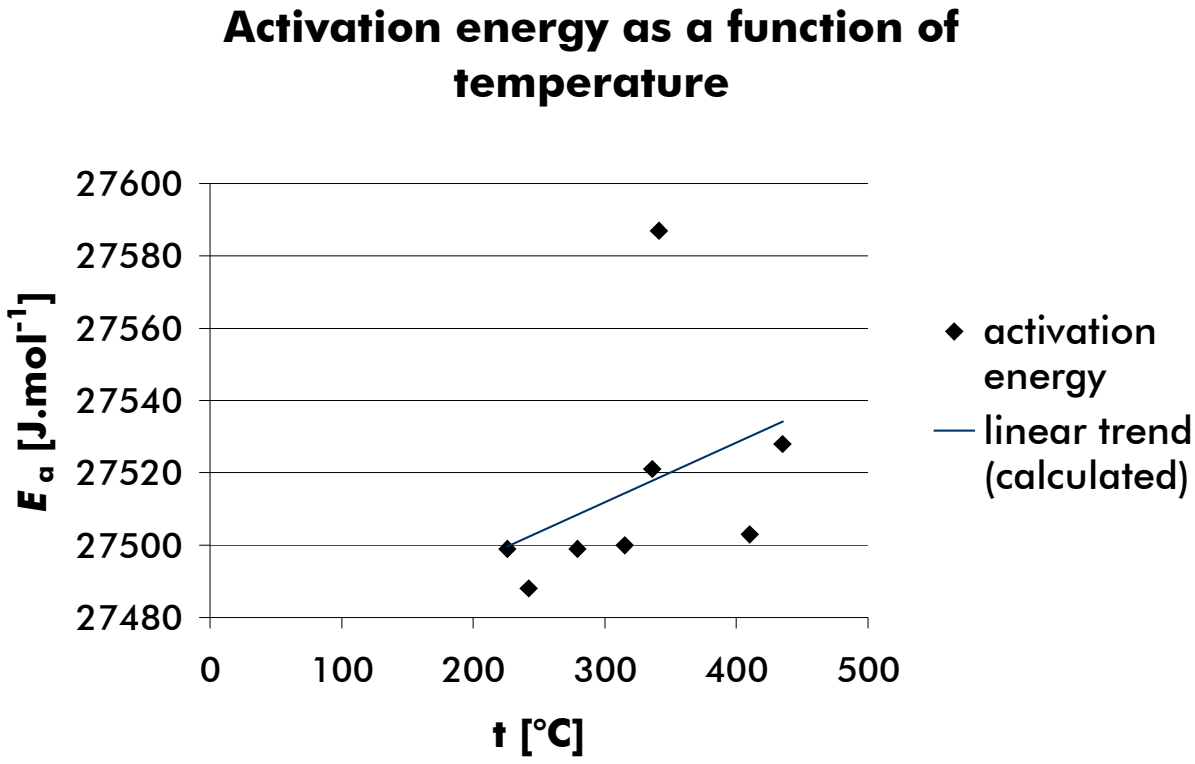

Fig. 37: Activation energy as a function of temperature.

Globally, results connected to activation energy are consisten with expectations (the mean value is equal to 27 512 $J.mol^{-1}$). Besides, the results obtained after numerical treatment remain grouped in a relatively narrow bracket of values, between 27 500 and 27 590 $J.mol^{-1}$.

However, even these results must be taken with caution. In actuality, as per the chosen kinetic model, this parameter is integrated into an exponential. Therefore, parametric identification tends to keep a value that is just little away from the initialisation value, as it happens, 27 440 $J.mol^{-1}$.

Conclusion

The model developed by Pascali and Herrera [1997] proposes simple kinetics of lignin pyrolysis. Its programming in MatLab allowed application to the degradation of the type of lignin used in the thesis (Kraft lignin from Aldrich).

By virtue of exploitation of results, it was made possible to consider validity of the chosen model.

Analysis of theoretical and experimental mass loss evolution makes it possible to suppose that the choice of model was pertinent as both traces superpose very well.

Global analysis of kinetic parameters permits to suppose that the reaction order remains constant for all selected temperatures, and the activation energy doesn't practically change. On contrary, in respect of frequency factor, analysis is more difficult. In fact, the value of frequency factor is about 40 to 150 times inferior than values expected basing on the paper by Pascali and Herrera [1997].

3.3.2 Ethylene vinyl acetate

Let us remind that the thermal degradation of EVA is a process running in two distinct stages. The first stage corresponds to de-acetylating of copolymer chain leading firstly, among other minor phenomena, to the massive creation of gaseous acetic acid (eliminated from the pyrolysis furnace by a fixed flow of nitrogen). After it, a plateau with no mass loss occurs (reaction rate is practically zero), and then again, the second stage of mass loss appears, all the more so since polyethylene – to the detriment of vinyl acetate – is present in EVA.

After pyrolysis, no solid residue is left. Among released gases and beyond acetic acid, carbon monoxide and carbon dioxide can be identified. It seems that methan is also released in the reactions, although it is less important. Other compounds not identified formally are supposedly ketones and the like.

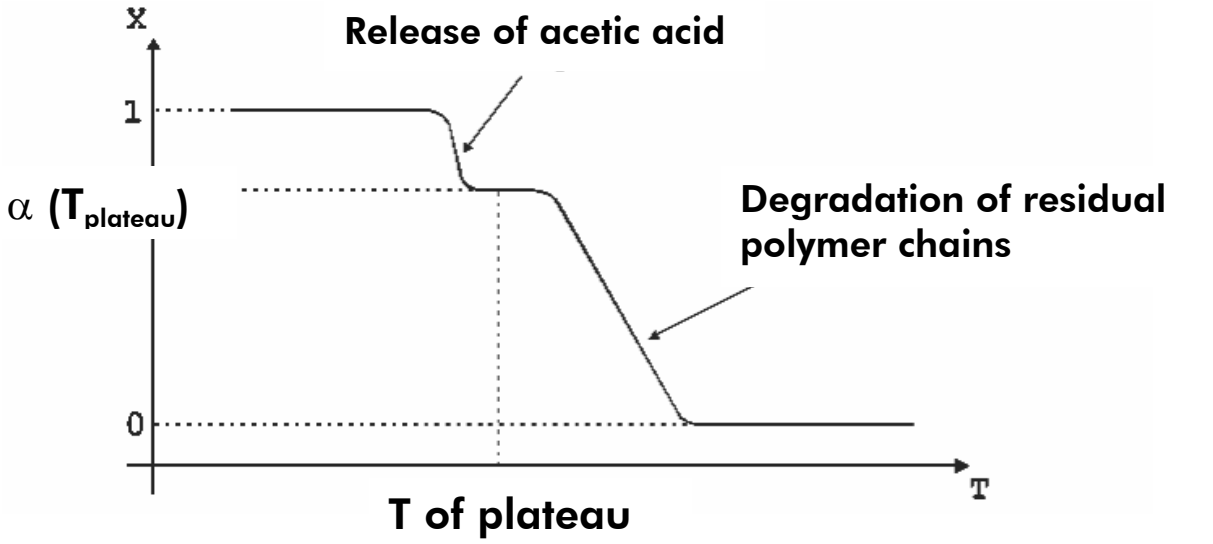

Fig. 38: A simple graphical representation of appearance of TGA/DTA charts obtained by pyrolysis of EVA.

The temperature of the first mass loss (taken at the point of maximal rate of mass loss) does not seemingly depend on the mass fraction of VA and crops always up between 340 and 370 °C in our experiments, pursuant to the heating rate (effect of thermal inertia).

The temperature of intermediate plateau (taken at the point of the lowest reaction rate) also does not seem to depend on or to respond to the mass fraction of vinyl acetate. Commensurate with the heating rate, it occurs between 380 and 410°C, agreeably to the heating rate. Finally, the temperature of the second rate of mass loss (taken at the point of maximal rate of mass loss) does not either depend on abundance of relevant polymers in this copolymer. This one takes place between 455 and 485 °C, still in consonance with the heating rate.

Following the bibliographical study on the kinetics of thermal degradation of EVA, it was decided that only the reaction scheme given the highest credit in the available literature in view of analysis of correspondence with experiments would be studied. As was expected, the scheme is very good.

Generally accepted kinetic scheme is the following [Marcilla et al., 1995b]:

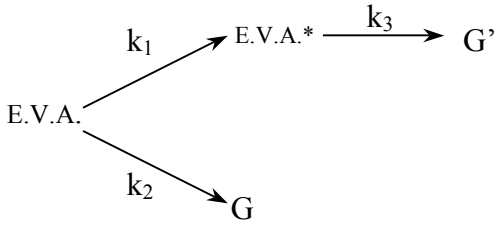

The solution of simulations gives the following kinetic parameters:

Tab. 19: Kinetic parameters for EVA.

Reaction 1	A_1 [min^{-1}]	E_{a1} [$J.mol^{-1}$]	n
	= f(% V.A.)	198037	1
Reaction 2	A_2 [min^{-1}]	E_{a2} [$J.mol^{-1}$]	m
	$8{,}06.10^{16}$	207948	1
Reaction 3	A_3 [min^{-1}]	E_{a3} [$J.mol^{-1}$]	p
	$0{,}94.10^{19}$	272357	1

A remarkable result concerning EVA is that the frequency factor of the first stage is a function of mass fraction of vinyl acetate (contained in EVA copolymer). A purely mathematic correlation between A_1 and mass fraction of vinyl acetate was searched for. Extrapolations to non-tested samples allowed verification of the model by detailed tests (see later in the thesis). These results are really satisfactory and enabled to trace the

graph of mass loss rates of the sum of EVA and EVA* (where EVA* designates the reaction intermediate).

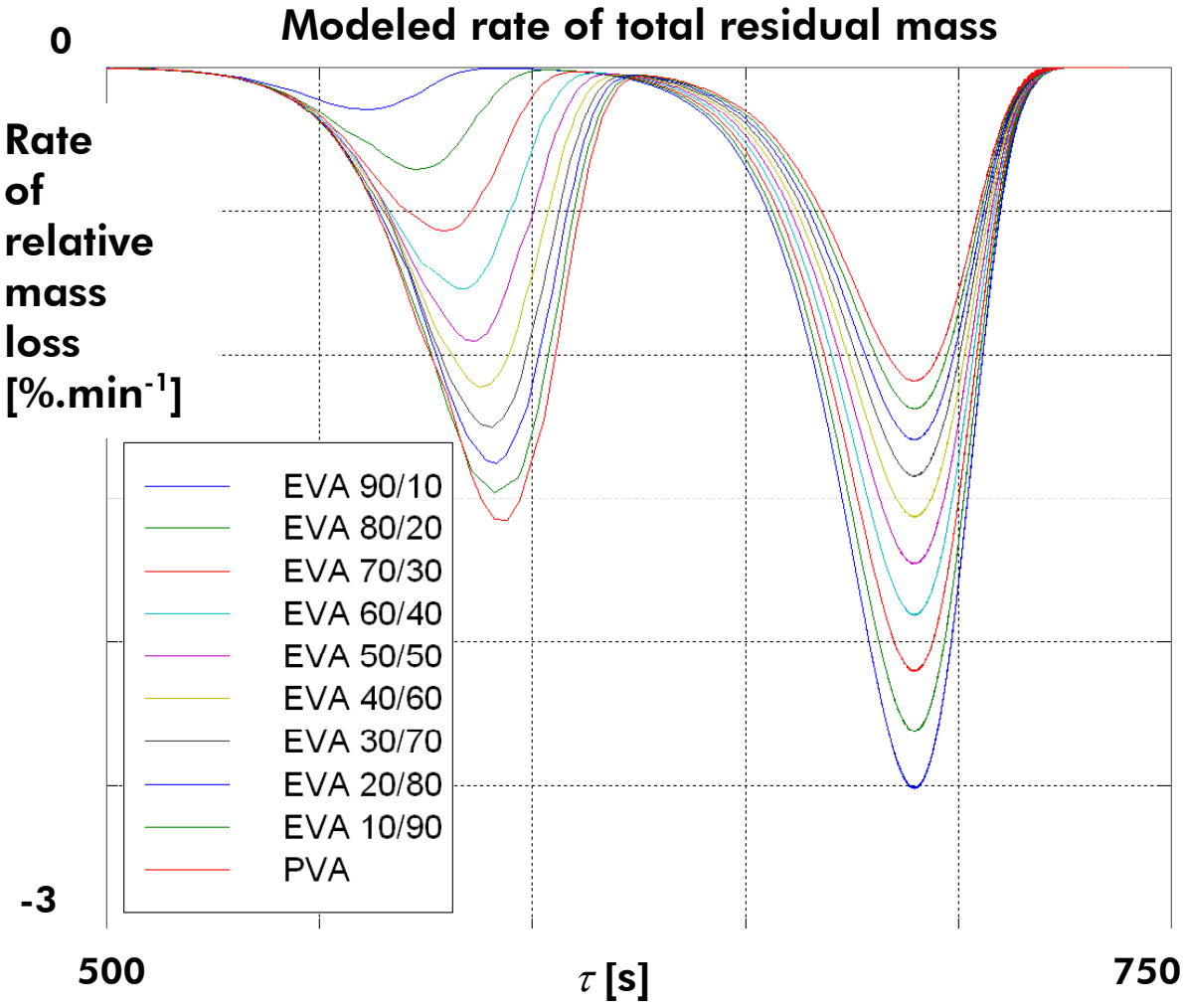

Fig. 39: Mass loss rates as a function of time for different types of EVA. These results are extrapolated from the model for all types of EVA.

Numerical solution of the accepted kinetic model

O.D.E. kinetic equations are numerically solved by the means of *ode45.m* function, distributed along with the standard MatLab licence. It was decided to integrate the influence of the percentage of vinyl acetate on kinetic coefficients, more precisely on the frequency factor A1, that seems to be by far the most sensitive to the mass fraction of VA.

Kinetic equations

In conformity with the preceding kinetic scheme, we can write (Kinetic equation of the model [Marcilla et al. 1995b]):

$$\left[\frac{dw}{dt} = -A_1 \exp\left(\frac{-E_{A1}}{RT}\right) w^n - A_2 \exp\left(\frac{-E_{A2}}{RT}\right) w^m\right]_K, \tag{24}$$

$$\left[\frac{dw^*}{dt} = -A_1 \exp\left(\frac{-E_{A1}}{RT}\right) w^n - A_3 \exp\left(\frac{-E_{A3}}{RT}\right) w^{*p}\right]_K, \tag{25}$$

where:

t	time of degradation progression, [min]
n, m, p	reaction orders
A_1, A_2, A_3	frequency factors, [min^{-1}]
E_{a1}, E_{a2}, E_{a3}	activation energy, [$J.mol^{-1}$]
R	ideal gas constant, = 8.3136 [$J.mol^{-1}.K^{-1}$]
T	sample temperature in time = K.t + T_0, [K]
T_0	initial temperature of the sample in time, [K]
K	temperature increase rate (dynamic slope), [$K.min^{-1}$]
w	EVA mass in time, [g]
w_0	initial mass of EVA, [g]
x	mass fraction of residual EVA in time τ; = w/w_0
x*	mass fraction of EVA* (reaction intermediate) in time τ; = w^*/w_0

Initialisation of kinetic parameters of the model

Activation energy depends a priori on the size of macromolecules used, i.e. on their VA contents. It would also seem justified to think that it depends on heating rate (different mechanisms according to their thermal inertia or occurrence of transfer phenomena of variable nature with temperature and its transitions). The chosen initialisation

parameters are the ones from the paper [Marcilla 1995b], excluding A1, which is a particular case that will be discussed later on.

Tab. 20: Initialization parameters of the optimization programme.

Reaction 1	A_1 [min^{-1}]	E_{a1} [$J.mol^{-1}$]	n
	$1.48.10^{15}$	197,200	1
Reaction 2	A_2 [min^{-1}]	E_{a2} [$J.mol^{-1}$]	m
	$8.79.10^{16}$	207,400	1
Reaction 3	A_3 [min^{-1}]	E_{a3} [$J.mol^{-1}$]	p
	$8.23.10^{18}$	272,300	1

MatLab code corresponding to the model:

```
function ypoint=modelkineva(t,y)
global A1 A2 A3 Ea1 Ea2 Ea3 K R n m p wini
ypoint(1)=-(A1/K)*wini ^ (n-1)*exp(-Ea1/(R*t))*(y(1)) ^ n-(A2/K)*wini ^ (m-1)*
        exp(-Ea2/(R*t))*(y(1)) ^ m;
ypoint(2)=(a*A1/K)*(wini ^ n)*exp(-Ea1/(R*t))*(y(1)) ^ n-(A3/K)*
        exp(-Ea3/(R*t))*(y(2)) ^ p;
YPOINT=YPOINT';
```

The whole set of obtained values (the experiment EVA 75/25 at 10°C.min^{-1} was eliminated because of an error in experimental procedure) is coherent with data from the paper by Marcilla [1995b], with the exception of A_1, in the case of which the differences are clearly significant. The most important deviation concerns the activation energy E_{a1}. The values in the second column of the table below correspond to the mean value of 15 parameters calculated for 3 types of EVA at 5 different heating rates.

Tab. 21: Values of frequency factor and activation energy.

Values from publication	**Values from simulation**
$A_1 = 1{,}48.10^{15}$ min^{-1}	--|--
$A_2 = 8{,}79.10^{16}$ min^{-1}	$A_2 = 8{,}06.10^{16}$ min^{-1}
$A_3 = 8{,}23.10^{18}$ min^{-1}	$A_3 = 8{,}46.10^{18}$ min^{-1}
E_{a1} = 197.2 kJ	E_{a1} = 198.0 kJ
E_{a2} = 207.4 kJ	E_{a2} = 207.9 kJ
E_{a3} = 272.3 kJ	E_{a3} = 272.4 kJ

The most surprising result concerns the frequency factor A_1, whose initialisation values had to be determined 'manually' before optimisation, so that the convergence of the programme was assured first. Therefore, these values are very distant from the values of the paper by Marcilla [1995b]. Moreover, A_1 also strongly changes in function of mass fraction of VA in the tested sample of EVA.

First of all, let us note that it was decided to let vary A_1 at the level of its initialisation, and in order to reach the convergence of the computer programme, rather than another parameter. And this for two reasons:

1) A_1 is, after all parameters were tested, the one that has the greatest influence on the intermediate plateau pitch; that seems evidently to be a phenomenon leading to the divergence in the model from a certain threshold of deviation from the optimum. (E_{a3} has also a great influence on the pitch of the plateau.)

2) A_1 is, physically, one of the only factors (with E_{a1}) that could influence the plateau pitch as it cannot depend on anything other than the first reaction, whose parameters are exactly A_1 and E_{a1}.

From these two enunciations, it seems that only A_1 has to be considered for re-evaluation, which is far away from the proposition of the publication; only thus convergence can be ensured. In addition, this allows solving an important problem that is answered by just a few publications:

How to take into account the pitch of the plateau on TGA/DTA curves corresponding to the intermediate in the discussed model that is varying in experiments in function of the mass fraction of vinyl acetate in EVA?

It is interesting to search for a correlation between three points of the abscissa of VA percentage (mass fraction of vinyl acetate in EVA) and of the A_1 on ordinate (frequency factor of the first equation of the kinetic model). A relation established from just three points should be taken with caution. Still, we should remember that we search just to formalise in a best possible way the observed tendency.

This study was undertaken with *GtkGraph* software that allows to search for a correlation that corresponds visually with the observed trend; furthermore, the least possible residue from the mean square method (mean square error) is searched out.

An equation of the type A_1=B.(% VA).M was found, GtkGraph provided the following values of the parameters: B = $446.803.10^{16}$ min^{-1}; M = -1.38914; residue = 0.0138466.

This equation and its coefficients are thereupon put into a new MatLab programme that makes traces for all possible types of EVA and all heating rates with the relative mass loss in function of time. This trace is parameterised in function of VA percentage (not of heating rate). An extrapolation to all types of EVA from 10 to 100 % of VA is realized, thus giving the following chart:

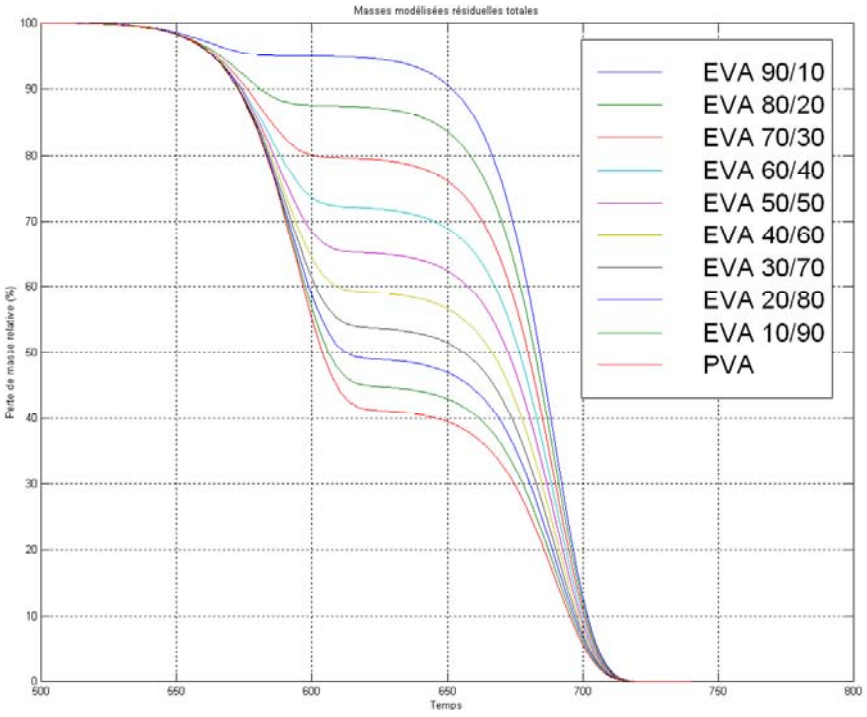

Fig. 40: Relative mass loss curves (EVA + EVA*) represented as a function of time and defined (parameterised) by VA percentage. X: time in seconds, from 500 to 800, Y: relative mass, from 0 to 100 %.

Actually, various plateau pitches expected are obtained that have a congruous appearance with experimental curves (reduced to a temporal study). Time scale is in seconds.

In order to evaluate the exactness of these curves, the percentages of VA were subsequently recalculated on the basis of the equation % VA = $1.434.(1\text{-}x_{T_{plateau}})$. Thereafter, it was put into the equation that was intended to be modelled.

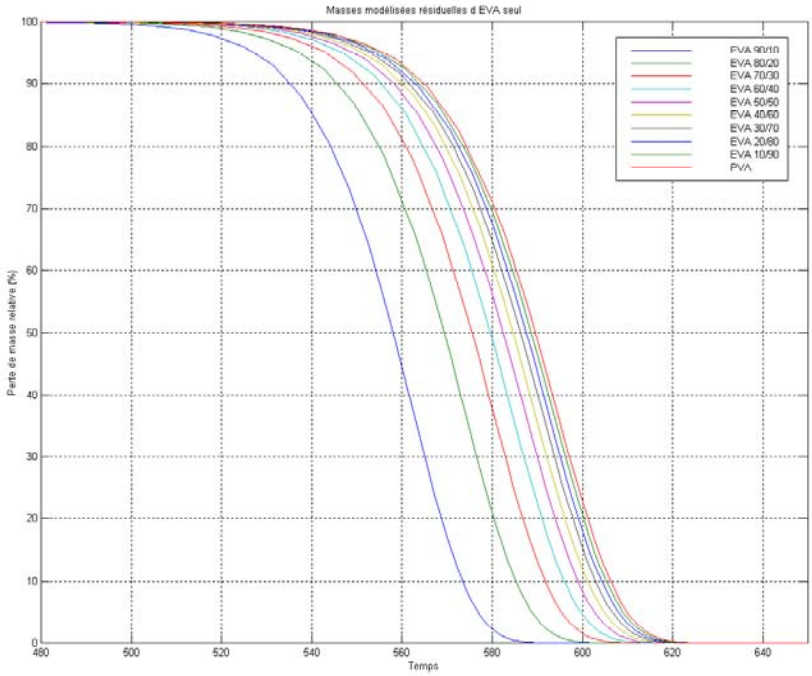

Fig. 41: On the same model as the preceding curves, this one represents the mass loss for the single EVA (the first stage). X: time from 190 to 640 by 10 s, Y: 0 to 100 %.

The following table summarizes calculations of VA percentage determined from the plateaus' pitches. The absolute and relative errors are calculated in relation to what was envisaged to be modelled (parameters of MatLab programme called improperly "VA percentage provider").

Tab. 22: Calculation of VA percentage form plateau pitches.

EVA type [% EVA/VA]	$X(T_{plateau})$	Calculated VA percentage [%]	VA percentage provider [%]	Absolute error	Relative error
EVA90/10	0.95	7.17	10	2.83	0.283
EVA80/20	0.88	17.208	20	2.792	0.1396
EVA70/30	0.79	30.114	30	-0.114	-0.0038
EVA60/40	0.72	40.152	40	-0.152	-0.0038
EVA50/50	0.65	50.19	50	-0.19	-0.0038
EVA40/60	0.59	58.794	60	1.206	0.0201
EVA30/70	0.53	67.398	70	2.606	0.03717
EVA20/80	0.48	74.568	80	5.432	0.0679
EVA10/90	0.45	78.87	90	11.13	0.1236
PVA	0.41	84.606	100	15.394	0.153

In MS Excel, (VA percentage provider) = f(EVA type) and (Calculated VA percentage) = g(EVA type) is firstly traced. The curves are amazingly near one another. This is leading us to represent subsequently relative errors in function of EVA type, so that the value bracket in which the extrapolation turns out to be exact is better visualised. Thus, we can consider that for EVA 30 to EVA 70, relative error is inferior to 5 %, i.e. the extrapolation is perfectly acceptable. For higher contents of vinyl acetate, a slight divergence can be observed.

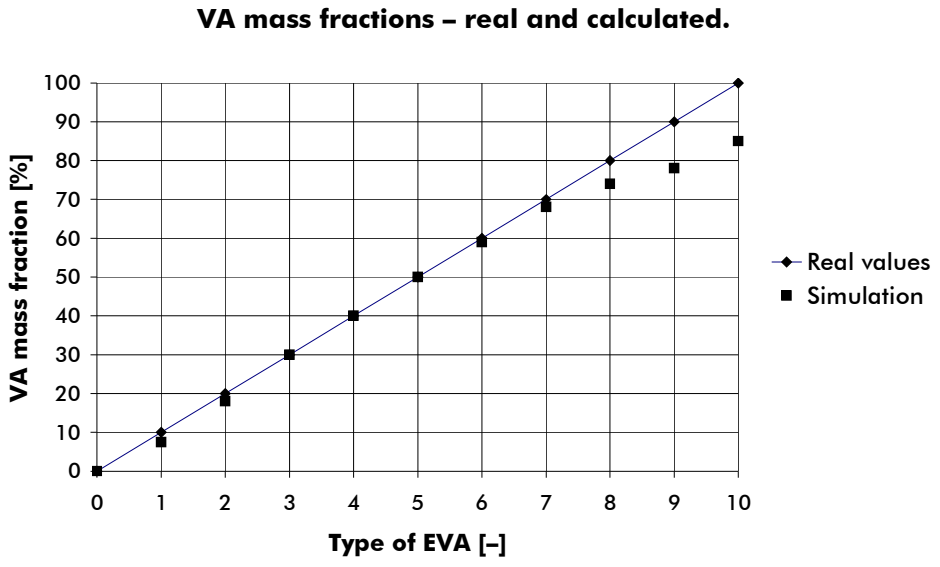

Fig. 42: Points corresponding to the table of calculations of VA percentage in order to visualise errors in function of EVA type considered for modelling. N.B.: See the next page!

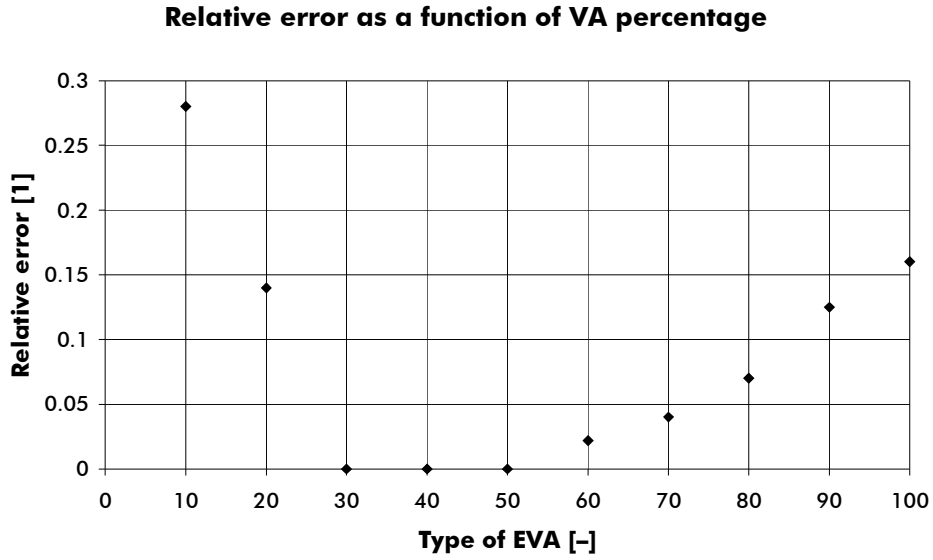

Fig. 43: Relative errors as a function of VA percentage.

Conclusion

The programme presented for computer-aided modelling of EVA pyrolysis works brilliantly. It is important to note that in this thesis, one of very few existing studies on EVA pyrolysis considering at the same time vinyl acetate percentage in EVA and different heating rates of the TGA/DTA furnace is rendered.

3.3.3 Study of the degradation kinetics of binary mixtures of polymers

Polymers valorised by pyrolysis are generally in the form of mixtures. It is therefore interesting to know behaviour of these mixtures, especially existence or non-existence of interactions. Consequently, a study of mixtures will be considered now; consistently with interests of CEA, these mixtures will always contain EVA as one constituent.

The alpha incinerator of "Directorate of military applications" (*Direction des applications militaires*) at Valduc (Côte-d'Or, France) treats combustible wastes like PVC, neoprene, latex, polyethylene, cellulose, that are contaminated by plutonium in boxes on gloves, whose activity does not allow a surface admission and storage. Coming from the Iris procedure (*Installation de recherche en incinération des solides* or Installation for research of incineration of solids) developed at CEA Marcoule in collaboration with CEA Valduc, and realized by SGN, it aims at reduction of volumes of treated materials and at safe storage without inhibiting the reversibility of treatment and the eventual recovery of plutonium. Since 1999, when its activity was initiated, the incinerator has allowed to reduce volumes of waste by factor 20. The new ash form of wastes imprison nearly 93 % of their initial activity, the remaining plutonium is consequently recuperated in the dust from electrofilters and residues from cleaning.

Fig. 44: CEA personnel in the middle of manipulating plutonium with plastic gloves.

The "French Atomic Energy Commission" (*Commissariat à l'Energie Atomique*), particularly the "nuclear safety" department, produces a lot of plastic wastes. These wastes are composed primarily of polymer mixtures such as ethylene vinyl acetate (EVA) with PVC or PS. Thus, the Commission takes interest in information about the kinetics of degradation of mixtures containing these polymers.

EVA is a polymer that is used, among other things, in nuclear industry, where it replaces PVC, used for production of maintenance tools (gloves, boots, …). Their composition is following: 5 % of cotton, 5 % of kleenex, 17 % of neoprene, 17 % of latex, 20 % of EVA, and the rest is PVC.

In CEA, once used, gloves are disposed of in the incinerator (pyrolysis at 500 °C and calcination at 900 °C). However, PVC poses problems during its incineration, because it releases chlorine. Ashes are stabilized by vitrification, but the presence of chlorine makes the vitrification or solidification difficult due to hard insertion of this element into the matrix.

Therefore, CEA endeavours to master the thermal degradation of polymer mixtures containing EVA to favour its utilization to the detriment of utilization of PVC.

The objective is to master, first on pilot-scale, the incineration process using pyrolysis for degradation of wastes with composition varying in time. The pilot facility on the site Valrho of CEA is able to process around 90 kg of wastes per day. In the medium term, elaborated kinetics will allow to know "what is going on" in the furnace according to raw materials on input. Later on, this will enable to optimise the conditions of functioning of the furnace in consonance with products that one wants to obtain (their phase, nature, …).

In the following part of the study, samples are binary mixtures with one part being always EVA. Polymers are mixed in three different ratios: 25/75, 50/50, and 75/25, except for EVA/Cellulose mixture, where only one ratio was used: 50/50.

It is fundamental to understand that in simulations of kinetic models of degradation of mixtures, an *a priori* hypothesis is always made in the sense that the degradation concerned is independent.

Study of the mixture EVA/PS

This chapter aims at determining of kinetics of the degradation of binary mixtures EVA/PS. Three proportions – 25/75, 50/50, and 75/25 – and three heating rates, 5, 10, and 20 °C.min^{-1} were studied.

Experimental conditions

Initial mass of samples is situated around approx. 25 mg. The differences of values of the initial sample mass is not a problematic agent as relative mass progression is being monitored. Regarding the placement of polymer samples in the crucible, a precise and rigorous experimental protocol was followed. The sequence of introduction of pure compounds is the same for all experiments.

Heating rate conditions are also different from one experiment to the other. In total, 3 values were used: 5°C.min^{-1}, 10°C.min^{-1}, 20°C.min^{-1}.

Reminder of results regarding pure polymers

The following tables present temperature of different DTG peaks observed during the pyrolysis of pure polymers.

These temperatures will make it easier to identify a compound degrading during pyrolysis of mixtures. In fact, temperature plateaus can be partly identical for both polymers. It is therefore *a priori* more difficult to determine which one corresponds to which polymer.

EVA: Two stages of mass loss are observed.

Tab. 23: Results (temperature and DTG) of EVA (single) pyrolysis.

Heating rate [°C.min^{-1}]	DTG peak temperature [°C]		DTG value [%.min^{-1}]	
	1st loss	2nd loss	1st loss	2nd loss
5	340	457	-2.2	-9.7
10	355	475	-3.9	-21.2
20	364	476	-9.6	-42.5

PS: Single stage of mass loss is observed.

Tab. 24: Results (temperature and DTG) of PS (single) pyrolysis.

Heating rate [°C.min^{-1}]	DTG peak temperature [°C]	DTG value [%.min^{-1}]
5	413	-14.7
10	426	-24.6
20	440	-42.9

Analysis of experimental curves

In examination of curves, the following data were recovered:

– percentage of mass loss,

– temperatures of different observed DTG peaks,

– value of this DTG.

Temperatures and values of DTG are interpreted graphically. The recording of mass loss corresponds to the percentage of loss relative to the initial mass placed in the crucible. It can happen that their sum is not exactly equal to 100; this would signify that a solid residue remains in the crucible at the end of pyrolysis.

Next, the moment of the beginning of degradation of each polymer was identified by comparison of temperature peaks of mixtures with those of pure compounds. This method implicates the hypothesis of an independent degradation of polymers.

EVA/PS mixture

Here, three stages of mass loss are observed.

Temperatures and values of DTG are interpreted graphically. The recording of mass loss corresponds to the percentage of loss relative to the initial mass placed in the crucible. In the case that their sum is not exactly equal to 100, it means that a solid residue remains in the crucible at the end of pyrolysis. The following table presents different values isolated on curves.

Tab. 25: Recap of graphical observations of experimental curves for EVA/PS mixture.

	Heating rate [°C.min^{-1}]	Peak temperature [°C]			DTG value [%.min^{-1}]			Mass loss [%]		
		1st loss	2nd loss	3rd loss	1st loss	2nd loss	3rd loss	1st loss	2nd loss	3rd loss
25 % EVA	5	329	408	454	-0.7	-11.4	-2.6	10.2	70.6	19.2
	10	343	420	463	-1.6	-20.5	-5.4	8.5	67.2	21.2
	20	359	430	473	-2.6	-37.4	-12.1	9.2	65.4	22.3
50 % EVA	5	335	408	458	-1.1	-7.8	-5.3	11.0	54.1	34.9
	10	350	422	471	-2.5	-15.7	-11.1	10.0	47.3	42.7
	20	355	424	477	-4.6	-26.8	-24.6	10.0	48.5	39.4
75 % EVA	5	338	410	463	-1.6	-4.6	-9.5	14.1	40.8	45.1
	10	353	426	467	-3.4	-8.9	-14.8	13.9	27.3	55.8
	20	366	433	476	-6.5	-18.3	-30.2	13.9	38.5	45.2

Identification of chronological order of the degradation

The first stage of degradation, whose maximal degradation rate is situated around 330-365°C, can be correlated with the first mass loss of pure EVA that occurs within the same zone (340-365°C).

The second part of the degradation is situated between 405 and 435°C, which corresponds to the degradation temperature of single polystyrene: 410-440°C.

The last degradation stage, between 455 and 480°C, corresponds to the second mass loss of pure EVA, situated between 455 and 480°C as well.

Generally, degradation temperatures shift to higher values when heating rate is increased.

Confirmation of the chronological order

Analysis of DTG values confirms the hypothesis.

These values are compared:

– experimental mass loss DTG (i),

– theoretical value calculated by the following equation.

$$Xa(T,i).DTGa(i), \qquad (26)$$

where

Xa(T,i) is the proportion of (a) degraded in mass loss (i),

DTGa(i) is the DTG mass loss value (i) at the same conditions of the heating rate for single polymer (a).

Example: for the EVA(25)/PS(75) mixture, at 5°C.min^{-1}

1st loss: 1st stage of EVA degradation

real value: -0.7 %.min^{-1}

theoretical value: 0.25 × -2.2 = -0.55 %.min^{-1}

2nd loss: PS degradation

real value: -11.4 %.min^{-1}

theoretical value: 0.75 × -14.7 = -11.0 %.min^{-1}

3rd loss: 2nd stage of EVA degradation

real value: -2.6 %.min^{-1}

theoretical value: 0.25 × -9.7 = -2.4 %.min^{-1}

Values are found to be of the same order, which is consistent with the hypothesis of the chronological order of degradation.

Another point of comparison is the DTG value of a mass loss in function of the polymer proportion. It is observed that this value evolves in the same sense as the proportion of polymer degrading in this stage of mass loss.

Generally speaking, DTG value increases with the increasing heating rate. Thus, degradation rate is increasing with heating rate. Mass loss values validate identification.

Heating rate value seems to have no influence on mass loss percentage. On the other hand, mass loss percentage evolves in the same direction as polymer proportion that degrades at this moment.

Conclusion on analysis of experimental results concerning EVA/PS mixtures

Mass loss analysis, analysis of degradation temperatures and of DTG values confirms the hypothesis of independent degradation of polymers. The three mass losses observed on curves correspond to the first stage of EVA mass loss, PS mass loss, and the second stage of EVA mass loss, respectively.

Numerical solution of kinetic models for the EVA/PS mixture

Source of models

For EVA: The same model as in the preceding study on single EVA pyrolysis is used.
For PS: Marcilla et al. [1995b].

Modelling of EVA/PS mixture pyrolysis

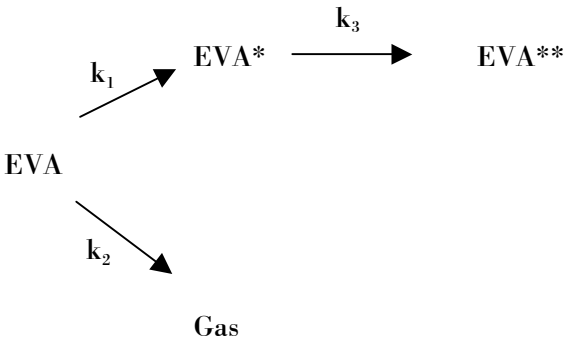

$$dEVA = -k_1.\exp(-E_{a1}/RT)_{[EVA]} - k_2.\exp(-E_{a2}/RT)_{[EVA]} \quad (27)$$

$$dEVA^* = k_1.\exp(-E_{a1}/RT)_{[EVA]} - k_3.\exp(-E_{a3}/RT)_{[EVA^*]} \quad (28)$$

$$dEVA_{total} = dEVA + dEVA^* \quad (29)$$

$$dEVA_{total,\ mixture} = (\text{EVA mass \%}).dEVA_{total} \quad (30)$$

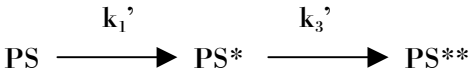

$$dPS = -k_1'.\exp(-E_{a1}'/RT)_{[PS]} \quad (31)$$

$$dPS^* = k_1'.\exp(-E_{a1}'/RT)_{[PS]} - k_3'.\exp(-E_{a3}'/RT)_{[PS^*]} \quad (32)$$

$$dPS_{total} = dPS + dPS^* \quad (33)$$

$$dPS_{total,\ mixture} = (\text{PS mass \%}).dPS_{total} \quad (34)$$

$$d(\text{EVA/PS mixture}) = dEVA_{total,\ mixture} + dPS_{total,\ mixture} \quad (35)$$

Let us remind the initial hypothesis of independent degradation of individual compounds. Thus, the assumption that the variation of mixture mass is the sum of independently taken variations of mass of each and every constituent of the mixture can be made.

EVA/PS mixture degradation can be described by 10 parameters that are now to be determined: k_1, E_{a1}, k_2, E_{a2}, k_3, E_{a3}, k_1', E_{a1}', k_3', E_{a3}'.

MatLab 6.0 simulation consists of three programmes:

(i) ***modelcin.m***, defining reaction kinetic equations,

(ii) ***evapsA1evastat.m***, allowing optimisation of a single parameter of reaction kinetic equations,

(iii) ***essaidessin.m***, allowing to trace curves needed for modelling.

In the ***evapsA1evastat.m*** programme, bibliographic values of various parameters are set according to literature data. These values will serve as a reference for all comparison with values calculated by the programme. The parameters are chosen as follows:

Tab. 26: Selection of parameter initialisation values.

Mixture	Heating rate [°C.min^{-1}]	Origin of parameters
EVA/PS	5	*EVA:* work on single EVA and PS. *PS:* work on single EVA and PS.
	10	*EVA:* work on single EVA and PS. *PS:* work on single EVA and PS.
	20	*EVA:* work on single EVA and PS. *PS:* work on single EVA and PS.

Pages refer to the work by Soudais et al. [2003].

Tracing of curves: essaidessin.m

This programme calculates, from all resulting optimal values, mass data in time, and represents them thereafter in graphical form. On these charts, experimental mass is outlined in green and theoretical mass in blue.

Analysis of frequency factors and activation energies

The values obtained for these parameters are presented below in tabular form. The table just below is an example.

Tab. 27: Example of table with results obtained in MatLab for EVA/PS mixture in 25/75 ratio, respectively, and at 10 °C.min^{-1}.

Coefficient	Reference value	Calculated value	Relative error	Correlation factor
A_1 EVA [min^{-1}]	$4.00.10^{17}$	$8.43.10^{16}$	78.9	0.0001
A_2 EVA [min^{-1}]	$7.50.10^{16}$	$7.71.10^{16}$	-2.77	0.0004
A_3 EVA [min^{-1}]	$1.00.10^{19}$	$8.43.10^{18}$	15.7	0.00008
E_{a1} EVA [J.mol^{-1}]	$1.98.10^{5}$	$1.97.10^{5}$	0.51	0.003
E_{a2} EVA [J.mol^{-1}]	$2.08.10^{5}$	$2.16.10^{5}$	-3.85	0.0005
E_{a3} EVA [J.mol^{-1}]	$2.72.10^{5}$	$2.73.10^{5}$	-0.141	0.0008
A_1 PS [min^{-1}]	$4.00.10^{14}$	$2.06.10^{14}$	1.58	0.0004
A_3 PS [min^{-1}]	$2.70.10^{16}$	$3.09.10^{16}$	-14.3	0.0012
E_{a1} PS [J.mol^{-1}]	$1.92.10^{5}$	$1.89.10^{5}$	1.72	0.0007
E_{a3} PS [J.mol^{-1}]	$2.16.10^{5}$	$2.13.10^{5}$	1.32	0.0039
Maximum relative error in masses:				**0.99 %**

This table indicates results for each parameter, and compares it with literature data by the mean value calculated from evaluation of relative errors.

The column with correlation factor represents the precision of obtained values. This value is calculated by the least squares method from mass data (experimental mass is compared with the theoretic – i.e. calculated – one). The nearer the results are to zero, the better is the coherence between theory and experiments.

The table below gives intervals of relative errors to facilitate their exploitation.

Tab. 28: Relative errors of frequency factors and activation energy values.

Mixture	Proportions of EVA/PS [%]	Heating rate [°C.min^{-1}]	Error range [%]	
			Frequency factors	Activation energies
EVA/PS	25/75	5	42-182	0-9
	50/50		37-250	0-10
	75/25		44-1700	1-10
	25/75	10	1-79	1-15
	50/50		0-280	2-9
	75/25		21-273	0-25
	25/75	20	8-175	0-26
	50/50		13-50	0-2
	75/25		0-376	0-9

The values of relative errors of frequency factors may seem to be very high. It appears, that it is due to the fact that these values have a great order (from 10^{12} to 10^{20}). Therefore, it would be preferable to base our analysis on activation energy values, where orders are more limited, and their inclusion in an exponential diminishes fluctuation of errors. Values of relative errors are contained between 0 and 26 % but the majority of them are around 8 %. Errors concerning activation energy are most often approx. 5 %, which corroborates our hypotheses.

Analysis of mass variations

Analysis of mass variations in time allows confirmation of our hypotheses. Evolutions of theoretical and experimental mass in time are traced in the same chart to make comparison more easy. The figure below is an example of this.

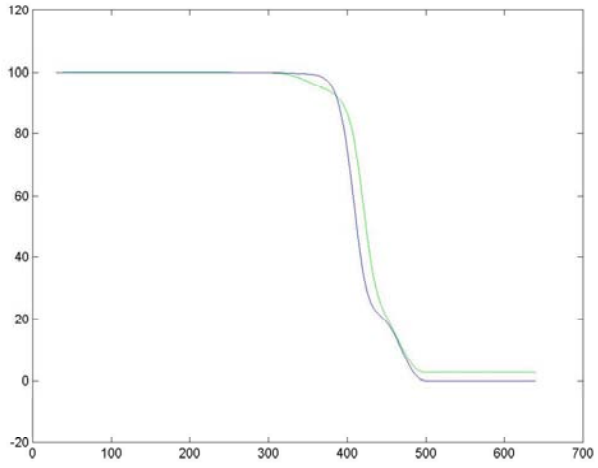

Fig. 45: Representation of mass in time for EVA/PS mixture (25/75 ratio) for the heating rate of 10 °C.min^{-1}. X: time from 0 to 700 by 100 s, Y: -20 to 120 by 20 %. *N.B.: Experimental mass is in green, theoretical in blue.*

We will notice a good coherence of these curves for EVA/PS mixture. Just the first stage of mass loss is not represented very well by theoretical curve; however, the same number of degradation stages at similar temperatures is found.

A more detailed analysis of relative errors of mass illustrates good foundation of our hypothesis as well.

The next table shows maximum values of relative errors of mass.

Tab. 29: Table of relative errors of mass data.

Mixture	Proportions of EVA/PS [%]	Heating rate [°C.min^{-1}]	Maximum relative error [%]
EVA/PS	25/75	5	5
	50/50		8
	75/25		10
	25/75	10	0.99
	50/50		0.06
	75/25		0.5
	25/75	20	60 (excluded)
	50/50		5.5
	75/25		5

Save one curve, maximum errors for EVA/PS are contained between 0.06 and 10 %. It is therefore facile to confirm our hypotheses concerning EVA/PS mixture.

The figure below presents the result of simulation of theoretical curves calculated from variation of each component – EVA/PS/PS*/EVA*.

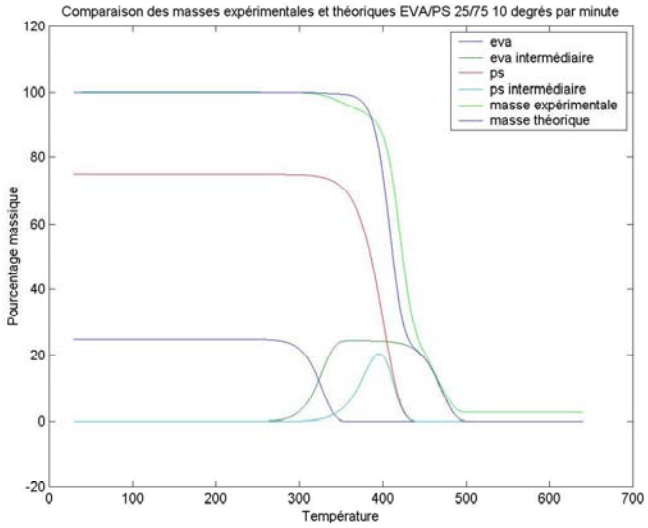

Fig. 46: Representation of mass variations in time for EVA/PS mixture (25/75 ratio) at the heating rate of 10 °C.min^{-1}. X: temperature from 0 to 700 by 100 °C, Y: sample mass from -20 to 120 by 20 %.

The results concerning the order of disappearance of various components for each experiment are cited in the table below:

Tab. 30: Chronological disappearance orders of reactants and reaction intermediates.

Mixture	Proportions of EVA/PS [%]	Heating rate [°C.min^{-1}]	Disappearance order [—]
EVA/PS	25/75	5	EVA/PS/PS*/EVA*
	50/50		EVA/PS/PS*/EVA*
	75/25		EVA/PS/PS*/EVA*
	25/75	10	EVA/PS/PS*/EVA*
	50/50		EVA/PS/PS*/EVA*
	75/25		PS/EVA/PS*/EVA*
	25/75	20	PS/EVA/EVA*/PS* (excluded, a lot of errors)
	50/50		EVA/PS/PS*/EVA*
	75/25		PS/EVA/PS*/EVA*

Examining these results, hypotheses are confirmed, the order of disappearance of components seem to be EVA/PS/PS*/EVA*; observed errors can result from approximations done in MatLab programming.

Conclusion concerning modelling

It is affirmed that for the EVA/PS mixture, kinetic model is validated.

The degradation of these polymer mixtures is the sum of degradations of single polymers, it seems that there is no interaction.

To sum up

Analysis of pyrolysis experiments monitored by thermogravimetrie allowed pronouncing a provisional hypothesis about chronological order of degradation. For EVA/PS mixture, we notice three stages of mass loss: EVA/PS/EVA*. For EVA/PS mixture, the hypothesis of one independent polymer degradation seems to be verified.

The MatLab simulation confirms previously expressed results. The study of theoretical and calculated mass traces show that curves coincide (with error from 0 to 10 %). This is

confirmed by a study of chronological disappearance orders of reactants and intermediates, by which the order EVA/PS/EVA* is established.

Thus, the hypothesis of independent degradation of polymers in the case of EVA/PS mixture is confirmed.

Study of the mixture EVA/PVC and EVA/Cellulose

Note: For this part of the study, new TGA/DTG experiments were carried out with single polymers (especially with EVA), and then for mixtures. The values used come from these new experiments.

In parallel, EVA/PVC and EVA/Cellulose mixtures will be studied here. This will be justified by similar degradation behaviour of these two mixtures, which will be shown in the course of our study.

Experimental conditions

Initial mass of samples is situated between approx. 25 mg. The differences of values of the initial sample mass is not a problematic agent as relative mass progression is being monitored. Regarding the placement of polymer samples in the crucible, a precise and rigorous experimental protocol was followed. The sequence of introduction of pure compounds is the same for all experiments.

Samples are binary mixtures with one part being always EVA. Polymers are mixed in three different ratios for EVA-PVC mixtures: 25/75, 50/50, 75/25 and only one ration 50/50 in the case of EVA-Cellulose mixture.

Heating rate conditions are: 5, 10, 20, 30°C.min^{-1} in the case of single EVA and PVC polymers and EVA-PVC mixture, and 10, 20°C.min^{-1} in the case of EVA-Cellulose.

In investigating of curves, the following data were recovered:

– percentage of mass loss,

– temperatures of different observed DTG peaks,

– value of this DTG.

Next, the moment of the beginning of degradation of each polymer was identified by comparison of temperature peaks of mixtures with those of pure compounds. This method implicates the hypothesis of an independent degradation of polymers.

Temperatures and values of DTG are interpreted graphically. The recording of mass loss corresponds to the percentage of loss relative to the initial mass placed in the crucible. It can happen that their sum is not exactly equal to 100; this would signify that a solid residue remains in the crucible at the end of pyrolysis.

The following tables present temperature results obtained for pyrolyses of pure polymers: EVA, PVC, and Cellulose, with heating rates of 5, 10, 20, and 30°C.min^{-1}.

Experimental results for EVA

Two stages of mass loss are observed.

Tab. 31: Mass loss, DTG, and DTG peak temperature values for pure EVA.

Heating rate [°C.min^{-1}]	DTG peak temperature [°C]		DTG value [%.min^{-1}]		Mass loss [%]	
	1st loss	2nd loss	1st loss	2nd loss	1st loss	2nd loss
5	345	461	-1.9	-10.5	22.4	77.6
10	355	474	-3.6	-20.5	25.8	67.2
20	367	483	-6.8	-29.8	27.2	72.8
30	375	489	-8.75	-37.25	28.4	91.6

Experimental results for PVC

Three stages of mass loss are observed.

Tab. 32: Mass loss, DTG, and DTG peak temperature values for pure PVC.

Heating rate [°C.min^{-1}]	DTG peak temperature [°C]			DTG value [%.min^{-1}]			Mass loss [%]		
	1st loss	2nd loss	3rd loss	1st loss	2nd loss	3rd loss	1st loss	2nd loss	3rd loss
5	270	325	458	-9.5	-1.2	-2.2	56.3	10.9	25.6
10	283	336	470	-15.5	-2.3	-3.9	58.1	10	25.6
20	300	350	480	-22.3	-6.3	-6.5	58	10.6	24.4
30	312	—	483	-26.6	—	-8.6	56.3	13.1	23.1

It was found that for the heating rate of 30°C.min^{-1}, only 2 peaks are present. However, three stages of mass loss are still present. This phenomenon is caused by the fact that for this rapid heating rate, degradations are simultaneous ans it isn't possible to differentiate the peaks visually.

Experimental results for Cellulose

In these experiments, just two heating rates were employed: 10°C.min^{-1} and 30°C.min^{-1}.

One and only stage of mass loss was observed.

Tab. 33: Mass loss, DTG, and DTG peak temperature values for pure pyrolysis.

Heating rate [°C.min^{-1}]	DTG peak temperature [°C]	DTG value [%.min^{-1}]	Mass loss [%]
	1 and only loss	*1 and only loss*	*1 and only loss*
10	345	-23.3	83
30	364	-37	83

Analysis of experimental results for single polymers

Identification of temperature of these diverse peaks will enable identifying of each and every compound during the pyrolysis of mixtures. Nevertheless, it can immediately be noted that PVC and EVA have common temperature zones around 350 °C and 480 °C. Cellulose peak is situated in the surrounding of 350 °C; this coincides with the first EVA peak. It can therefore be already said that it is difficult – only from thermogravimetric data – to determine the constitution in respective mass value of each polymer in the signal of mass loss for pyrolysis of mixtures.

Analysis of experimental results for mixtures

As well as for pure polymers, data concerning each mixture were registered.

EVA/PVC mixture

Three stages of mass loss are observed.

Tab. 34: Mass loss, DTG, and DTG peak temperature values for EVA/PVC mixture.

	Heating rate [°C.min^{-1}]	Peak temperature [°C]			DTG value [%.min^{-1}]			Mass loss [%]		
		1st loss	*2nd loss*	*3rd loss*	*1st loss*	*2nd loss*	*3rd loss*	*1st loss*	*2nd loss*	*3rd loss*
25 % EVA	5	265	333	464	-7.4	-1.1	-3.9	44.4	13.1	36.3
	10	231	336	475	-12.2	-2.2	-7.4	45.0	13.1	36.3
	20	346	355	483	-17.6	-4.6	-12.0	45.0	15.0	34.4
	30	308	—	494	-21.4	—	-15.6	43.8	10.6	38.1
50 % EVA	5	265	330	465	-4.75	-1.4	-6.25	30.0	13.3	50.7
	10	277	347	476	-8.8	-2.48	-11.2	36.3	11.9	48.9
	20	294	350	487	-12.9	-5.0	-18.3	31.9	15.0	48.1
	30	308	—	494	-15.4	—	-22.3	32.5	13.1	51.3
75 % EVA	5	268	328	464	-2.3	-1.6	-8.15	16.7	18.0	62.0
	10	278	346	476	-4.3	-3.1	-14.5	18.0	17.0	61.3
	20	300	358	488	-6.8	-5.5	-23.5	16.0	21.6	62.4
	30	308	369	494	-8.3	-7.5	-29.1	18.0	19.0	60.3

The same phenomenon as the one observed for single PVC is found for the heating rate of 30 °C.min^{-1}: just 2 peaks can be visually discerned, even if there are 3 mass loss stages. This phenomenon partially explains variations in the calculation of mass loss stages actually observed.

EVA/Cellulose mixture

As it was also encountered in the case of experiments concerning cellulose, only experiments with the heating rates of 10 and 30 °C.min^{-1} were carried out, and just for one mixture with the 50/50 ratio.

Two stages of mass loss are observed:

Tab. 35: Mass loss, DTG, and DTG peak temperature values for EVA/Cellulose mixture.

	Heating rate [°C.min^{-1}]	DTG peak temperature [°C]		DTG value [%.min^{-1}]		Mass loss [%]	
		1st loss	*2nd loss*	*1st loss*	*2nd loss*	*1st loss*	*2nd loss*
50 % EVA	10	346	476	-13.0	-9.1	54.4	39.4
	30	368	492	-22.9	-18.9	55.6	39.4

The results concerning the second stage of mass loss seem to be perfectly identical, which could appear paradoxal in comparison with other experimental results. However, this result can be explained by a deep slope of TGA curve. In fact, a slight error in determining of tangents has a repercussion on calculation of mass loss and this all the more the slope is more marked.

Analysis of results for EVA/PVC mixture

Let us recapitulate results obtained by TGA. As an example, data from experiments with the heating rate of 20 °C.min^{-1} will be taken. Generally speaking, degradation temperature increases with the increasing value of heating rate.

Pure EVA: dm1 : 30 % at 350°C, dm2 : 70 % at 480°C;

Pure PVC: dm1 : 50 % at 300°C, dm2 : 20 % at 350°C,
dm3 : 30 % at 480°C;

EVA/PVC mixture (50/50 ratio) – 3 stages of mass loss are observed:

dm1 : 30 % at 300°C dm2 : 20 % at 350°C

dm3 : 50 % at 480°C

The chart below shows different profiles obtained:

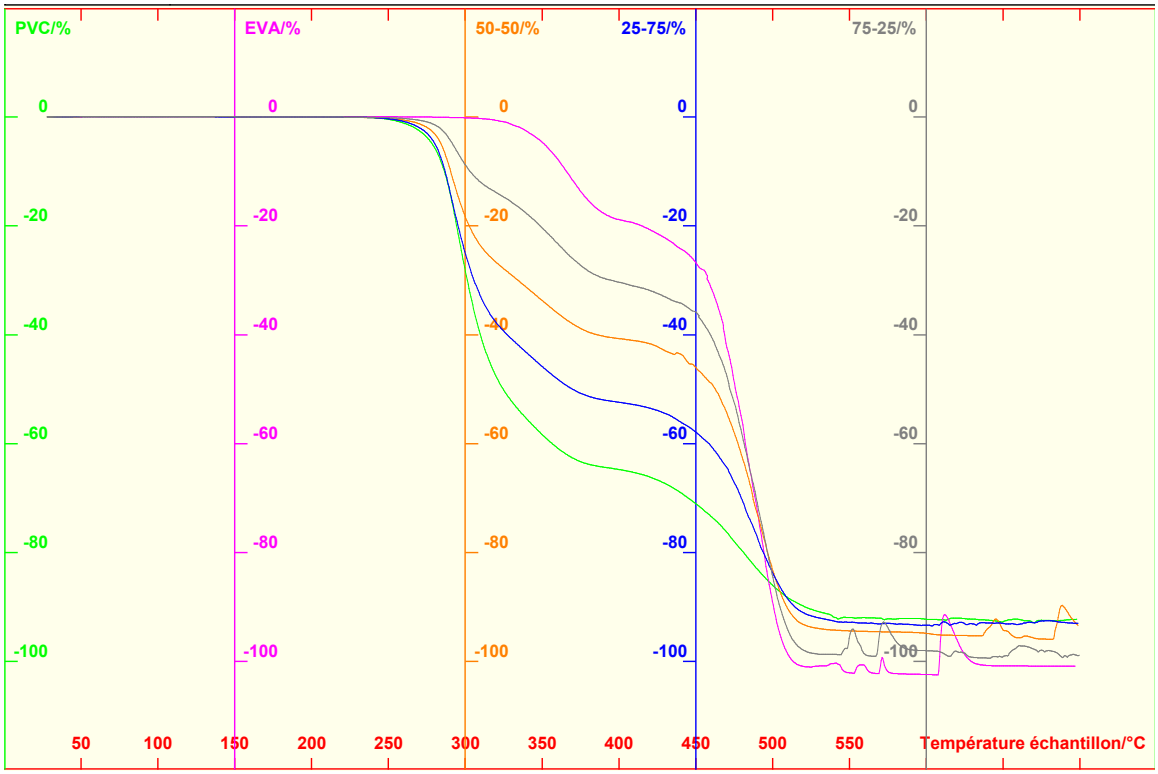

Fig. 47: Superposition of TGA curves for pure EVA, pure PVC, and the mixture of both, at three different ratios (X-Y %, where X stands for EVA, and Y stands for PVC). X: temperature from 50 to 550 by 50 °C, Y: sample mass from -100 to 0 by 20 %.

Identification of chronological order of EVA/PVC mixture degradation

The first stage of degradation, whose maximum rate is situated around 300°C, can be attributed to the first stage of mass loss of PVC that occurs in the same temperature zone when degraded individually.

The second stage of degradation takes place at approx. 350°C. This temperature corresponds at the same time to the first stage of mass loss of EVA and to the second stage of mass loss of PVC. It can be said that in this region, analysis of relevant phenomena is more complex, as there is a superposition of degradation zones of pure polymers. FTIR analysis of pyrolysis gases should provide us with more information enabling us to make conclusions about the actual character of the degradation process. And finally, the third

stage of degradation occurs around 480°C (at the same temperature as in the preceding case); in this temperature zone, the second mass loss of EVA and the last stage of PVC mass loss take place simultaneously.

Analysis of results for EVA/Cellulose mixture

Let us summarise results concerned by TGA

– for pure EVA, 2 stages of mass loss are observed, with the following approximative results: dm1: 30 % at 350°C, dm2: 70 % at 480°C;

– for pure Cellulose, 1 stage of mass loss is observed: dm1 at 350°C;

– for EVA/Cellulose mixture (50/50 ratio), 2 stages of mass loss are observed: dm1 – 60 % at 350°C, dm2 – 40 % at 480°C.

Identification of chronological degradation order for EVA/Cellulose mixture

The first stage of degradation, whose maximum degradation rate is situated around 350 °C, can resemble the superposition of the first mass loss of EVA and the one of cellulose, as they can take place in the surroundings of this temperature when single polymers are degraded.

The second stage of degradation is situated around 480 °C, which corresponds to the temperature of the second and last stage of mass loss of EVA.

Confirmation of chronological order

In order to validate the hypothesis concerning the order of degradation for polymers constituting the mixture, DTG values can be analyzed. Especially, as it was also done for the EVA/PS mixture, DTG value corresponding to the mass loss (i) obtained during an experiment is compared with the theoretical or calculated value, which amounts to:

$$Xa(T,i)*DTGa(i), \quad (36)$$

where Xa(T,i) designates the ratio of component (a) degraded during the mass loss (i), and DTGa(i) is the DTG value of mass loss (i) taken for the same heating rate conditions as for the individual polymer.

Example

For EVA(50)/cellulose(50) mixture at 10°C.min^{-1}

1st loss: 1st stage of EVA degradation and (at the same time) cellulose degradation

real value: -13 %.min^{-1}

theoretical value: $0.5 \times (-3.6) + 0.5 \times (-23.3) =$ -13.45 %.min^{-1}

2nd loss: 2nd stage of EVA degradation

real value: -9.1 %.min^{-1}

theoretical value: $0.5 \times (-20.2) =$ -10.1 %.min^{-1}

It can be said that the values are of the same order, which is in concordance with the hypothesis concerning the chronological order of degradation.

Concluding words on TGA/DTA experiments of EVA/PVC and EVA/Cellulose mixtures

Analyses of loss mass for mixtures seem to show a good fitting between the temperature plateaus of individual and mixed polymers. However, the results from MatLab simulation, and, of course, FTIR analysis, should be awaited to conclude about a possible independence of degradations and the validation of kinetic models that was proposed.

The next part will provide arguments enabling to answer questions like:

- which is the kinetic scheme adapted to pyrolysis of each studied mixture?
- is there any interaction between constituents during the degradation?

3.3.4 Simulation of kinetic models in MatLab

Choosing a model

With respect to the fact that the scientific community did not propose any kinetic model for EVA/PVC and EVA/Cellulose mixtures (or at least not in papers and bibliographical sources available for our thesis), the hypothesis of independence of degradation of individual polymers in mixtures during their pyrolysis is *a priory* accepted.

Modelling of EVA

The model for EVA remains identical to the one used in previous studies.

Reminder: It assumes a decomposition in two stages of mass loss according to a series and a parallel scheme.

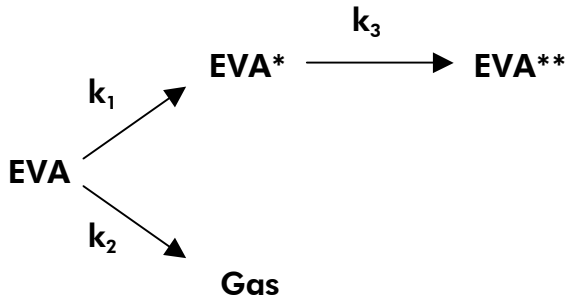

Fig. 48: Kinetic scheme of EVA degradation.

$$dEVA = -k_1 \exp(-E_{a1}/RT)_{[EVA]} - k_2 \exp(-E_{a2}/RT)_{[EVA]} \quad (37)$$

$$dEVA^* = k_1 \exp(-E_{a1}/RT)_{[EVA]} - k_3 \exp(-E_{a3}/RT)_{[EVA^*]} \quad (38)$$

$$dEVA_{total} = dEVA + dEVA^* \quad (39)$$

$$dEVA_{total,mixture} = (\%\ \text{masse EVA})\ dEVA_{total} \quad (40)$$

Fig. 49: Mathematical expression of the kinetic model of EVA pyrolysis.

Chart of PVC modelling:

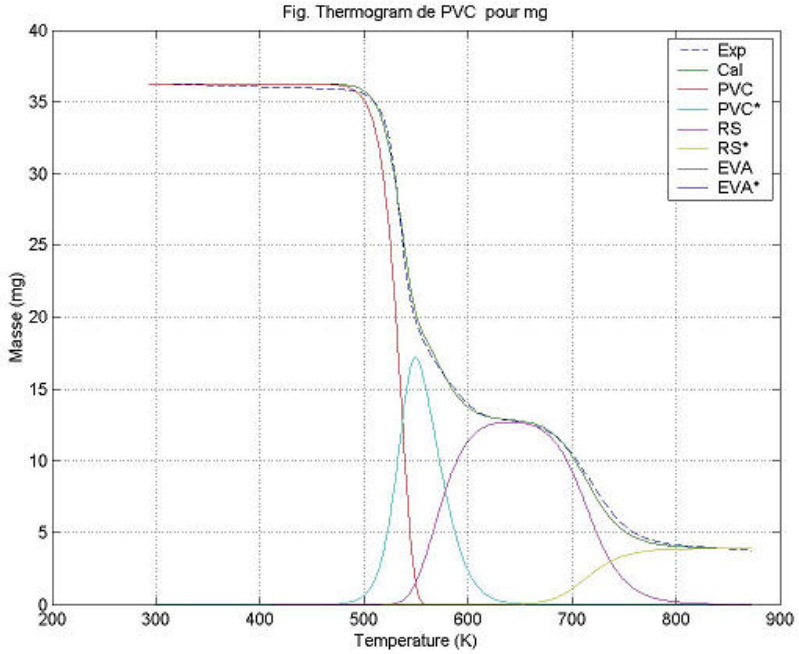

Fig. 50: Comparison of experimental and calculated curves for pure PVC. X: temperature from 200 to 900 by 100 K, Y: mass from 0 to 40 by 5 mg.

The model can be described in this way:

$$\mathbf{PVC} \xrightarrow{k_1} \mathbf{a\ HCl + b\ PVC^*}, \tag{41}$$

$$\mathbf{b\ PVC^*} \xrightarrow{k_2} \mathbf{c\ G + e\ RS}, \tag{42}$$

$$\mathbf{e\ RS} \xrightarrow{k_2} \mathbf{f\ G' + g\ RS^*}, \tag{43}$$

Fig. 51: Kinetic scheme of PVC degradation.

$$\mathbf{dPVC = -k_1' \exp(-E_{a1}'/RT)_{[PVC]}} \tag{44}$$

$$\mathbf{dPVC^* = b\ (k_1' \exp(-E_{a1}'/RT)_{[PVC]} - k_2' \exp(-E_{a2}'/RT)_{[PVC^*]})} \tag{45}$$

$$dRS = e\,(k_2'\exp(-E_{a2}'/RT)_{[PVC^*]} - k_3'\exp(-E_{a3}'/RT)_{[RS]}) \quad (46)$$

$$dRS^* = g\,(k_3'\exp(-E_{a3}'/RT)_{[RS]}) \quad (47)$$

$$dPVC_{total} = dPVC + dPVC^* + dRS \quad (48)$$

$$dPVC_{total,mixture} = (\text{PVC mass \%})\,dPVC_{total} \quad (49)$$

Fig. 52: Kinetic model of PVC expressed mathematically.

The model mentioned above comes from the paper by Marcilla and Beltrán [1995c].

The cited article contains several parallel and series models. From the curves obtained in the course of our study, it seems that the parallel model chosen is perfectly adapted to PVC, which is not truth for the series model.

Cellulose modelling

It is assumed that cellulose decomposes in two parallel reactions, agreeably to the following scheme:

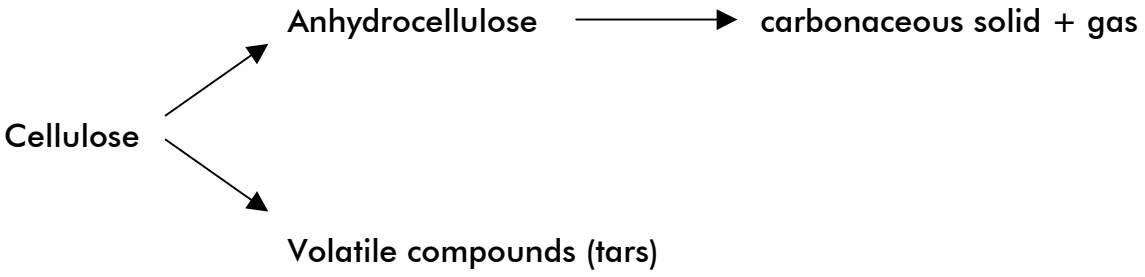

Fig. 53: Broido-Schafizadeh reaction scheme.

In literature, complex kinetic models can be found (e.g. those in the paper by Di Blasi [1998]). They come from a multi-step reaction mechanism exemplified in the Fig. 53. However, the thermal degradation is most often limited to a single stage, and the corresponding kinetics is summarized in the following "simple expression":

$$dCellulose = k_0.\exp(-E_a/RT)\,(1 - [Cellulose])\,.\,[Cellulose]0,5 \quad (50)$$

$$dCellulose_{total,mixture} = (EVA\ mass\ \%)\ dCellulose \quad (51)$$

This kinetic scheme is coming from the paper by Khezami et al. [2003].

The experimental procedure in this paper consists in carrying out dynamic thermogravimetric analyses and in subsequent discriminating of the kinetic equations proposed in literature for thermal decomposition of solid matter.

The form of the reaction rate expression is the following:

$$d\alpha/dt = k_0 \exp(-E_a/RT).f(\alpha), \quad (52)$$

where α represents conversion ratio of the solid and $f(\alpha)$ is a mathematical function depending on an assumed reaction mechanism. For example, for a kinetic mechanism of the first order, $f(\alpha)$ is equal to $1-\alpha$.

The results obtained in this study lead to an assumption that the equation that is most adapted to modelling of cellulose kinetics is the Prout-Tompkins equation. For this reason, the same equation was used in the thesis.

The modelling results present deviations when correlated with experiments. Nevertheless, the model remains close to the reality, with the exception of the final phase of the experiment.

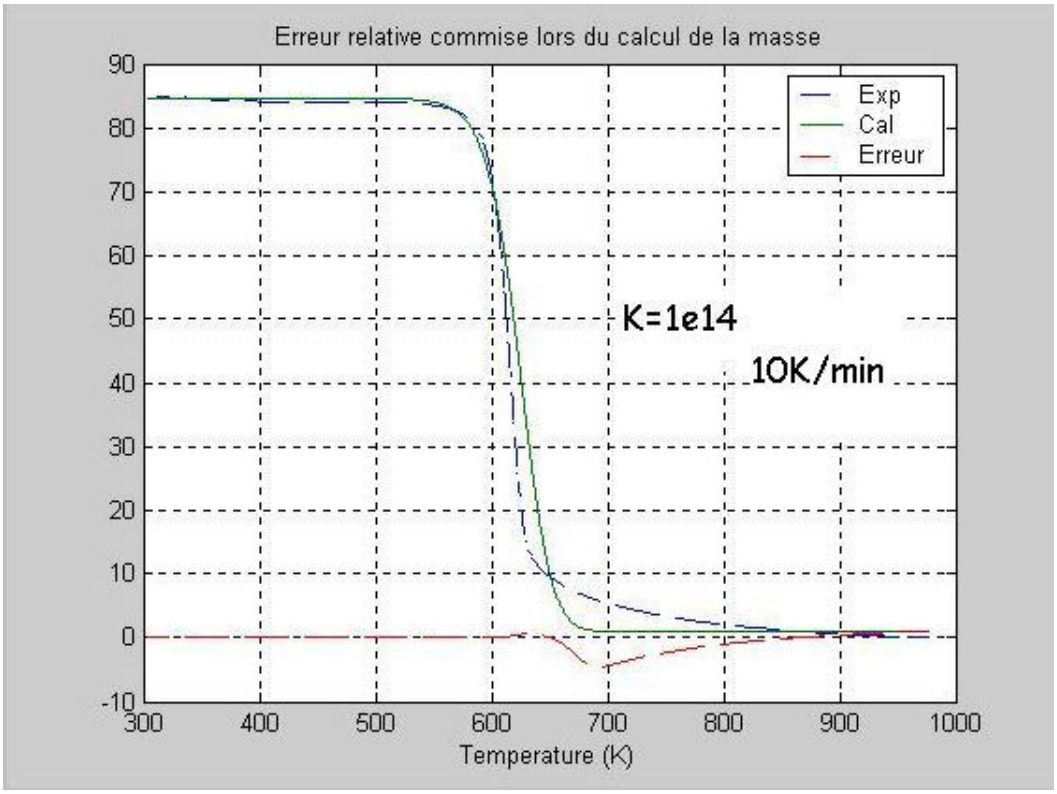

Fig. 54: Comparison of the experimental and calculated curve for the pure cellulose pyrolysis. X: temperature from 300 to 1,000 by 100 K, Y: mass from -10 to 90 by 10 %.

Modelling of mixtures

Reminder: In the case of mixtures, the independence hypothesis leads to this "simple superposition" of models:

$$d(\text{EVA/PVC mixture}) = dEVA_{\text{total, mixture}} + dPVC_{\text{total, mixture}} \quad (53)$$

$$d(\text{EVA/Cellulose mixture}) = dEVA_{\text{total, mixture}} + dCellulose_{\text{total, mixture}} \quad (54)$$

EVA/PVC mixture

With respect to the experimental curve below, the independence hypothesis seems to be totally out of question. In fact, the kinetic models used for pure PVC and pure EVA are adapted perfectly.

The problem of incoherence between experimental and calculated results cannot therefore be explained in any other way than by an existing interdependence between the compounds when mixed.

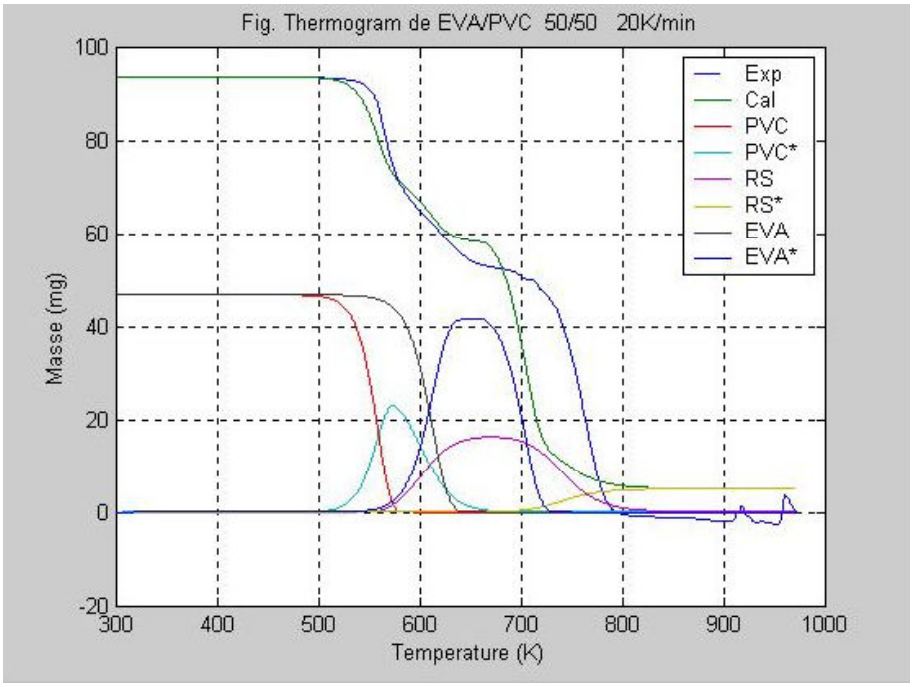

Fig. 55: Comparison of experimental and calculated curve for EVA/PVC mixture. X: temperature from 300 to 1,000 by 100 K, Y: mass from –20 to 100 by 20 %.

Thus, it can be supposed that there is an **interaction of PVC with the EVA degradation** in the course of the pyrolysis of mixture.

A detailed analysis of relative errors: $\frac{\left|mass_{experimental} - mass_{calculated}\right|}{mass_{experimental}}$ illustrates the solidity of our conclusions as well. The following table (Tab. 36) shows maxima of relative errors for mass data.

Tab. 36.: Maximal relative errors of the mass loss from the correlation of experimental and calculated curves.

Mixture	Proportions [%/%]	Heating rate [°C.min^{-1}]	Maximum relative error [%]
EVA/PVC	25/75	5	12.53
	50/50		14.3
	75/25		5.56
	25/75	10	10.0
	50/50		16.32
	75/25		16.58
	25/75	20	10.63
	50/50		26.6
	75/25		—
	25/75	30	11.03
	50/50		—
	75/25		—

After analysing experimental results from FTIR spectrometry, we could find more about phenomena (concerning interactions) that take part in the course of polymer mixture pyrolysis.

EVA/Cellulose mixture

For the mixture of EVA and Cellulose, it is more difficult to draw conclusions. In fact, just two curves could be analysed.

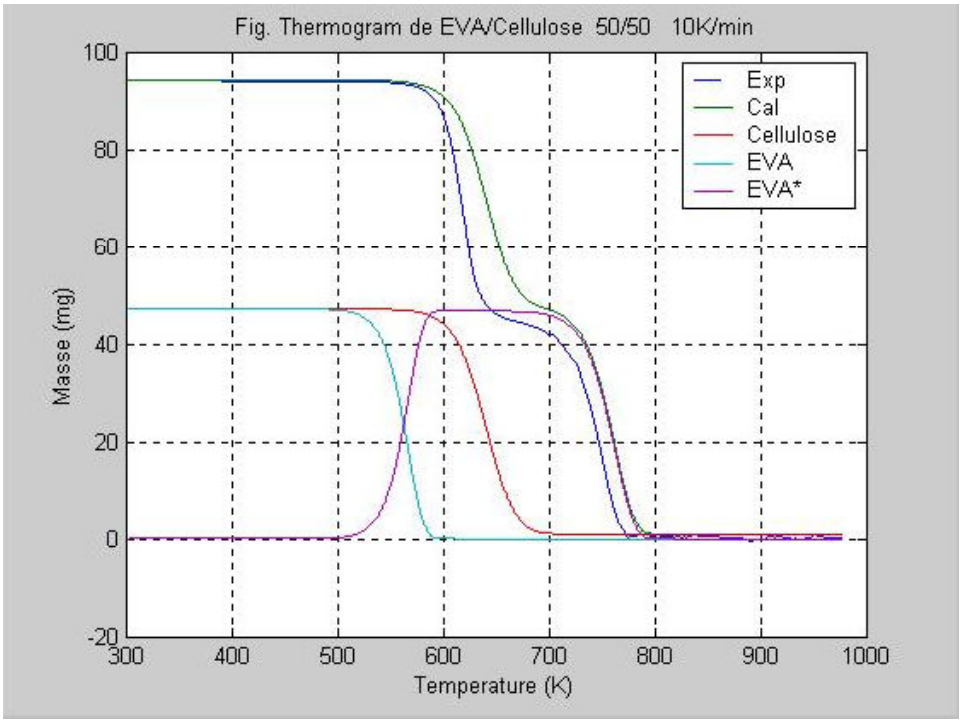

Fig. 56: Comparison of experimental and calculated curves for EVA/Cellulose mixture pyrolysis. X: temperature from 300 to 1,000 by 100 K, Y: mass from -20 to 100 by 20 %.

Notwithstanding, certain hypotheses can be pronounced with respect to phenomena that take place in the course of the mixture pyrolysis.

During its degradation, EVA produces acetic acid. Even of this acid is not strong, it is probable that it acts on basic parts of the cellulose molecule and thus accelerates its degradation (which can be observed by comparing experimental and calculated curve).

In the following curve representing a superposition of the degradation curves for pure cellulose, pure EVA, and 50/50 mixture of both, it can be noticed that pure cellulosis degrading up to 85 % of its total mass is degraded more in the mixture as its total mass loss amounts to 95 %. The curve of the mixture should occur exactly "in the middle" of two curves of pure compounds because the ratio is 50/50. Therefore, the difference stems from a "surplus degradation" of cellulose, that should be provoked by acetic acid.

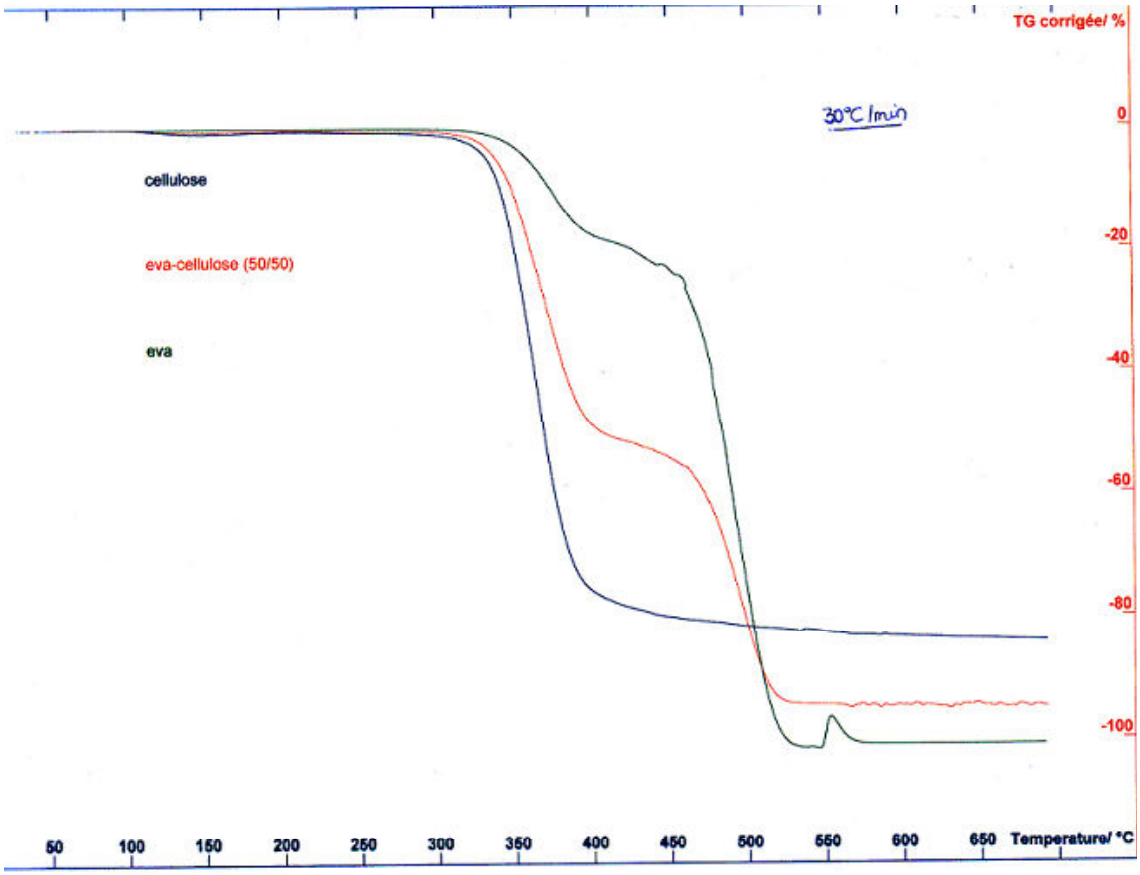

Fig. 57: Superposition of TGA experimental curves of pure cellulose, pure EVA and of the mixture of both. X: temperature from 50 to 650 by 50 °C, Y: mass from -100 to 0 by 20 %.

Conclusion on MatLab simulation results

Results from MatLab simulation has lead us to refute the independence hypothesis for the EVA/PVC mixture. FTIR analysis will enable a deeper understanding of observed interaction phenomena taking place during the relevant pyrolysis and thus conclude on reasons of this degradation (inter)dependence.

Regarding the EVA/Cellulose mixture, FTIR analysis will, in this case as well, provide some proof of the influence – with consideration of the simulation results – of acetic acid on cellulose degradation, as a difference between experimental and calculated curves exists. However, it remains minute in comparison to the one observed in the case of the EVA/PVC pyrolysis.

3.3.5 FTIR analysis of released gases

Now, infra-red spectra of gases released and registered during pyrolysis experiments will be studied. These results will be compared to TGA results. The most important objectives of this study are to:

- indentify diverse compounds produced in the cours of pyrolysis,
- specify the moment of their formation,
- find a direct relation with TGA.

It is interesting to be able to connect the result from analyses of FTIR spectra with mass variations registered by thermogravimetre. We can express the relation joining together the time as monitored on the corresponding Gram-Schmidt, for each and every moment τ, with the registred FTIR spectrum, at the temperature value visible on thermogramme.

Expression of temperature as the function of time

FTIR analyser (Fourrier-transform infra-red) is coupled with TGA-DTA analyser unit. Gases released in the course of pyrolysis are conducted by a vector of gas flow (in our case, the gas used is nitrogen, with the concentration 99.995 %) in the area of heat insulated case, where it is subsequently analysed by infra-red spectrometry.

The beginning of Gram-Schmidt registration (registration of spectra in function of time) is electronically synchronised with the initiation of heating of thermal analyser. This moment is considered as time τ_0 in each experiment:

- τ_{IR} is time in seconds corrsponding to an FTIR spectre obtained from registering of Gram-Schmidt,
- τ_{RS} is time in seconds of the transfer of gases released during pyrolyris, from TGA to the FTIR cell ; this time is directly the function of configuration of our installation and the flow of gas vector (its value, experimentally measured, amounts to 110 seconds),
- β is the hating rate, in $^{o}C.min^{-1}$,
- T is the sample temperature registred on thermogramme, in °C.

Thus :

$$T = [(\tau_{IR} + \tau_{RS})\,\beta]/\,60 \qquad (55)$$

Principle of infra-red spectrometry

Infra-red (IR) radiation is situated in the domain of electromagnetic spectre comprised between the visible region and the micro-wave region. A spectrum of infra-red absorption represents the variation of intensity of radiation emitted by a sample in function of wave length or of the radiation frequency. Molecules absorb the energy of these radiations and modify their vibration energy. Intensity of radiation is represented by transmission, which is a percentage of transmitted intensity. The wavelength is expressed in cm^{-1}, absorption frequency depends on relative masses of atoms, constant of bond forces, and on geometry of atoms. The graphical representation of the percentage of absorbed energy (absorption) in function of the wavelength constitutes infra-red spectrum.

Conventional spectrophotometers work in a domain from 400 to 4000 cm^{-1}. This interval is, for an organic chemist, the most interesting range of investigations. The Fourrier transformation infra-red (FTIR) spectrometry has been very developed lately and it can offer some advantages. The radiation comprising all IR wavelengths (from 5000 to 400 cm^{-1}) is divided in two beams. One of them has a fixed trajectory, the other has to pass through a pathway with variable distance (shifting mirror). When the difference in the optical path between beams corresponds to a whole multiple of the wavelength, a constructive interference is thus formed. A destructive interference appears when this difference is an entire multiple odd to the quarter of the wavelength. The result of a variation of intensities is an oscillating series of destructive or constructive combinations called an interferogramme. The Fourrier transformation converts this interferogramme with a time scale into a chart with frequencies, which is a more familiar form of the relation. A slight continual variation of the length of a piston adjusts the position of the mirror and imposes variations onto beam length. The Fourrier transformation in succeeding points along the whole set of variations produces a complete IR spectrum. The passage of this radiation through sample puts the compound through a wide energy band. In principle, an analysis of a single passage of the radiation containing the whole energy band through a sample produces a complete infra-red spectrum.

Essentially, infrared spectrometric analysis is a consequence of absorption of electromagnetic radiations at frequency values corresponding to the vibration of chemical bonds of molecules. It is important to note that the energy of a molecule is formed by an addition of diverse energetic terms:

$$E_{total} = E_{electronic} + E_{vibrational} + E_{rotational} + E_{translational}. \quad (56)$$

The translational energy shows a deplacement of molecules in the space. Rotational energy is a result of energy absorption in the region of microwaves. Electronic constituent is related to the transition energy of electrons that are distributed in the molecule. Vibrational factor corresponds to the energy of constituents of an atom that vibrate around the centre of the bonds.

Bibliographical summary

According to Munteanu et al. [1977], the FTIR results for EVA pyrolysis gases (12 % VA, 300°C) are:

- acetoxy group for the following peaks: 1736, 1240 1022, 947 et 794 cm^{-1},
- C=CH group for the peak at 964 cm^{-1} attributed to the C=C bond.

According to Dutta et al. [1995], FTIR results for pyrolysis gases of EVA with 12 % of VA and heating rate between 20°C and 550°C are:

- for =C=O, absorption stems from the stretching at 1737 cm^{-1},
- for $=CH_2$, absorption comes from scissoring at 1470 cm^{-1},
- for CH_2=CH-, the absorption comes from a deformation at 962 cm^{-1}.

According to Maurin [1991], FTIR results for EVA pyrolysis gas with 40 % of EVA, at the heating rate of 40°C.min^{-1}, temperature varying from 25 to 650 °C are: acetic acid, ethylene, methane and carbon dioxide.

According to the McGrattan [1993], the FTIR results for the EVA pyrolysis gases with 33 % of VA, the heating rate of 20°C.min^{-1} and temperature varying between 250 and 550 °C, are the following: acetic acid, carbon monoxide, carbon dioxide, and 1-hexadecene.

Analysis of results of FTIR for pure compounds

Pure EVA

Reminder: FTIR analysis provides a Gram-Schmidt representing the evolution of absorption of pyrolysis gases as a function of time. From the heating rate and the time of transfer of pyrolysis gas from TGA to FTIR analyser (approx. 110 s), corresponding temperature can be deducted.

Example of calculation of temperature for the time of 933,59 s:

$$t = \frac{(933.59 + 110)}{60} \times 20 = 347.86°C \tag{57}$$

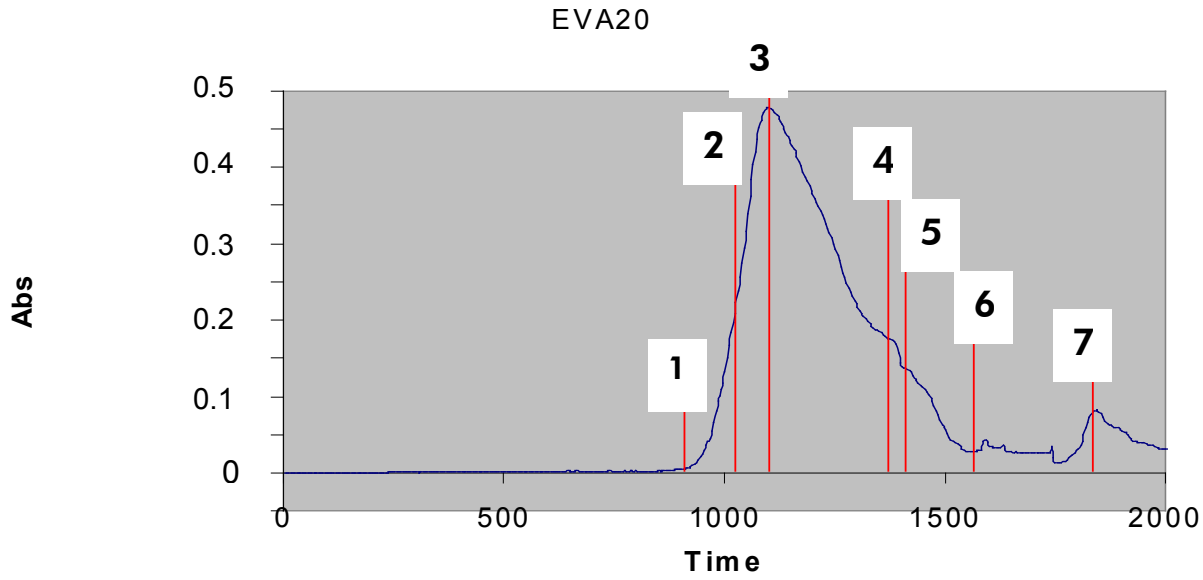

Fig. 58: Gram-Schmidt of pure EVA.

On the previous chart (Fig. 58), the following data were ascertained:

1. time = 933.59 s, T = 348°C

Appearance of the first characteristic peaks of acetic acid can be identified.

2. time = 1,006.87 s, T = 372°C

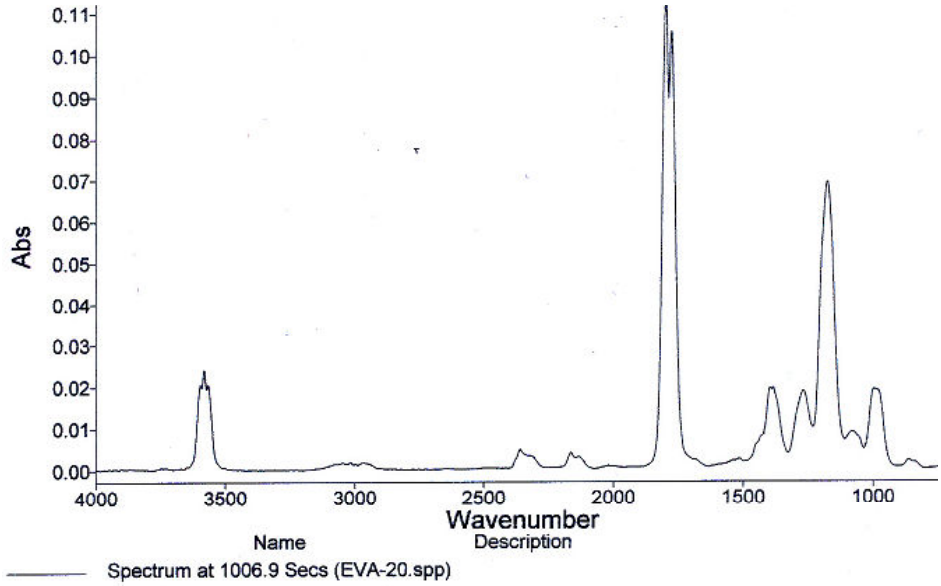

Fig. 59: Absorption spectrum during the EVA degradation at 1,006.87 s.

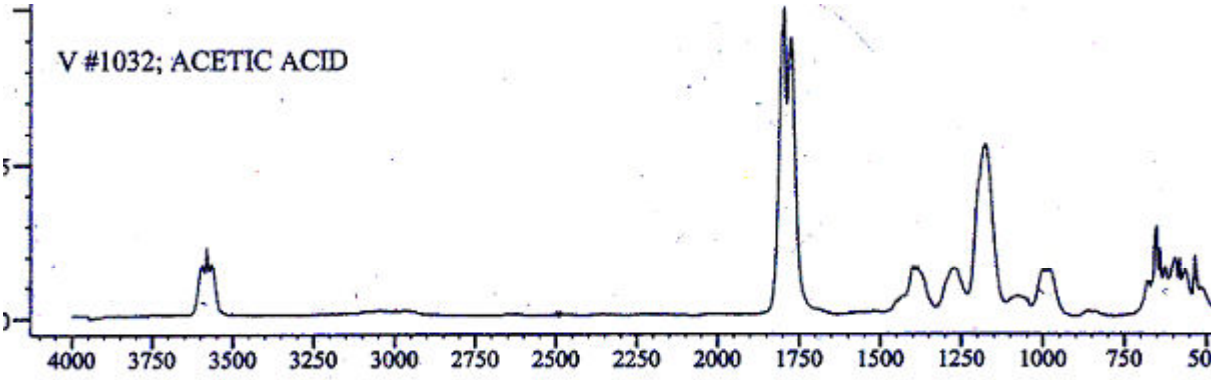

Fig. 60: Characteristic spectrum of acetic acid.

Considering the previous two curves (Fig. 59 and 60), the presence of acetic acid in the absorbency spectrum of EVA degradation can very easily be ascertained.

3. time = 1,097.16 s, T = 402°C.

Spectrum corresponding to the maximum release of acetic acid.

4. time = 1,385.52 s, T = 498°C.

Diminishing of the intensity of absorption peaks of acetic acid, but new peaks appear (in the region of 3,000 cm^{-1}) corresponding to the second stage of degradation of EVA.

5. time = 1,419.01 s, T = 510°C.

The persistent presence of acetic acid peaks and detection of "new ones" previously observed that become more intense.

6. time = 1,579.19 s, T = 563°C.

Evolution of peaks obtained previously is observed (presence of acetic acid is still to be noticed).

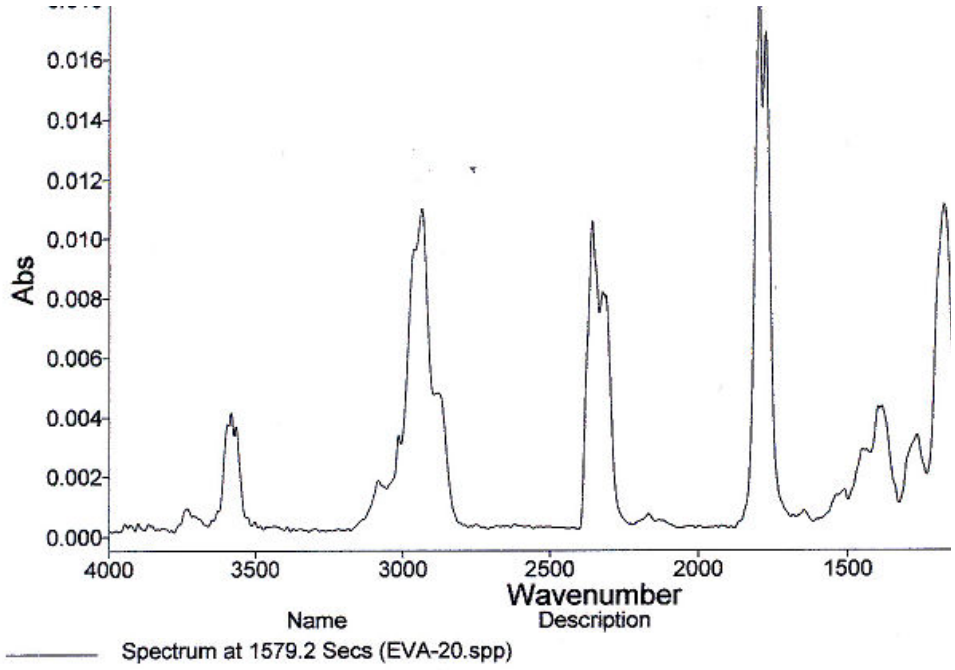

Fig. 61: Absorption spectrum during the degradation of EVA at 1,579.19 s.

7. time = 1,837.34 s, T = 649°C.

The peaks of acetic acid disappear and new peaks remain (in the surroundings of 3,000 cm^{-1}).

Pure PVC

In the same way as for EVA, spectra for specific moments of pyrolysis are extracted from the Gram-schmidt:

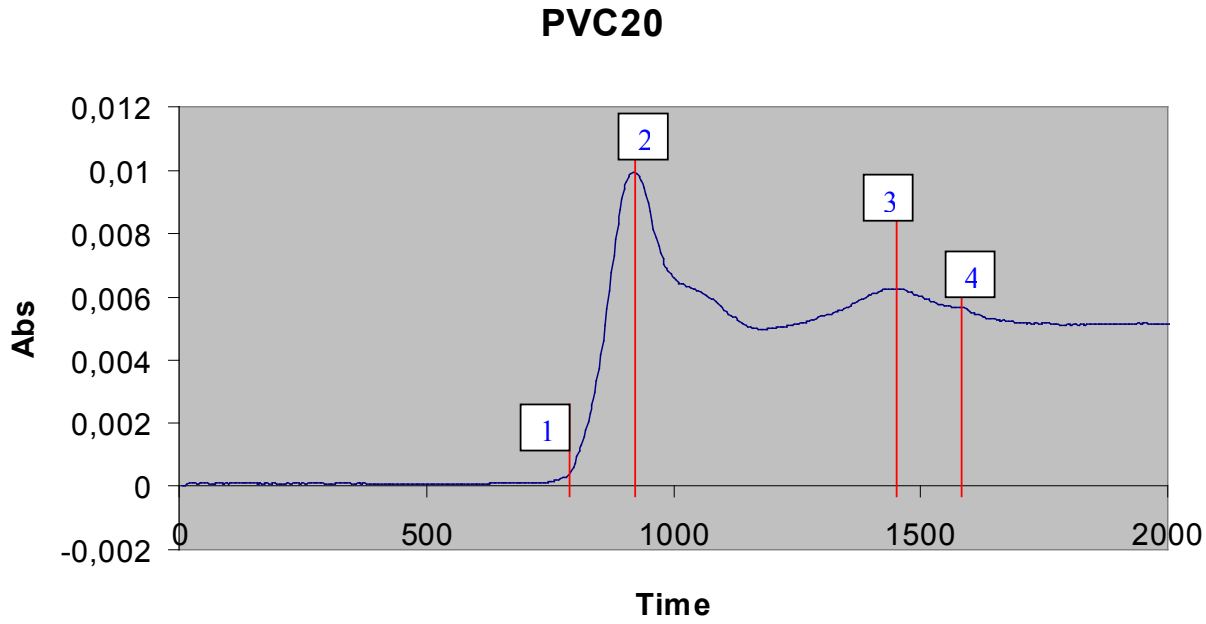

Fig. 62: Gram-Schmidt of the pure PVC.

1. time = 775.85 s, T = 295°C.

Slight peaks characteristic for hydrochloric acid appear (very easily discernable, corresponding to the rotation spectrum).

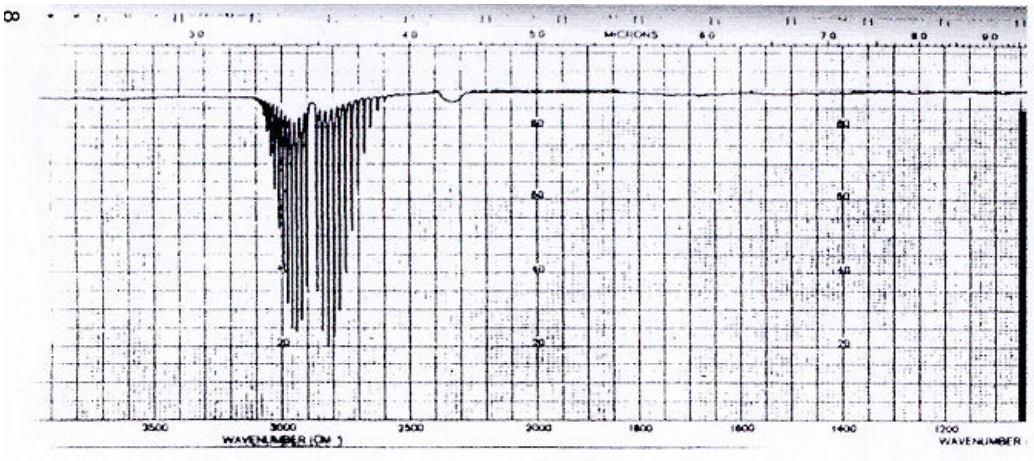

Fig. 63: Characteristic transmitance spectrum (= 1 – absorbance) of hydrochloric acid.

2. time = 922.60 s, T = 344°C.

The peaks of hydrochloric acid are very easily discernable.

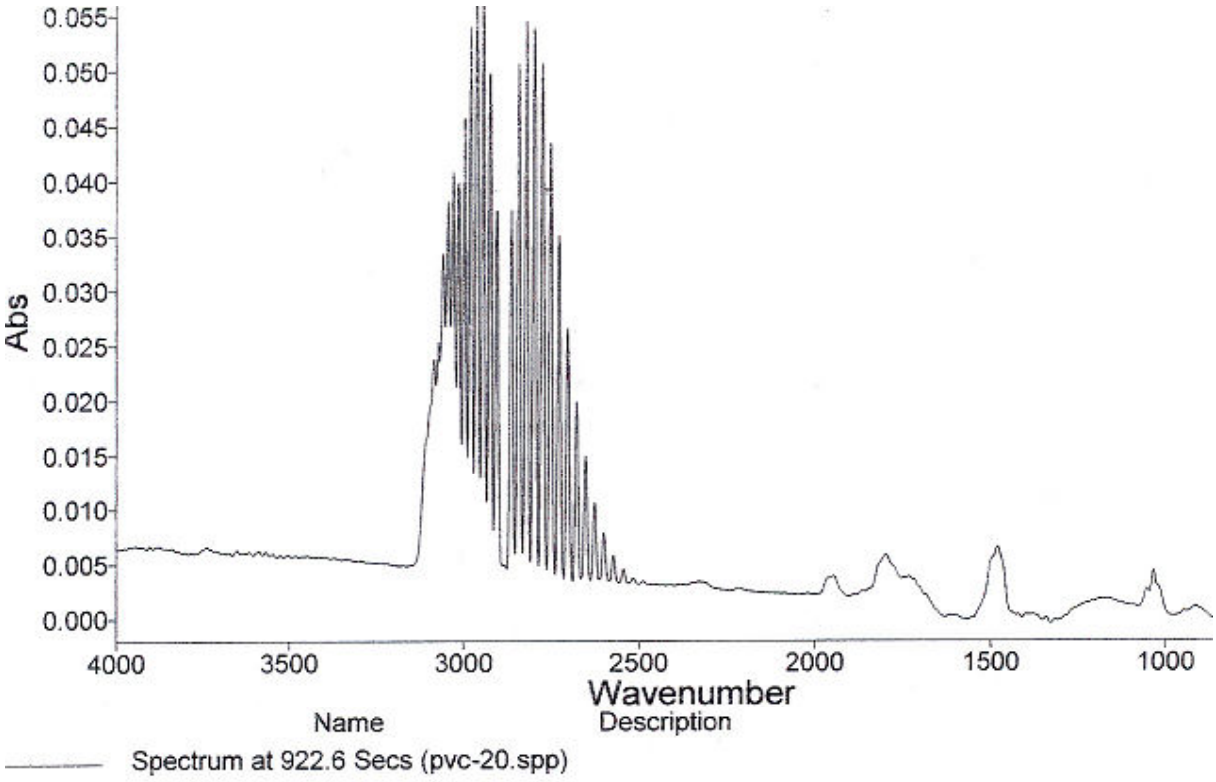

Fig. 64: Absorption spectrum during the PVC degradation at 922.6 s.

3. time = 1,457.82 s, T = 523°C.

The peaks of hydrochloric acid disappear almost totally and new peaks appear (around 3,000 cm^{-1} and between 1,500 and 1,000 cm^{-1}), corresponding to the last stage of the degradation of PVC.

4. time = 1,587.44 s, T = 566°C.

The last peaks evolve.

Analysis of experimental FTIR results in the case of the EVA/PVC mixture

The following Gram-Schmidt chart was obtained:

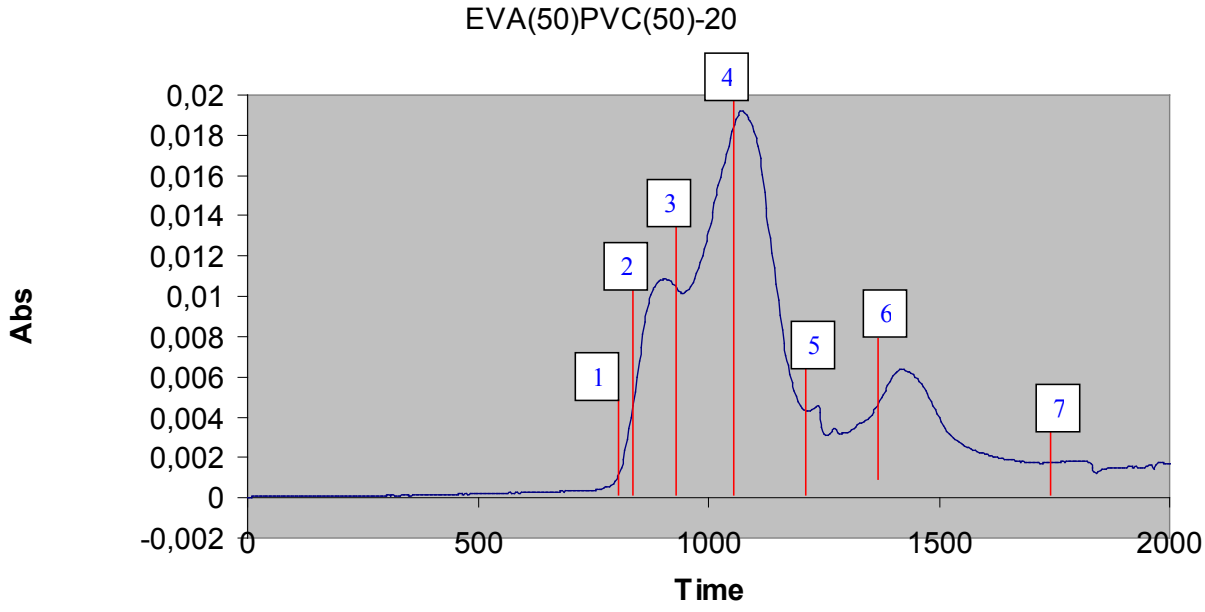

Fig. 65 : Gram-Schmidt of EVA/PVC mixture.

1. time = 785.23 s, T = 298°C.

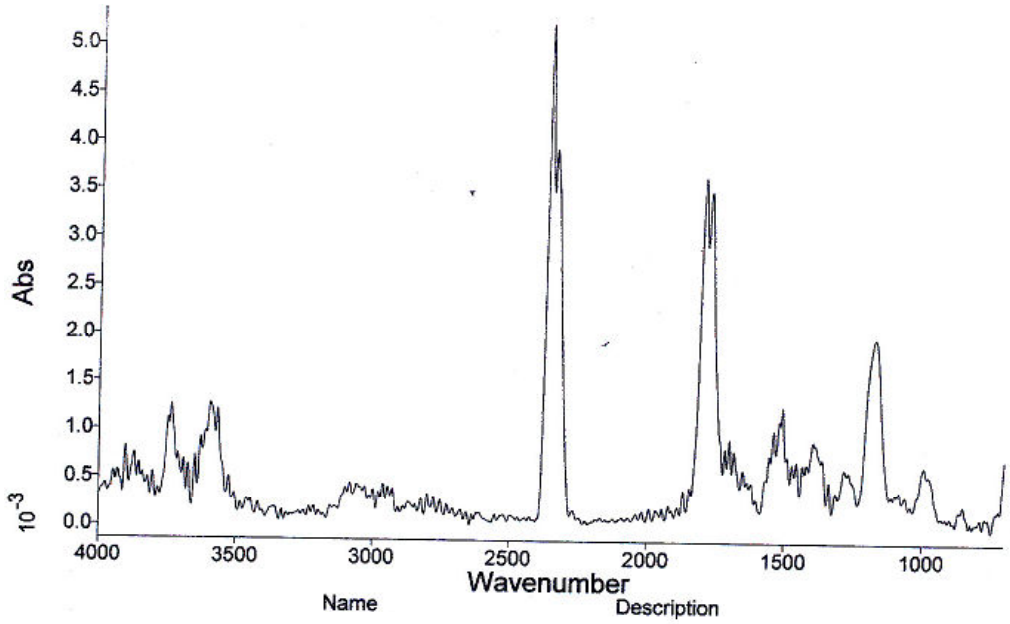

Fig. 66: Absorption spectrum during the degradation of the EVA/PVC mixture at 785.23 s.

Weak peaks of acetic acid can be observed.

2. time = 823.51 s, T = 311°C.

A simultaneous presence of acetic acid and hydrochloric acid peaks can be observed.

3. time = 856.8 s, T = 322 °C.

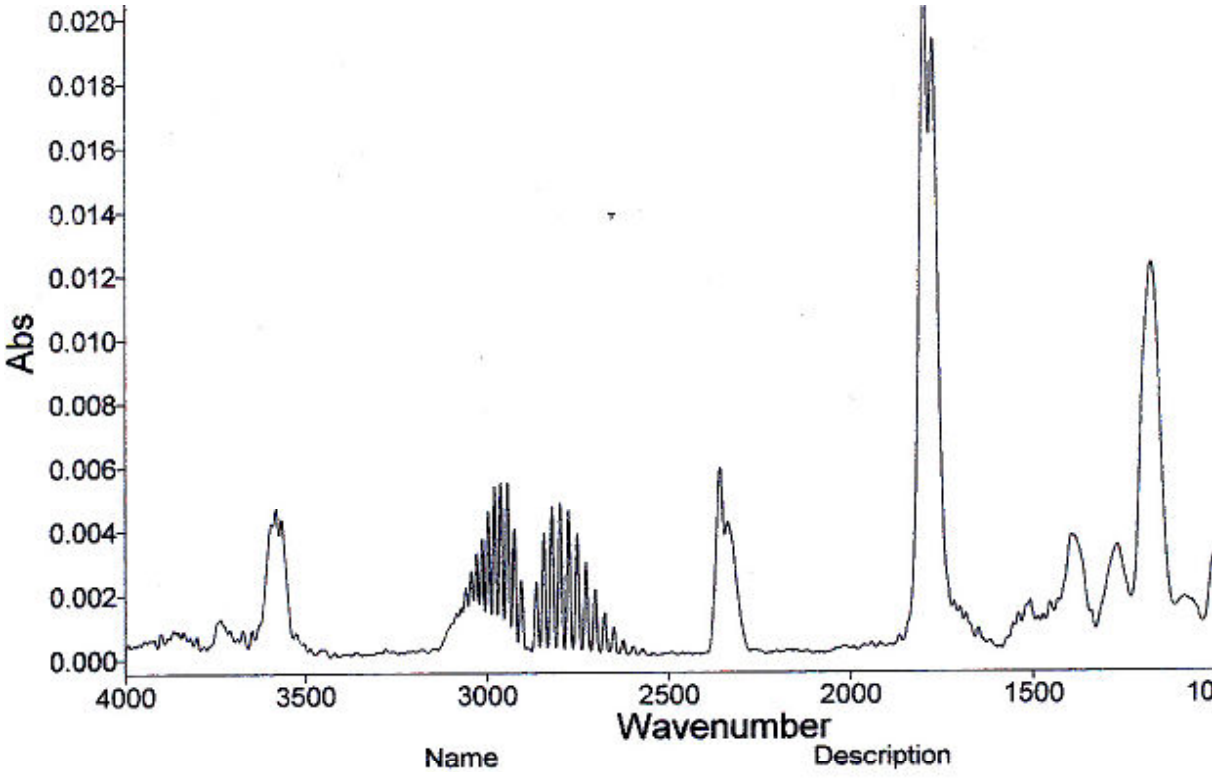

Fig. 67: Absorption spectrum for the degradation of EVA/PVC mixture at 856.8 s.

The peaks of acetic acid are still present, the peaks of hydrochloric acid become more intense.

4. time = 1,073.53 s, T = 395°C.

Acetic acid peaks remain present, whereas hydrochloric acid peaks begin to disappear.

5. time = 1,232.07 s, T = 447°C.

A residue of acetic acid still remains, the peaks of hydrochloric acid remain and appearance of new peaks around 3,000 cm^{-1} can be observed.

6. time = 1,422.98 s, T = 511°C.

The intensity of the peaks of acetic acid weakens, still new peaks at 3,000 cm^{-1} are observed and also little peaks at 1,500 and 1,000 cm^{-1}.

7. time = 1,845.79 s, T = 652°C.

A progressive disappearance of the whole set of peaks can be observed.

Conclusion about FTIR pyrolysis

It can be noticed that around 300°C, signs of acetic acid appear. This marks the degradation of EVA. At this temperature, pure EVA has not yet began its degradation. On the contrary, this temperature plateau corresponds to the first stage of the mass loss of PVC. However, the appearance of hydrochloric acid is slightly lagging behind compared to the pure PVC.

Next, for the temperatures in the surroundings of 350 °C and 480 °C, FTIR analysis confirms that the PVC degradation takes place at the same time as the degradation of EVA, which could be supposed when considering the superposition of temperature values for the peaks of pure polymers.

Thus, the above results confirm the MatLab simulation: the degradation is interdependent. It can be clearly seen that the degradation of EVA is accelerated: it occurs at 300 °C, though it should not appear until 350 °C. Conversely, PVC degrades theoretically first and at the surroundings of 300 °C. But the appearance of the peaks of hydrochloric acid, that are characteristic for its degradation, are not observed.

Conclusions corroborated by a recent paper:

In an article by Matsuzawa at al. [2001], a series of results that can be compared to what was observed in the case of EVA/PVC mixture can be found.

In fact, the publication presents experimental results of co-polymerisation of cellulose and some other polymers, as e.g. polyethylene, polypropylene, polystyrene and especially PVC. Even if the publication does not concern the EVA/PVC mixture, conclusions deduced from this series of experiments ally to the results that could be observed in the behaviour of our mixture:

• In the pyrolysis of mixtures, no interactions were confirmed other than those between cellulose (that could be assimilated to EVA in our case) and PVC. Cellulose degraded independently and with all the studied polymers with the exception of PVC.

This result is important in our identification methodology (in the precise case of this publication) of EVA together with cellulose.

In fact, as well as the EVA/PS mixture, the cellulose/PS mixture confirms the independence hypothesis. This actuality, together with the fact that cellulose has interacted only with PVC (as well as EVA), guides us to think that the behaviour of EVA in the mixture is noticeably similar to that of cellulose.

• In the mixture, cellulose degrades at a lower temperature than pure cellulose; this was observed for EVA in the mixture of EVA/PVC in our study.

• Experimentally obtained residual mass is more important than the one stemming from calculations, and this is corroborated in our case also.

Consequently, all the results converge to the same conclusion:

There is an interdependence of degradation phenomena for PVC and EVA.

Thus, the hypothesis can be enunciated that the apparition of hydrochloric acid can have a catalytic effect on the EVA degradation.

3.3.6 Discussion and conclusions

Analyses performed on the EVA/PVC mixtures and EVA/cellulose mixtures have allowed us to voice some conclusions concerning pyrolysis degradation of mixtures. For the EVA/PVC mixture, with respect to results from numerical simulation and FTIR, we are totally authorized to think that the phenomena are connected and that the polymers interact in the mixture. These interaction phenomena seem to have its cause in the catalytic effect of hydrochloric acid, released by PVC, on the EVA degradation.

For the EVA/cellulose mixture, conclusions are not as easy to pronounce, and this especially by reason of a very limited number of TGA experiments performed. However, these data seem to direct the conclusions to the non-validity of the proposed model, i.e. the dependency of compounds during their degradation in mixture. Interaction phenomena seem to be less clear-cut than in the case of the EVA/PVC mixture.

A hypothesis can be presented that for the mixture studied above, EVA plays the role of PVC in the mixture EVA/PVC. Actually, the degradation of EVA has lead to the formation of acetic acid in the first stage. Subsequently, this acid promotes the degradation of cellulose as an acid catalyst, just as HCl promotes the degradation of EVA as an acid catalyst.

Finally, in the case of the EVA/PVC mixture, the presence of gaseous HCl plays and enhances the role of a catalyst, via the interaction between hydrogen and oxygen, as proposed Munteanu and Turcu in their reaction scheme (see p. 87, Fig. 30) for active methylene.

In the case of EVA/cellulose mixture, a similar catalytic action of hydrogen of acetic acid formed in the first stage of the EVA degradation can be proposed for the rupture of ether glucosic bonds in cellulose.

4. Discussion and conclusion

In the presented thesis, evaluation of kinetic parameters of pyrolysis from thermogravimetric data based on the Ozawa-Flynn-Wall method (Popescu's modification) and on simulation of kinetic models in MatLab was realized.

Polymers studied include: polyvinyl chloride, lignin, cellulose, ethylene vinyle acetate copolymer, and polystyrene.

The present work on pyrolysis of polymers being developed on laboratory scale, it would surely prove valuable to conduct a comparative study of pyrolysis behaviour on pilot scale, which was not possible during this thesis due to technical reasons. Conclusions enriched by taking into account such pilot-scale study would be more appealing to mankind's industrial interests.

However, the thermogravimetric apparatus used, connected to FTIR spectrometer, has permitted to correlate mass loss data with pyrolysis behaviour under different heating rate values, represented by sets of spectra corresponding to specific moments of the degradation process. Kinetic parameters calculated by means of the Popescu's variant of the Ozawa-Flynn-Wall integral method were in good agreement with reference data.

On the whole, the results proved that the initial analysis of suitability of various computational methods in the field of polymer pyrolysis based on an extensive and accurate study of available literature was valuable.

Moreover, the study of polymer mixtures by the model-fitting method, promoted by the FTIR analysis of spectra of gases released has allowed to demonstrate the absence of interactions in the case of the thermal degradation of the EVA-PS mixture. Contrariwise, in the case of the EVA-PVC and EVA-Cellulose mixtures, the thermal degradation vents itself by interactions. With respect to the EVA-PVC mixture, the interactions are strong, in relation to the EVA-Cellulose mixture, the interactions are not so pronounced. The most verisimilar interpretation of these interactions can be presented as a phenomenon induced by the acid catalysis caused by the acid nature of gaseous compounds (HCl, CH_3COOH) released during the first stage of the degradation of PVC and EVA. Finally, it is important to note that the totality of these results has contributed to a better managing

of the α reactor operation by CEA, by virtue of a better understanding of phenomena occurring during thermal degradations.

5. References

ACS, American Chemical Society: United States Synthetic Rubber Program, 1939-1945 – http://www.rockbridgegroup.com/review/new_nhcl/nhcl_2/landmarks/rbb/rbb_begin.html.

Adachi, S., Tanimoto, M., Tanaka, M., Matsuno, R., Chemical Engineering Journal 49 (1992) B17.

APME, Recommendations to improve the competitiveness of plastics recycling, Association of plastic manufacturers in Europe (APME), Recycling World magazine, 1999 report, p. 4, Brussels.

APME, Plastic Recovery in perspective; Plastics Consumption and recovery in Western Europe 1995, Association of Plastic Manufacturers in Europe (APME), Brussels, Belgium, 1996.

Arnold, M., Veress, G. E., Paulik, J., Paulik, F., The applicability of the Arrhenius model in thermal analysis, Analytica Chimica Acta 124 (1981) 341-350.

Avni, E., Coughlin, R. W., Thermochim. Acta 90 (1985) 157-167.

Ballistreri, A., Foti, S., Montaudo, G., Scamporrino, E., J Polym Sci, Polym Chem Ed 18 (1980) 1147. (a)

Ballistreri, A., Foti, S., Montaudo, G., Scamporrino, E., J Polym Sci, Polym Chem Ed 18 (1980) 3101. (b)

Banyasz, J. L., Li, S., Lyons-Hart, J. L., Shafer, K. H., Cellulose pyrolysis: the kinetics of hydroxyacetaldehyde evolution, Journal of Analytical and Applied Pyrolysis 57 (2001) 223-248.

Barbooti, M. M., The possibility of resolving overlapping decomposition reactions by the kinetic plots of thermogravimetric data, Thermochimica Acta 68 (1983) 363-370.

Billa, E., Koukios, E. G., Monties, B., Investigation of lignins structure in cereal crops by chemical degradation methods, Polymer Degradation and Stability 59 (1998) 71-75.

Bockhorn, H., Hornung, A., Hornung, U., Teepe, S., Weichmann, J., Combustion Science and Technology, 116-117 (1996), 129-151.

Britt, Ph. F., Buchanan, A. C., III, Thomas, K. B., Lee, S.-K., Pyrolysis mechanisms of lignin: surface-immobilized model compound investigation of acid-catalyzed and free-radical reaction pathways, Journal of Analytical and Applied Pyrolysis 33 (1995) 1-19.

Brown, H. A., Penski, E. C., Callahan, J. J., Thermochim. Acta 3 (1971) 271.

Brown, M. E., Introduction to Thermal Analysis – Techniques and Applications, Chapman and Hall, London – New York, 1988.

Brown, M. E., Maciejewski, M., Vyazovkin, S., Nomen, R., Sempere, J., Burnham, A., Opfermann, J., Strey, R., Anderson, H. L., Kemmler, A., Keuleers, R., Janssens, J., Desseyn, H. O., Chao-Rui Li, Tong B. Tang, Roduit, B., Málek, J., Mitsuhashi, T., Computational aspects of kinetic analysis, Part A: The ICTAC kinetics project-data, methods and results, Thermochimica Acta 355 (2000), 125-143.

Burnham, A. K., Computational aspects of kinetic analysis. Part D: The ICTAC kinetics project — multi-thermal-history model-fitting methods and their relation to isoconversional methods, Thermochimica Acta 355 (2000) 165-170.

Caballero, J. A., Font, R., Marcilla, A., Study of the primary pyrolysis of Kraft lignin at high heating rates: yields and kinetics, Journal of Analytical and Applied Pyrolysis 36 (1996) 159-178.

Caldwell, K. M., Gallagher, P. K., Johnson, D. W., Thermochimica Acta 18 (1977), 15.

Camino, G., Sgobbi, R., Z., Colombier, S., Scelza, C. Fire Matter 24 (2000) 85-90.

CDS Analytical, Inc. Degradation Mechanisms – Random Scission 2000.

CDS Analytical, Inc. Degradation Mechanisms – Side Group Elimination 2000.

Chang, E. P., Salovey, R., Polym Sci Polym Chem Ed 12 (1974) 2927.

Clark, Jim, http://www.chemguide.co.uk/atoms/bonding/vdw.html.

Chiu, S. J., and Cheng, W. H., Thermal degradation and catalytic cracking of poly(ethylene terephthalate), Polymer Degradation and Stability 63 (1999) 407-412.

Christmann W, Kasioke D., Klöppel K. D., Partocht H., Rotard W., Chemosphere 19, 1-6 (1989), 387.

Coats, A. W., Redfern, J. P., Analyst 88 (1963), 906.

Collins, D. E., Richey, F. A., Jr., Synthetic organic chemicals, In: Kent, J. A., ed., Riegel's handbook of industrial chemistry, 9th ed. New York, Van Nostrand Reinhold, 1992, pp. 800-862.

Cordero T., Rodríguez-Maroto, J. M., Thermochim. Acta 164 (1990) 135-144.

Day, M., Cooney, J. D., Touchette-Barrette, C., Sheehan, S. E., Pyrolysis of mixed plastics used in the electronics industry, Journal of Analytical and Applied Pyrolysis 52 (1999) 199-224.

DeClerq, M., Duval, C., Anal. Chim. Acta 5 (1951), 282.

Di Blasi, C., Comparison of semi-global mechanisms for primary pyrolysis of lignocellulosic fuels, Journal of Analytical and Applied Pyrolysis, 47 (1998) 43-64.

Domburgs, G., Sergeeva, V. N., Kalnis, A., Khim. Drev. 7 (1971) 59.

Dorrestijn, E., Laarhoven, L. J. J., Arends, I. W. C. E., Mulder, P., The occurrence and reactivity of phenoxyl linkages in lignin and low rank coal, Journal of Analytical and Applied Pyrolysis 54 (2000) 153-192.

Doyle, C. D., Kinetic analysis of thermogravimetric data, Journal of Applied Polymer Science, Vol. V 15 (1961) 285-292.

Doyle, C. D., J. Appl. Polym. Sci. 6 (1962) 639.

Drysdale, D., An Introduction to Fire Dynamics. Chichester: John Wiley and Sons, 1985.

Dunn, J. G., Chem. Aust. 47 (1980) 281.

Dutta, S. K., Bhowmick, A. K., Mukunda, P. G., Chaki, T. K., Thermal degradation studies of electron beam cured ethylene-vinyl acetate copolymer, Polymer Degradation and Stability 50 (1995) 75-82.

Ebert, K. H., Ederer, H. J., Schröder, U. K. O., Hamielec, A. W., On the Kinetics and Mechanism of Thermal Degradation of Polystyrene, Makromolekulare Chemie – Macromolecular Chemistry and Physics 183 (1982) 1207-1218.

Escola, J. M., Reciclado químico de poliolefinas con catalizadores zeolíticos, Ph. D. thesis, Universidad Complutense de Madrid, 1998.

Flynn, J.H., Wall, L.A., General treatment of the thermogravimetry of polymers, Journal of Research of the National Bureau of Standards-A. Physical and Chemical Vol. 70A, N°6, (Nov-Dec. 1966), 487.

Fontana, A., La thermolyse au service du traitement des déchets: Actualité et perspectives. Université Libre de Bruxelles, Faculté des Sciences Appliquées, Faculté des Sciences Sociales, Politiques et Economiques, Ecole de Commerce Solvay, EFE-Paris, octobre 1998.

Fontana, A., Laurent, Ph., Kestemont, C., Braekman-Danheux, C., Municipal waste pyrolysis (1) – The Behaviour of Chlorine with Cellulose and Lignin, Erdöl Erdgas Kohle, 116/2 (Feb. 2000), 89-92.

Gilby, G. W., Ethylene-vinyl acetate copolymers. In : Developments in rubber technology – 3. London : Applied Science Publishers Ltd., 1982.

Grassie, N., Kerr, W. W., Trans. Faraday Soc. 55 (1959) 1050.

Grassie, N., Kerr, W. W., Makromol. Chem. 51 (1962) 130.

Guyot, A., Bert, M., Journal of Applied Polymer Science 17 (1973) 753.

Hergert, H. L., Infrared Spectra, in Sarkanen, K. V., and Ludwing, C. H. (Eds.), Lignins: Occurrence, formation, structure and reaction (1971), 268-272.

Hinz B., Hoffmockel M., Pohlmann K., Schädel S., Schimmel I., Sinn, H., Journal of Analytical and Applied Pyrolysis, 1994, 30-35.

Horatius = Q. Horatius Flaccus, Satirae, 1, 10, 34.

Hoyt, C. H., Goheen, D. W., in: Sarkanen, K. V., Ludwig, C. H. (Eds.), Lignins, Wiley-Interscience, New York, 1971, Chapter 20, p. 833.

Hrdina, K. E., et al., Detect formation during binder removal in ethylene vinyl acetate filled system, Journal of Materials Science 34 (1999) 3281-3290.

Hsiung, C., Chang, C. Y., Hor, J. L., Waste Management, 13 (1993), 221-235.

Ida T., Nakanishi M., Goto K., Polym Chem Ed 12 (1974) 737.

Jakab, E., Faix, O., Till, F., Thermal decomposition of milled wood lignins studied by thermogravimetry/mass spectrometry, Journal of Analytical and Applied Pyrolysis, 40-41 (1997) 171-186.

Jellinek, H. H. G., Journal of Polymer Science 3 (1948) 850.

Karaduman, A., Simsek, Çiçek, B., Bilgesü, A. Y., Flash pyrolysis of polystyrene wastes in a free-fall reactor under vacuum, Journal of Analytical and Applied Pyrolysis 60 (2001) 179-186.

Khezami, Capart, Evaluation de différents modèles cinétiques appliqués à la pyrolyse de la cellulose, 9ème congrès SFGP St Nazaire, 9-11 sept 2003.

Knümann, R., Bockhorn, H., Combustion Science and Technology, 39/3 (1994), 860-865 (cited in Fontana et al.).

Lecomte, D., Bodoira, N., Mise au point et validation de techniques d'analyses couplées: TG/FTIR & TG/DSC/CPG/SM, Projet de Fin d'Etudes à CPE-LYON, effectué au Centre Energétique et Environnement de l'Ecole des Mines d'Albi-Carmaux, 2002.

Lin, S. Y., Lin, I. S., Lignin, Ullmann's encyclopedia of industrial chemistry, Vol. A-15, Edition Elvers, Hawkins et Schulz, 1990, 305-314.

Liptay, G., J. Thermal Anal. 25 (1982) 235.

Lombardi, G., For Better Thermal Analysis, 2nd ed., ICTA, Rome, 1980.

Lukaszewski, G. M., Redfern, J. P., Lab. Pract. 30 (1961) 469.

Maciejewski, M., Computational aspects of kinetic analysis. Part B: The ICTAC Kinetics Project — the decomposition kinetics of calcium carbonate revisited, or some tips on survival in the kinetics minefield, Thermochimica Acta 355 (2000) 145-154.

Mackenzie, R. C., Thermochimica Acta 28 (1979) 1.

Mackenzie, R. C., Isr. J. Chem. 22 (1982) 22.

Madorsky, S. L., Thermal degradation of organic polymers. In: Mark, H. F. and Immergut, E. H., ed. Polymer reviews, Vol 7, New York: John Wiley & Sons, 1964.

Marcilla, A., Beltrán, M., Polymer Degradation and Stability 48 (1995a) 219.

Marcilla, A., Beltrán, M., Kinetic study of the thermal decomposition of polystyrene and polyethylene-vinyl acetate graft copolymers by thermogravimetric analysis, Polymer Degradation and Stability 50 (1995b) 117-124.

Marcilla, A., Beltrán, M., Thermogravimetric kinetic study of poly(vinylchloride) pyrolysis, Polymer Degradation and Stability (1995c) 117-124.

Marcilla, A., Gómez, A., Reyes-Labarta, J. A., MCM-41 catalytic pyrolysis of ethylene-vinyl acetate copolymers: kinetic model, Polymer 42 (2001) 8103-8111.

Mardosky, S. L., McIntyre, D., O'Mara, J. H., Straus, S., J. Res. Natl Bur. Stand. Sect. A 66 (1962) 307.

Masuda, T., Miwa, Y., Tamagawa, A., Mukai, S. R., Hashimoto, K., Ikeda, Y., Degradation of waste poly(ethylene terephthalate) in a steam atmosphere to recover terephthalic acid and to minimize carbonaceous residue, Polymer Degradation and Stability 58 (1997) 315-320.

Mathias, L. J., http://www.psrc.usm.edu/macrog/natupoly.htm (see PSRC entry).

Mathot, V. B. F., Thermal analysis and calorimetry beyond 2000: challenges and new routes, Thermochimica Acta 355 (2000) 1-33.

Matsuzawa, J., Ayabe, M., Nishino, J., Acceleration of cellulose co-pyrolysis with polymer, Polymer degradation and stability, 71/3 (2001), 435-444.

Maurin, M. B., Dittert, L. W., and Hussain, A. A. Thermagravimetric analysis of ethylene-vinyl acetate copolymers with Fourier transforme infrared analysis of the pyrolysis products. Thermochim Acta, 186 (1991) 97-102.

McGrattan, B. J., Applied Spectroscopy, 48/12 (1993) 1472-1476.

McNeill. Comprehensive polymer science, vol. 6. Oxford : Pergamon Press, 1989.

McNeill, I. C., Bounekhel, M., Thermal Degradation Studies of Terephtalate Polyesters: 1. Poly(alkylene terephtalates), Polymer Degradation and Stability 34 (1991) 187-204.

Miller, R. R., et al. Styrene production, use and human exposure. Critical reviews of toxicology 24 (1994) 1-11.

Milosavljevic, I., Oja, V., and Suuberg, E. M., Thermal Effects in Cellulose Pyrolysis: Relationship to Char Formation Processes, Ind. Eng. Chem. Res. 35 (1996) 653-662.

Miranda, R., Yang, J., Roy, Ch., Vasile, C., Vacuum pyrolysis of PVC - I. Kinetic study, Polymer Degradation and Stability 64 (1999) 127-144.

Moskala, E. J., Lee, D. W., Polymer Degradation and Stability 25 (1989) 11.

Mothé, C. G., Tavares, M. I. B., Study of recycling and biodegradability of ethylene-co-vinyl acetate reject by thermal analysis, Polymer Degradation and Stability 57 (1997) 183-186.

Munteanu, D., Turcu, S., Studiul mecanismului reacțiilor de descompunere termică a copolimerilor grefați ai poli(etilenei) cu acetatul de vinil, Materiale Plastice 14/3 (1977) 144-147.

Munteanu, D., Turcu, S., Journal of Thermal Analysis 20 (1981) 281.

Murty, M. V. S., Rangarajan, P., Grulke, E. A., Bhattachara, D., Fuel Process. Tech., 49 (1996), 75-90.

Nernst, W., Riesenfeld, E. H., Ber. 36 (1903), 2086.

Newkirk, A. E., Anal. Chem. 32 (1960) 1558.

Newkirk, A. E., Aliferis, I., Anal. Chem., 30 (1958), 982.

Nunn, T. R., Howard, J. B., Longwell, J. P., Peters, W. A., Ind. Eng. Chem. Process Des. Dev. 24 (1985) 844.

Oakes, W. G., Richards, R. B., J. Chem. Soc. (1949) 2929-2935.

Odian, G. Principles of polymerization. 3rd ed. New York : Wiley, 1991.

Oliveira, A. A. M., Kaviany, M., Hrdina, K. E., Halloran, J. W., Mass diffusion-controlled bubbling and optimum schedule of thermal degradation of polymeric binders in molded powders, International Journal of Heat and Mass Transfer 42 (1999) 3307-3329.

Ozawa, T., Critical investigation of methods for kinetic analysis of thermoanalytical data, Journal of Thermal Analysis 7 (1975) 601-617.

Ozawa, T. [2], Bull. Chem. Soc. Jpn. 38 (1965) 1881.

Ozawa, T., Thermal analysis — review and prospect, Thermochimica Acta 355 (2000) 35□42.

Pascali, C. E. L., Herrera, H., Pyrolysis of lignin and IR analysis of residues, Thermochimica Acta, 293 (1997) 39-46.

Patel, R., Velasquez, A., Calderon, H. S., Brown, G. R., J. Appl. Polym. Sci., 46 (1992), 179 (cited in Fontana et al.).

Paulik, F., Paulik, T., Thermochimica Acta 4 (1972) 189.

COL (Physical Chemistry On Line, http://www.pcol.ch.iup.edu/polymers/Resources/Classification.htm.

Perkin-Elmer Model TGS-1 Thermobalance Brochure, Perkin-Elmer Co., Norwalk, C.

Plastiques et Elastomeres Magazine 54-1, Janvier/Fevrier 2002, 58.

Pinorini, M. T., La suie comme indicateur dans l'investigation des incendies. Thesis Dissertation. Lausanne: Institut de police scientifique et de criminologie 1992.

Popescu, C., Integral method to analyze the kinetics of heterogenous reactions under non-isothermal conditions. A variant on the Ozawa-Flynn-Wall method. Thermochimica Acta 285 (1996) 309-323.

Popescu, C., personal communications, 2003.

PR.COM (PlasticsRescource.com, The American Plastics Council, http://www.plasticsresource.com/s_plasticsresource/sec.asp?TRACKID=&CID=126&DID=228.

PSRC, University of Southern Mississippi, Department of Polymer Science, http://www.psrc.usm.edu / macrog/ vinyl.htm.

Ramakrishna, U., Aravamudan, M., Aravamudan, G., Curr. Sci. 39 (1970) 206.

Rice, F.O., Rice, K. K., The aliphatic free radicals, John Hopkins Press, Baltimore, MD, 1936.

Richards, D. H., Salter, D. A., Polymer 8 (1967) 153.

Roduit, B., Maciejewski, M., Baiker, A., Influence of experimental conditions on the kinetic parameters of gas-solid reactions – parametric sensitivity of thermal analysis, Thermochimica Acta 282/283 (1996) 101-119.

Roduit, B., Computational aspects of kinetic analysis. Part E: The ICTAC Kinetics Project—numerical techniques and kinetics of solid state processes, Thermochimica Acta 355 (2000) 171-180.

Sakata, Y., Uddin, M. A., Koizumi, K., Murata, K., Thermal degradation of polyethylene mixed with poly(vinyl chloride) and poly(ethyleneterephthalate), Polymer Degradation and Stability 53 (1996) 111-117.

Salamone, M. F., Westlake, G., Vinyl chloride – an annotated bibliography with emphasis on genotoxicity and carcinogenicity, Ontario Ministry of the Environment, September 1998, ISBN: 0-7778-7908-5.

Serra, R., Nomen, R., Sempere, J., J. Thermal Anal. 52 (1998) 933.

Seymour, R. B., Journal of Chemical Education 65 (1988) 327-334.

Simha, R., Wall, L. A., Bram, J., J. Chem. Phys. 29 (1958) 894.

Simons, E. L., Newkirk, A. E., Talanta 11 (1964) 549.

Soudais, Y., Lemort, F., Blažek, J., Cassagne, S., Corbel, E., Jardot, Ch., Spinu, M., Thomas, S., Etude de la pyrolyse de mélanges de polymères: Cas des mélanges binaires EVA/PS et EVA/PVC, Rapport de projet 16, IFI 3, Ecole Nationale Supèrieures des Techniques Industrielles et des Mines d'Albi-Carmaux, Avril 2003.

Stamm, A. J., Ind. Eng. Chem. 48 (1956) 413.

Starnes, W. H., Jr., Girois, S., Polymer Yearbook, 1996, p. 105 (cited in Fontana et al.).

Suuberg, E. M., Peters, W. A., Howard, J. B., Ind. Eng. Chem. Process Des. Dev. 17 (1978) 37.

Syndicat des Producteurs de Matières Plastiques, http://www.proplast.org/spmp.

Šatava, V., Mechanism and kinetics from non-isothermal TG traces, Thermochimica Acta 2 (1971) 423-428.

Tang, W. K., U. S. For. Serv. Res. Pap. FPL 71 (1967).

TRP Project (Technology Reinvestment Program, Tutorial on Polymer Composite Molding, Michigan State University and the University of Delaware, http://islnotes.cps.msu.edu/trp/).

Turi, E. A., editor, Thermal characterization of polymeric materials, 2nd edition (1997, 1981), Academic Press, Inc.

Urbain, G., Compt. Rend. 154 (1912) 347.

US EPA. Characterization of municipal solid waste in the United States 1990 update. EPA 530-SW-90-042. Environmental Protection Agency, Office of Solid Waste and Emergency Response, 1990.

Vyazovkin, S., Computational aspects of kinetic analysis. Part C. The ICTAC Kinetics Project — the light at the end of the tunnel?, Thermochimica Acta 355 (2000) 155-163.

Wall, L. A., Straus, S., McIntyre, D., Simha, R. H., J. Phys. Chem. 70 (1966) 53.

Wall, L. A., Madorsky, S. L., Brown, D. W., Straus, S., Simha, R., J. Am. Chem. Soc. 76 (1954) 3430.

Wampler, T. P., Analytical Pyrolysis: An Overview, In: Wampler, T. P., ed. Applied Pyrolysis Handbook. New York: Marcel Dekker, 1995: 1–29.

Wendlandt [1], W. Wm., Thermal Analysis, 3rd Edition, John Wiley & Sons, February 1986, ISBN: 0-471-88477-4.

Wendlandt, W. Wm., Thermochimica Acta 36 (1980) 393.

Wenzl, H. F. J., The Chemical Technology of Wood, Academic Press, New York, 1970.

6. References – selected papers on kinetics

Agherghinei, I., Thermogravimetry. Analysis of the parameters of the DTG maximum, Thermochimica Acta 285 (1996) 57-65.

Atkinson, J., MacCallum, J.R., Kinetics of thermal decomposition of polymer. II, Journal of Polymer Science: part A-2, Vol. 10, 811-822 (1972).

Bagchi, T.P., Sen, P.K., Combined differential and integral method for analysis of non-isothermal kinetic data, Thermochimica Acta 51 (1981) 175-189.

Bagchi, T.P., Sen, P.K., redindancy of isothermal kinetic data to back up non-isothermal kinetic data, Thermochimica Acta 70 (1983) 363-365.

Baitalow, F., Schmidt, H.-G., Wolf, G., Formal kinetic analysis of processes in the solid state, Thermochimica Acta, 337 (1999) 111-120.

Bate, D.M., Lehrle, R.S., The effect of blending on polymer stability: kinectics and mechanisms, Polymer Degradation and stability 62 (1998) 57-66.

Beckman, I.N., Zheleznov, A.V., Balek, V., Evaluation of thermal analysis experimental data, Journal of Thermal Analysis, Vol 37 (1991) 1479-11495.

Bounaceur, R., Warth, V., Marquaire, P.-M., Scacchi, G., Dominé, F., Dessort, D., Pradier, B., Brevart, O., Modeling of hydrocarbons pyrolysis at low temperature. Automatic generation of free radicals mechanism, Journal of Analytical and Applied Pyrolysis, 64 (2002) 103-122.

Broido, A., A simple sensitive graphical method of training thermogravimetric analysis data, Journal of Polymer Science: part A-2, Vol. 7, 1961-1773, 1969.

Brown, M.E., Flynn, R.M., Flynn, J.H., Report on the ICTA kinetics committee (august 1992 to september 1994), Thermochimica Acta 256 (1995) 477-483.

Buekens, A.G., mertens, J.J.R., Schoeters, J.G.E., Steen, P.C., Experimental techniques and mathematical models in the study of waste pyrolysis and gasification, Conservation and Recycling, 1979, Vol 3, pp. 1-23.

Caballero, J.A., Conesa,J.A., Mathematical considerations for nonisothermal kinetics in thermal decomposition, Journal of Analytical and Applied Pyrolysis, 7“ (2005) 85-100.

Cao, J., Mathematical studies of modulated differentiel scanning calorimetry-II. Kinectic and non – kinetic components, Thermochimica Acta 329 (1999) 89-95

Caots, A.W., Redfern, J.P., Thermogravimetric analysis: a review, Analyst, Vol. 88, pp. 906-924, 1963.

Caots, A.W., Redfern, J.P., Kinetic parameters from thermogravimetric data, Nature, january 4, 1964, Vol. 201, pp. 68-69.

Carrol, B;, Kinetic analysis of chemical reactions for non-isothermal procedure, Thermochimica Acta 3 (1972) 449-459.

Conesa, J. A., Marcilla, A., Caballero, J. A., Font, R., Comments on the validity and utility of the different methods for kinetic analysis of thermogravimetric data, Journal of Analytical and Applied Pyrolysis, 58-59 (2001) 617-633.

Criado, J.M., Morales, J., Rives, V., Computer kinetic analysis of simultaneously obtained TG and DTG curves, Journal of Thermal Analysis, Vol. 14 (1978) 221-228.

Da Silva, S.A., Da Conceiçao, M.M., De Souza, A.G., Macêdo, R.O., Calorimetric and kinectic parameters of manioc derivatives, Thermochimica Acta, 328 (1999) 177-181

Doyle, C.D., Kinetic analysis of thermogravimetric data, Journal of Applied Polymer Science, Vol. V, Issue N°15, pp. 285-292 (1961).

Draper, A.L., Sveum, L.K., The analysis of thermal data, Thermochimica Acta 1 (1970) 345-365.

Elder, J.P., reconciliation of Arrhenius and iso-conversional analysis kinetics parameters of non-isothermal data, Thermochimica Acta 272 (1996) 41-48.

Fan, L.T., Fan, L.S., Miyanami, K., Chen, T.Y., Walawender, P., A mathematical model for pyrolysis of a solide particle, The canadian Journal of Chemical Engineering, Vol. 55, February, 1977.

Flynn, J.H., The temperature integral – Its use and abuse, Thermochimica Acta 300 (1997) 83-92.

Font, R., Garcia, A.N., Application of the transition state theory to the pyrolysis of biomass and tars, J. Anal. Appl. Pyrolysis 35 (1995) 249-258.

Font, R., Marcilla, A., Garcia, A.N, caballero, J.A., Conesa, J.A., Kinetic models for the thermal degradation of heterogeous materials, J. Anal. Appl. Pyrolysis 32 (1995) 29-39.

Freeman, E.S., Carroll, B., The application of thermoanalytical techniques to reaction kinetics. The termogravimetric evaluation of the kinetics of the decomposition of calcium oxalate monohydrate, Journal of Physical Chemistry, Vol. 62, pp. 394-397, April 1958.

Friedman, H.,L., Kinetics of thermal degradation of char-forming plastics from thermogravimetry. Application to a phenolic plastic, Journal of polymer Science:part C, N°6, pp. 183-195.

Friedman, H.L;, Errors in vacuum thermogravimetry, Analytical Chemistry, Vol. 37, N° 6, 768-769, May 1965.

Fuoss, R.M., Salyer, I., Wilson, H.S., Evaluation of rate constants from thermogravimetric data, Journal of Polymer Science: part A, Vol. 2, pp. 3147-3151 (1964).

Galway, A.K., Brown, M.E., Arrhenius parameters and compensation behaviour in solid-state decomposition, Thermochimica Acta 300 (1997) 107-115.

Heal, G. R., Evaluation of the integral of the Arrhenius function by a series of Chebyshev polynomials — use in the analysis of non-isothermal kinetics, Thermochimica Acta 340-341 (1999) 69-76.

Heikkinen, J. M., Hordijk, J. C., de Jong, W., Spliethoff, H., Thermogravimetry as a tool to classify waste components to be used for energy generation, J. Anal. Appl. Pyrolysis (2004), article in press, accepted 3 December 2003.

Helsen, L., Van den Bulck, E., Kinetics of the low-temperature pyrolysis of chromated copper arsenate-treated wood, Journal of Analytical and Applied Pyrolysis, 53 (2000) 51-79.

Horowitz, H.H., Metzger, G., A new analysis of thermogravemetric traces, Analytical Chemistry, Vol. 35, N° 10, 1464-1468, september 1963.

Houser, T.J., Kinetics of polymer pyrolysis from surface regression rates, The Journal of Chemical Physics, Vol. 45, N°3, 1031-1037, 1 august 1966.

Johnson, D.W., Gallagher, P.K., Comparaison of dynamic with isothermal techniques for the study of solid state decomposition kinetics, The Journal of Physical Chemistry, Vol. 76, N° 10, 1972.

Kim, S., Park, J.K., Chun, H.D., Pyrolysis kinectics of scap tire rubbers using DTG and TGA, Journal of Environmental Engineering, July 1995, 507-514.

Kissinger, H.E., Variation of peak temperature with heating rate in differential thermal analysis, Journal of Research of the National Bureau of Standards, Vol. 57, N°4, pp. 217-221, October 1956.

Korobov, A., heterogeneous chemical kinetics in two dimensions: two ways of discrete description, Thermochimica Acta 279 (1996) 191-204.

Liu, J.S., Zeng, X.C., Tian, A.M., Deng, Y., Development and applications of a method for kinetic analysis of consecutive reactions under isothermal conditions, Thermochimica Acta 273 (1996) 53-60.

Liu, N. A., Fan W. C., Critical consideration on the Freeman and Carroll method for evaluating global mass loss kinetics of polymer thermal degradation, Thermochimica Acta, 338 (1999), 85-94.

Liu, N. A., Fan. W., Dobashi, R., Huang, L., Kinetic modeling of thermal decomposition of natural cellulosic materials in air atmosphere, Journal of Analytical and Applied Pyrolysis, 63 (2002) 303-325.

Llopiz, J., Romero, M.M., Jerez, A., laureiro, Y., Generalization of the Kissinger equation for several kinetic models, Thermochimica Acta 256 (199() 205-211.

Lyon, R.E., Pyrolysis kinectics of char forming polymers, Polymer Degradation and stability 61 (1998) 201-210.

Maffezzoli, A., Kenny, J.M., Torre, L., On the physical dimensions of the Avrami constant, Thermochimica Acta 269/270 (1995) 185-190.

Malek, J., Criado, J.M., Gotor, F.J., Sestak, J., Some comments about a correct estimation of the kinectic exponent for non-isothermal solid-state processes using Augis and Bennettt method, Thermochimica Acta 322 (1998) 77-82.

Marcilla, A., Reyes-Labarta, J. A., Sempere, F. J., DSC kinetic study of the transitions involved in the thermal treatment of polymers. Methodological considerations, Polymer 42 (2001), 5343-5350.

Martín-Gullón, I., Gómez-Rico, M. F., Fullana, A., Font, R., Interrelation between the kinetic constant and the reaction order in pyrolysis, J. Anal. Appl. Pyrolysis, 68-69 (2003) 645-655.

Matsuzawa, Y., Ayabe, M., Nishino, J., Kubota, N., Motegi, M., Evaluation of char fuel ratio in municipal pyrolysis waste, Fuel (2004), article in press, received 11 April

2003, revised 5 February 2004, accepted 6 February 2004, available online 4 March 2004.

Ortega, A., The incorrectness of the temperature criterion, Thermochimica Acta 276 (1996) 189-198.

Ortega, A., Perez-Mquedea, L., Criado, J.M., The problem of discerning Avrami-Erofeev kinetic models from the new controlled rate thermal analysis with constant acceleration of the transformation, Thermochimica Acta 25 (1995) 147-152.

Ortega, A., Perez-Maqueda, LA.A., Criado, J.M., A new point of view on the evaluation of the temperature integral, Thermochimica Acta 282/283 (1996) 29-34.

Ozawa, T., A new method of analysing thermogravimetric data, XXXX , Vol 38, N011, pp.1881-1886, Nov. 1965.

Ozawa, T., Kinetic analysis of derivative curves in thermal analysis, Journal of Thermal Analysis, Vol 2 (1970) 301-324.

Ozawa, T., Estimation of activation energy by isoconversion methods, Thermochimica Acta 203 (1992) 159-165.

Ozawa, T., Controlled rate thermogravimetry. New usefulness of controlled rate thermogravimetry revealed by decomposition of polyimide. Journal of Thermal Analysis and Calorimetry, 59 (2000) 375-384.

Ozawa, T., Kinetic analysis by repeated temperature scanning. Part I. Theory and methods, Thermochimica Acta, 356 (2000) 173-180.

Ozawa, T., Temperature control modes in thermal analysis, Journal of Thermal Analysis and Calorimetry, 64 (2001) 109-126.

Pananokis, D., Abel, E.W., A comparaison of method for the deconvolution of isothermal DSC data, Thermochimica Acta 315 (1998) 107-119.

Perez-Maqueda, L.A., Ortega, A., Criado, J.M., The use of master plots for discriminating the kinetic model of solid-state reactions from a single constant-rate thermal analysis (CRTA) experiment, Thermochimica Acta 277 (1996) 165-173.

Peters, B., Schröder, E., Bruch, Ch., Measurements and particle resolved modelling of the thermo- and fluid dynamics of a packed bed, J. Anal. Appl. Pyrolysis 70 (2003) 211-231.

Poutsma, M. L., Fundamental reactions of free radicals relevant to pyrolysis reactions, Journal of Analytical and Applied Pyrolysis, 54 (2000) 5-35.

Rajeshwar, K., The kinetics of the thermal decomposition of green river oil shale kerogen by non-isothermal thermogravimetry, Thermochimica Acta 45 (1981) 253-263.

Reich, L;, A rapid estimation of activation energy from thermogravimetric traces, Polymer Letters, Vol. 2, pp. 621-623 (1964).

Reich, L., Use of spreadsheets in the kinetic analysis of two consecutive first-order reactions, Thermochimica Acta 273 (1996) 113-118.

Reich, L., Use of databases in the kinetic analysis of two competitive consecutive second-order reactions, Thermochimica Acta 293 (1997) 179-183.

Reich, L, Stivala, S.S., Computer-determination kinetic parameters from TG curves, part XI, Thermochimica Acta 71 (1983) 281-285.

Reich, L, Stivala, S.S., Computer-determination kinetic parameters from TG curves, part VIII, Thermochimica Acta 68 (1983) 379-381.

Reich, L, Stivala, S.S., Computer-analysis of non-isothermal TG data for mechanism and activation energy, part I, Thermichimica Acta 73 (1984) 165-172.

Savage, P. E., Mechanisms and kinetics models for hydrocarbon pyrolysis, Journal of Analytical and Applied Pyrolysis, 54 (2000) 109-126.

Sbirrazzuoli, N., Simulations for evaluation of kinetic methods in differential scanning calorimetry. Part 2 - Effect of additional noise on single peak methods, Thermochim. Acta, 1996, 273, 169-184.

Sbbirrazzuoli, N., Girault, Y., Elegant, L., Simulations for evaluation of kinetic methods in differential scanning calorimetry. Part 3 – Peak maximum evolution methods and isoconvertional methods, Thermochimica Acta 293 (1997) 25-37.

Sbbirrazzuoli, N., Vincent, L., Vyazovkin, S., Comparaison of several computational procedures for evaluating the kinetics of thermally stimulated condensed phase reactions, Chemometrics and intelligent laboratory systems 5‘ (2000) 53-60.

Sharp, J.H., Wentworth, S.A., Kinetic analysis of thermogravimetric data, Analytical Chemistry, Vol. 41, N° 14, december 1969.

Simon, P, Kinetics of polymer degradation involving the splitting off of small molecules: part II- concluding remarks, Polymer Degradation and stability 47 (1995) 265-273.

Smith, G.W., A method for determination of Avrami parameters directly from isothermal calorimetry data, Thermochimica Acta 291 (1997) 59-64.

Starink, M.J., A new method for the derivation of activation energies from experiments performed at constant heating rate, Thermochimica Acta 288 (1996) 97-104.

Šesták, J., Errors of kinetic data obtained from thermogravimetric curves at increasing temperature, Presented at the symposium on Thermal Analysis, Northern Polytechnic, London, 13-13 april, 1965, Talanta, 1966, Vol 13, pp. 567-579.

Šesták, J., Berggren, G., Study of the kinetics of the mechanism of solid state reactions at increasing temperatures, Thermochimica Acta 3 (1971) 1-12.

Tanaka, H.; Thermal analysis and kinetics of solid state reactions, Thermochimica Acta 267 (1995) 29-44.

Turner, R.C., Hoffman, I., Chen, D., Thermogravimetry of the dehydratation of Mg(OH)2, Canadian Journal of Chemistry, Vol. 41 (1963), pp. 243-251.

Van Krevelen, D.W., Van Heerden, C., Huntjens, F.J., physical aspects of the pyrolysis of coal and related organic compounds, Fuel XXX-11, pp. 253-259, 1951.

Várhegyi, G., Szabó, P., Jakab, E., Till, F., Least squares criteria for the kinetic evaluation of thermoanalytical experiments. Examples from a char reactivity study, Journal of Analytical and Applied Pyrolysis, 57 (2001) 203-222.

Vyazovkin, S., Sbirrazzuoli, N., Kinetic methods to sudy isothermal and nonisothermal epoxy-anhydride cure. Macromol. Chem. Phys. 200, 2294-2303 (1999).

Vyazovkin, S., Linert Wolfgang, Detecting isokinetic relationships in non-isothermal systems by isoconvertional method, Thermochimica Acta 269/270 (1995) 61-72.

Vyazovkin, S., Sbirrazzuoli, N., Effects of viscosity on the kinetics of initial cure stages, Macromol. Chem. Phys. 201/2, (2000) 199-203.

Wilburn, F. W., Kinetics of overlapping reactions, Thermochimica Acta, 354 (2000) 99-105.

Wilburn, F. W., The determination of kinetic parameters from DTG curves — fact or fiction?, Thermochimica Acta 340-341 (1999) 77-87.

Zeng, X.-Ch., Chen, Y., Chen, X.-N., Xie, J.-Q., Jiang, F.-B., Thermo-kinetic research method for faster reactions: modifier method of distorted thermoanalytical curve, Thermochimica Acta, 332 (1999) 97-102.

Appendices

Appendix A

Working protocol
– identification, analysis, and interpretation of FTIR spectra –

In this chapter, working protocol is presented that enabled getting divers results of this study.

The used software was the following:
– TIME BASE by Perkin Elmer.
– KNOW IT ALL [analytical edition] by Bio-Rad.

The Time Base tool allows browsing and investigating files of the .spp format, which display absorbance as the function of time [RMS]. Then, the spectrum corresponding to a chosen point of the RMS chart can be opened and examined. The software allows creating various files containing all spectra isolated from the RMS chart. When all the spectra needed are collected in files of the .sp format, the KnowItAll software tool will enable to search for known spectra. In certain cases, it is relatively easy to make predictions as to found results from the character of studied molecules. But generally, it depends on complexity of their structure.

To analyse results, a preliminary study of theoretical possibilities concerning molecule scissions is performed. When a general idea about results is conceived, analyses with the help of various software tools in hand can follow. After that, TimeBase is used.

TIME BASE

First, Time Base software by Perkin Elmer is launched. After using the File-Open menu, Pel_Data folder is searched for. There, opening various files with .spp extension allows expecting spectra as a function of time [RMS], at any time scale desired. In Time Base, charts can also be printed or saved in separate files in order to be put into reports. A simple searching engine is available as well to enable spectra analysis, but it does not reach the power of KnowItAll software tool.

Opening an ".spp" file will provoke appearance of a window on the screen. There, two charts are displayed, one with a spectrum at the moment t of RMS, the other enabling to produce all the spectra of the superior window as a function of time, by moving a vertical line representing time of RMS. The whole evolution of spectra in time can thus be displayed.

KNOW IT ALL

When all necessary spectra with the extension .sp were obtained, KnowItAll by BioRad can be launched. With this software tool, several ways of searching the molecules present in pyrolysis gas can be used. There are especially four modes, called SearchIt IR, AnalyzeIt IR, MineIt IR, and RefineIt IR, that constitute handy means of exploring spectra.

SearchIt IR

In this mode, spectra similar to the opened one are looked for. Measure of Euclidean distances between all the points of the two charts compared is checked. A database containing FTIR spectra of pure or industrial compounds is used for this comparison. More than 350,000 spectra is contained therein.

AnalyzeIt IR

In this mode, elementary chemical groups that can be connected with the spectrum chosen are searched. Moreover, other characteristic peaks of the same molecular group

are visualized. This tool is very practical for mixtures of molecules. In fact, with Search IR, it is very difficult to find reliable results in that case. In this case, it is preferable to work with AnalyzeIt IR as different molecular groups can be told apart.

Once the file is opened, a magnifying glass connected to a vertical and a horizontal line appears. A movement of mouse is correspondingly reflected upon the motion of the magnifying glass. When placed on a peak, all possible types of bonds are displayed, as well as their properties [on choosing "Analyzing Correlations…" in the "Analyze" menu]. When "Correlating Individual Peak" is chosen, a small window appears where the exact frequency of a spectrum that is to be analysed is demanded. In the "Analyze" menu, option "Browse a functional group…" is also located, allowing to choose functional groups in each peak.

MineIt IR

Results from searching with Search IR appear in MineIt IR. A list of the most probable spectra is presented [by default, the number of items in the list is 50, but it can be modified]. The list is sorted by decreasing degree of probability, in consonance with the measure of the Euclidean distance. Each spectrum can be superposed with the one to which the corresponding spectrum is being searched for so that a visual inspection of the concordance between peaks can be performed.

RefineIt IR

With this tool, spectra can be opened and observed more in detail. Also, a superposition of several spectra can be performed to enable an overall vision of their evolution in time [pseudo-3D representation].

Appendix B

— experimental results, EVA kinetic model —

Tab. B-1: Results for EVA from simulations.

		Sample 1 88/12	Sample 2 75/25	Sample 3 60/40
Mass fraction of vinyl acatate, v		0.12	0.25	0.4
Mole fraction of vinyl acetate, w		0.0425	0.098	0.1784
Mole mass, M_w [g/mol]				
Mean mole mass, M_m [g/mol]				
Polymerisation degree, DP				
Mass fraction of VA calculated from TGA		0.1246	0.2907	0.4211
Heating rate				
5 K.min^{-1}	Pyrolysed mass, w_0 [mg]	32.849	26.721	25.916
	Temperature of degradation initiation, T_i [°C]	304	292	280
	Temperature of degradation end, T_f [°C]	494	492	492
	Temperature of intermediate plateau, T_p [°C]	379	380	380
	Maximal degradation rate temperature for EVA + EVA*, stage 1, $T_{d,max1}$ [°C]	341	340	340
	Maximal degradation rate, stage 1, v_1 [%.min^{-1}]	-1.1	-2.1	-3.2
	Maximal degradation rate temperature for EVA*, stage 2, $T_{d,max2}$ [°C]	457	457	463
	Maximal degradation rate, stage, v_2 [%.min^{-1}]	-13.2	-9.7	-11
	Frequency factor, A_1 [min^{-1}]	$1.27.10^{17}$ [0.0014]	$2.93.10^{16}$	$3.11.10^{16}$
	Frequency factor, A_2 [min^{-1}]	$6.87.10^{16}$ [0.0014]	$6.89.10^{16}$	$1.25.10^{17}$
	Frequency factor, A_3 [min^{-1}]	$6.94.10^{18}$ [0.0015]	$1.52.10^{19}$	$1.65.10^{19}$
	Activation energy, E_{a1} [J.mol^{-1}]	199010 [0.0015]	198240	198180
	Activation energy, E_{a2} [J.mol^{-1}]	208830 [0.0014]	208240	207730
	Activation energy, E_{a3} [J.mol^{-1}]	272480	272270	272290
7 K.min^{-1}	Pyrolysed mass, w_0 [mg]	29.96	25.892	24.478
	Temperature of degradation initiation, T_i [°C]	313	297	286
	Temperature of degradation end, T_f [°C]	502	496	497
	Temperature of intermediate plateau, T_p [°C]	386	382	386
	Maximal degradation rate temperature for EVA + EVA*, stage 1, $T_{d,max1}$ [°C]	350	343	345
	Maximal degradation rate, stage 1, v_1 [%.min^{-1}]	-1.4	-2.8	-4.3
	Maximal degradation rate temperature for EVA* stage 2, $T_{d,max2}$ [°C]	465	461	459
	Maximal degradation rate, stage 2, v_2 [%.min^{-1}]	-18.3	-14.3	-16.4
	Frequency factor, A_1 [min^{-1}]	$1.40.10^{17}$ [0.0016]	$3.51.10^{16}$	$2.97.10^{16}$
	Frequency factor, A_2 [min^{-1}]	$6.22.10^{16}$ [0.0016]	$7.15.10^{16}$	$1.19.10^{17}$
	Frequency factor, A_3 [min^{-1}]	$6.89.10^{18}$ [0.0016]	$1.26.10^{19}$	$2.97.10^{19}$
	Activation energy, E_{a1} [J.mol^{-1}]	198520 [0.0014]	197940	197890
	Activation energy, E_{a2} [J.mol^{-1}]	207980 [0.0016]	207760	207720
	Activation energy, E_{a3} [J.mol^{-1}]	272460	272280	272310
10 K.min^{-1}	Pyrolysed mass, w_0 [mg]	30.272	28.382	26.848
	Temperature of degradation initiation, T_i [°C]	314	-|-	291
	Temperature of degradation end, T_f [°C]	506	-|-	506
	Temperature of intermediate plateau, T_p [°C]	-|-	-|-	389
	Maximal degradation rate temperature			

	for EVA + EVA* stage 1, $T_{d,max1}$ [°C]	357	-|-	349
	Maximal degradation rate, stage 1, v_1 [%.min^{-1}]	-2.2	-|-	-6.3
	Maximal degradation rate temperature			
	for EVA stage 2, $T_{d,max2}$ [°C]	471	-|-	475
	Maximal degradation rate, stage 2, v_2 [%.min^{-1}]	-28.2	-|-	-17.9
	Frequency factor, A_1 [min^{-1}]	1.56.10^{17} [0.0024]	*4.21.10^{16}*	2.83.10^{16} [0.0025]
	Frequency factor, A_2 [min^{-1}]	7.44.10^{16} [0.0024]	*7.51.10^{16}*	8.21.10^{16} [0.0023]
	Frequency factor, A_3 [min^{-1}]	6.83.10^{18} [0.0018]	*9.20.10^{18}*	7.99.10^{18} [0.0023]
	Activation energy, E_{a1} [J.mol^{-1}]	198190 [0.0018]	*197610*	197560 [0.0022]
	Activation energy, E_{a2} [J.mol^{-1}]	208220 [0.0018]	*207780*	207730 [0.0020]
	Activation energy, E_{a3} [J.mol^{-1}]	272470 [0.0018]	*272300*	272320 [0.0021]
15 K.min^{-1}	Pyrolysed mass, w_0 [mg]	48.149	27.82	26.977
	Temperature of degradation initiation, T_i [°C]	318	304	295
	Temperature of degradation end, T_f [°C]	516	514	511
	Temperature of intermediate plateau, T_p [°C]	400	398	396
	Maximal degradation rate temperature			
	for EVA + EVA* stage 1, $T_{d,max1}$ [°C]	361	361	357
	Maximal degradation rate, stage 1, v_1 [%.min^{-1}]	-3.3	-6.1	-9.5
	Maximal degradation rate temperature			
	for EVA stage 2, $T_{d,max2}$ [°C]	476	475	479
	Maximal degradation rate, stage 2, v_2 [%.min^{-1}]	-40.3	-27.3	-30
	Frequency factor, A_1 [min^{-1}]	1.43.10^{17}	5.52.10^{16} [0.0030]	2.90.10^{16} [0.0032]
	Frequency factor, A_2 [min^{-1}]	5.72.10^{16}	8.08.10^{16} [0.0029]	8.14.10^{16} [0.0030]
	Frequency factor, A_3 [min^{-1}]	6.12.10^{18}	9.06.10^{18} [0.0027]	9.81.10^{18} [0.0024]
	Activation energy, E_{a1} [J.mol^{-1}]	199260	197520 [0.0026]	197490 [0.0023]
	Activation energy, E_{a2} [J.mol^{-1}]	208330	207800 [0.0025]	207750 [0.0022]
	Activation energy, E_{a3} [J.mol^{-1}]	272520	272290 [0.0025]	272300 [0.0022]
20 K.min^{-1}	Pyrolysed mass, w_0 [mg]	31.355	27.425	23.667
	Temperature of degradation initiation, T_i [°C]	320	312	302
	Temperature of degradation end, T_f [°C]	520	518	518
	Temperature of intermediate plateau, T_p [°C]	400	401	402
	Maximal degradation rate temperature			
	for EVA + EVA* stage 1, $T_{d,max1}$ [°C]	363	364	359
	Maximal degradation rate, stage 1, v_1 [%.min^{-1}]	-4.3	-7.7	-13.5
	Maximal degradation rate temperature			
	for EVA stage 2 $T_{d,max2}$ [°C]	484	476	476
	Maximal degradation rate, stage 2, v_2 [%.min^{-1}]	-49.8	-35.2	-39.4
	Frequency factor, A_1 [min^{-1}]	1.89.10^{17} [0.0063]	5.49.10^{16} [0.0041]	2.91.10^{16} [0.0039]
	Frequency factor, A_2 [min^{-1}]	8.11.10^{16} [0.0062]	8.09.10^{16} [0.0040]	8.10.10^{16} [0.0036]
	Frequency factor, A_3 [min^{-1}]	6.00.10^{18} [0.0029]	1.09.10^{19} [0.0020]	1.02.10^{19} [0.0029]
	Activation energy, E_{a1} [J.mol^{-1}]	198280 [0.0027]	197290 [0.0020]	197570 [0.0027]
	Activation energy, E_{a2} [J.mol^{-1}]	207810 [0.0026]	207780 [0.0020]	207760 [0.0025]
	Activation energy, E_{a3} [J.mol^{-1}]	272490 [0.0026]	272280 [0.0020]	272300 [0.0025]
30 K.min^{-1}	Pyrolysed mass, w_0 [mg]	35.081	33.299	22.635
	Temperature of degradation initiation, T_i [°C]	312	313	305
	Temperature of degradation end, T_f [°C]	533	530	527
	Temperature of intermediate plateau, T_p [°C]	411	406	411
	Maximal degradation rate temperature			
	for EVA + EVA* stage 1, $T_{d,max1}$ [°C]	364	368	364
	Maximal degradation rate, stage 1, v_1 [%.min^{-1}]	-7.3	-10.6	-19.5
	Maximal degradation rate temperature			
	for EVA stage 2, $T_{d,max2}$ [°C]	488	484	482
	Maximal degradation rate, stage 2, v_2 [%.min^{-1}]	-76.7	-46	-58.3
	Frequency factor, A_1 [min^{-1}]	-|-	-|-	-|-

Frequency factor, A_2 [min^{-1}]	-|-	-|-	-|-
Frequency factor, A_3 [min^{-1}]	-|-	-|-	-|-
Activation energy, E_{a1} [$J.mol^{-1}$]	-|-	-|-	-|-
Activation energy, E_{a2} [$J.mol^{-1}$]	-|-	-|-	-|-
Activation energy, E_{a3} [$J.mol^{-1}$]	-|-	-|-	-|-
Variation coefficient of degraded masses	0.204693269	0.091372417	0.077621688

In parenthesis: variation coefficients
Nitrogen flow: 0.27 $Nm^3.min^{-1}$ Values in italics are very probably wrong .
Orders n, m, p: 1, 1, 1
-|- : calculation failed

Mean values for K = 5, 7, 10, 15, 20	88/12	75/25	60/40
Frequency factor, A_1 [min^{-1}]	$1.51.10^{17}$	$4.33.10^{16}$	$2.94.10^{16}$
Frequency factor, A_2 [min^{-1}]	$6.87.10^{16}$	$7.54.10^{16}$	$9.77.10^{16}$
Frequency factor, A_3 [min^{-1}]	$6.56.10^{18}$	$1.14.10^{19}$	$7.42.10^{18}$
Activation energy, E_{a1} [$J.mol^{-1}$]	198652	197720	197738
Activation energy, E_{a2} [$J.mol^{-1}$]	208234	207872	207738
Activation energy, E_{a3} [$J.mol^{-1}$]	272484	272284	272304

Accumulation of EVA*	88/12	75/25	60/40
for K=5, [%]	95	75	63
for K=7, [%]	95	77	64
for K=10, [%]	95	81	72
for K=15, [%]	95	84	72
for K=20, [%]	95	84	72
for K=30, [%]	-|-	-|-	-|-

Appendix C
Detailed description of the thermobalance

The thermogravimetric unit TGA 92 is composed of a thermobalance (including balance, furnace, gas circuit and power supply), a control unit CS 32 and a PC (Fig. C-1). This setup is completed by a printer for printing of thermogravimetric curves.

Fig. C-1: Thermogravimetric unit TGA 92.

Microbalance B92

The electronic microbalance (Fig. C-2) uses a system of a balance beam. The balance beam (1) is fixed, by means of a torsion band (2), between two springs (3). It is maintained in the same position by the following mechanism:

• The optic slot shutter (4) integrally bound together with the balance beam partially hides the light beam coming from the source (5) aiming at two solid photoresistors (6). The carrier of the shutter is equipped by two highly stable permanent magnets (7). The extremities of these magnets, magnetizated inversely in order to eliminate the influence of

external magnetic fields, are embedded into four solid solenoids (8). One pair of these solenoids serves to tare, the other, connected to the photoelectric mechanism, constitutes the equilibrating circuit.

• The signal of photo resistors is amplified by a strong amplifier (9). The outgoing current of the amplifier circulates in the couple of solenoids, which continually work upon magnets with such a power that retains the balance beam in equilibrium.

• The overall position stability is assured by the correcting circuit (10), associated with the amplifier. The proportional relation between the current intensity and the equilibrating electromagnetic power associates the extent of current variations with the extent of weight variations.

• The potential difference proportional to the counterbalancing current is amplified (11) and consequently numerically processed in the control unit coupled with the PC.

• Two bands (12) assure the connection of balancing beam with the hooks suspending

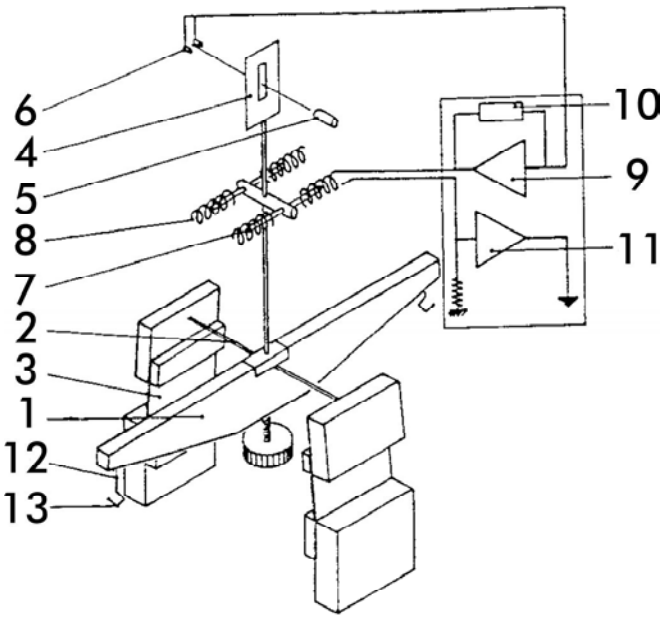

the weights.

Fig. C-2: Microbalance B92.

Furnace

The furnace used within the thermoanalyser TGA 92 for experiments at high temperatures is equipped with a graphite resistor, whose operating temperature ranges between room temperature and 1750°C.

Description of the furnace: in the tubular axle, there is a graphite tube serving as a heater resistor (1). The resistor is insulated by an aluminium tubular protective case (2) and an enclosure from graphite felt (3). The cooling of the furnace is realized by circulating water. Outer impermeable casing is equipped with an input (4) and an output (5) orifice through which circulates the purging gas, thus protecting the graphite resistor. The back valve (6) secures impermeability on the exit. Temperature control is assured by control unit CS 32 connected to a thermocouple situated in the analysis chamber of the furnace.

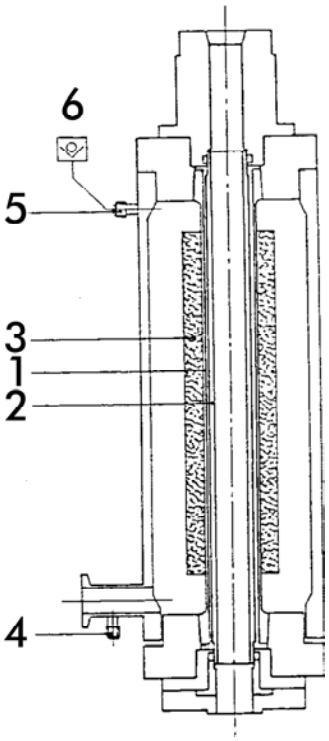

Fig. C-3: Furnace.

Appendix D
FTIR spectrophotometer Perkin-Elmer, model Spectrum 2000 FT-IR Spectrometer

Technical parameters

Principle: one-beam Michelson interferometer (see Fig. D-1, next page) with a bidirectional stationary rotating scanning beam separator. Automatic adjustment of interferometer, magnetic control.

Optic unit: beam separators cover a region of wavelength between 15000 and 30 cm^{-1}. Optical parts are hermetically sealed and desiccated. Cleaning is possible, but not necessary.

Emission source

Near IR: wolfram lamp with quartz cover, air-cooled, with stabilized tension.

Middle and distant IR: spool with operating temperature of 1350 K, air-cooled, with stabilized tension.

Detectors

Near IR: InSb detector cooled by liquid nitrogen. FR-DTGS (Fast Recovery Deuterated TriGlycine Sulfate) detectors near IR have a window made from calcium fluoride.

Middle IR: Detector MCD (Mercury Cadmium Telluride) cooled by liquid nitrogen with broad, middle and narrow bands, with a KBr window. It is also possible to use FR-DTGS detectors with a CsI window.

Distant IR: Detectors FR-DTGS and a polyethylene window.

J-stop: fix: from 2 to 16 cm^{-1}, up to 15,000 cm^{-1}; variable: from 0.2 to 16 cm^{-1}, up to 15,000 cm^{-1}.

Abscissa: 15,000-30 cm^{-1}, with an appropriate combination of beam splitters, sources and detectors.

Signal/noise ratio: 45000:1 (r.m.s.), 9000:1 (peak-to-peak); time measurement: 5 s.

The above mentioned data were obtained under these conditions: DTGS detectors, optimised beam splitter (from KBr), resolution at 4000 cm^{-1} = 4 cm^{-1}, scan rate: 0.2 $cm.s^{-1}$, strong apodisation, bilateral bidirectional scanning, measured in intervals of 50 cm^{-1}, in the surroundings of 2000 cm^{-1}.

Resolution: from 0.2 to 64 cm^{-1} (available model 1 cm^{-1}).

Scan rate: variable from 0.05 to 5.0 $cm.s^{-1}$ of the speed of difference of the optic trajectory.

Apodisation: weak, middle or strong Beer-Norton, triangular, cosine, filling, Kaiser-Bessel or box.

Emplacement of samples/accessories: energy passage on the Monitor dialog panel.

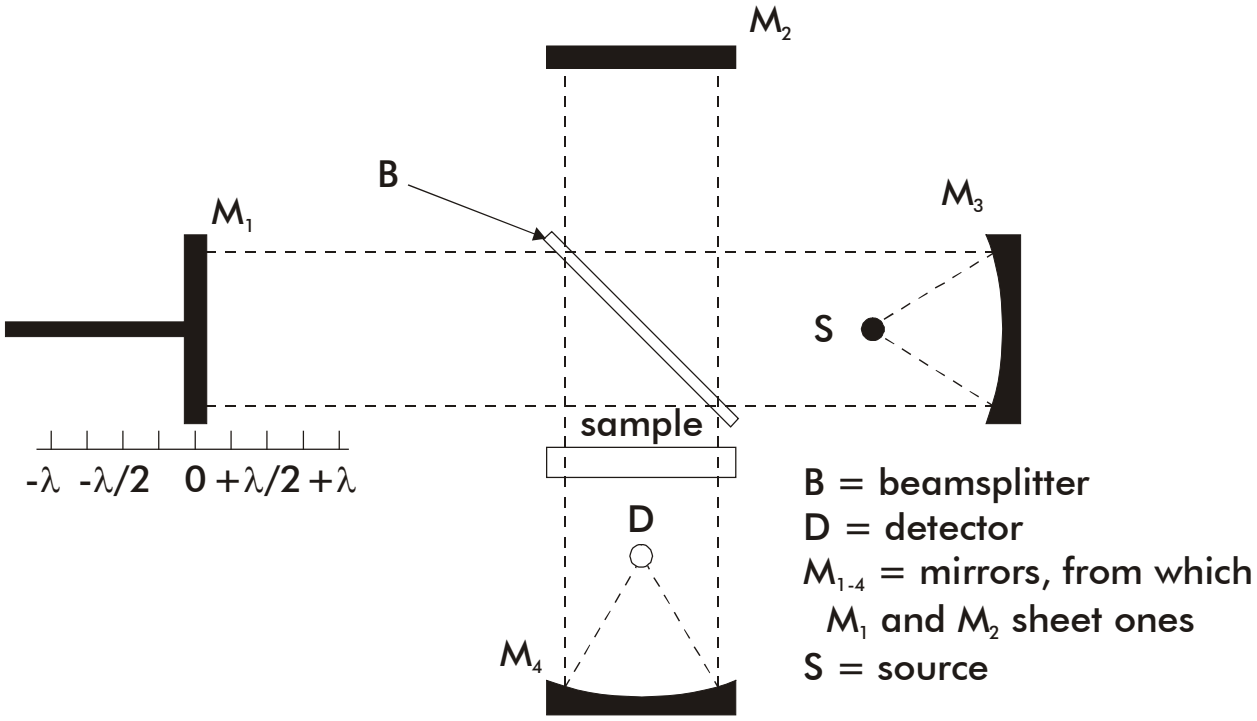

Fig. D-1: Scheme of the Michelson interferometer.

Annexe E
– Tables for Part 1 –

Tab. E-1: Lignin pyrolysis frequency factors.

Frequency factors for D3 and F1 models, respectively.				
α	A [s^{-1}]			
	D3 (Diffusion model 3)		F1 (Reaction order = 1)	
0.2—0.3	7.51E+29	7.51E+29	1.35E+31	1.35E+31
0.2—0.4	4.85E+31	4.85E+31	7.20E+32	7.20E+32
0.2—0.5	7.07E+32	7.07E+32	8.87E+33	8.87E+33
0.2—0.6	5.19E+36	5.19E+36	5.60E+37	5.60E+37
0.2—0.7	7.24E+38	7.24E+38	6.82E+39	6.82E+39
0.2—0.8	2.37E+25	2.37E+25	1.97E+26	1.97E+26
0.2—0.9	1.31E+13	*excluded*	9.68E+13	*excluded*
0.4—0.5	1.37E+37	1.37E+37	1.39E+38	1.39E+38
0.4—0.6	2.21E+42	2.21E+42	2.00E+43	2.00E+43
0.4—0.7	2.24E+45	2.24E+45	1.83E+46	1.83E+46
0.4—0.8	1.47E+28	1.47E+28	1.09E+29	1.09E+29
0.4—0.9	9.51E+13	*excluded*	6.49E+14	*excluded*
Mean value	**1.87E+44**	**2.25E+44**	**1.53E+45**	**1.84E+45**
Std. dev.	6.20E+44	6.73E+44	5.07E+45	5.50E+45
Sup. value	2.24E+45	2.24E+45	1.83E+46	1.83E+46
Inf. value	1.31E+13	2.37E+25	9.68E+13	1.97E+26
Δ(Sup; Inf)	2.24E+45	2.24E+45	1.83E+46	1.83E+46

Tab. E-2: Activation energy.

Lignin 10, 20, and 30 $K.min^{-1}$		
α	E_a [$J.mol^{-1}$]	
0.2—0.3	366,686	366,686
0.2—0.4	392,318	392,318
0.2—0.5	411,610	411,610
0.2—0.6	465,660	465,660
0.2—0.7	506,703	506,703
0.2—0.8	356,517	356,517
0.2—0.9	213,328	*excluded*
0.4—0.5	476,647	476,647
0.4—0.6	550,507	550,507
0.4—0.7	606,208	606,208
0.4—0.8	404,986	404,986
0.4—0.9	231,777	*excluded*
Mean value	**415,246**	**453,784**
Std. dev.	111,922	78,126
Sup. value	606,208	606,208
Inf. value	213,328	356,517
Δ(Sup; Inf)	392,880	249,690

Tab. E-3: Cellulose pyrolysis frequency factors.

Frequency factors for AE2 and F1 models, respectively.				
α	A [s^{-1}]			
	D3 (Diffusion model 3)		F1 (Reaction order = 1)	
0.2—0.3	1.93E+14	1.93E+14	3.46E+15	3.46E+15
0.2—0.4	5.38E+13	5.38E+13	7.98E+14	7.98E+14
0.2—0.5	1.86E+13	1.86E+13	2.34E+14	2.34E+14
0.2—0.6	6.04E+12	6.04E+12	6.53E+13	6.53E+13
0.2—0.7	1.61E+12	1.61E+12	1.52E+13	1.52E+13
0.2—0.8	4.98E+11	4.98E+11	4.13E+12	4.13E+12
0.2—0.9	9.28E+13	*excluded*	6.85E+14	*excluded*
0.4—0.5	2.18E+12	2.18E+12	2.20E+13	2.20E+13
0.4—0.6	7.47E+11	7.47E+11	6.77E+12	6.77E+12
0.4—0.7	2.17E+11	2.17E+11	1.78E+12	1.78E+12
0.4—0.8	1.01E+11	1.01E+11	7.49E+11	7.49E+11
0.4—0.9	8.50E+13	*excluded*	5.80E+14	*excluded*
Mean value	**3.79E+13**	**2.76E+13**	**4.90E+14**	**4.61E+14**
Std. dev.	5.70E+13	5.72E+13	9.41E+14	1.03E+15
Sup. value	1.93E+14	1.93E+14	3.46E+15	3.46E+15
Inf. value	1.01E+11	1.01E+11	7.49E+11	7.49E+11
Δ(Sup; Inf)	1.93E+14	1.93E+14	3.46E+15	3.46E+15

Tab. E-4: Activation energy from partial sets of cellulose pyrolysis experimental data.

Cellulose 10 (a), 20, 30 K.min^{-1}			Cellulose 10 (b) – 30 K.min^{-1}			Cellulose 10 (c) – 30 K.min^{-1}		
α	E_a [J.mol^{-1}]		α	E_a [J.mol^{-1}]		α	E_a [J.mol^{-1}]	
0.1—0.3	181,290	181,290	—0.3	199,552	199,552	—0.3	189,890	189,890
0.1—0.4	174,203	174,203	—0.4	191,443	191,443	—0.4	181,698	181,698
0.1—0.5	167,258	167,258	—0.5	185,927	185,927	—0.5	174,920	174,920
0.1—0.6	160,125	160,125	—0.6	180,133	180,133	—0.6	167,968	167,968
0.1—0.7	151,808	151,808	—0.7	174,204	174,204	—0.7	160,154	160,154
0.1—0.8	141,506	141,506	—0.8	173,670	173,670	—0.8	155,516	155,516
0.1—0.9	143,959	*excluded*	—0.9	235,475	*excluded*	—0.9	219,027	*excluded*
0.4—0.5	153,991	153,991	—0.5	175,055	175,055	—0.5	162,153	162,153
0.4—0.6	147,442	147,442	—0.6	169,605	169,605	—0.6	155,800	155,800
0.4—0.7	139,711	139,711	—0.7	164,504	164,504	—0.7	148,726	148,726
0.4—0.8	131,045	131,045	—0.8	167,060	167,060	—0.8	147,213	147,213
0.4—0.9	142,960	*excluded*	—0.9	236,635	*excluded*	—0.9	221,417	*excluded*
Mean value	**152,941**	**154,838**	∅	**187,772**	**178,115**	∅	**173,707**	**164,404**
Std. dev.	14,464	15,147	S.D.	23,668	10,614	S.D.	24,126	13,377
Sup. value	181,290	181,290	Sup	236,635	199,552	Sup	221,417	189,890
Inf. value	131,045	131,045	Inf	164,504	164,504	Inf	147,213	147,213
Δ(Sup; Inf)	50,244	50,244	Rng	72,132	35,048	Rng	74,204	42,677

Tab. E-5: EVA 12 frequency factors, the 1st degradation step.

Frequency factors for R3 and F1 models, respectively.				
α	A [s^{-1}]			
	R3 (Contracting volume 3)		F1 (Reaction order = 1)	
0.2—0.3	6.54E+15	6.54E+15	2.16E+16	2.16E+16
0.2—0.4	4.21E+15	4.21E+15	1.43E+16	1.43E+16
0.2—0.5	4.84E+15	4.84E+15	1.69E+16	1.69E+16
0.2—0.6	4.81E+15	4.81E+15	1.74E+16	1.74E+16
0.2—0.7	5.58E+15	5.58E+15	2.11E+16	2.11E+16
0.2—0.8	5.16E+15	5.16E+15	2.08E+16	2.08E+16
0.2—0.9	5.34E+15	*excluded*	2.39E+16	*excluded*
0.4—0.5	8.30E+15	8.30E+15	3.04E+16	3.04E+16
0.4—0.6	7.26E+15	7.26E+15	2.76E+16	2.76E+16
0.4—0.7	9.03E+15	9.03E+15	3.60E+16	3.60E+16
0.4—0.8	8.16E+15	8.16E+15	3.47E+16	3.47E+16
0.4—0.9	9.01E+15	*excluded*	4.26E+16	*excluded*
Mean value	**6.52E+15**	**6.39E+15**	**2.56E+16**	**2.41E+16**
Std. dev.	1.69E+15	1.62E+15	8.36E+15	7.24E+15
Sup. value	4.21E+15	4.21E+15	1.43E+16	1.43E+16
Inf. value	9.03E+15	9.03E+15	4.26E+16	3.60E+16
Δ(Sup; Inf)	4.82E+15	4.82E+15	2.83E+16	2.17E+16

Tab. E-6: EVA 12 frequency factors, the 2nd degradation step.

Frequency factors for R3 and F1 models, respectively.				
α	A [s^{-1}]			
	R3 (Contracting volume 3)		F1 (Reaction order = 1)	
0.2—0.3	2.84E+17	2.84E+17	9.39E+17	9.39E+17
0.2—0.4	2.95E+18	2.95E+18	9.99E+18	9.99E+18
0.2—0.5	2.73E+18	2.73E+18	9.54E+18	9.54E+18
0.2—0.6	1.96E+18	1.96E+18	7.09E+18	7.09E+18
0.2—0.7	2.64E+18	2.64E+18	1.00E+19	1.00E+19
0.2—0.8	2.37E+18	2.37E+18	9.55E+18	9.55E+18
0.2—0.9	2.02E+18	*excluded*	9.05E+18	*excluded*
0.4—0.5	2.25E+18	2.25E+18	8.23E+18	8.23E+18
0.4—0.6	1.22E+18	1.22E+18	4.62E+18	4.62E+18
0.4—0.7	2.28E+18	2.28E+18	9.10E+18	9.10E+18
0.4—0.8	1.98E+18	1.98E+18	8.42E+18	8.42E+18
0.4—0.9	1.66E+18	*excluded*	7.84E+18	*excluded*
Mean value	**2.03E+18**	**2.07E+18**	**7.87E+18**	**7.75E+18**
Std. dev.	6.95E+17	7.51E+17	2.54E+18	2.75E+18
Sup. value	2.84E+17	2.84E+17	9.39E+17	9.39E+17
Inf. value	2.95E+18	2.95E+18	1.00E+19	1.00E+19
Δ(Sup; Inf)	2.66E+18	2.66E+18	9.08E+18	9.08E+18

Tab. E-7: EVA 25 frequency factors, the 1st degradation step.

Frequency factors for R3 and F1 models, respectively.				
α	A [s^{-1}]			
	R3 (Contracting volume 3)		F1 (Reaction order = 1)	
0.2—0.3	1.29E+15	1.29E+15	4.26E+15	4.26E+15
0.2—0.4	1.47E+15	1.47E+15	4.98E+15	4.98E+15
0.2—0.5	1.91E+15	1.91E+15	6.68E+15	6.68E+15
0.2—0.6	2.77E+15	2.77E+15	1.00E+16	1.00E+16
0.2—0.7	3.06E+15	3.06E+15	1.16E+16	1.16E+16
0.2—0.8	2.61E+15	2.61E+15	1.05E+16	1.05E+16
0.2—0.9	1.79E+15	*excluded*	8.01E+15	*excluded*
0.4—0.5	2.98E+15	2.98E+15	1.09E+16	1.09E+16
0.4—0.6	4.62E+15	4.62E+15	1.76E+16	1.76E+16
0.4—0.7	4.44E+15	4.44E+15	1.77E+16	1.77E+16
0.4—0.8	3.25E+15	3.25E+15	1.38E+16	1.38E+16
0.4—0.9	1.98E+15	*excluded*	9.36E+15	*excluded*
Mean value	**2.68E+15**	**2.84E+15**	**1.05E+16**	**1.08E+16**
Std. dev.	1.03E+15	1.06E+15	4.14E+15	4.44E+15
Sup. value	1.29E+15	1.29E+15	4.26E+15	4.26E+15
Inf. value	4.62E+15	4.62E+15	1.77E+16	1.77E+16
Δ(Sup; Inf)	3.33E+15	3.33E+15	1.34E+16	1.34E+16

Tab. E-8: EVA 25 frequency factors, the 2nd degradation step.

Frequency factors for R3 and F1 models, respectively.				
α	A [s^{-1}]			
	R3 (Contracting volume 3)		F1 (Reaction order = 1)	
0.2—0.3	6.56E+21	6.56E+21	2.17E+22	2.17E+22
0.2—0.4	5.75E+21	5.75E+21	1.95E+22	1.95E+22
0.2—0.5	4.68E+21	4.68E+21	1.63E+22	1.63E+22
0.2—0.6	7.40E+21	7.40E+21	2.68E+22	2.68E+22
0.2—0.7	3.67E+21	3.67E+21	1.39E+22	1.39E+22
0.2—0.8	2.37E+21	2.37E+21	9.56E+21	9.56E+21
0.2—0.9	5.64E+20	*excluded*	2.53E+21	*excluded*
0.4—0.5	3.48E+21	3.48E+21	1.27E+22	1.27E+22
0.4—0.6	9.54E+21	9.54E+21	3.63E+22	3.63E+22
0.4—0.7	3.15E+21	3.15E+21	1.26E+22	1.26E+22
0.4—0.8	1.87E+21	1.87E+21	7.95E+21	7.95E+21
0.4—0.9	3.53E+20	*excluded*	1.67E+21	*excluded*
Mean value	**4.12E+21**	**4.85E+21**	**1.51E+22**	**1.77E+22**
Std. dev.	2.67E+21	2.31E+21	9.50E+21	8.22E+21
Sup. value	3.53E+20	1.87E+21	1.67E+21	7.95E+21
Inf. value	9.54E+21	9.54E+21	3.63E+22	3.63E+22
Δ(Sup; Inf)	9.19E+21	7.67E+21	3.46E+22	2.83E+22

Tab. E-9: E_a for EVA 12, β = 1, 2, 5, 7, 10, 20, and 30 K.min^{-1}.

EVA 12, 1st degradation step.			EVA 12, 2nd step.		
α	E_a [J.mol^{-1}]			E_a [J.mol^{-1}]	
0.2—0.3	199,104	199,104	—0.3	260035	260,035
0.2—0.4	197,044	197,044	—0.4	274084	274,084
0.2—0.5	197,837	197,837	—0.5	273541	273,541
0.2—0.6	198,004	198,004	—0.6	271490	271,490
0.2—0.7	198,991	198,991	—0.7	273452	273,452
0.2—0.8	198,977	198,977	—0.8	272903	272,903
0.2—0.9	199,982	*excluded*	—0.9	272281	*excluded*
0.4—0.5	201,208	201,208	—0.5	272453	272,453
0.4—0.6	200,889	200,889	—0.6	268782	268,782
0.4—0.7	202,365	202,365	—0.7	272944	272,944
0.4—0.8	202,354	202,354	—0.8	272298	272,298
0.4—0.9	203,885	*excluded*	—0.9	271686	*excluded*
Mean value	**200,053**	**199,677**	∅	**271,329**	**271,198**
Std. dev.	2,015	1,806	S.D.	3,644	3,977
Sup. value	197,044	197,044	Max	260,035	260,035
Inf. value	203,885	202,365	Min	274,084	274,084
Δ(Sup; Inf)	6,841	5,322	Rng	14,049	14,049

Tab. E-10: E_a for EVA 25, β = 1, 2, 5, 7, 10, 20, and 30 K.min^{-1}.

EVA 12, 1st degradation step.			EVA 12, 2nd step.		
α	E_a [J.mol^{-1}]			E_a [J.mol^{-1}]	
0.2—0.3	189,951	189,951	—0.3	318,862	318,862
0.2—0.4	190,648	190,648	—0.4	318,203	318,203
0.2—0.5	192,080	192,080	—0.5	317,077	317,077
0.2—0.6	194,096	194,096	—0.6	319,943	319,943
0.2—0.7	194,832	194,832	—0.7	315,877	315,877
0.2—0.8	194,364	194,364	—0.8	313,467	313,467
0.2—0.9	193,099	*excluded*	—0.9	305,123	*excluded*
0.4—0.5	194,949	194,949	—0.5	315,998	315,998
0.4—0.6	197,441	197,441	—0.6	322,325	322,325
0.4—0.7	197,606	197,606	—0.7	315,867	315,867
0.4—0.8	196,461	196,461	—0.8	313,032	313,032
0.4—0.9	194,716	*excluded*	—0.9	303,314	*excluded*
Mean value	**194,187**	**194,243**	∅	**314,924**	**317,065**
Std. dev.	2,325	2,517	S.D.	5,403	2,714
Sup. value	189,951	189,951	Sup	303,314	313,032
Inf. value	197,606	197,606	Inf	322,325	322,325
Δ(Sup; Inf)	7,656	7,656	Rng	19,011	9,293

Tab. E-11: Temperatures at various degrees of conversion.

	PS 1	PS 2	PS 5	PS 7	PS 10	PS 15	PS 20
α	$T_1(\alpha)$	$T_2(\alpha)$	$T_5(\alpha)$	$T_7(\alpha)$	$T_{10}(\alpha)$	$T_{15}(\alpha)$	$T_{20}(\alpha)$
0.1	359.069	368.945	383.657	389.018	*382.370*	401.712	405.907
0.2	367.205	377.057	392.388	397.596	*395.779*	410.945	415.582
0.3	371.779	382.481	397.830	403.075	*403.459*	416.964	421.975
0.4	375.583	386.407	401.973	407.321	409.017	421.731	427.078
0.5	378.931	389.656	405.576	411.007	413.549	426.026	431.733
0.6	380.938	392.554	408.970	414.481	417.633	430.129	436.161
0.7	383.816	395.417	412.496	418.023	421.725	434.304	440.693
0.8	386.683	398.710	416.437	421.965	426.207	439.039	445.776
0.9	390.953	403.124	421.486	427.133	431.943	445.320	452.551

N.B. 1: The temperature values and heating rates are indicated without their respective units, for convenience, as the number following the designation of polymer. These are, respectively, degrees of centigrade and $K.min^{-1}$.
N.B. 2: Three temperatures bringing up discrepancy between the thermal degradation behaviour of seven experimental curves are presented in italics (reminder: see "PS 10").

Tab. E-12: PS pyrolysis frequency factors.

Frequency factors for AE2 and F1 models, respectively.				
α	A [s^{-1}]			
	AE2 (Avrami-Erofeev 2)		F1 (Reaction order = 1)	
0.2—0.3	1.17E+15	1.17E+15	1.25E+15	1.25E+15
0.2—0.4	1.01E+15	1.01E+15	1.20E+15	1.20E+15
0.2—0.5	6.75E+14	6.75E+14	8.81E+14	8.81E+14
0.2—0.6	1.93E+14	1.93E+14	2.76E+14	2.76E+14
0.2—0.7	1.06E+14	1.06E+14	1.66E+14	1.66E+14
0.2—0.8	4.73E+13	4.73E+13	8.23E+13	8.23E+13
0.2—0.9	2.36E+13	*excluded*	4.70E+13	*excluded*
0.4—0.5	1.57E+14	1.57E+14	2.42E+14	2.42E+14
0.4—0.6	1.19E+13	1.19E+13	1.99E+13	1.99E+13
0.4—0.7	9.55E+12	9.55E+12	1.73E+13	1.73E+13
0.4—0.8	4.95E+12	4.95E+12	9.82E+12	9.82E+12
0.4—0.9	3.53E+12	*excluded*	7.88E+12	*excluded*
Mean value	**2.84E+14**	**3.38E+14**	**3.50E+14**	**4.14E+14**
Std. dev.	4.03E+14	4.21E+14	4.55E+14	4.72E+14
Sup. value	1.17E+15	1.17E+15	1.25E+15	1.25E+15
Inf. value	3.53E+12	4.95E+12	7.88E+12	9.82E+12
Δ(Sup; Inf)	1.16E+15	1.16E+15	1.24E+15	1.24E+15

Tab. E-13: Activation energy from partial sets of experimental data.

PS 1, 2 K.min^{-1}			PS 5, 7, and 10 K.min^{-1}			PS 15, 20 K.min^{-1}		
α	E_a [J.mol^{-1}]			E_a [J.mol^{-1}]			E_a [J.mol^{-1}]	
0.1—0.2	241,206	*excluded*	—0.2	197,781	*excluded*	—0.2	210,777	*excluded*
0.1—0.3	211,007	211,007	—0.3	227,501	227,501	—0.3	199,571	199,571
0.1—0.4	213,405	213,405	—0.4	239,044	239,044	—0.4	190,745	190,745
0.1—0.5	220,213	220,213	—0.5	245,531	245,531	—0.5	181,495	181,495
0.1—0.6	200,607	200,607	—0.6	250,196	250,196	—0.6	175,005	175,005
0.1—0.7	204,633	204,633	—0.7	257,446	257,446	—0.7	168,288	168,288
0.1—0.8	199,158	199,158	—0.8	265,132	265,132	—0.8	163,530	163,530
0.1—0.9	200,947	*excluded*	—0.9	268,718	*excluded*	—0.9	156,907	*excluded*
0.4—0.5	239,823	239,823	—0.5	234,963	234,963	—0.5	152,578	152,578
0.4—0.6	177,536	177,536	—0.6	236,324	236,324	—0.6	150,615	150,615
0.4—0.7	193,783	193,783	—0.7	239,493	239,493	—0.7	146,132	146,132
0.4—0.8	187,058	187,058	—0.8	241,302	241,302	—0.8	144,526	144,526
0.4—0.9	193,096	*excluded*	—0.9	238,975	*excluded*	—0.9	140,399	*excluded*
Mean value	**206,344**	**204,722**	∅	**241,724**	**243,693**	∅	**167,736**	**167,249**
Std. dev.	18,085	16,750	S.D.	17,183	10,640	S.D.	21,570	18,246
Sup. value	241,206	239,823	Sup	268,718	265,132	Sup	210,777	199,571
Inf. value	177,536	177,536	Inf	197,781	227,501	Inf	140,399	144,526
Δ(Sup; Inf)	63,670	62,287	Rng	70,937	37,631	Rng	70,378	55,045

Tab. E-14: Detailed comparison of "5, 7, 10" and "5, 7" data sets.

PS 5, 7, and 10 K.min^{-1}			PS 5, and 7 K.min^{-1}		
α	E_a [J.mol^{-1}]		α	E_a [J.mol^{-1}]	
0.1—0.2	197,781	*excluded*	—0.2	245,582	*N/A*
0.1—0.3	227,501	227,501	—0.3	240,044	240,044
0.1—0.4	239,044	239,044	—0.4	234,058	234,058
0.1—0.5	245,531	245,531	—0.5	230,825	230,825
0.1—0.6	250,196	250,196	—0.6	228,422	228,422
0.1—0.7	257,446	257,446	—0.7	229,418	229,418
0.1—0.8	265,132	265,132	—0.8	231,165	231,165
0.1—0.9	268,718	*excluded*	—0.9	228,699	excluded
0.4—0.5	234,963	234,963	—0.5	223,501	223,501
0.4—0.6	236,324	236,324	—0.6	222,797	222,797
0.4—0.7	239,493	239,493	—0.7	228,049	228,049
0.4—0.8	241,302	241,302	—0.8	232,511	232,511
0.4—0.9	238,975	*excluded*	—0.9	229,696	*excluded*
Mean value	**241,724**	**243,693**	∅	**229,932**	**230,079**
Std. dev.	17,182	10,640	S. D.	4,361	4,758
Sup. value	268,718	265,132	Sup	240,044	240,044
Inf. value	197,781	227,501	Inf	222,797	222,797
Δ(Sup; Inf)	70,937	37,631	Rng	17,247	17,247

Tab. E-15: Activation energies of three sets of PS experiments.

PS 1, 2 K.min^{-1}			PS 5, 7, and 10 K.min^{-1}			PS 15, 20 K.min^{-1}		
α	E_a [J.mol^{-1}]			E_a [J.mol^{-1}]			E_a [J.mol^{-1}]	
0.2—0.3	177,473	177,473	—0.3	254,757	254,757	—0.3	186,430	186,430
0.2—0.4	198,044	198,044	—0.4	247,990	247,990	—0.4	178,604	178,604
0.2—0.5	212,969	212,969	—0.5	247,694	247,694	—0.5	169,764	169,764
0.2—0.6	188,746	188,746	—0.6	249,082	249,082	—0.6	164,343	164,343
0.2—0.7	196,578	196,578	—0.7	253,165	253,165	—0.7	158,471	158,471
0.2—0.8	191,796	191,796	—0.8	257,005	257,005	—0.8	154,857	154,857
0.2—0.9	195,944	*excluded*	—0.9	256,836	*excluded*	—0.9	149,324	*excluded*
0.4—0.5	239,823	239,823	—0.5	234,963	234,963	—0.5	152,578	152,578
0.4—0.6	177,536	177,536	—0.6	236,324	236,324	—0.6	150,615	150,615
0.4—0.7	193,783	193,783	—0.7	239,493	239,493	—0.7	146,132	146,132
0.4—0.8	187,058	187,058	—0.8	241,302	241,302	—0.8	144,526	144,526
0.4—0.9	193,096	*excluded*	—0.9	238,975	*excluded*	—0.9	140,399	*excluded*
Mean value	**196,070**	**196,380**	∅	**246,466**	**246,178**	∅	**158,004**	**160,632**
Std. dev.	15,970	17,466	S.D.	7,689	7,383	S.D.	13,580	13,261
Sup. value	239,823	239,823	Sup	257,005	257,005	Sup	186,430	186,430
Inf. value	177,473	177,473	Inf	234,963	234,963	Inf	140,399	144,526
Δ(Sup; Inf)	62,350	62,350	Rng	22,043	22,043	Rng	46,031	41,904

Tab. E-16: Comparison of 5, 7, 10, and 5, 7 data sets.

PS 5, 7, and 10 K.min^{-1}			PS 5, 7 K.min^{-1}		
α	E_a [J.mol^{-1}]			E_a [J.mol^{-1}]	
0.2—0.3	254,757	254,757	—0.3	235,880	235,880
0.2—0.4	247,990	247,990	—0.4	229,648	229,648
0.2—0.5	247,694	247,694	—0.5	227,491	227,491
0.2—0.6	249,082	249,082	—0.6	226,000	226,000
0.2—0.7	253,165	253,165	—0.7	228,553	228,553
0.2—0.8	257,005	257,005	—0.8	231,630	231,630
0.2—0.9	256,836	*excluded*	—0.9	229,572	*excluded*
0.4—0.5	234,963	234,963	—0.5	223,501	223,501
0.4—0.6	236,324	236,324	—0.6	222,797	222,797
0.4—0.7	239,493	239,493	—0.7	228,049	228,049
0.4—0.8	241,302	241,302	—0.8	232,511	232,511
0.4—0.9	238,975	*excluded*	—0.9	229,696	*excluded*
Mean value	**246,466**	**246,178**	∅	**228,777**	**228,606**
Std. dev.	7,689	7,383	S.D.	3,516	3,828
Sup. value	257,005	257,005	Sup	235,880	235,880
Inf. value	234,963	234,963	Inf	222,797	222,797
Δ(Sup; Inf)	22,043	22,043	Rng	13,083	13,083

Tab. E-17: Summary results for the whole set of experiments.

PS 1, 2, 5, 7, 10, 15, 20 K.min^{-1}					
α	E_a [J.mol^{-1}]		α	E_a [J.mol^{-1}]	
0.1—0.2	212,730	*excluded*	—	*N/A*	*N/A*
0.1—0.3	208,563	208,563	0.2—0.3	203,502	203,502
0.1—0.4	206,229	206,229	0.2—0.4	202,252	202,252
0.1—0.5	203,390	203,390	0.2—0.5	199,663	199,663
0.1—0.6	196,028	196,028	0.2—0.6	190,964	190,964
0.1—0.7	192,484	192,484	0.2—0.7	187,756	187,756
0.1—0.8	187,885	187,885	0.2—0.8	183,330	183,330
0.1—0.9	184,001	*excluded*	0.2—0.9	180,080	*excluded*
0.4—0.5	194,288	194,288	0.4—0.5	194,288	194,288
0.4—0.6	179,694	179,694	0.4—0.6	179,694	179,694
0.4—0.7	178,614	178,614	0.4—0.7	178,614	178,614
0.4—0.8	175,069	175,069	0.4—0.8	175,069	175,069
0.4—0.9	173,450	*excluded*	0.4—0.9	173,450	*excluded*
Mean value	**191,725**	**192,224**	Mean value	**187,388**	**189,513**
Std. dev.	12,708	11,233	Std. dev.	10,181	9,752
Sup. value	212,730	208,563	Sup. value	203,502	203,502
Inf. value	173,450	175,069	Inf. value	173,450	175,069
Δ(Sup; Inf)	39,280	33,494	Δ(Sup; Inf)	30,052	28,433

Tab. E-18: PVC pyrolysis frequency factors. The 1st degradation step.

Frequency factors for D3 and F1 models, respectively.				
α	A [s^{-1}]			
	D3 (Diffusion model 3)		F1 (Reaction order = 1)	
0.2—0.3	1.07E+10	1.07E+10	1.93E+11	1.93E+11
0.2—0.4	8.79E+09	8.79E+09	1.31E+11	1.31E+11
0.2—0.5	8.14E+09	8.14E+09	1.02E+11	1.02E+11
0.2—0.6	7.70E+09	7.70E+09	8.32E+10	8.32E+10
0.2—0.7	8.99E+09	8.99E+09	8.47E+10	8.47E+10
0.2—0.8	8.03E+09	8.03E+09	6.66E+10	6.66E+10
0.2—0.9	1.23E+10	*excluded*	9.09E+10	*excluded*
0.4—0.5	5.65E+09	5.65E+09	5.71E+10	5.71E+10
0.4—0.6	5.40E+09	5.40E+09	4.89E+10	4.89E+10
0.4—0.7	7.18E+09	7.18E+09	5.87E+10	5.87E+10
0.4—0.8	6.03E+09	6.03E+09	4.48E+10	4.48E+10
0.4—0.9	1.05E+10	*excluded*	7.14E+10	*excluded*
Mean value	**8.29E+09**	**7.66E+09**	**8.60E+10**	**8.70E+10**
Std. dev.	2.04E+09	1.58E+09	3.98E+10	4.33E+10
Sup. value	5.40E+09	5.40E+09	4.48E+10	4.48E+10
Inf. value	1.23E+10	1.07E+10	1.93E+11	1.93E+11
Δ(Sup; Inf)	6.93E+09	5.33E+09	1.48E+11	1.48E+11

Tab. E-19: PVC pyrolysis frequency factors. The 2nd degradation step.

Frequency factors for D3 and F1 models, respectively.				
α	A [s^{-1}]			
	D3 (Diffusion model 3)		F1 (Reaction order = 1)	
0.2—0.3	3.93E+15	3.93E+15	7.07E+16	7.07E+16
0.2—0.4	4.47E+15	4.47E+15	6.64E+16	6.64E+16
0.2—0.5	4.95E+15	4.95E+15	6.22E+16	6.22E+16
0.2—0.6	4.49E+15	4.49E+15	4.86E+16	4.86E+16
0.2—0.7	4.17E+15	4.17E+15	3.93E+16	3.93E+16
0.2—0.8	4.55E+15	4.55E+15	3.77E+16	3.77E+16
0.2—0.9	5.11E+15	*excluded*	3.77E+16	*excluded*
0.4—0.5	1.47E+16	1.47E+16	1.49E+17	1.49E+17
0.4—0.6	1.41E+16	1.41E+16	1.27E+17	1.27E+17
0.4—0.7	1.47E+16	1.47E+16	1.20E+17	1.20E+17
0.4—0.8	1.89E+16	1.89E+16	1.40E+17	1.40E+17
0.4—0.9	2.46E+16	*excluded*	1.68E+17	*excluded*
Mean value	**9.88E+15**	**8.89E+15**	**8.88E+16**	**8.61E+16**
Std. dev.	6.84E+15	5.60E+15	4.63E+16	4.10E+16
Sup. value	3.93E+15	3.93E+15	3.77E+16	3.77E+16
Inf. Value	2.46E+16	1.89E+16	1.68E+17	1.49E+17
Δ(Sup; Inf)	2.06E+16	1.50E+16	1.30E+17	1.11E+17

Tab. E-20: PVC pyrolysis frequency factors. The 3rd degradation step.

Frequency factors for D3 and F1 models, respectively.				
α	A [s^{-1}]			
	D3 (Diffusion model 3)		F1 (Reaction order = 1)	
0.2—0.3	4.67E+17	4.67E+17	8.39E+18	8.39E+18
0.2—0.4	4.33E+17	4.33E+17	6.42E+18	6.42E+18
0.2—0.5	1.04E+17	1.04E+17	1.31E+18	1.31E+18
0.2—0.6	6.34E+16	6.34E+16	6.85E+17	6.85E+17
0.2—0.7	5.75E+16	5.75E+16	5.42E+17	5.42E+17
0.2—0.8	5.62E+16	5.62E+16	4.66E+17	4.66E+17
0.2—0.9	5.24E+16	*excluded*	3.87E+17	*excluded*
0.4—0.5	6.89E+15	6.89E+15	6.96E+16	6.96E+16
0.4—0.6	8.30E+15	8.30E+15	7.52E+16	7.52E+16
0.4—0.7	1.07E+16	1.07E+16	8.74E+16	8.74E+16
0.4—0.8	1.24E+16	1.24E+16	9.21E+16	9.21E+16
0.4—0.9	1.27E+16	*excluded*	8.63E+16	*excluded*
Mean value	**1.07E+17**	**1.22E+17**	**1.55E+18**	**1.81E+18**
Std. dev.	1.56E+17	1.67E+17	2.67E+18	2.85E+18
Sup. value	6.89E+15	6.89E+15	6.96E+16	6.96E+16
Inf. value	4.67E+17	4.67E+17	8.39E+18	8.39E+18
Δ(Sup; Inf)	4.60E+17	4.60E+17	8.32E+18	8.32E+18

Tab. E-21: Activation energy values for the three degradation steps of PVC, 1-30 $K.min^{-1}$.

PVC, the 1st degradation step.			PVC, the 2nd step.			PVC, the 3rd step.		
α	E_a [$J.mol^{-1}$]		α	E_a [$J.mol^{-1}$]		α	E_a [$J.mol^{-1}$]	
0.2—0.3	123,258	123,258	—0.3	194,718	194,718	—0.3	269,952	269,952
0.2—0.4	120,887	120,887	—0.4	195,143	195,143	—0.4	269,214	269,214
0.2—0.5	119,311	119,311	—0.5	195,504	195,504	—0.5	260,333	260,333
0.2—0.6	118,002	118,002	—0.6	194,906	194,906	—0.6	257,052	257,052
0.2—0.7	117,751	117,751	—0.7	194,413	194,413	—0.7	256,229	256,229
0.2—0.8	116,264	116,264	—0.8	194,719	194,719	—0.8	256,058	256,058
0.2—0.9	117,173	*excluded*	—0.9	195,176	*excluded*	—0.9	256,158	*excluded*
0.4—0.5	115,860	115,860	—0.5	201,087	201,087	—0.5	244,425	244,425
0.4—0.6	114,930	114,930	—0.6	200,899	200,899	—0.6	245,521	245,521
0.4—0.7	115,567	115,567	—0.7	201,137	201,137	—0.7	247,065	247,065
0.4—0.8	114,026	114,026	—0.8	202,424	202,424	—0.8	248,174	248,174
0.4—0.9	115,742	*excluded*	—0.9	203,784	*excluded*	—0.9	249,079	*excluded*
Mean value	**117,397**	**117,586**	∅	**197,826**	**197,495**	∅	**254,938**	**255,402**
Std. dev.	2,548	2,734	S.D.	3,497	3,212	S.D.	8,208	8,778
Sup. value	114,026	114,026	Sup	194,413	194,413	Sup	244,425	244,425
Inf. value	123,258	123,258	Inf	203,784	202,424	Inf	269,952	269,952
Δ(Sup; Inf)	9,232	9,232	Rng	9,371	8,012	Rng	25,528	25,528

Appendix F

– Figures for PART A –

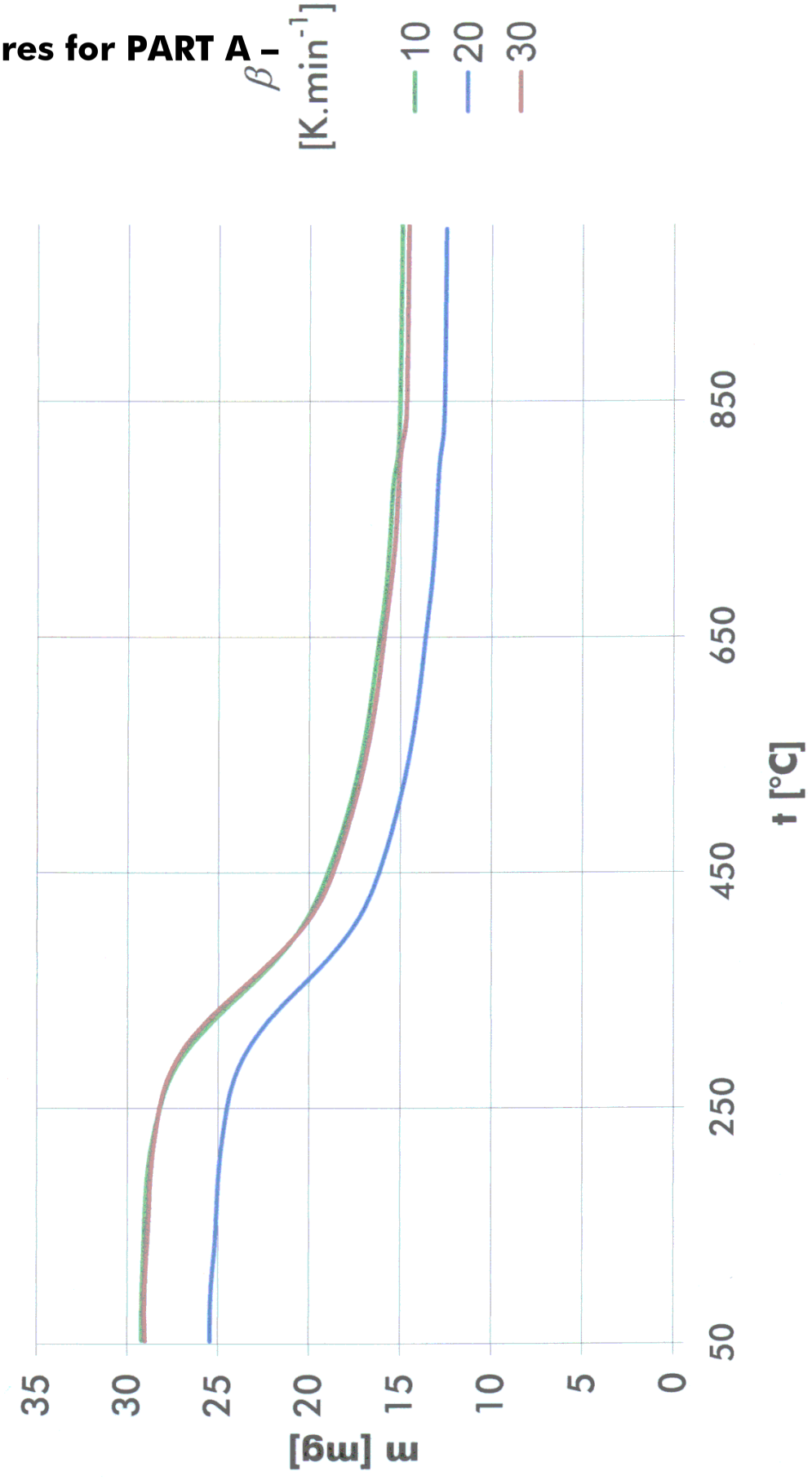

Fig. F-1: Lignin pyrolysis thermogravigram.

Fig. F-2: Lignin pyrolysis α = f(t).

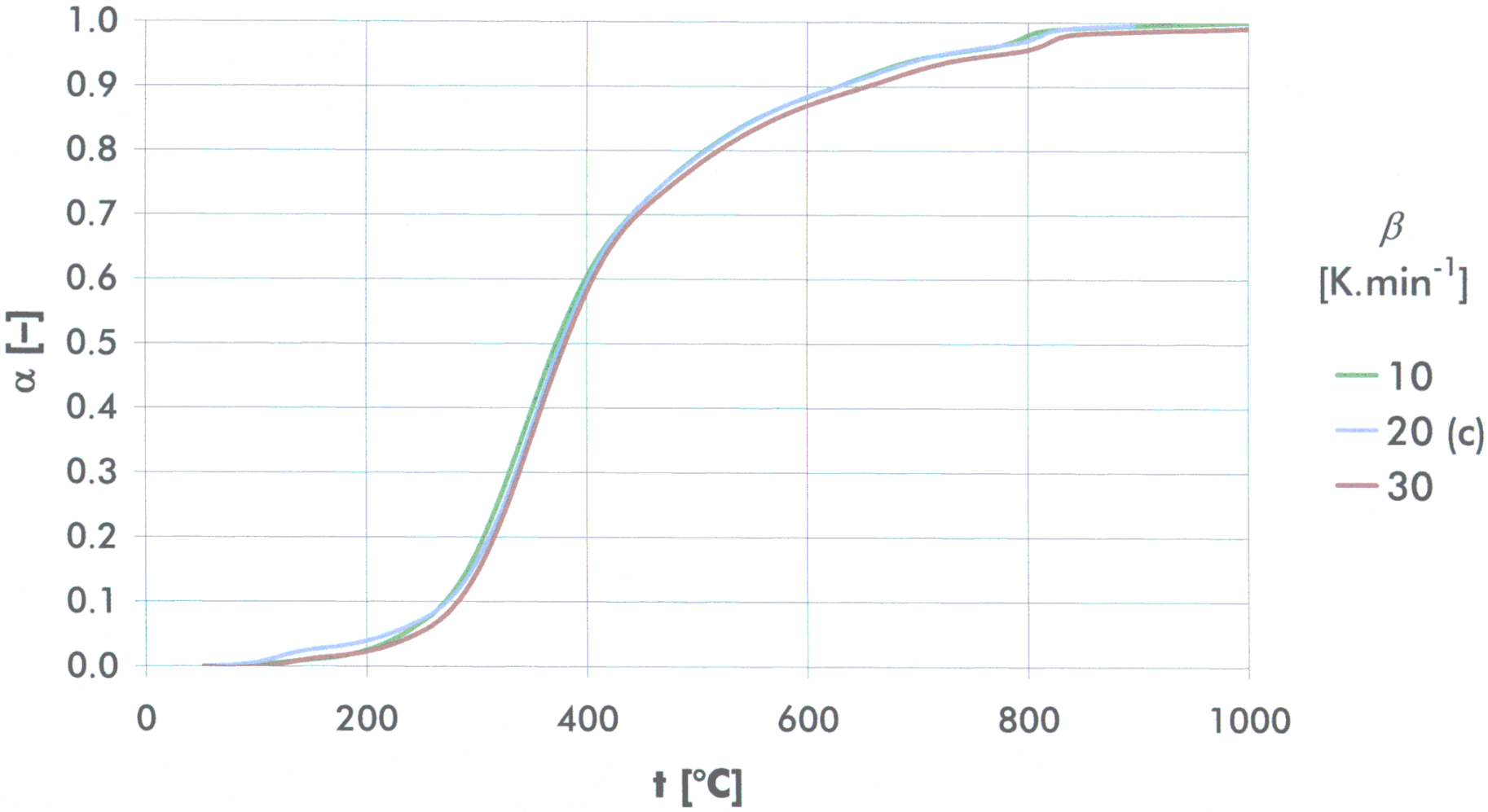

Fig. F-3: t = f(τ), the case of lignin.

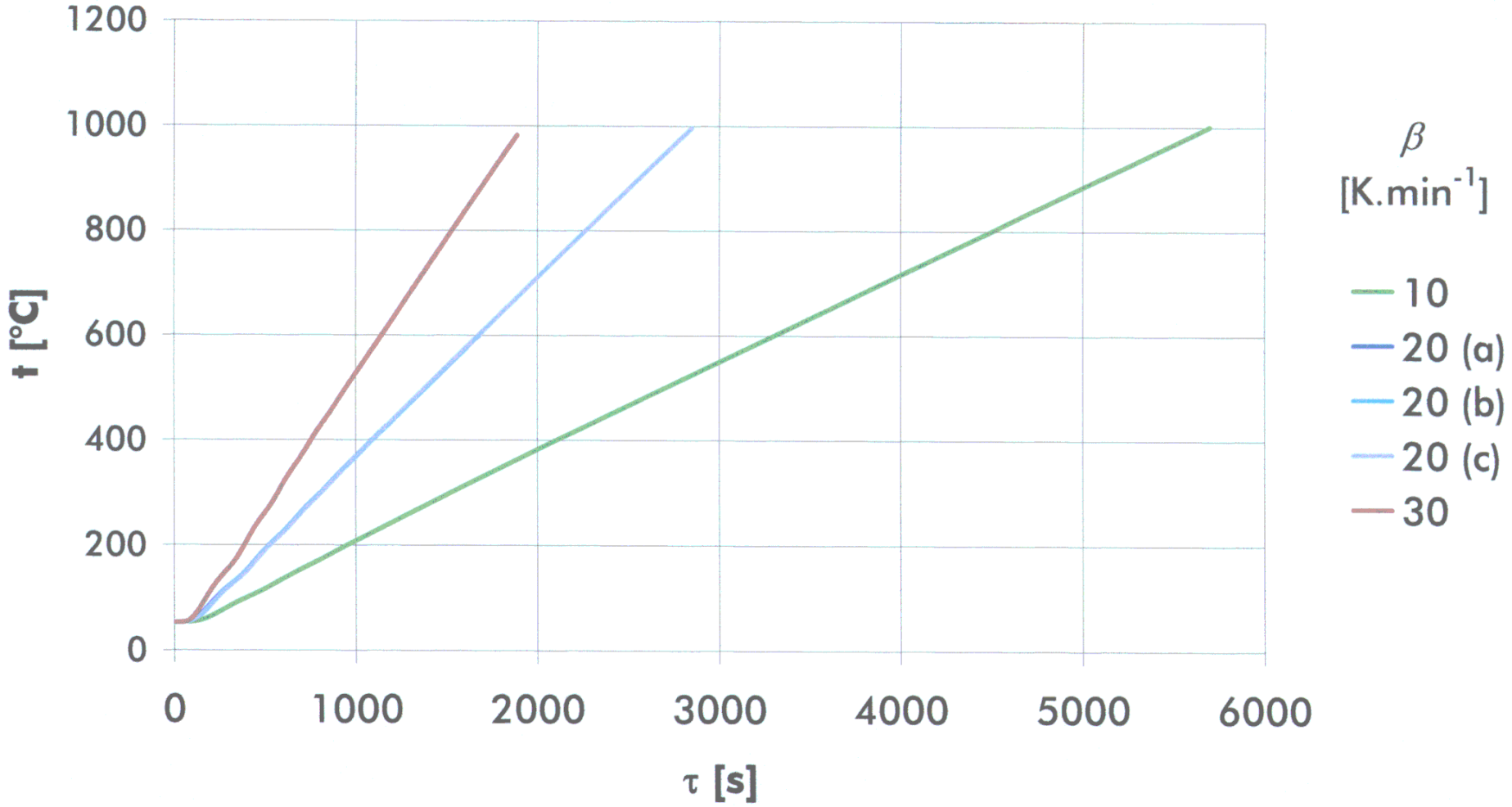

Fig. F-4: Detailed TGA of lignin 30 K.min^{-1} pyrolysis.

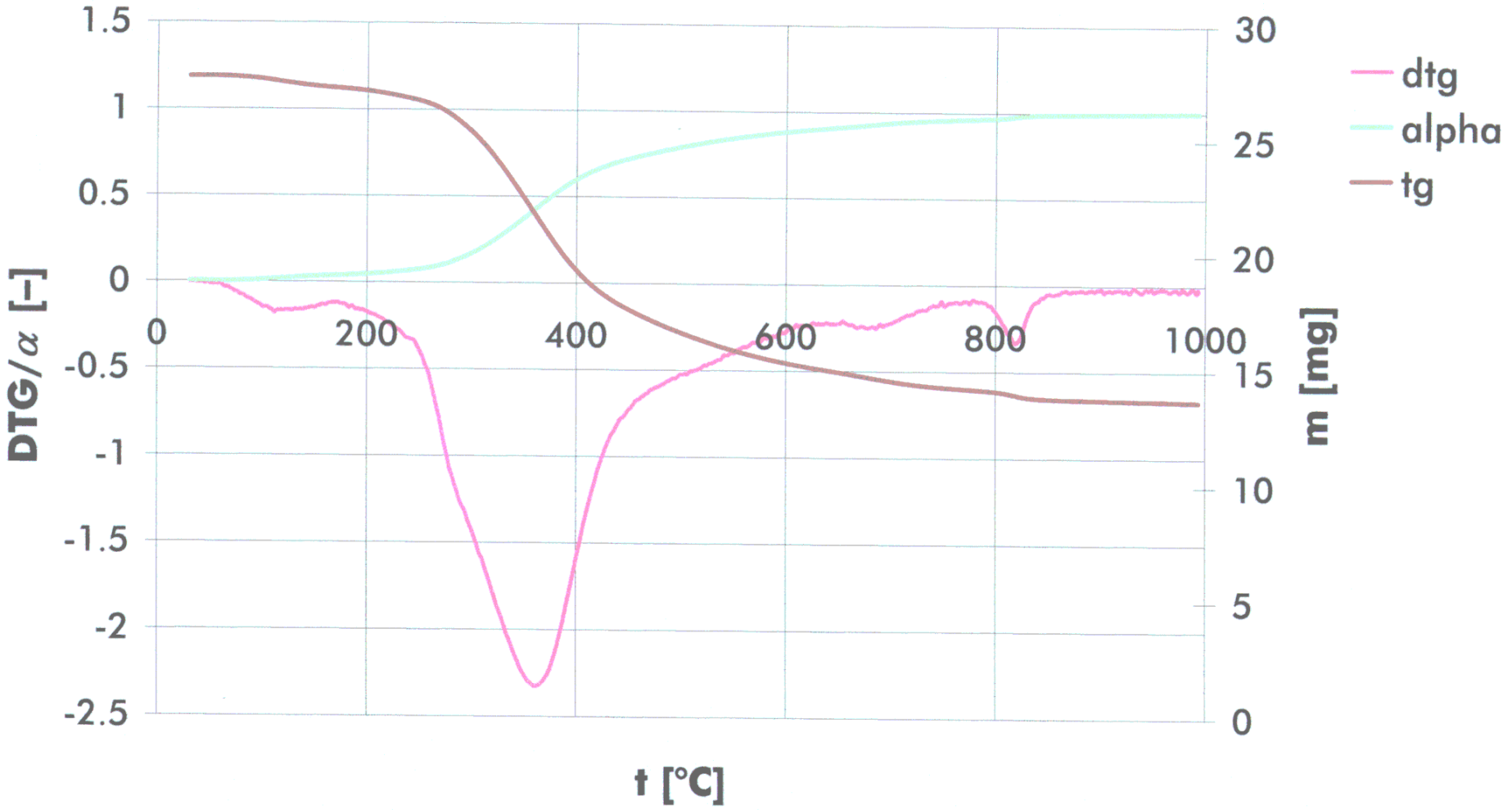

Fig. F-5: Cellulose pyrolysis curves.

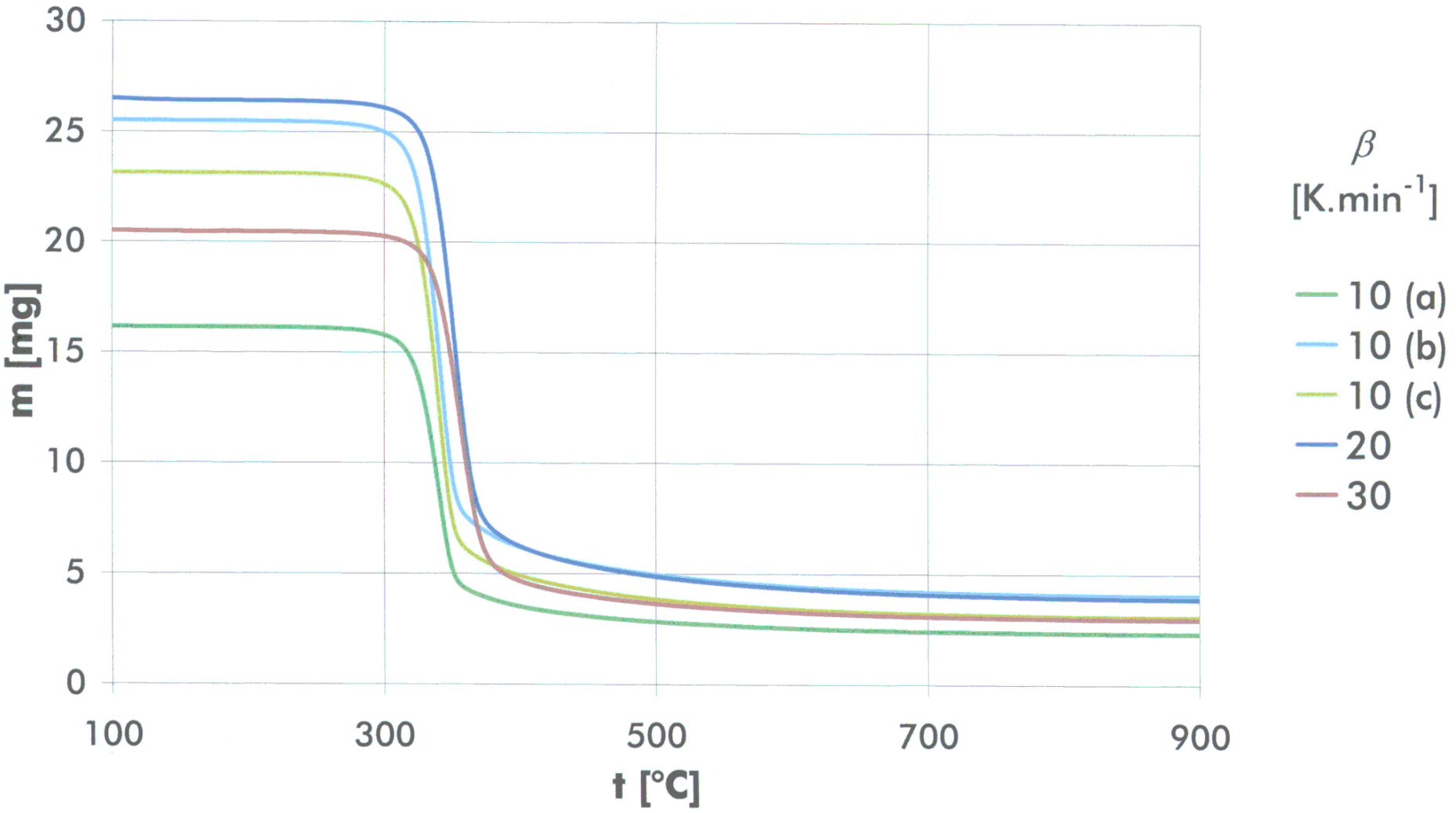

Fig. F-6: Cellulose pyrolysis α evolution.

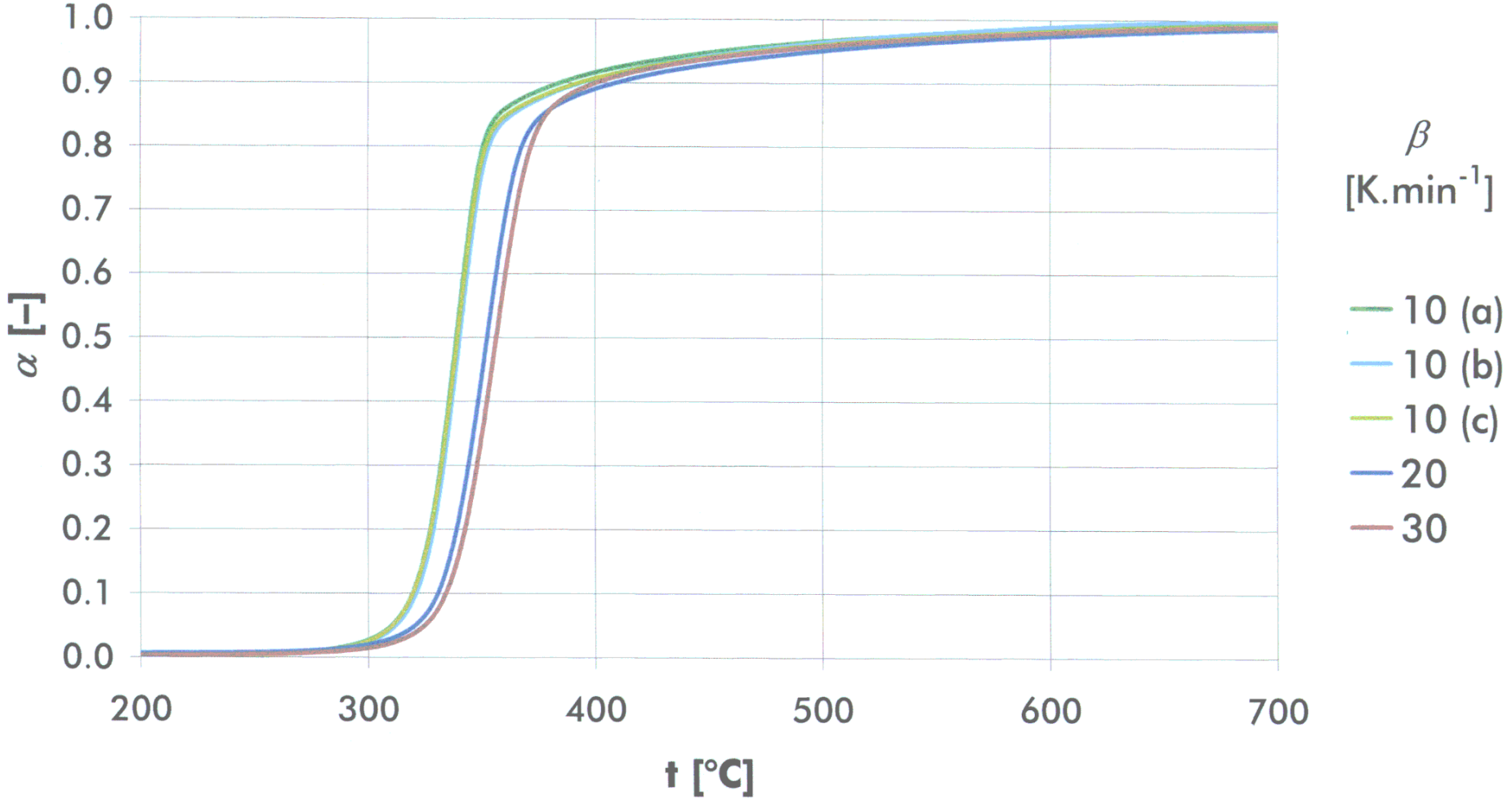

Fig. F-7: Cellulose pyrolysis t = f(τ) graph.

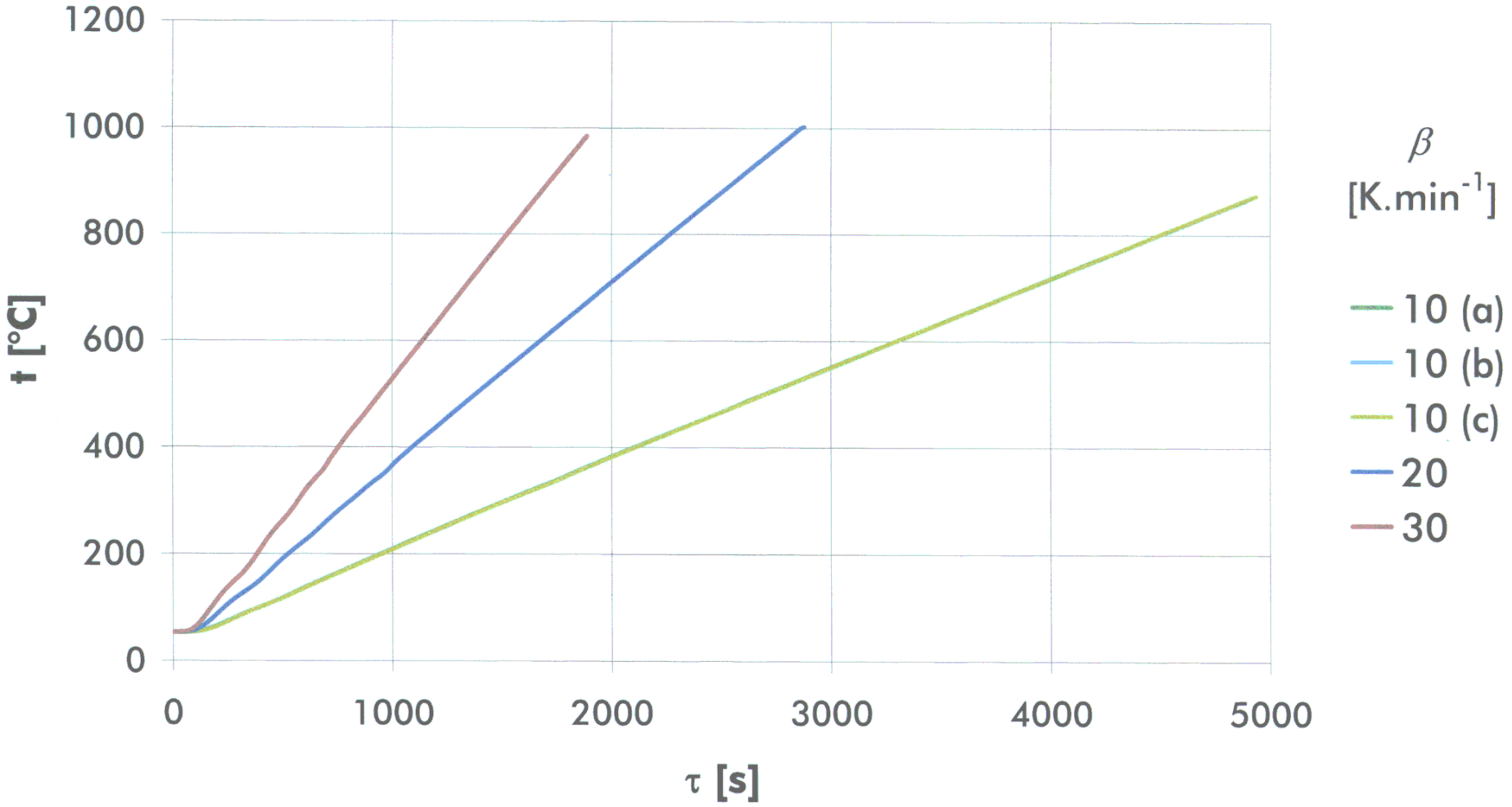

Fig. F-8: Energy of activation of cellulose pyrolysis.

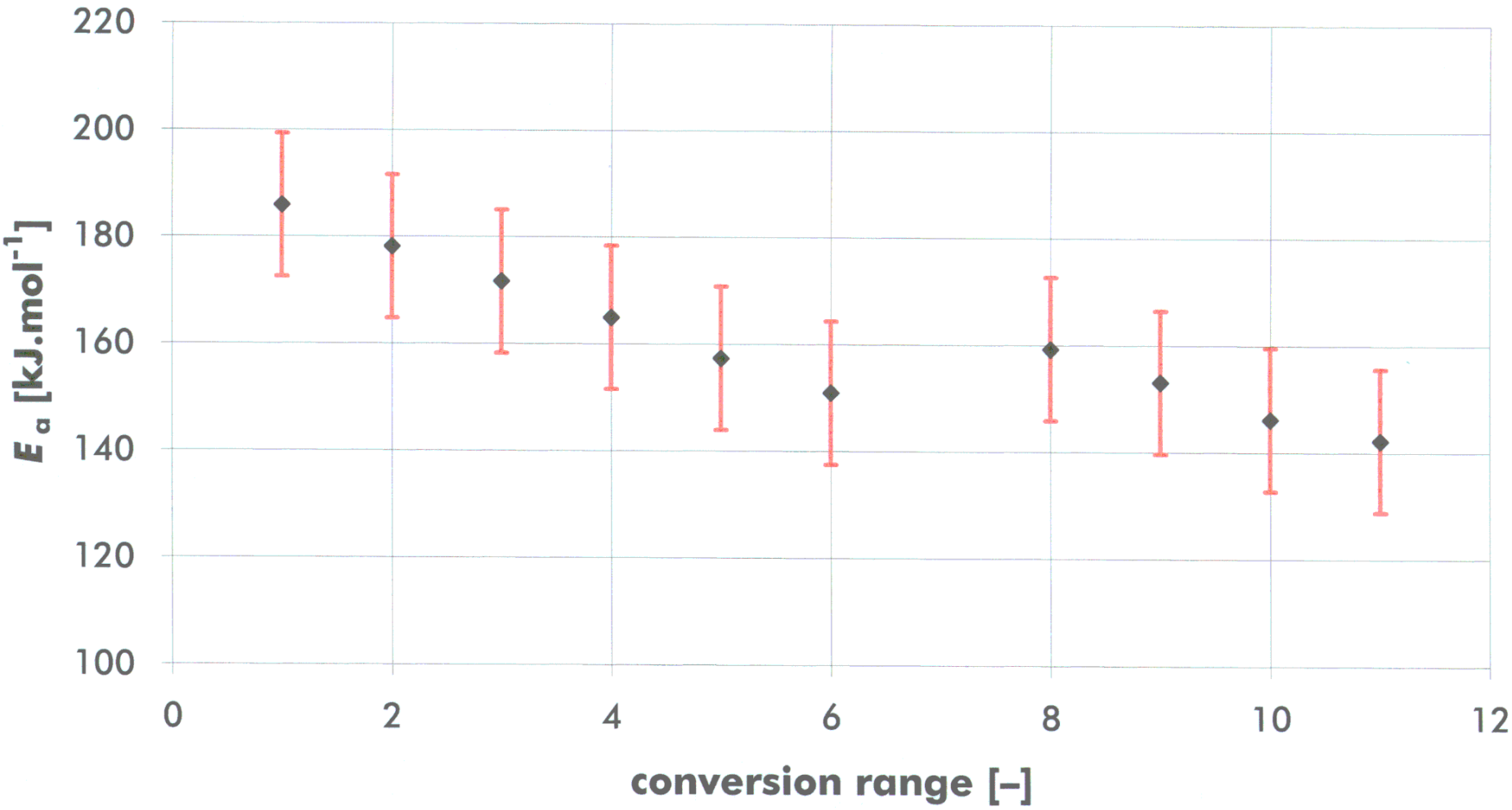

Fig. F-9: EVA "12" thermogravimetric analysis curves.

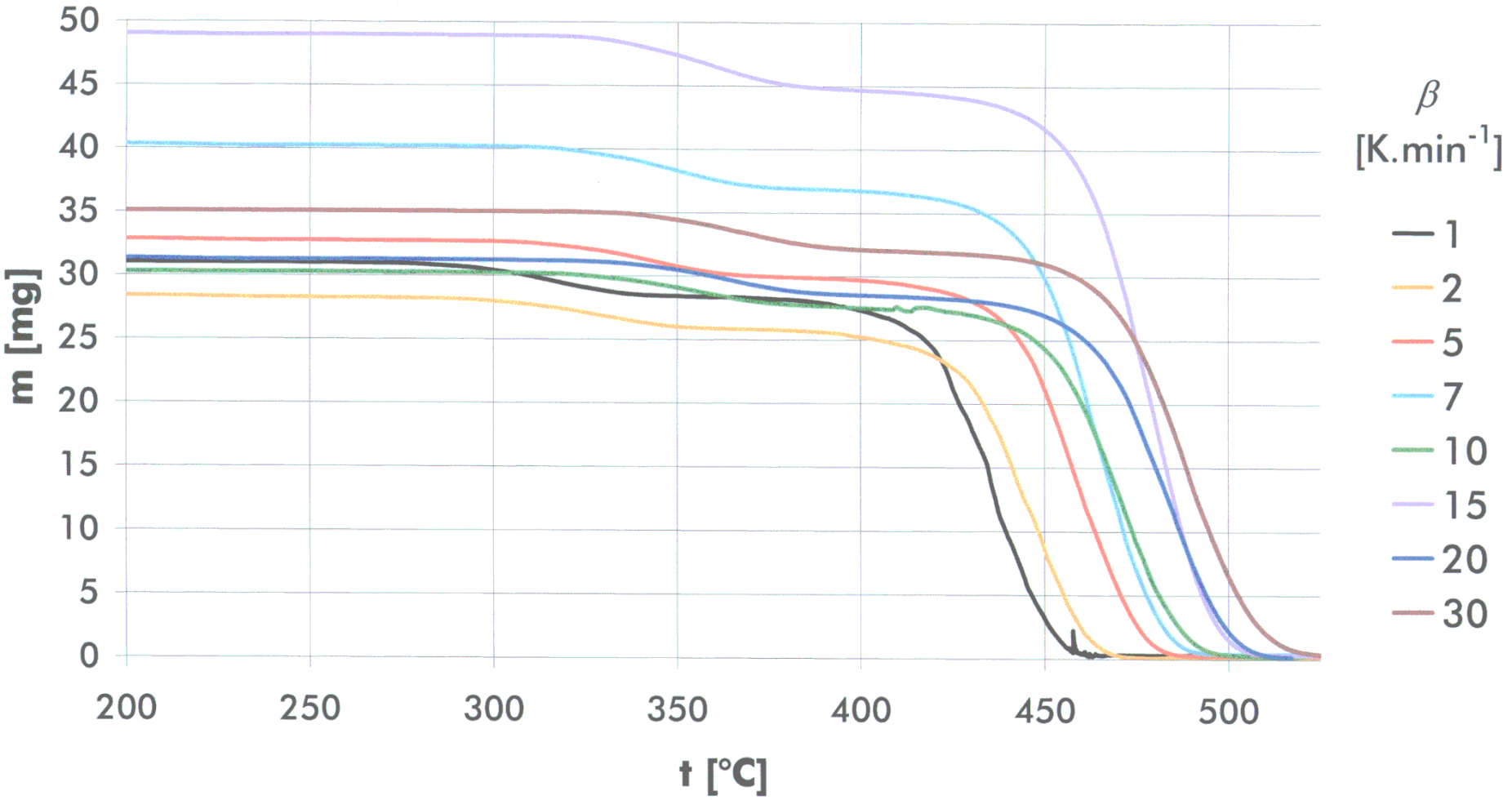

Fig. F-10: EVA "12" α = f(t) curves.

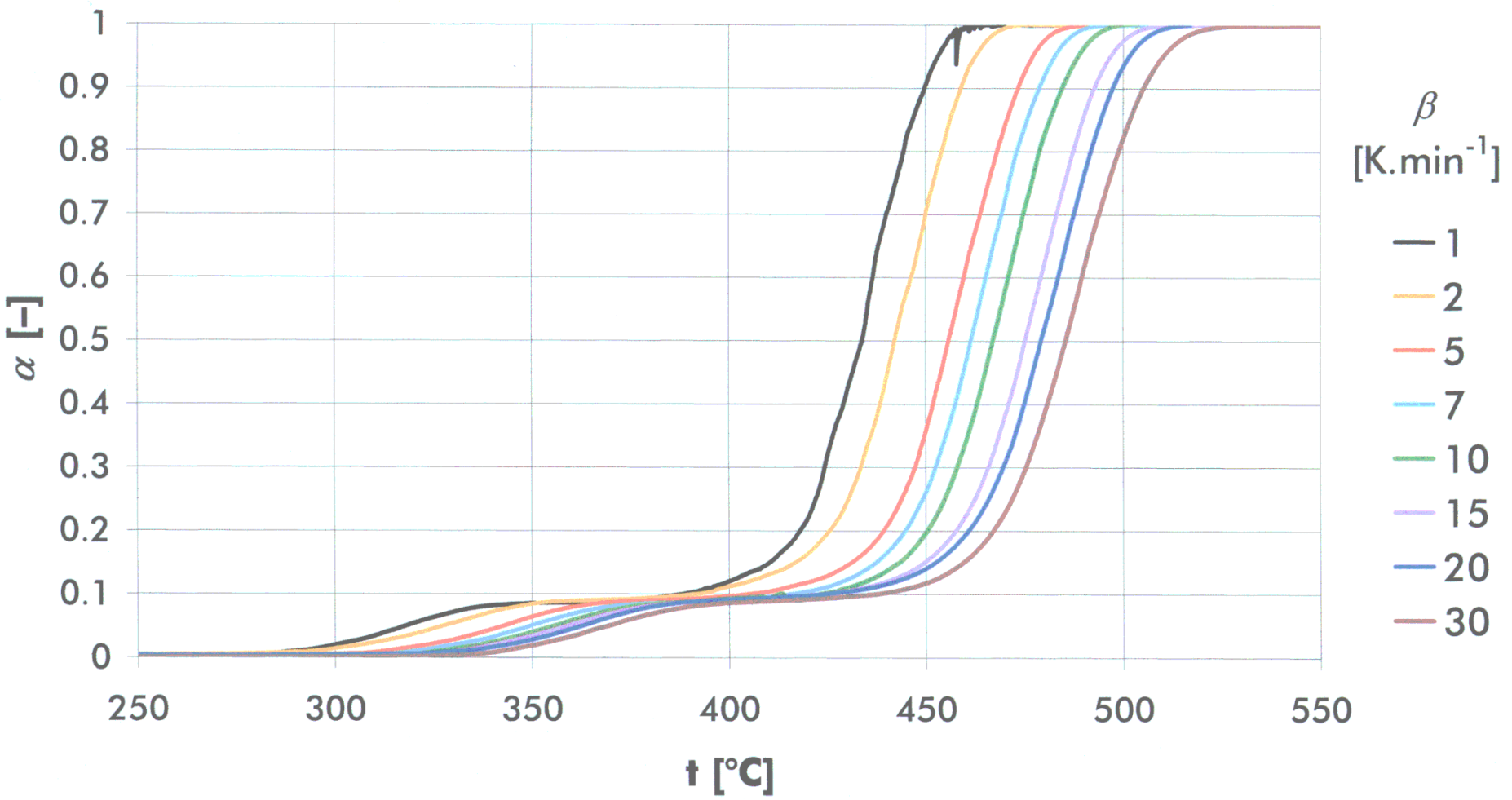

Fig. F-11: EVA "12" t = f(τ) curves.

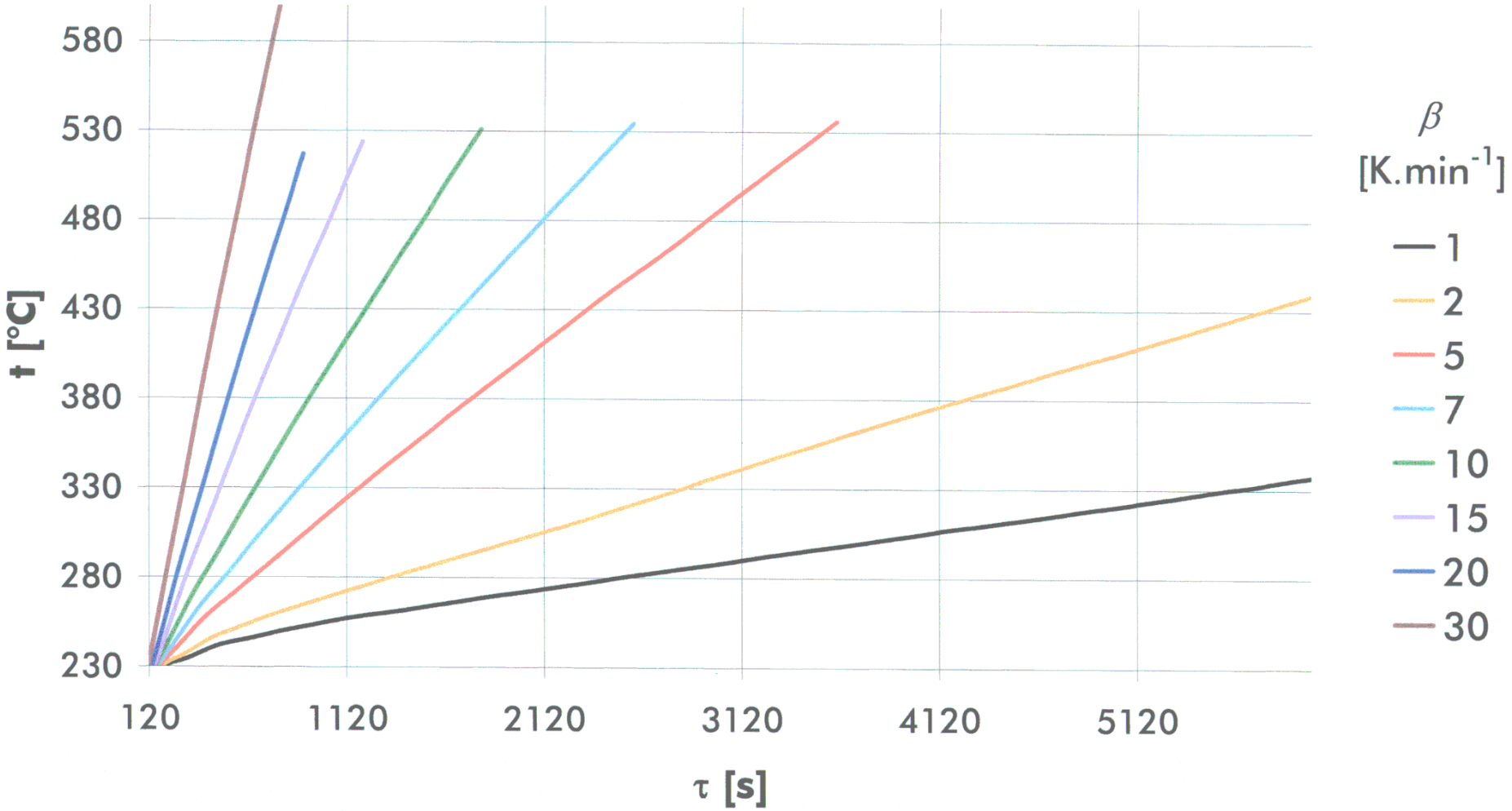

Fig. F-12: EVA "12" α = f(t) selected values.

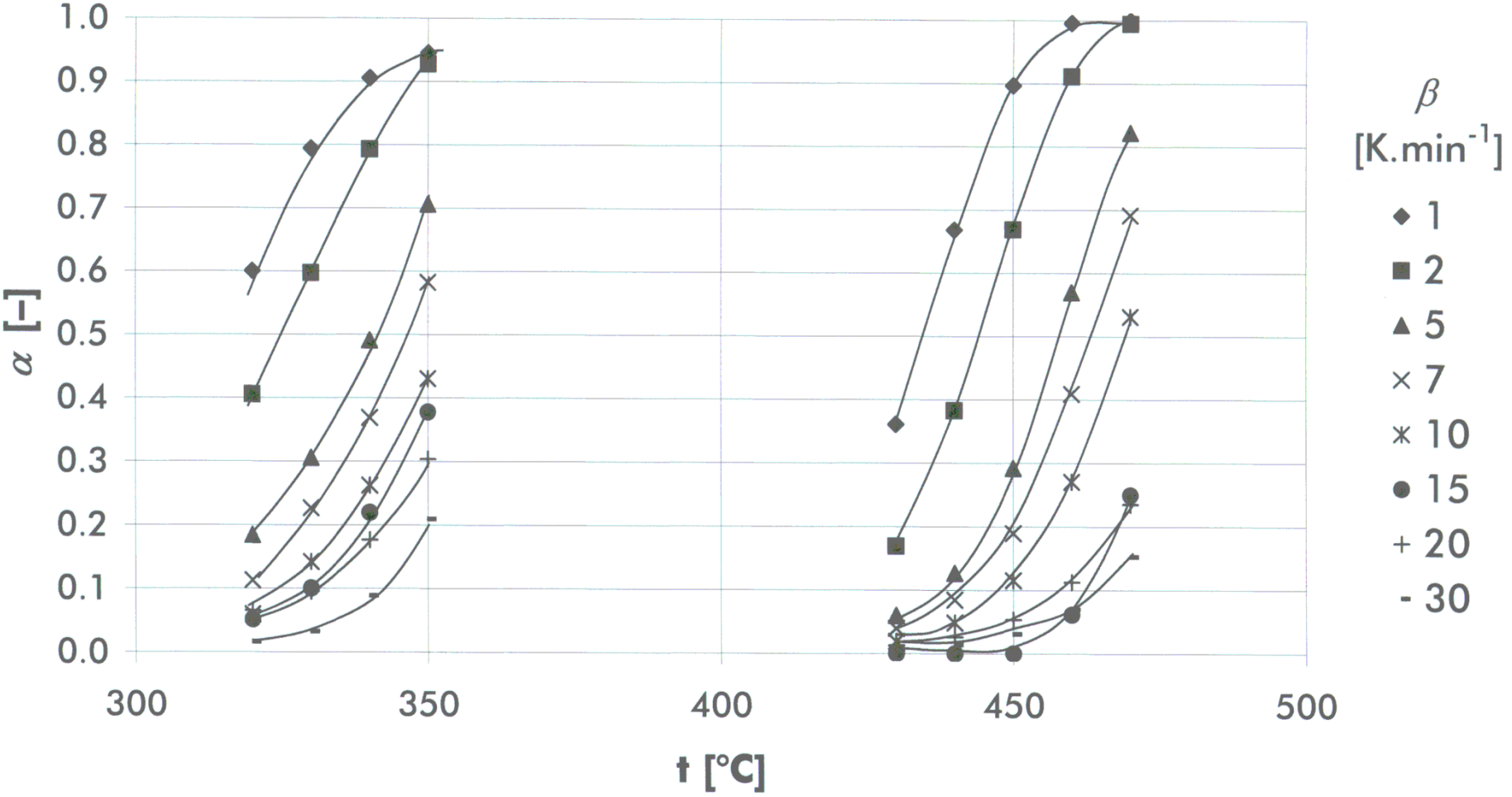

Fig. F-13: EVA "12" F graph – t ∈ <320; 330> [°C].

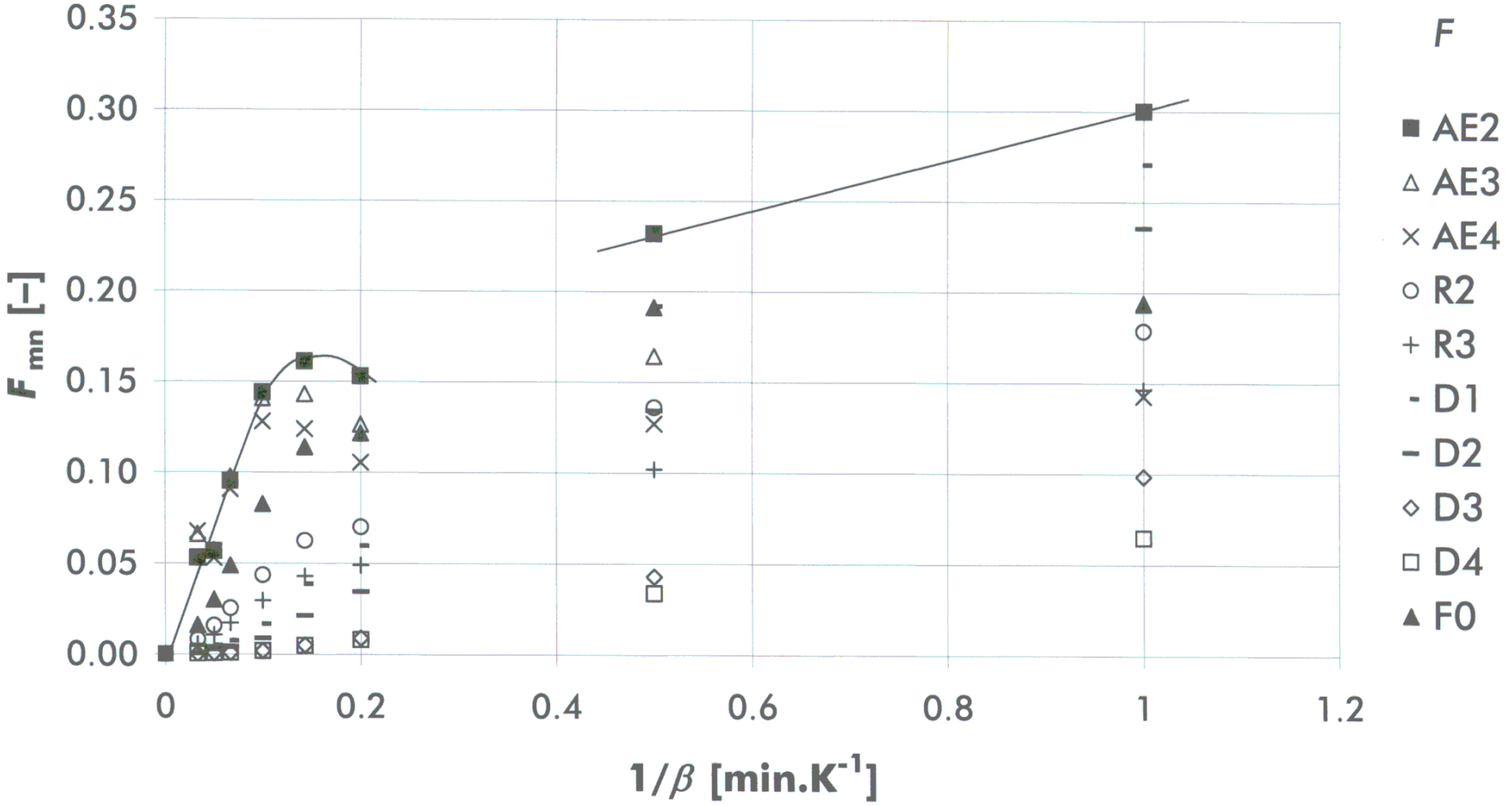

Fig. F-14: EVA "12" F graph – t ∈ <330; 340> [°C].

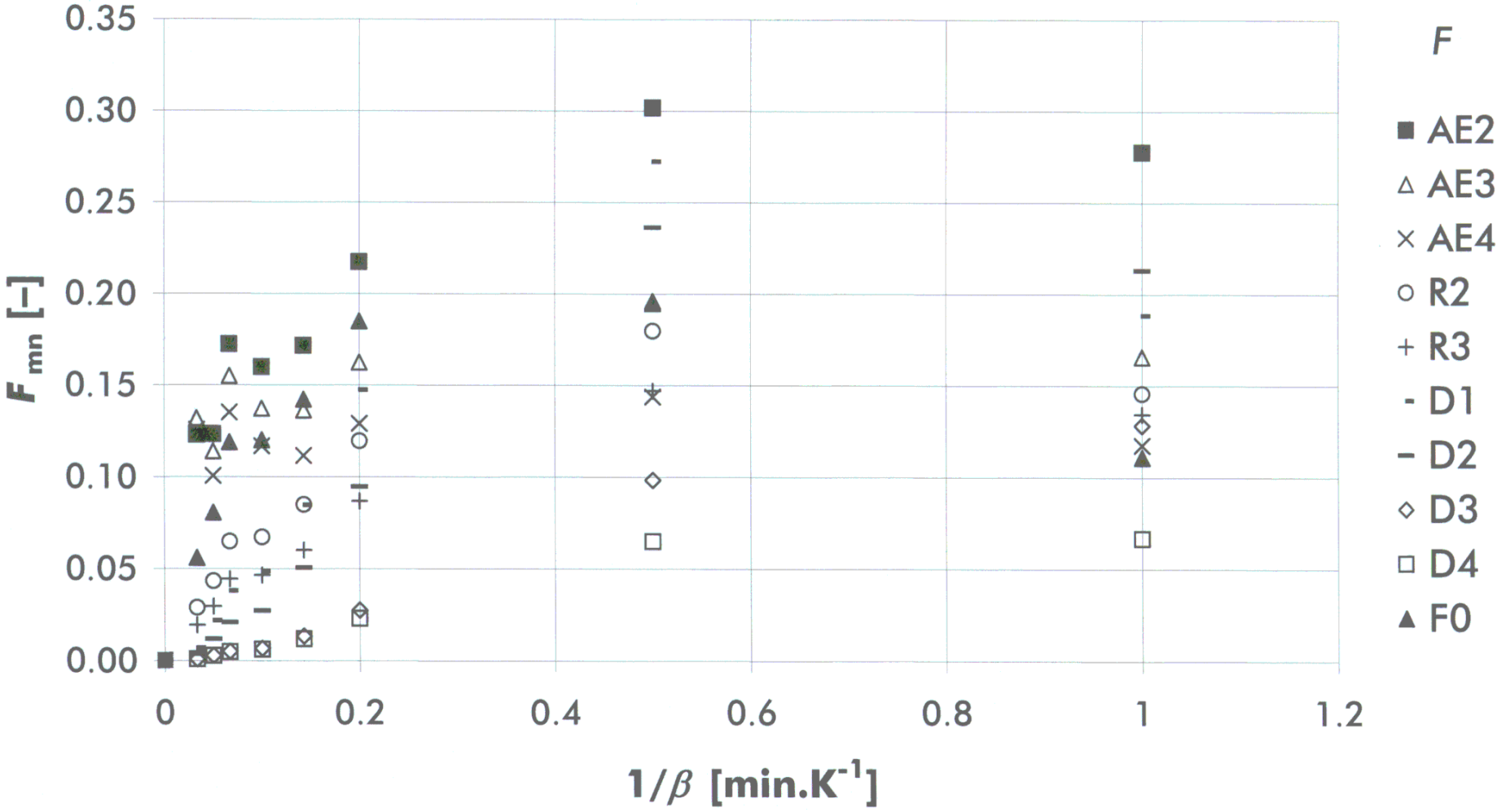

Fig. F-15: EVA "12" F graph – t ∈ <340; 350> [°C].

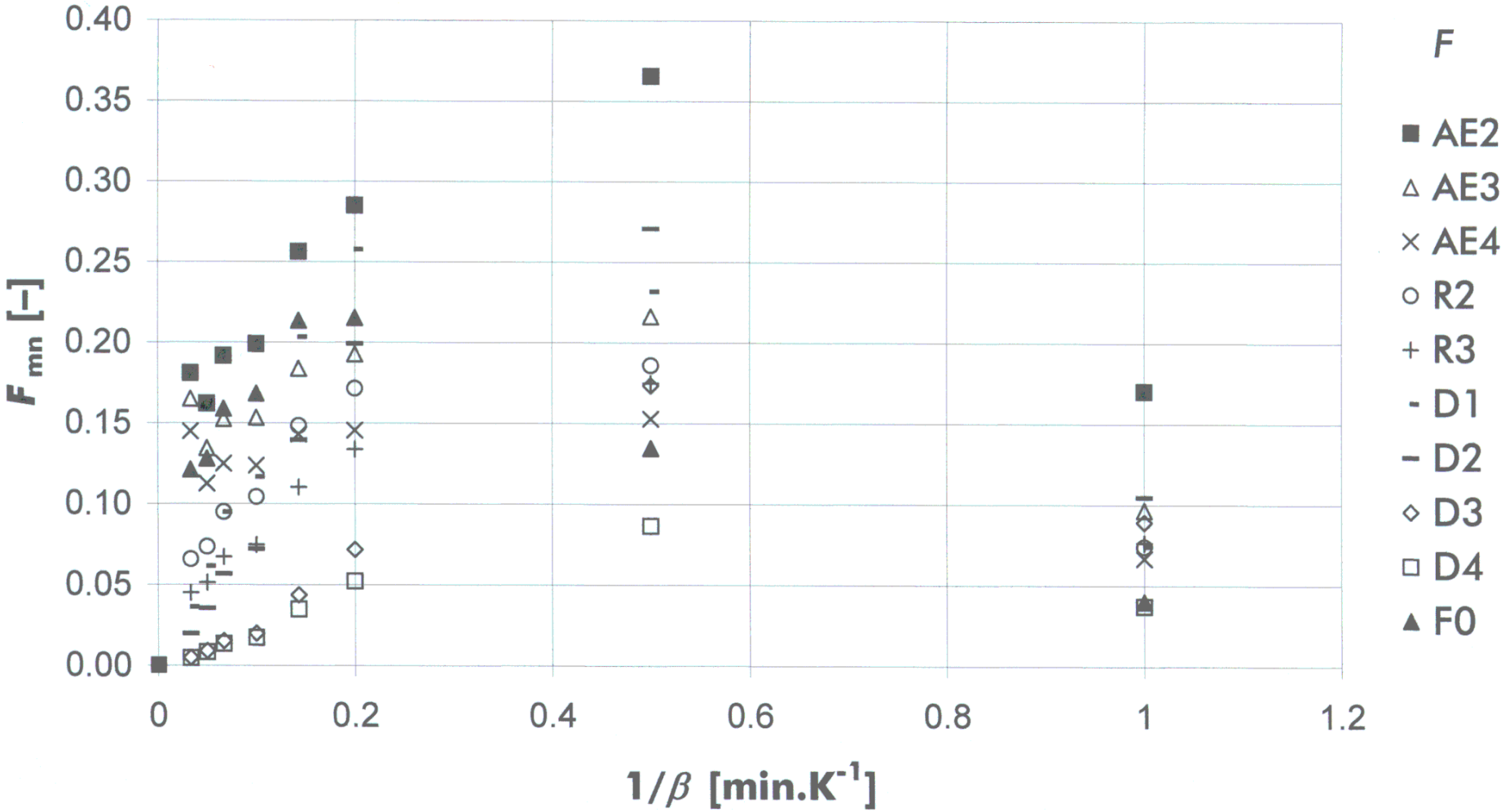

Fig. F-16: EVA "12" F graph – t ∈ <430; 440> [°C].

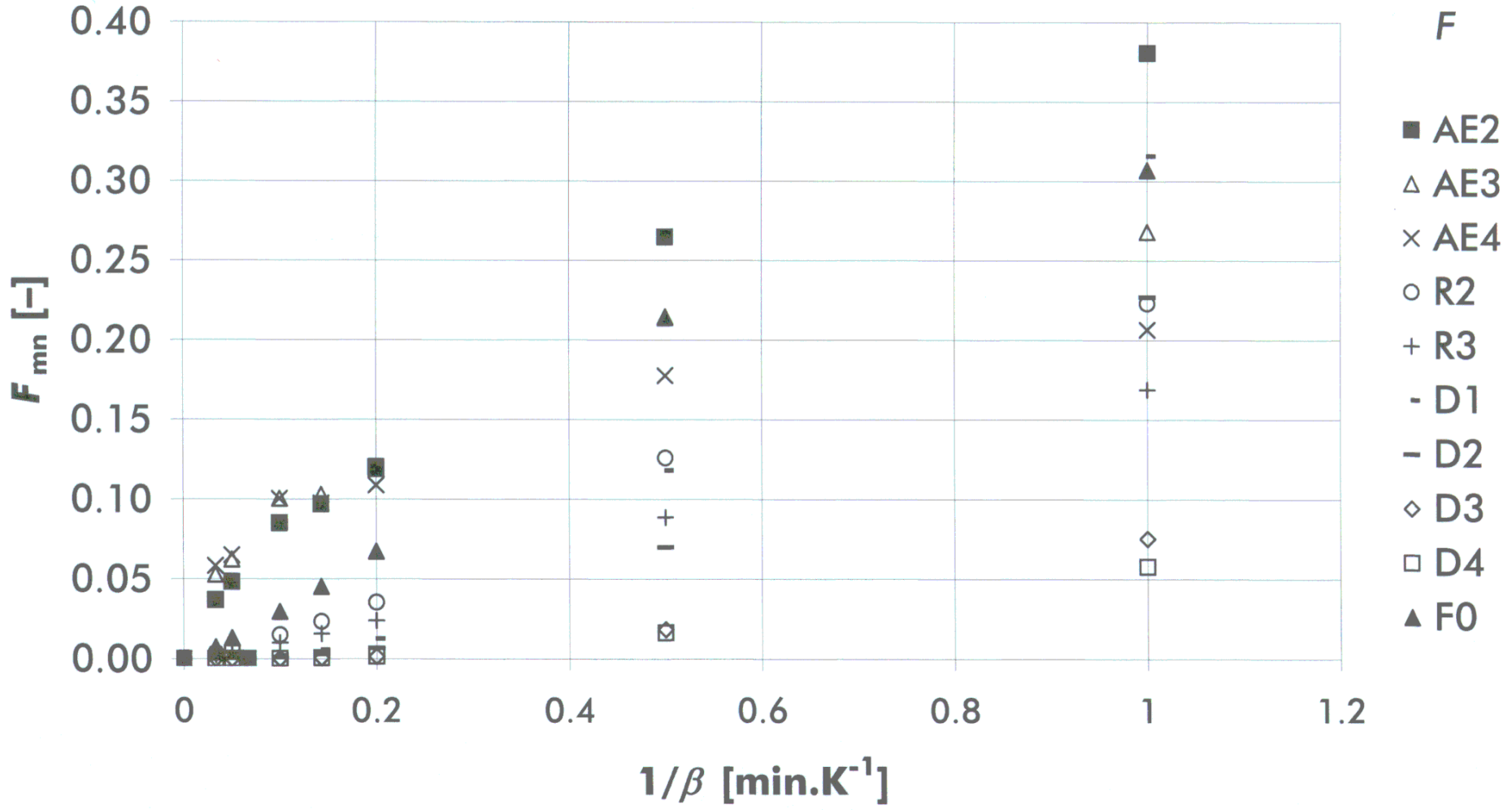

Fig. F-17: EVA "12" F graph – t ∈ <440; 450> [°C].

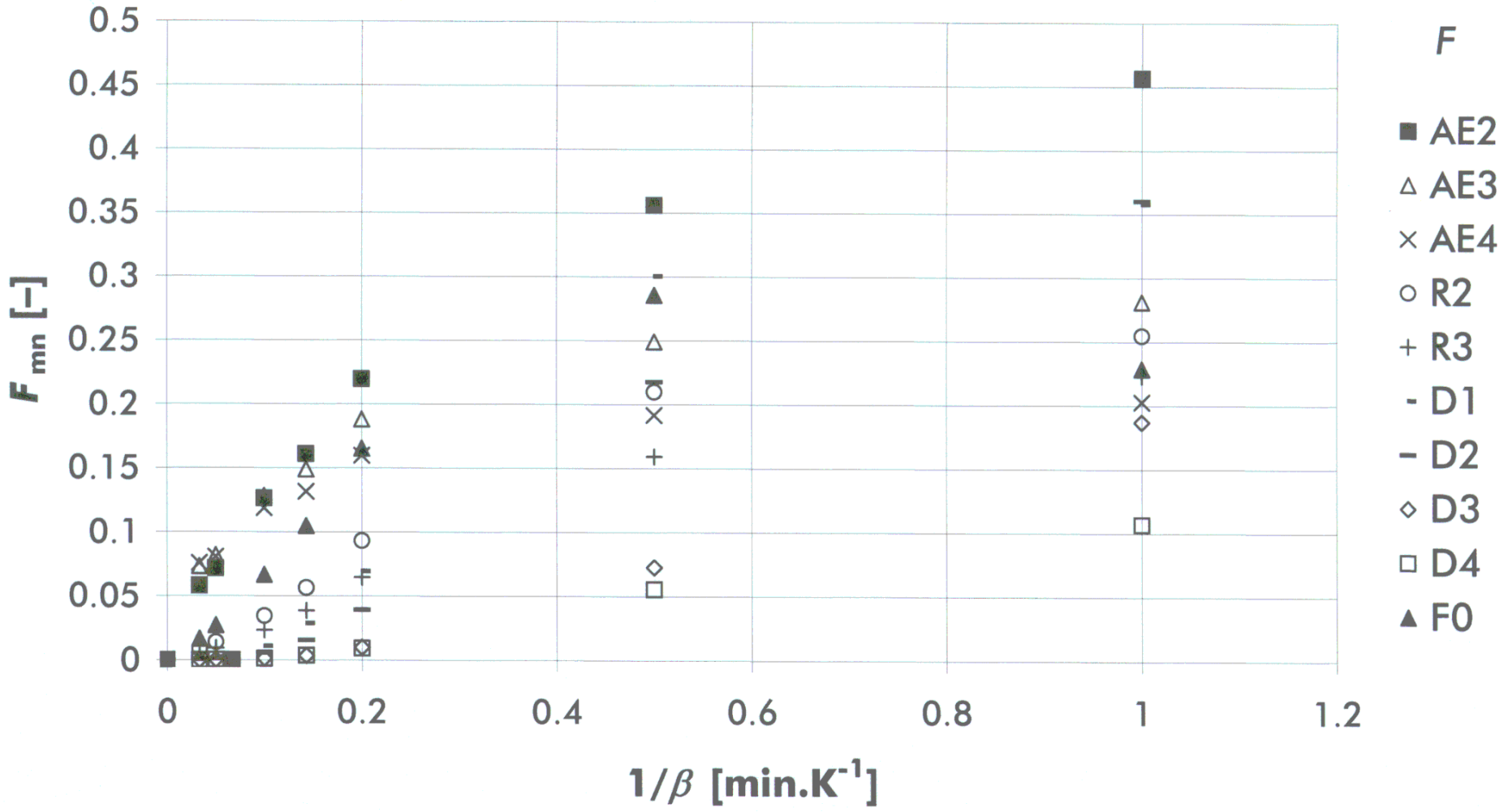

Fig. F-18: EVA "12" F graph – t ∈ <450; 460> [°C].

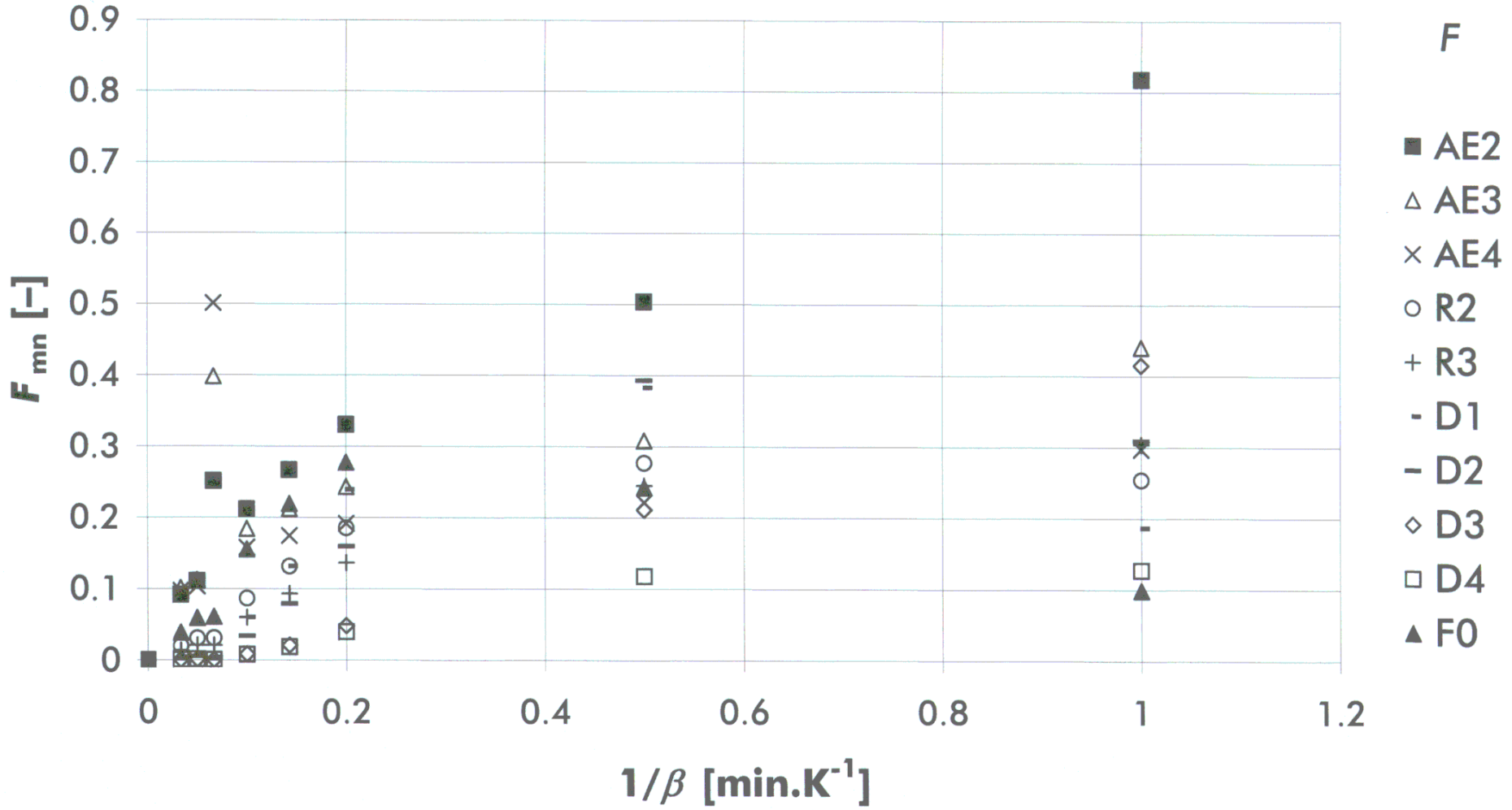

Fig. F-19: EVA "12" F graph – t ∈ <460; 470> [°C].

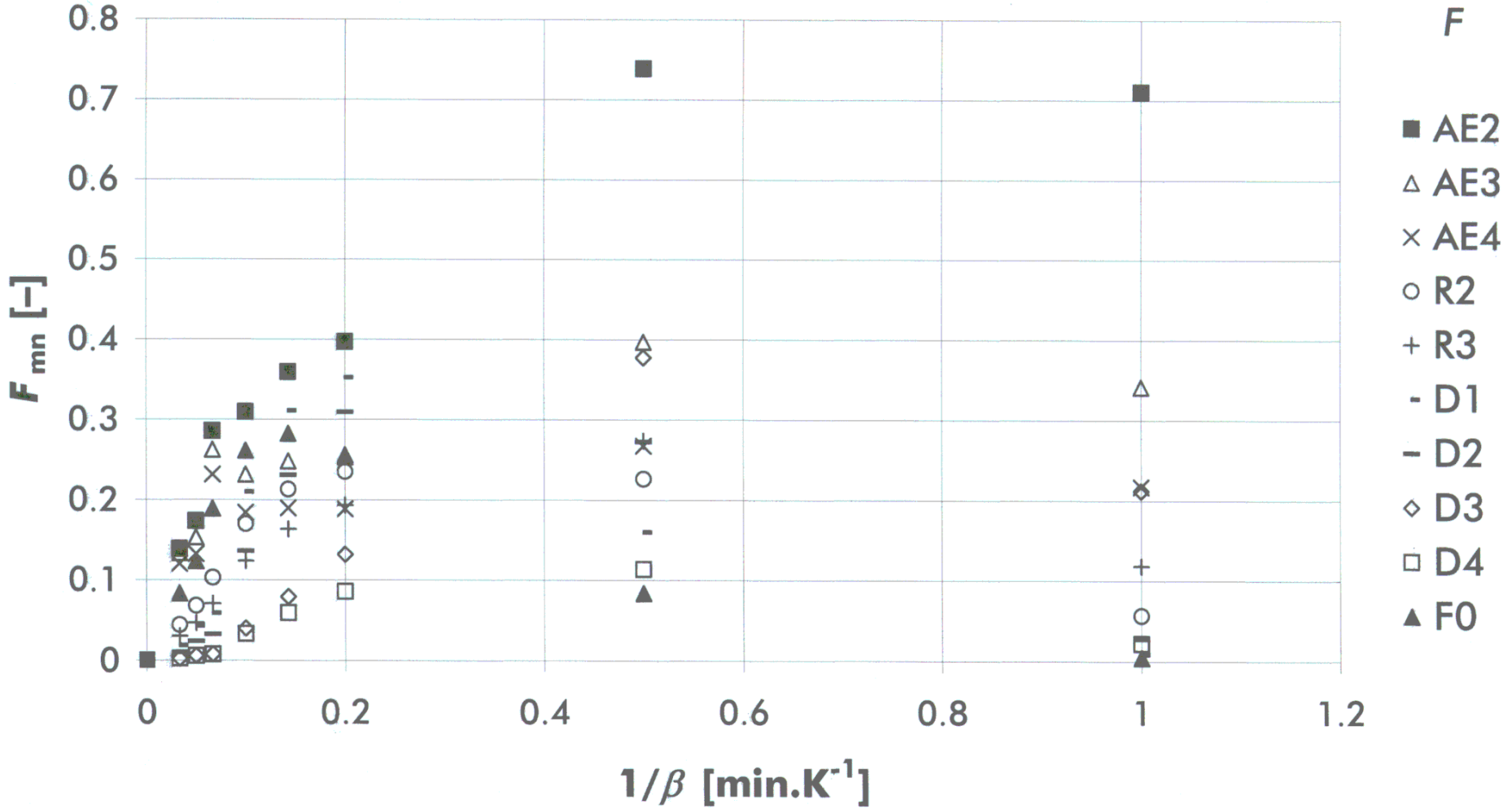

Fig. F-20: EVA "25" thermogravimetric analysis curves.

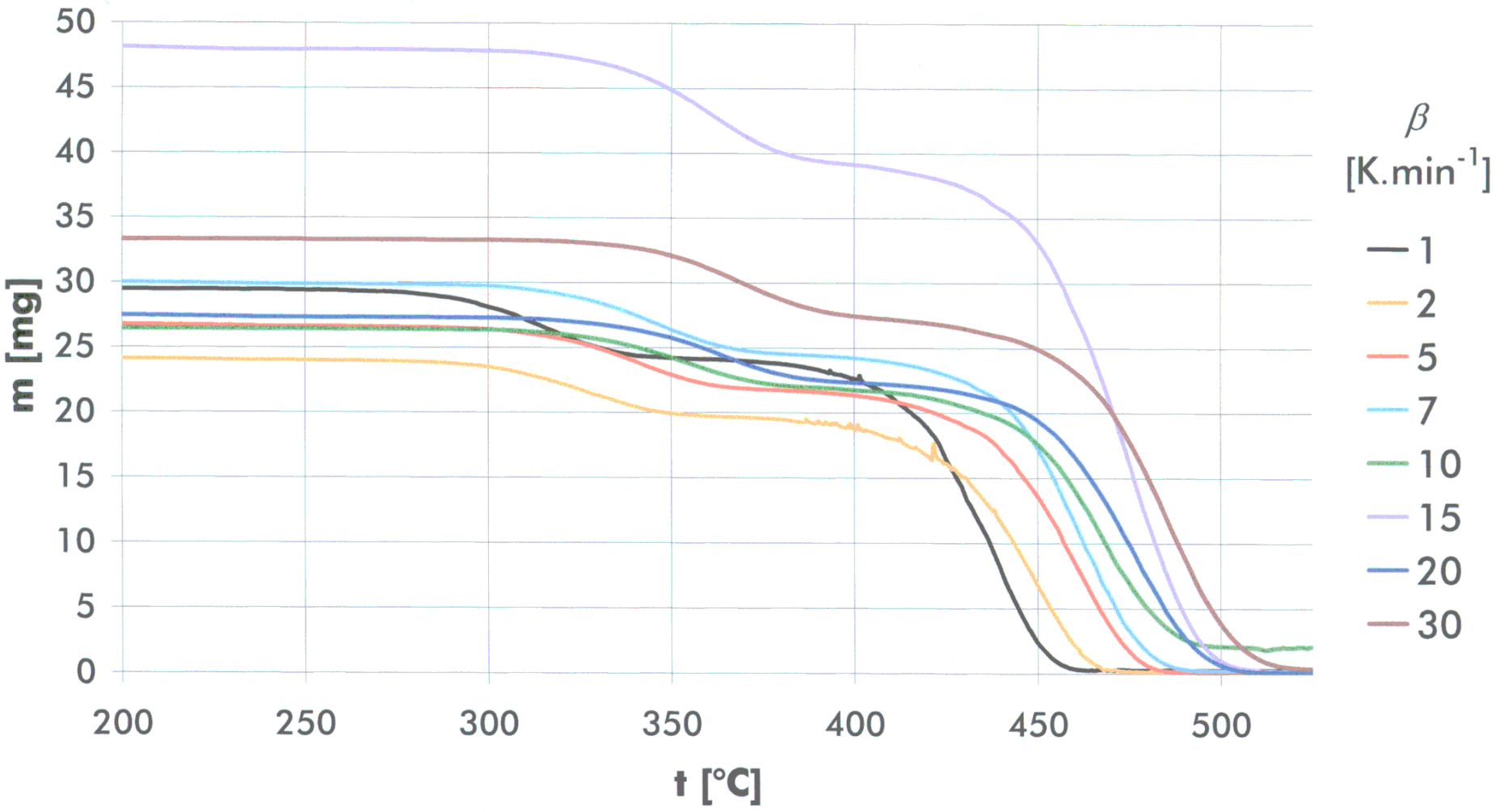

Fig. F-21: EVA "25" α = f(t) curves.

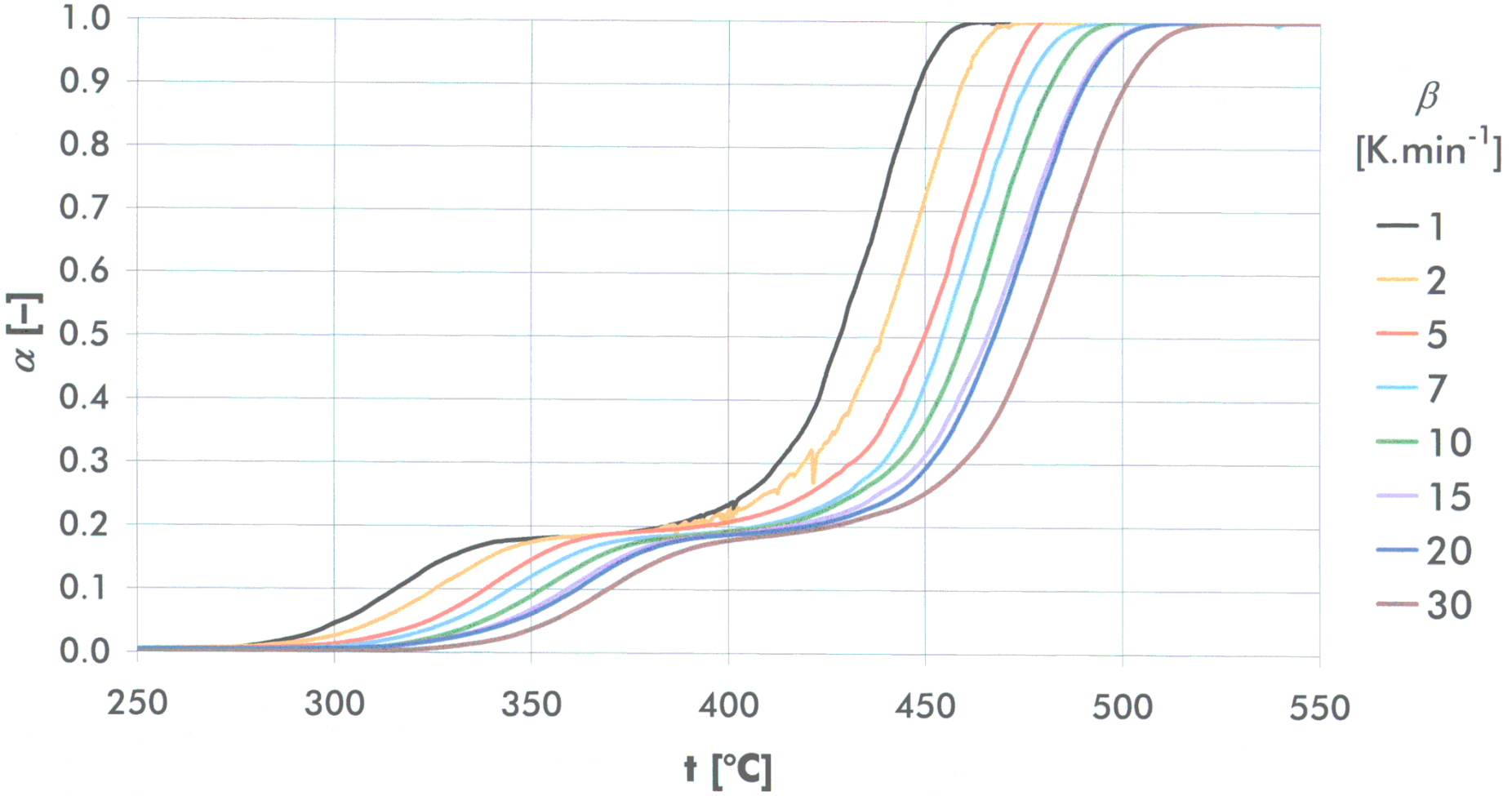

Fig. F-22: EVA "25" t = f(τ) curves.

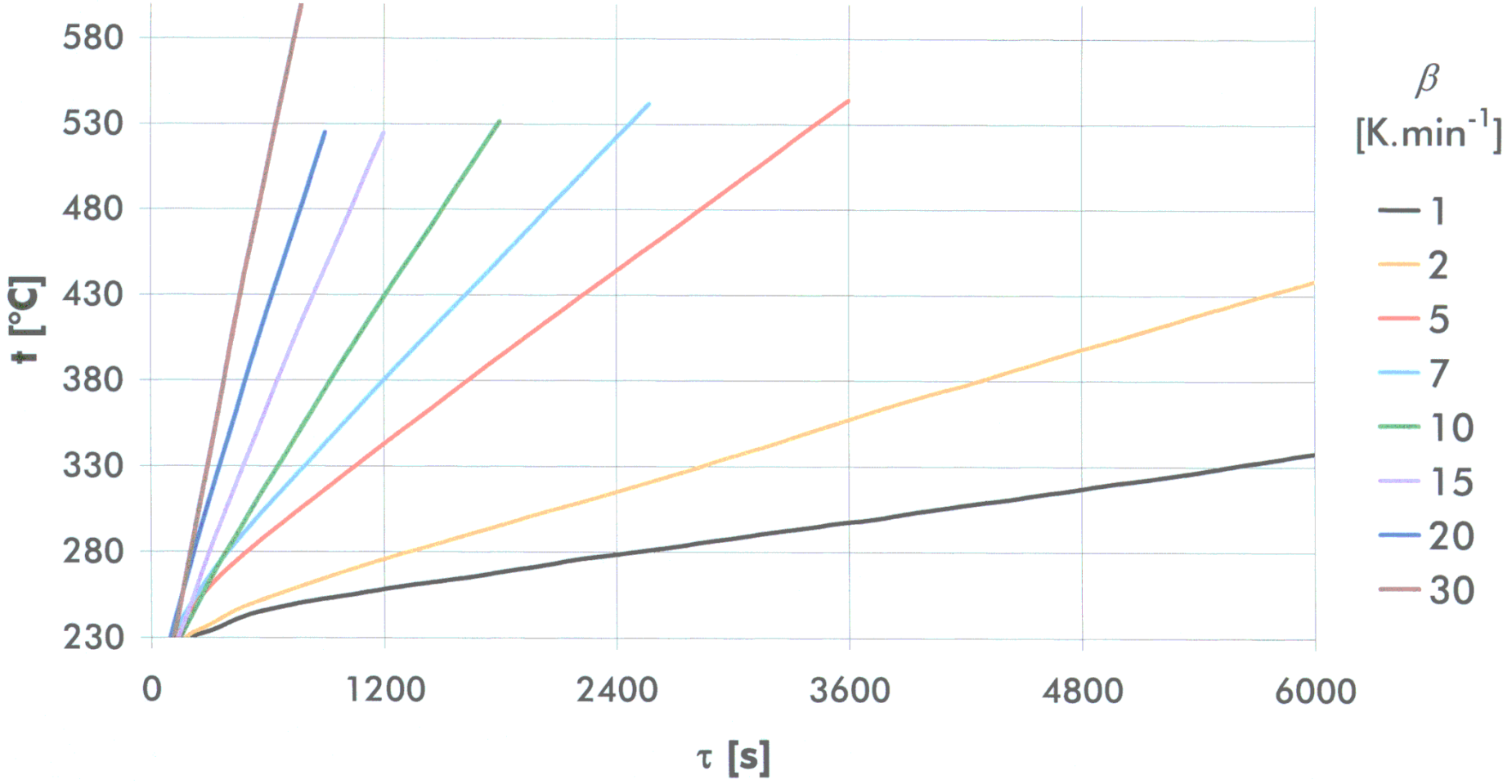

Fig. F-23: EVA "25" α = f(t) selected values.

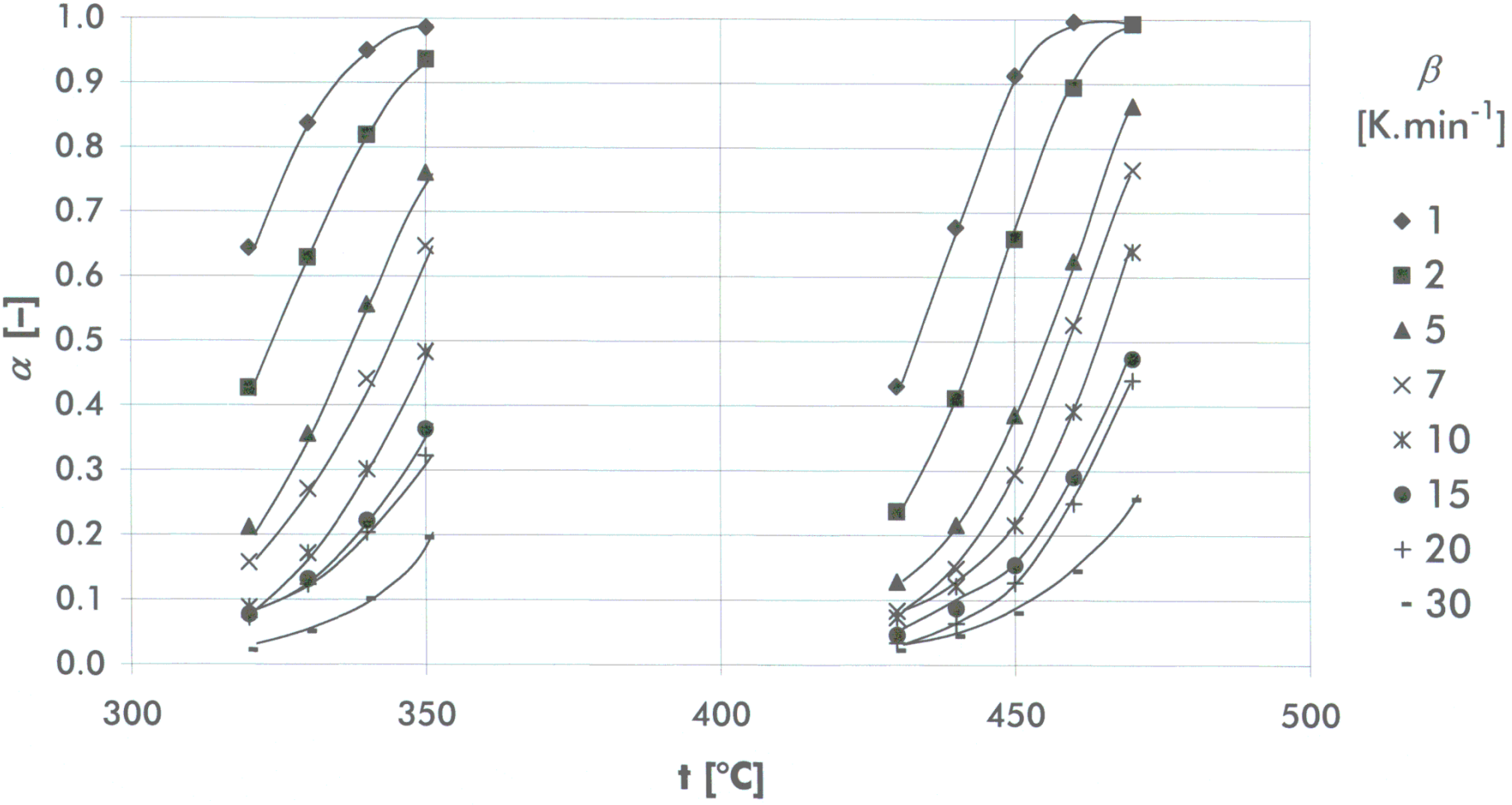

Fig. F-24: EVA "25" F graph – t ∈ <320; 330> [°C].

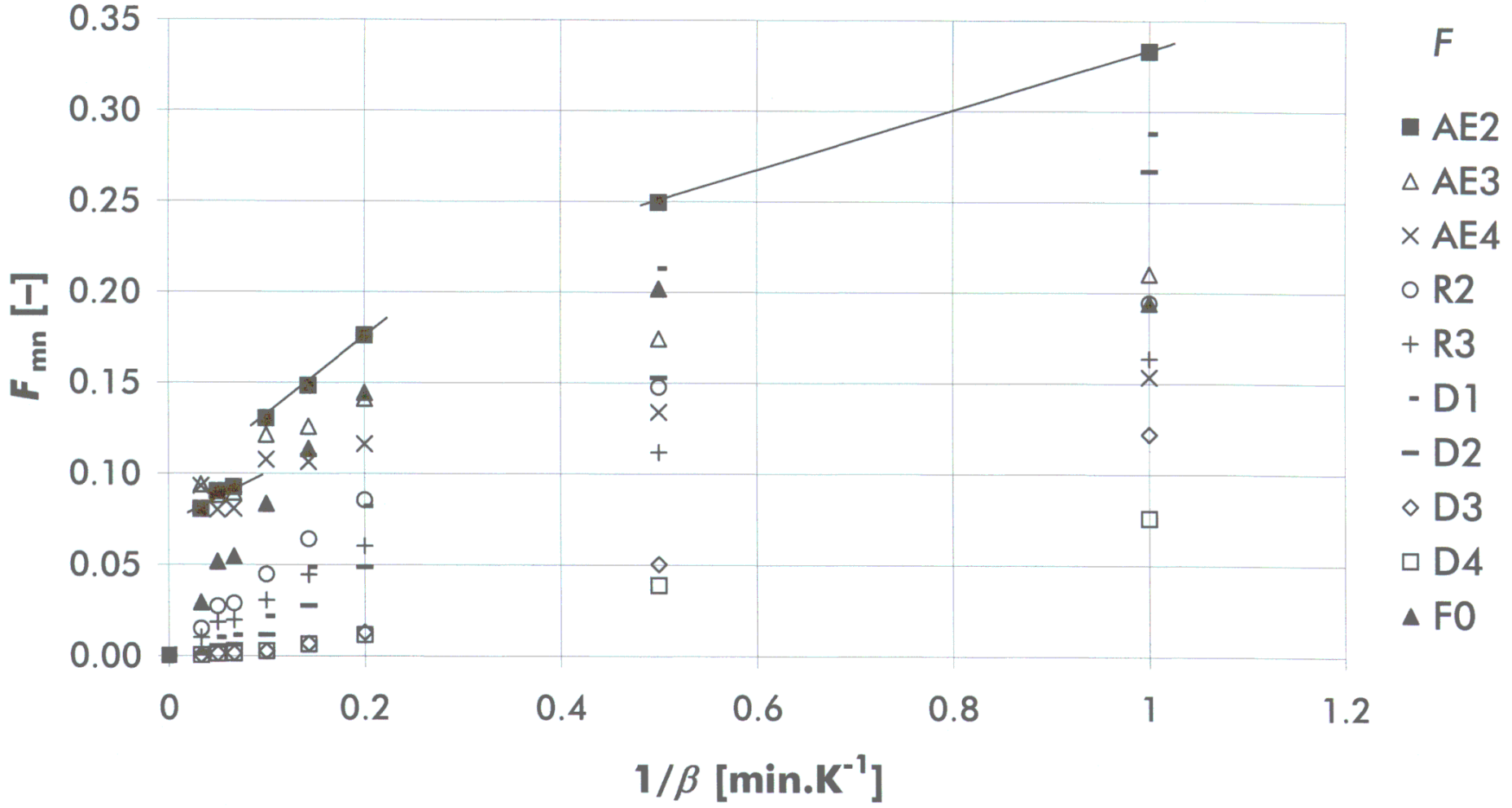

Fig. F-25: EVA "25" F graph – t ∈ <330; 340> [°C].

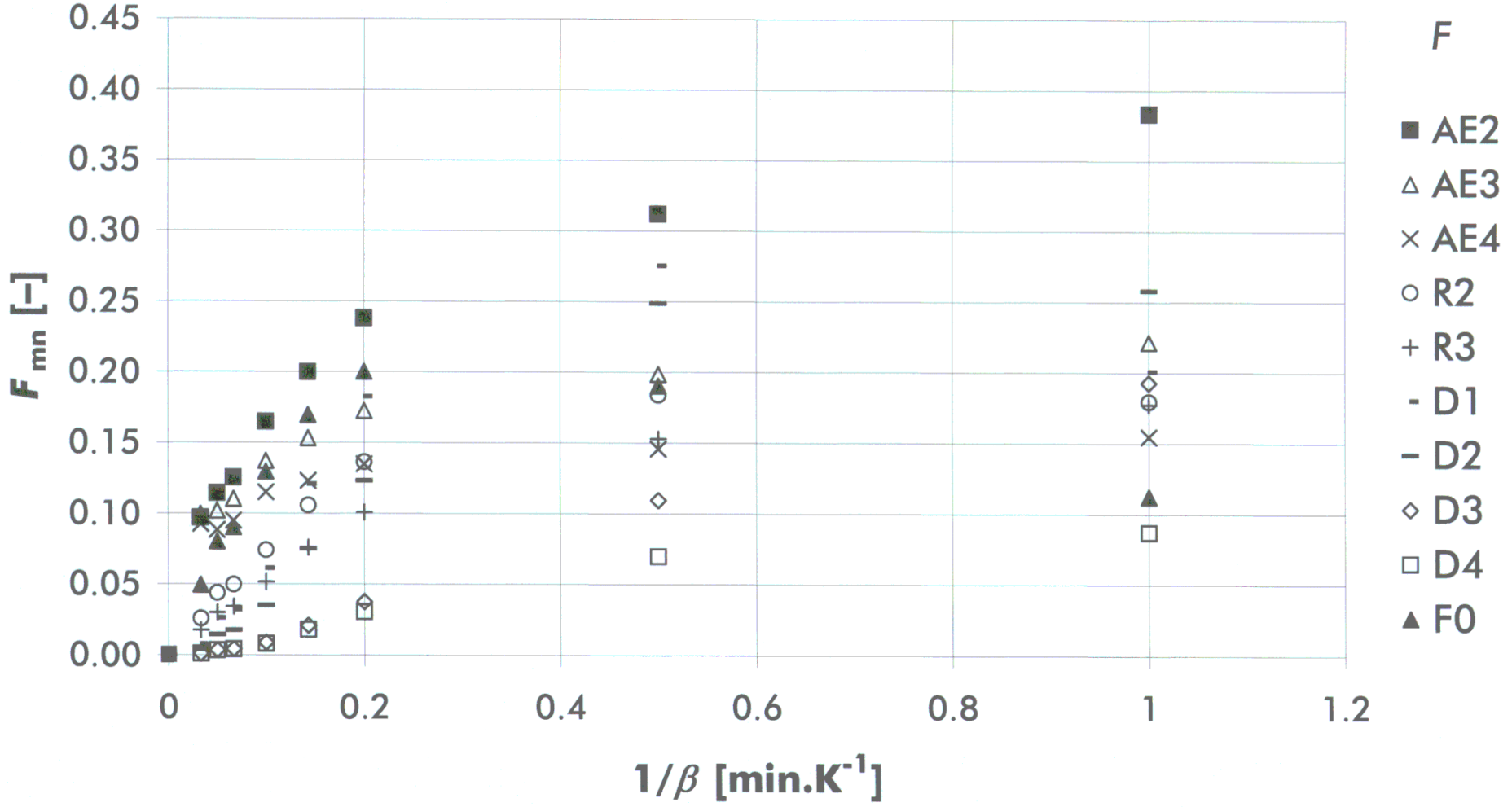

Fig. F-26: EVA "25" F graph – t ∈ <340; 350> [°C].

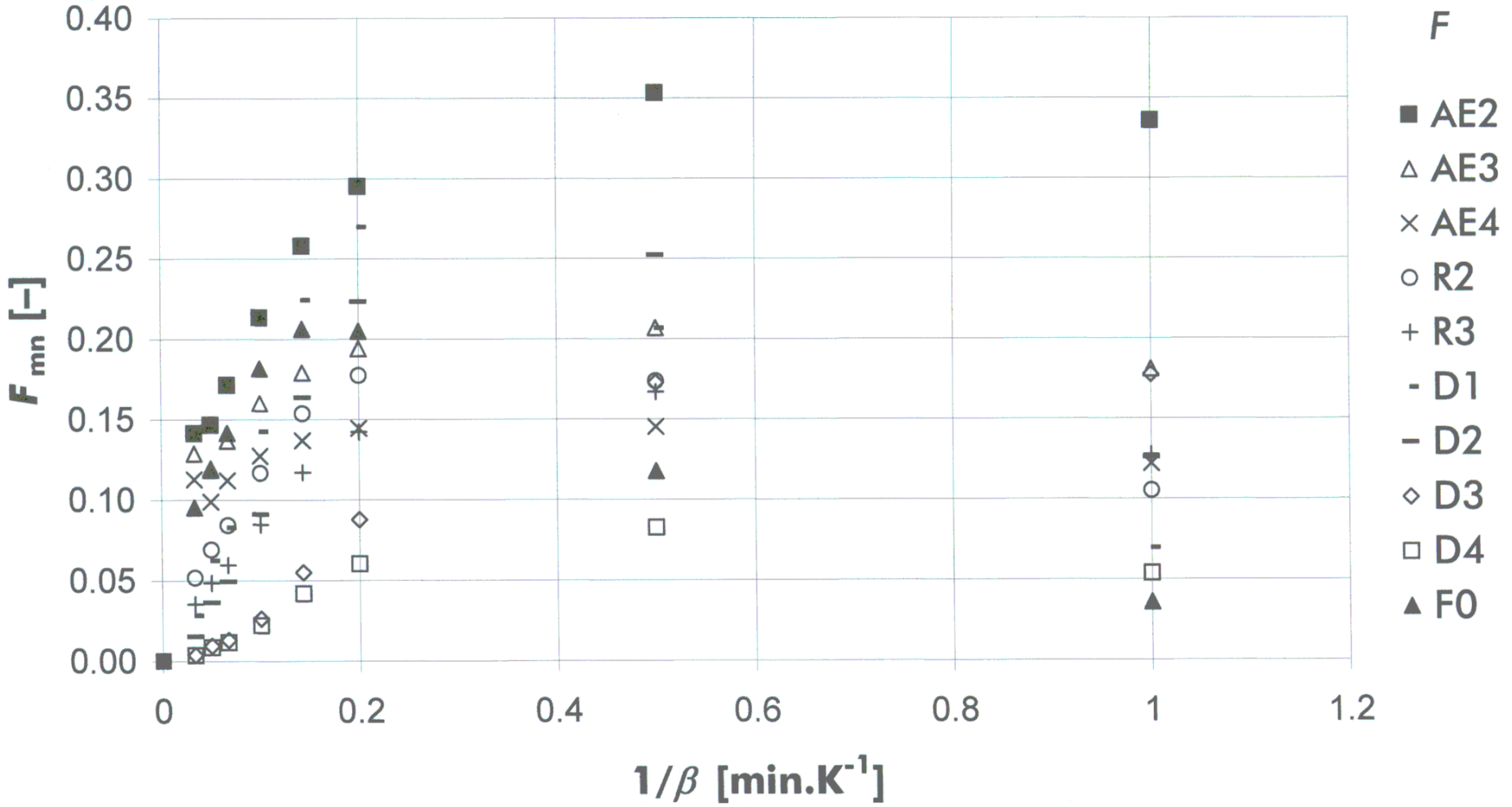

Fig. F-27: EVA "25" F graph – t ∈ <430; 440> [°C].

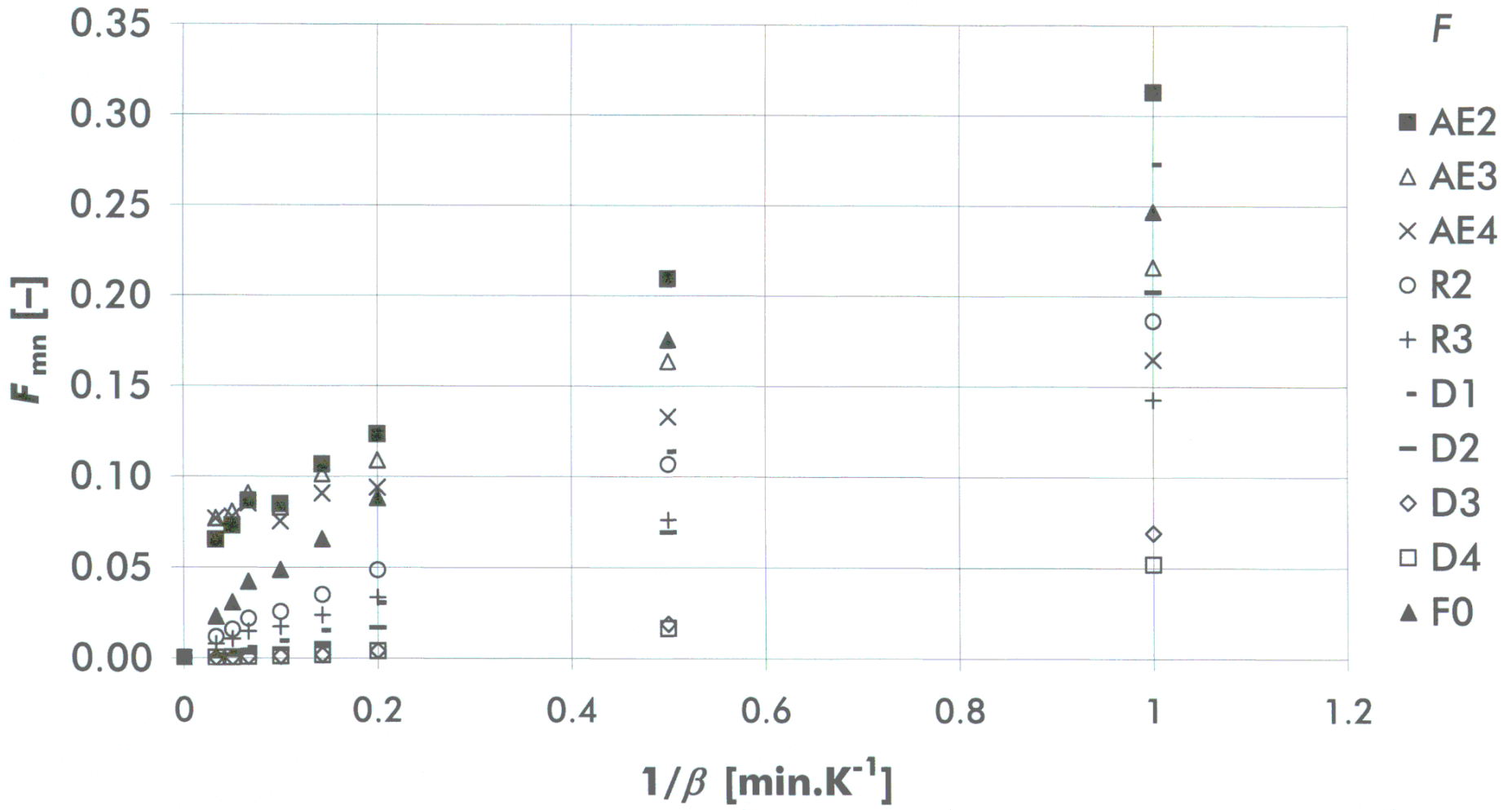

Fig. F-28: EVA "25" F graph – t ∈ <440; 450> [°C].

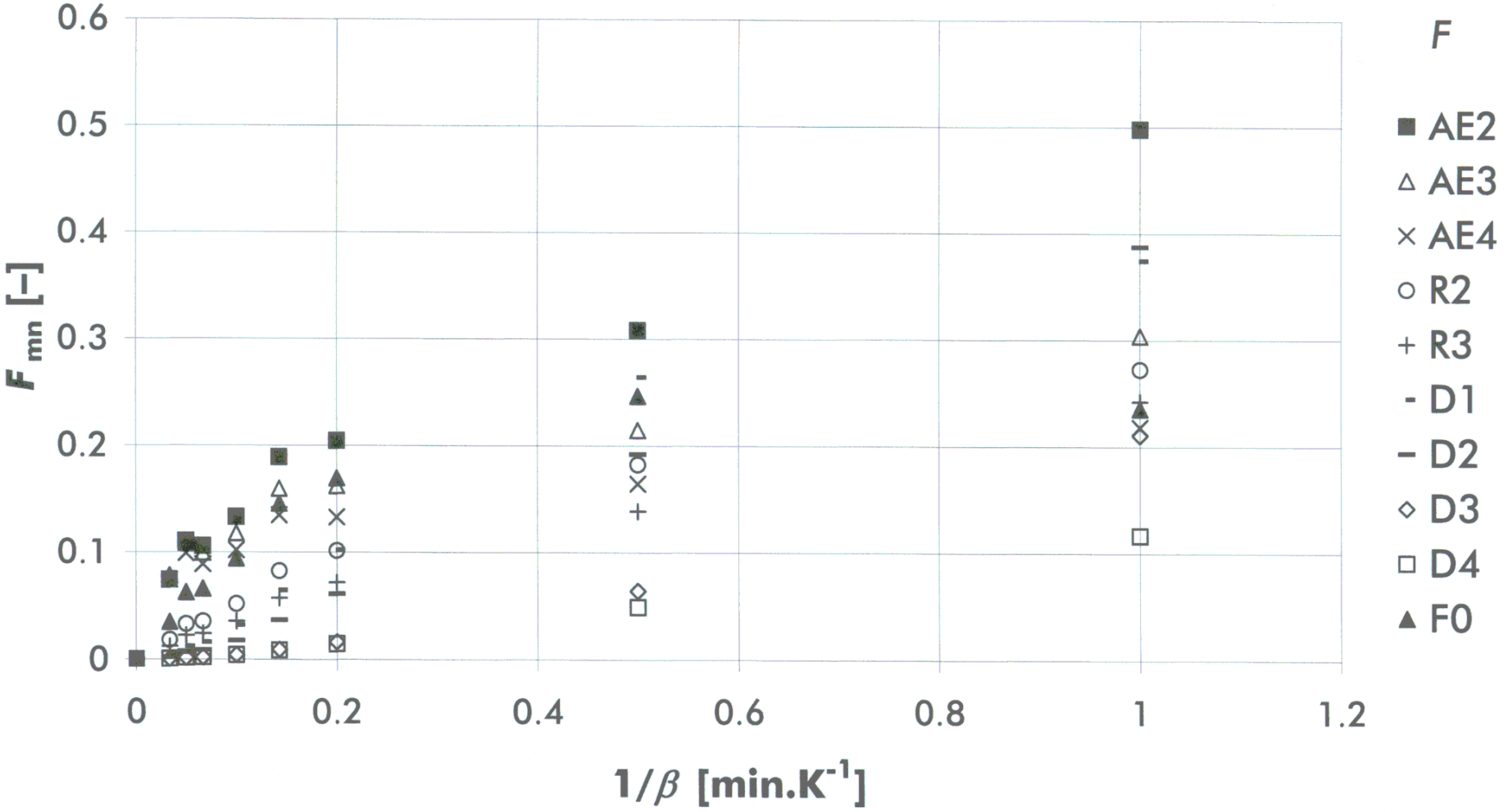

Fig. F-29: EVA "25" F graph – t ∈ <450; 460> [°C].

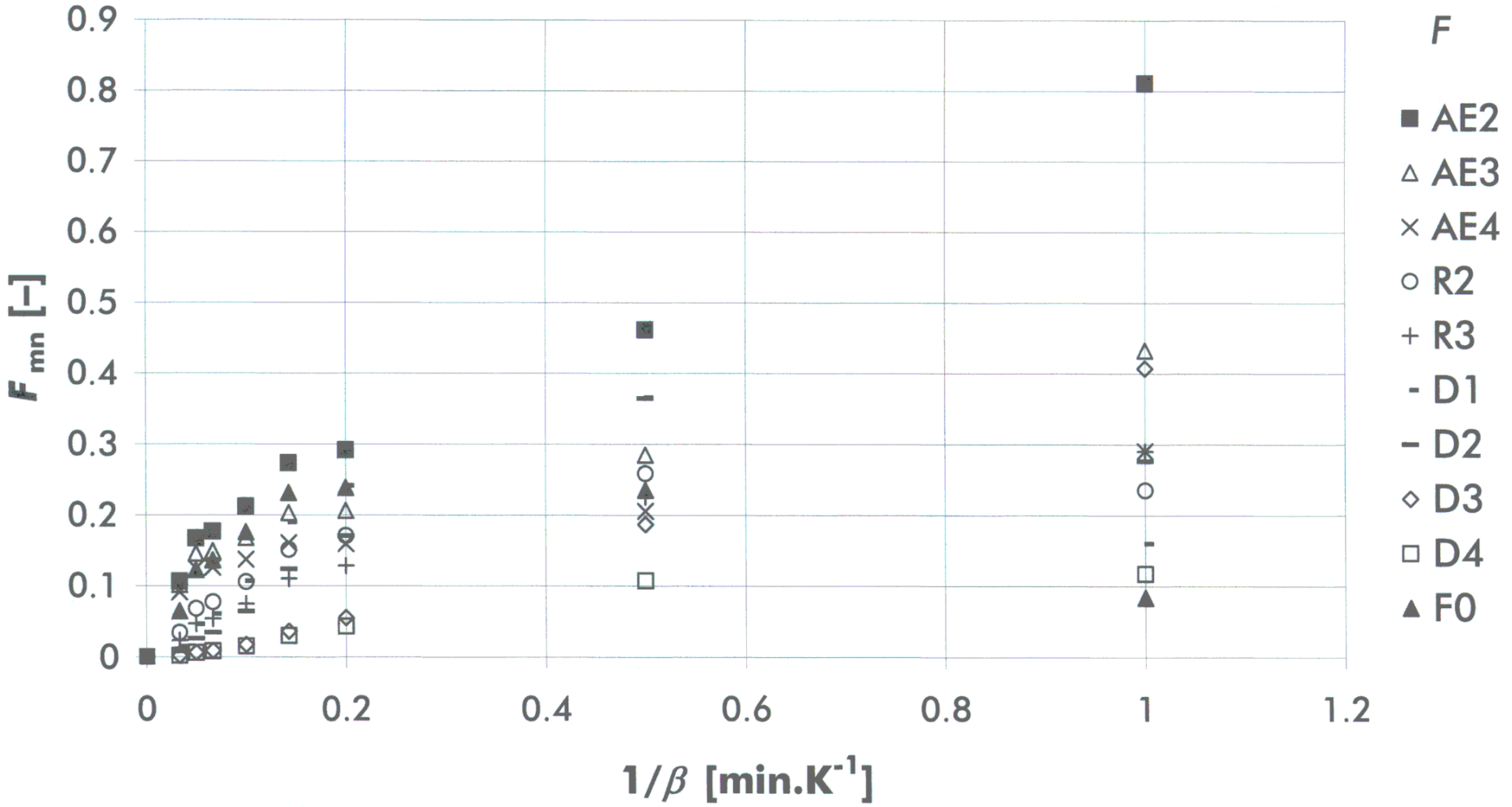

Fig. F-30: EVA "25" F graph – t ∈ <460; 470> [°C].

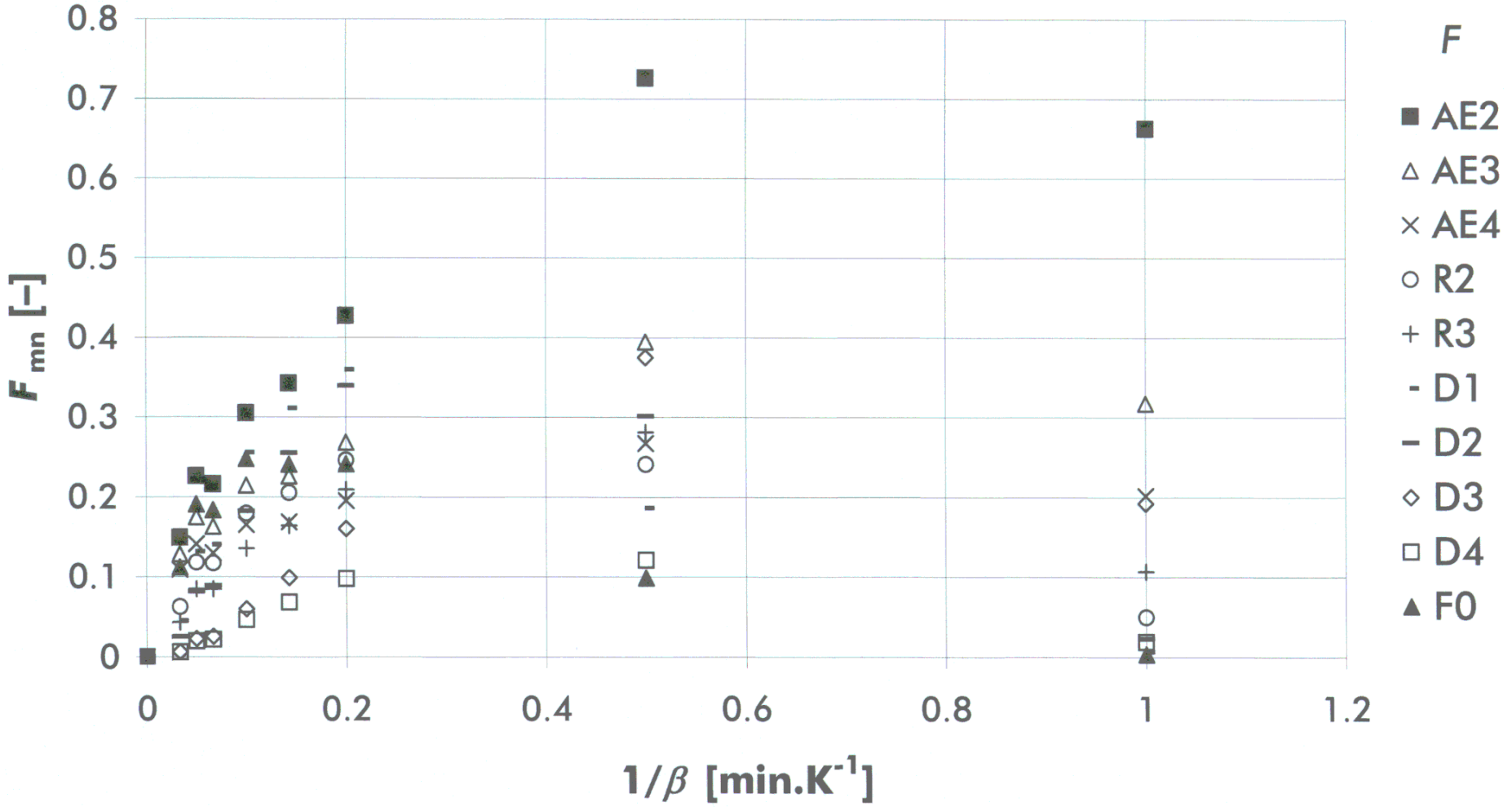

Fig. F-31: VA percentage influence on EVA TGA.

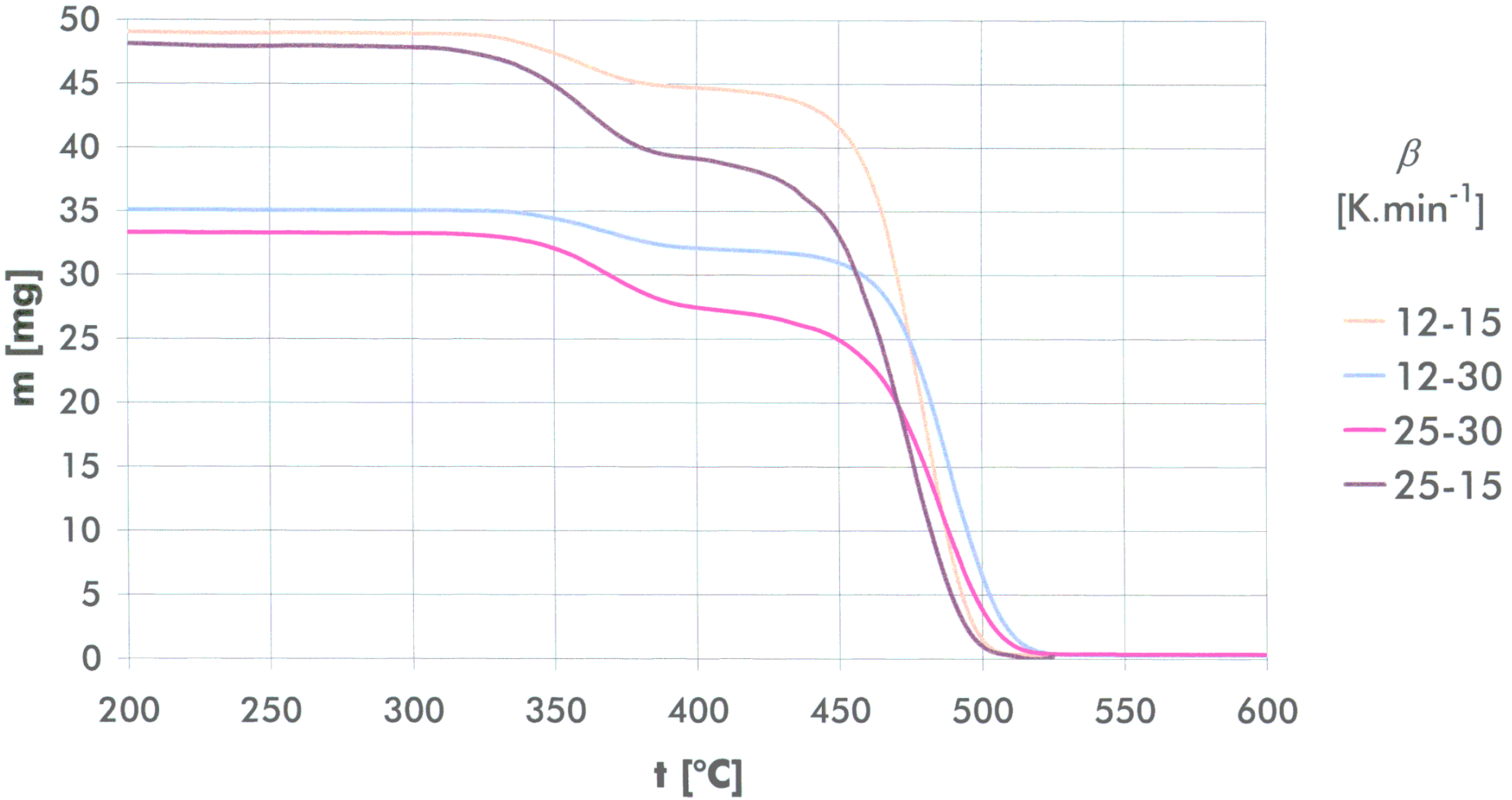

Fig. F-32: m = f(t) chart for PS with $\beta \in$ <1; 20> K.min^{-1}.

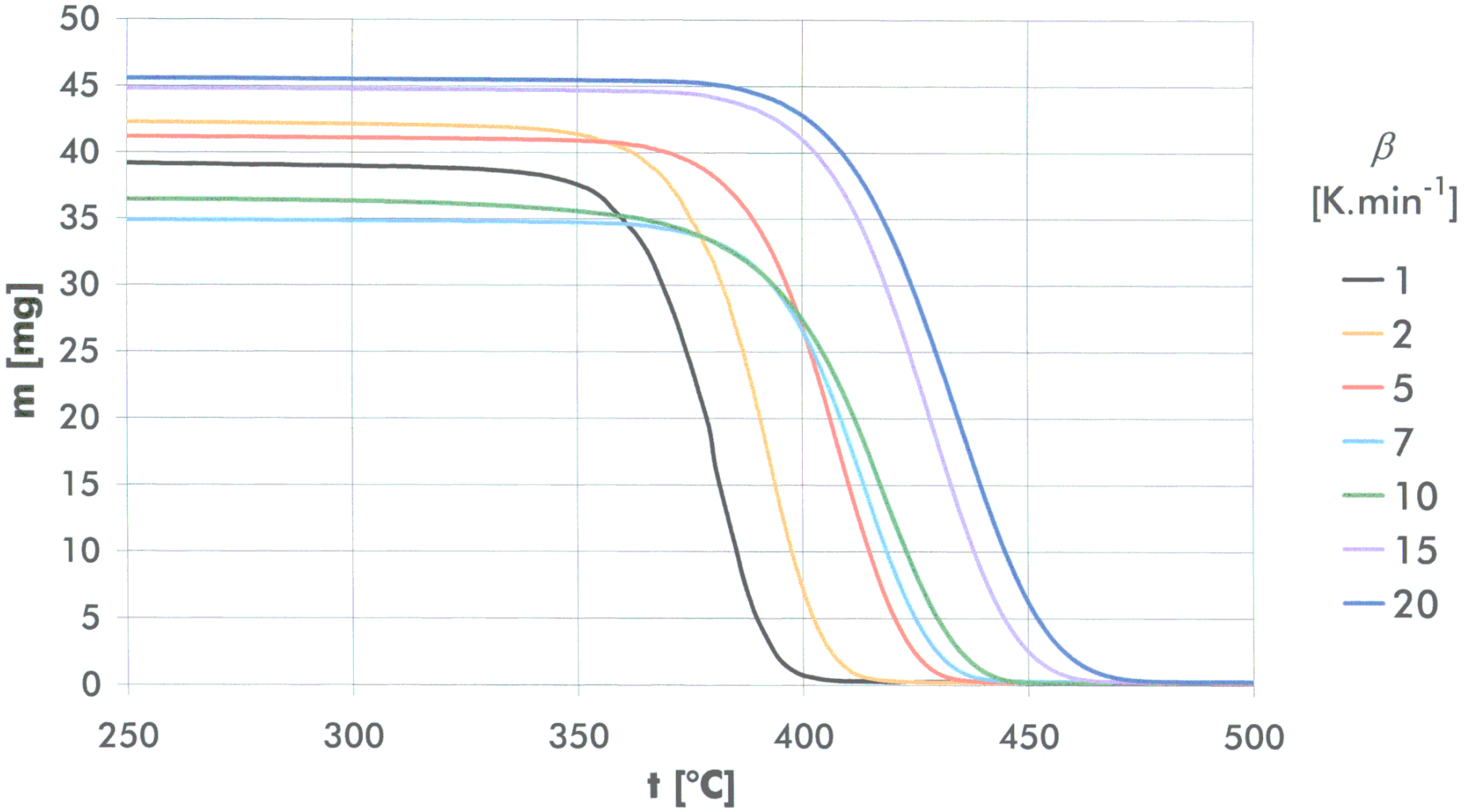

Fig. F-33: TG phenomenon exemplification.

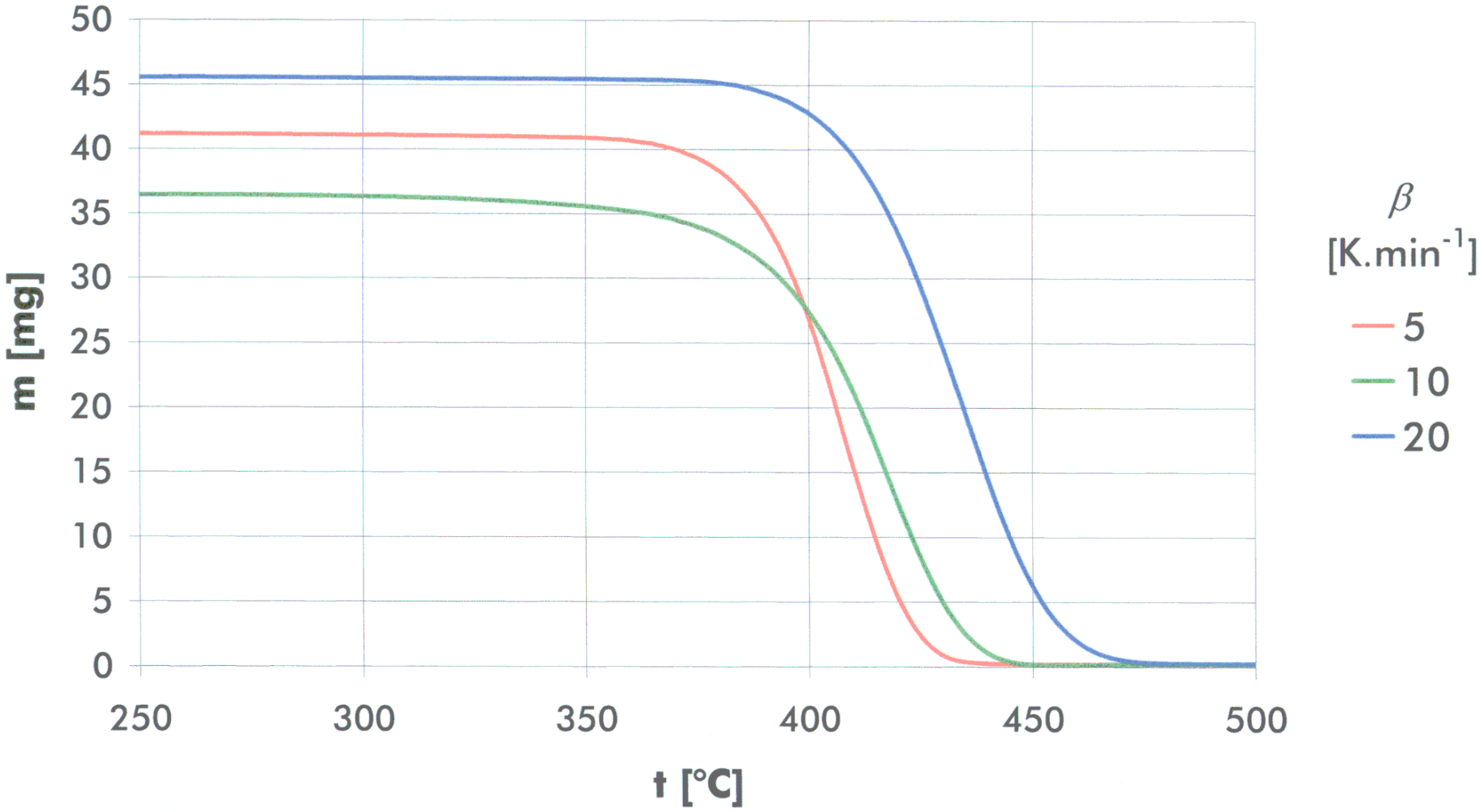

Fig. F-34: Conversion degree as a function of T, the case of PS.

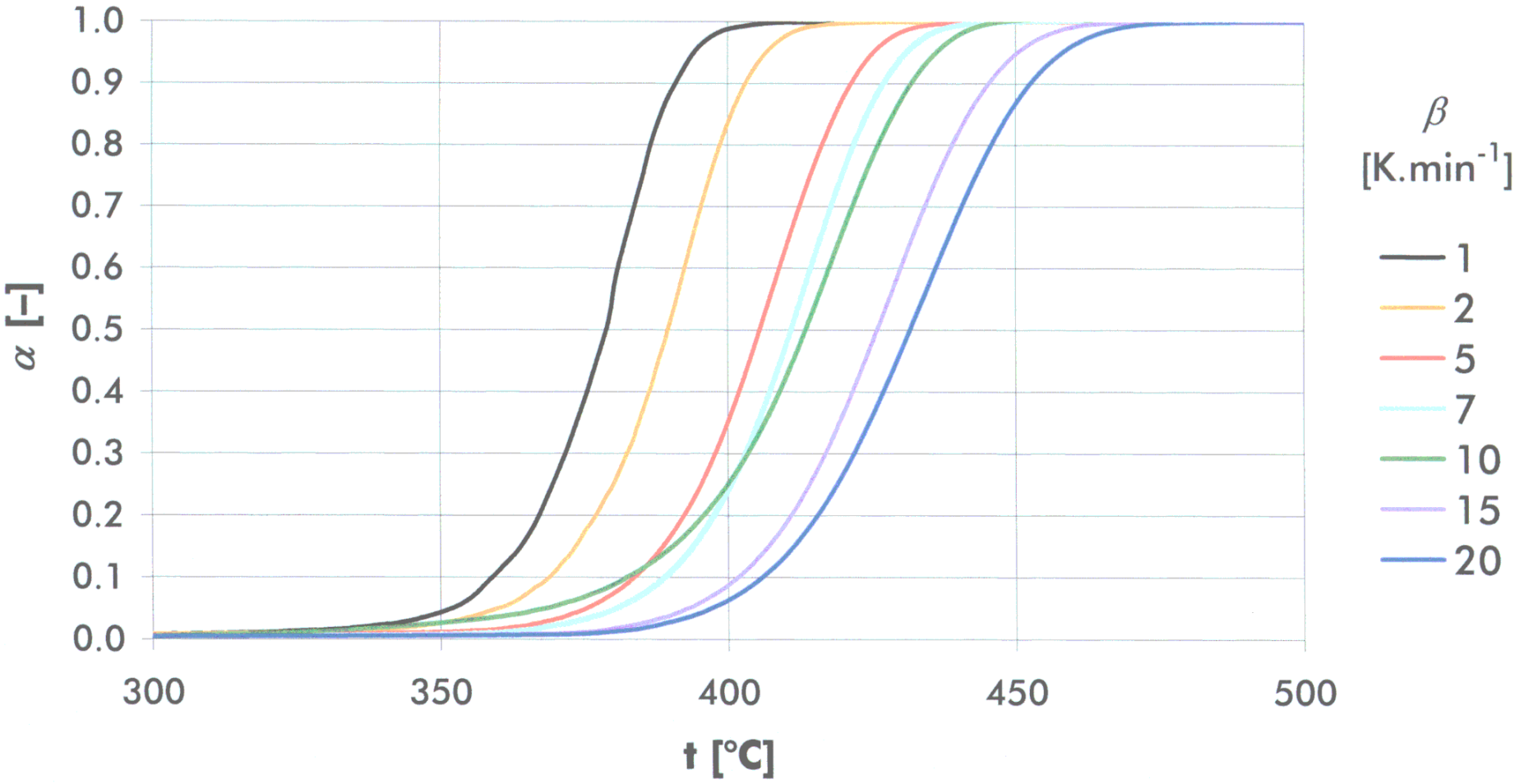

Fig. F-35: t = f(τ) aspect of PS pyrolysis.

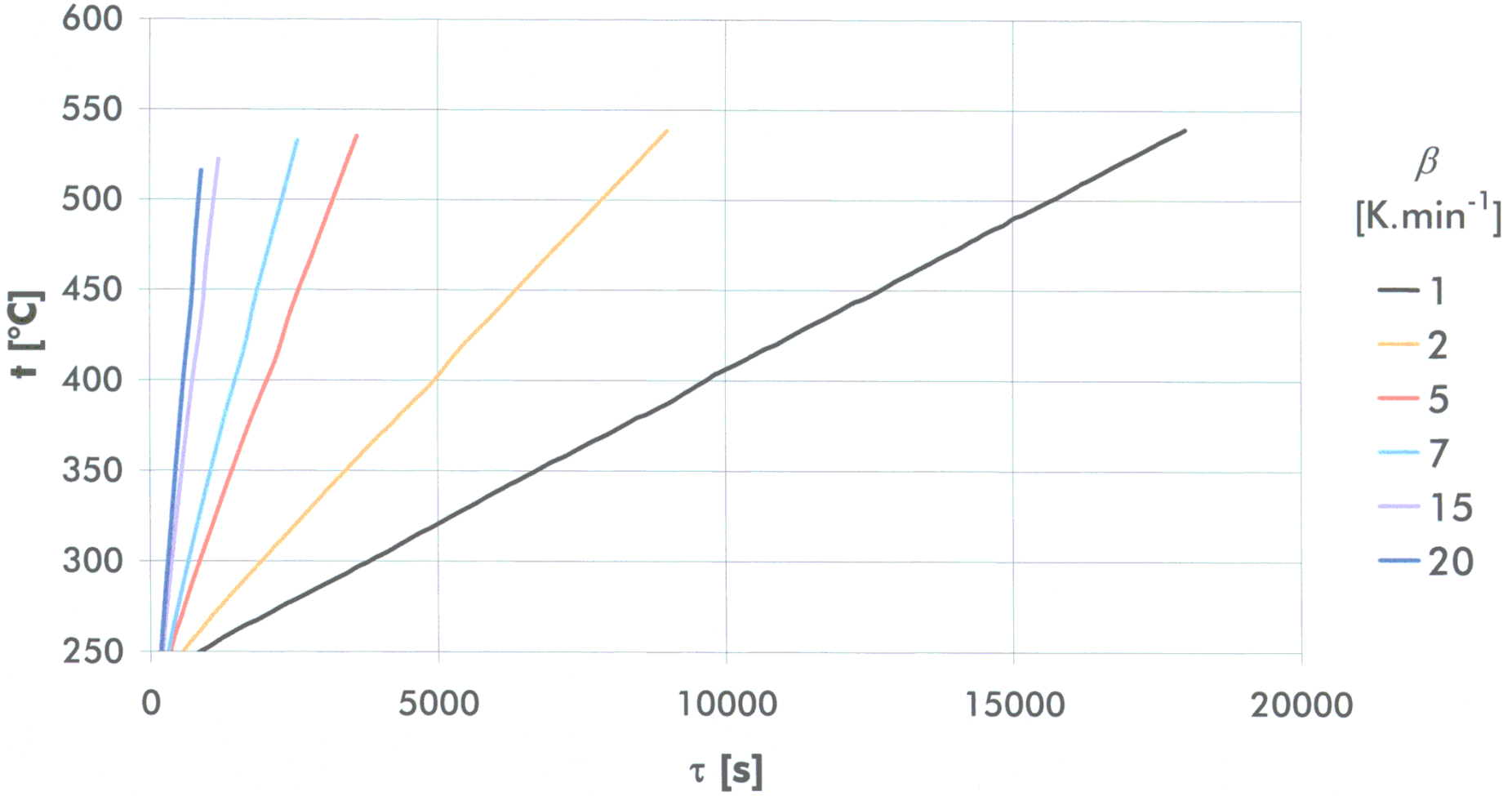

Fig. F-36: PVC thermogravimetric curve.

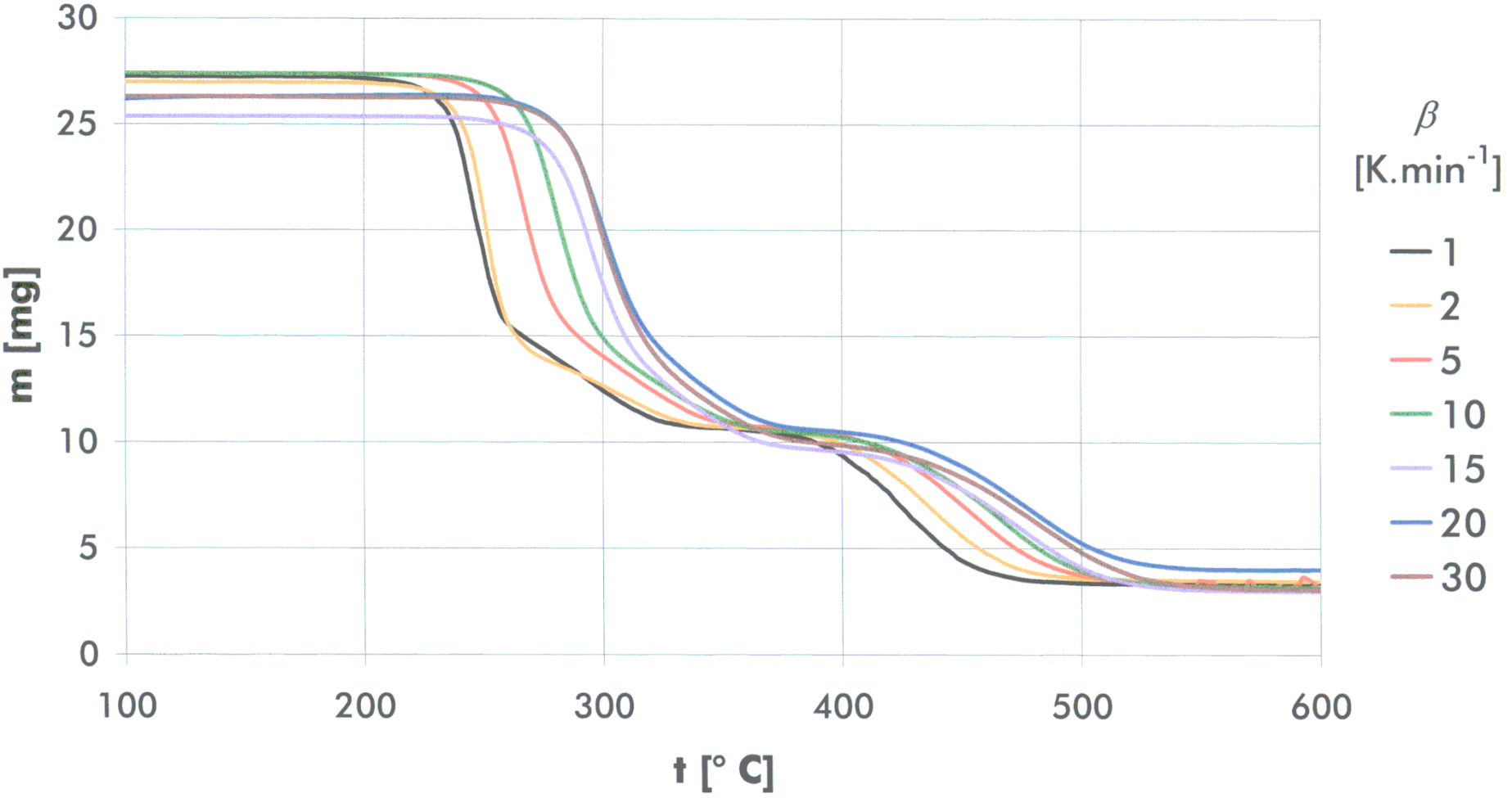

Fig. F-37: PVC pyrolysis α = f(t) aspect.

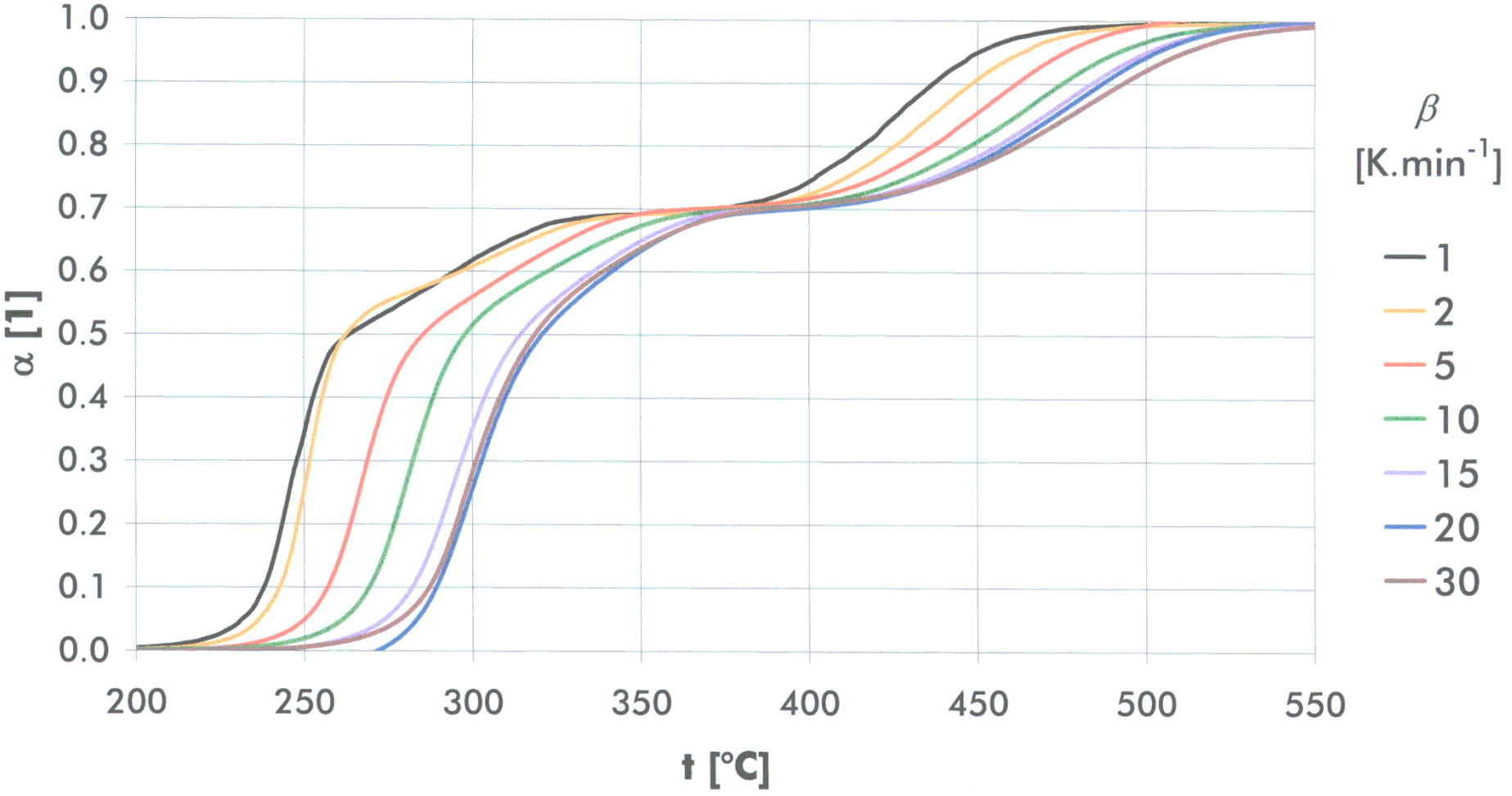

Fig. F-38: t = f(τ), the case of PVC.

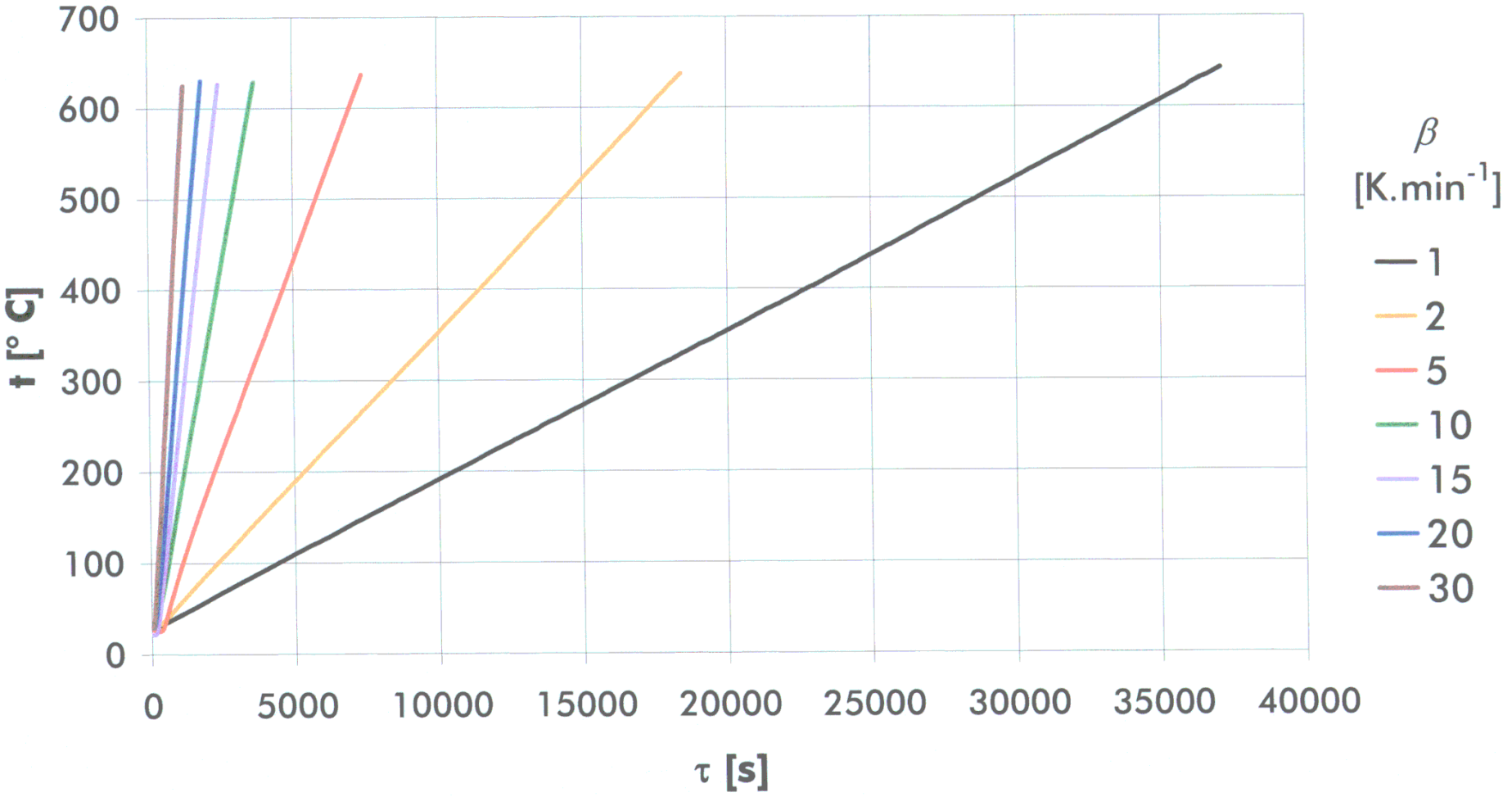

Appendix G

– Polymer generalities –

Below are a chart (Fig. G-1) and a table (Tab. G-1) representing the evolution of the consumption of some selected polymers in Europe, from 2000 to 2001 [*Plastiques et Elastomeres Magazine* 2002].

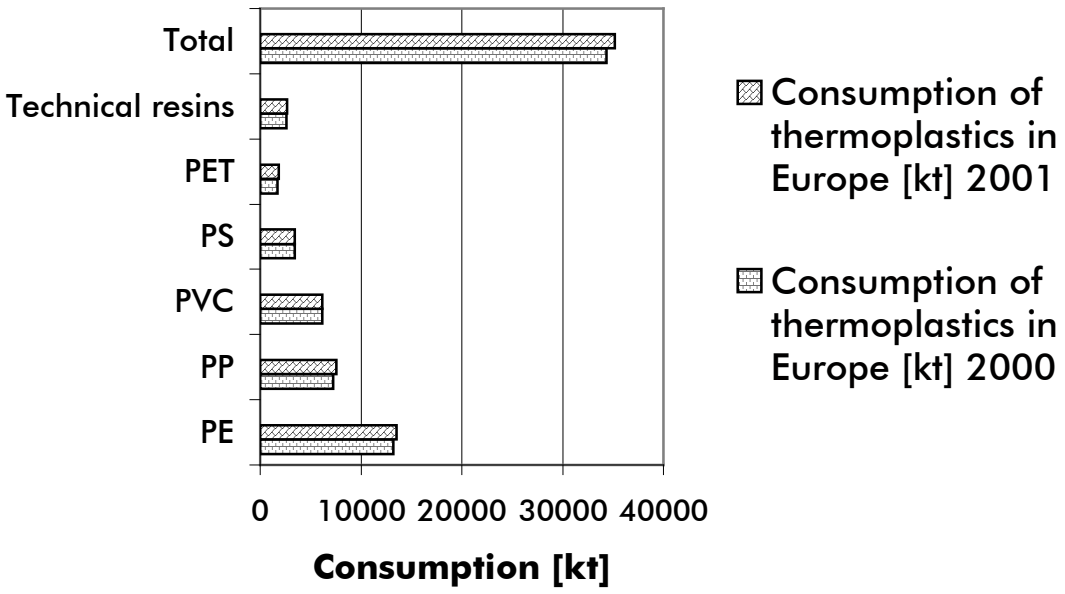

Fig. G-1: Consumption of thermoplastics in Europe in 2000 and 2001.

Tab. G-1: Consumption of thermoplastics in Europe (thousands of tons).

	2000	2001	Change in %
Polyethylene	13,194	13,495	2.3
Polypropylene	7,262	7,586	4.5
PVC	6,181	6,139	-0.7
PS	3,409	3,427	0.5
PET	1,697	1,841	8.5
Technical resins	2,603	2,658	2.1
Total	34,345	35,146	2.3

The following chart (Fig. G-2) represents the consumption of thermoplastics in Europe in 2001, by country. The corresponding table (Tab. G-2) contains the consumption in thousands of tons as well.

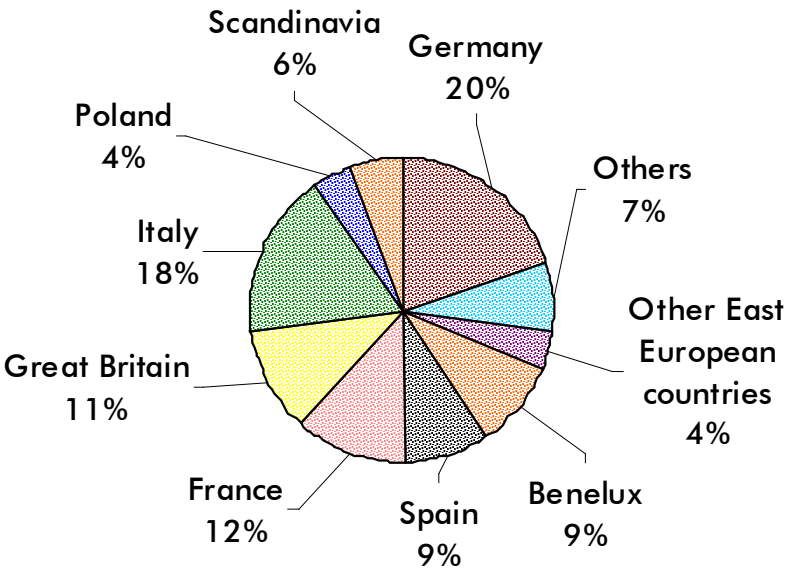

Fig. G-2: Consumption of thermoplastics in Europe in 2001.

Tab. G-2: Consumption of thermoplastics per country in 2001.

Country	Consumption [kT]	Consumption [%]
Benelux	3,266	9.3
France	4,280	12.2
Germany	7,075	20.1
Great Britain	3,851	11.0
Italy	6,175	17.6
Other	2,528	7.2
Other East-European countries	1,427	4.1
Poland	1,437	4.1
Scandinavia	1,993	5.7
Spain	3,113	8.9

Appendix H

List of publications and presentations of professional activities

Etude de la dégradation thermique de la lignine sous atmosphère inerte, Entropie (ISSN 0013 90 84; Francie), No. 235/236, 37ème année (1-126, 2001), p. 6-11 – J. Blažek, P. Buryan, D. Grouset, Y. Soudais, V. Tekáč • *paper in a journal.*

Etude et caractérisation de la pyrolyse de l'Ethyle vinyle acétate – J. Blažek, Y. Soudais • *internal research communication for CEA (Valrho, BP 17171, 30207 Bagnols sur Cèze Cedex) about the EVA pyrolysis.*

Modelové pokusy pyrolýzy hnědého uhlí z dolu Čs. armády, J. Blažek, P. Buryan • *research communication on possibilities of reducing tar production by pyrolysis in presence of various additives; for* Mostecká uhelná a.s. *joint-stock company.*

Conference contributions

Etude de la dégradation thermique de l'EVA sous atmosphère inerte, J. Blažek, P. Buryan, D. Lecomte, F. Lemort, Y. Soudais, V. Tekáč • *lecture – "33èmes Journées de Calorimétrie et d'Analyse Thermique" (JCAT 33), ENSIA Massy – Paris, France, 29-31/5/2002.*

Thermal Degradation of EVA Copolymers in the Inert Atmosphere, J. Blažek, P. Buryan, D. Lecomte, F. Lemort, Y. Soudais, V. Tekáč • *lecture; text published in conference proceedings – Pyrolysis 2002 conference, Leoben, Austria, 17-20/9/2002.*

The Pyrolysis of a Mixture of EVA and PS as Compared to That of the Individual Polymers, J. Blažek, P. Buryan, D. Lecomte, F. Lemort, Y. Soudais, V. Tekáč • *poster; text published in conference proceedings – Pyrolysis 2002 conference, Leoben, Austria, 17-20/9/2002.*

Study of the thermal degradation of lignin in the inert atmosphere, J. Blažek, P. Buryan, D. Grouset, Y. Soudais, V. Tekáč • *poster – conference "Biodegradable Polymers"; Queen's College, Oxford, England, 8-13/7/2001.*

Etude de la dégradation thermique de la lignine sous atmosphère inerte, J. Blažek, P. Buryan, D. Grouset, Y. Soudais, V. Tekáč • *poster – conference "Journées Polymères du Grand-Est", Nançy, France, 4/7/2001.*

Analysis of fluorides in the real contaminated soil, P. Arichtevová, J. Blažek, M. Kubal, H. Parschová • *poster; abstract published in conference proceedings – 5th International Symposium & Exhibition on Environmental Contamination in Central & Eastern Europe, Prague, Czech Republic, 12.-14.9.2000.*

Presentations on seminars with an expert audience

Etude de la pyrolyse des polymères • *lecture – Ecole des Mines d'Albi-Carmaux, Centre Energétique-Environnement, Séminaire sur l'ATG-DSC (Workshops on thermogravimetry and differential scanning calorimetry), Albi, France, March 2003.*

Etude de la pyrolyse de l'EVA • *lecture – Ecole des Mines d'Albi-Carmaux, UMR – CNRS 2392, Albi, France, 28/5/2002.*

Etude de la pyrolyse des polymères • *lecture – Université Libre de Bruxelles, Brussels, Belgium, May 2002.*

Etude de la pyrolyse de l'EVA et du PS • *lecture – Comissariat à l'Energie Atomique, Bagnols-sur-Cèze, France, 8/4/2002.*

Appendix I – Notation used

A	Frequency factor; also "pre-exponential factor"
ABS	Acrylonitrile Butadiene Styrene
E_a	Activation energy
$C_6H_{10}O_5$	Cellulose
$d\alpha/dt$	Rate of conversion
DSC	Differential Scanning Calorimetry
DTA	Differential Thermal Analysis
DTG	Derivative Thermogravimetry
EVA	Ethylene Vinyl Acetate
FTIR	Fourier Transformation Infra-Red (spectroscopy); Infra-Red spectroscopy using the Fourier transformation and the least square method
ICTAC	International Confederation for Thermal Analysis and Calorimetry
Inf	= "Inf. value"
Inf. value	Inferior value
IR	Infra-red
k	Rate coefficient in the Arrhenius equation, $k = A.\exp(-E_a/RT)$
n	Reaction order
PA	Polyamide
PBT	Polybutylene Terephthalate
PC	Polycarbonate
PCB	Polychlorinated Biphenyls (PCBs)
PCDD	Polychlorinated Dibenzodioxins
PCDF	Polychlorinated Dibenzofurans
PMME	Polymethyl Methacrylate
PP	Polypropylene
PPO	Polyphenylene Ether (Polyphenylene Oxide)
PS	Polystyrene
PVA	Polyvinyl Acetate
PVC	Polyvinyl Chloride
R	Universal/ideal gas constant
RMS	Root Mean Squared (Deviation); a common statistical measure of the differences between the atoms is the RMS between the atoms, or the RMS dev.
Rng	= "Range"; Δ(Sup; Inf)
Std. dev.	Standard deviation
Sup	= "Sup. value"
Sup. value	Superior value
t	Time
t; T	Temperature [°C]; [K]
TA	Thermal analysis
TG; TGA	Thermogravimetry, thermogravimetric; Thermogravimetric analysis
UHMWPE	Ultra high molecular weight Polyethylene
VA	Vinyl Acetate

RÉSUMÉ in French: L'objet de cette étude porte sur l'évaluation des paramètres cinétiques de la pyrolyse des polymères individuels. Les polymères étudiés ont été les polymères « naturels » et les polymères « industriels ». Comme polymères naturels, la lignine et la cellulose ont été choisies ; les polymères industriels ont été l'EVA, le PVC et le PS.

Les spectres IRTF des gaz émis pendant la pyrolyse ont été étudiés, sous la pression atmosphérique, dans le domaine des températures 20-1000°C. L'évolution de différents produits dans les étapes spécifiques des expériences a été comparée avec les schémas théoriques et les observations trouvées dans la littérature. Une concordance satisfaisante a été constatée.

Les résultats des essais ont été évalués par la méthode intégrale de Ozawa-Flynn-Wall (variante de Popescu). Les valeurs de sortie de cette méthode sont l'énergie d'activation E_a et le facteur préexponentiel A qui présentent une bonne concordance avec les paramètres cinétiques de référence. Les paramètres cinétiques principaux trouvés, par ex. pour l'EVA, le polymère le plus largement étudié, sont (pour l'EVA à 25 % du VA, montée en température allant de 1 à 30 $K.min^{-1}$) : E_a = 194 $kJ.mol^{-1}$ pour la première étape de dégradation, E_a = 317 $kJ.mol^{-1}$ pour la seconde étape de dégradation.

Une étude détaillée de la pyrolyse des mélanges binaires de l'EVA avec le PVC, le PS et la Cellulose, couplée avec l'analyse IRTF des gaz émis, a contribué à une meilleure maîtrise d'un procédé industriel, mis en œuvre par le CEA.

DOMAIN
In French (Discipline): Énergétique et transferts – Systèmes et procédés
In Czech (Obor PGS): Chemické a energetické zpracování paliv

MOTS-CLÉS	KLÍČOVÁ SLOVA	KEYWORDS
cinétique	kinetika	kinetics
pyrolyse	pyrolýza	pyrolysis
polymères	polymery	polymers

NAMES AND ADDRESSES OF THE U.F.R. OR LABORATORIES

Ecole des Mines d'Albi-Carmaux
Centre Energétique Environnement
UMR CNRS 2392 LGPSD
Campus Jarlard – Route de Teillet
81 013 Albi CT Cédex 09
République Française

Vysoká škola chemicko-technologická v Praze
(Institute of Chemical Technology, Prague)
Fakulta technologie ochrany prostředí
Ústav plynárenství, koksochemie a ochrany ovzduší
Technická 5, 166 28 Praha 6 – Dejvice
Czech Republic

ABSTRACT in English: The present work on pyrolysis of polymers was developed on laboratory scale. A thermogravimetric apparatus connected to FTIR spectrometer was used, the outputs of analyses were a set of mass loss data correlated with heating rates and a set of spectra corresponding to different moments of the degradation process. Kinetic parameters (E_a and A) were calculated by the means of the Popescu's variant of the Ozawa-Flynn-Wall integral method. A good agreement was found between calculated values and referential kinetic parameters.

Another method, 'fitting' experimental curves by the means of a special MatLab programs using differential equations solvers, was applied in the case of several polymers. It was used in the study of pyrolysis of individual polymers and their mixtures, and it did – together with examination of results from FTIR analysis – yield results that were applied on industrial niveau.

The polymers used were two "natural polymers", lignin and cellulose, and industry polymers: PVC, EVA, PS. In comparisons with reference kinetic parameters, a good accordance was observed in most cases. Principal results for the polymer examined most in detail, i. e. EVA (e.g. with 12 % of VA in molecules; 1-30 $K.min^{-1}$), are: E_a = 200 $kJ.mol^{-1}$ for the 1st degradation step and E_a = 271 $kJ.mol^{-1}$ for the 2nd degradation step.